THE UNIVERSITY
of EDINBURGH

Derivation of enkephalinergic medium spiny neurons from mouse embryonic stem cells

Chinnavuth Vatanashevanopakorn

Thesis presented for the degree of Doctor of Philosophy

The University of Edinburgh

2014

Declaration

I hereby declare that the work presented in this thesis is my own unless otherwise stated. This thesis has not been submitted to anywhere for any degrees or professional qualification except to The University of Edinburgh for the degree of Doctor of Philosophy.

Chinnavuth Vatanashevanopakorn

September 2014

Lay summary

Huntington's disease is an inherited neurodegenerative disease that results in the child of an affected person having a 50% chance of developing the disease. The major characteristics of the disease are the preferential degeneration of a sub-type of brain cell (medium spiny neuron) that produce a peptide called enkephalin. Loss of these particular neurons results in abnormal uncontrollable movements, impairment in comprehension, memory and psychiatric problems. Due to the fact that no effective treatment for the disease is available, development of a tool to explore the function of these neurons is essential. Use of embryonic stem cells is considered to be a potential approach for modelling neurodegenerative disorders including Huntington's disease. This strategy, however, needs a robust method to produce the specific cells of interest. Previous studies have generated medium spiny neurons from embryonic stem cells but failed to show whether they produced enkephalin. We show here that, the standard method for deriving medium spiny neurons from embryonic stem cells generates low numbers of neurons that make enkephalin. Interestingly, higher numbers are produced from a simpler culture condition and that these cells exhibit normal electrical properties of functional medium spiny neurons. We, therefore, conclude that the simpler culture condition is preferable for deriving enkephalin-expressing medium spiny neurons from embryonic stem cells.

Abstract

Medium spiny neurons (MSNs) play an important role in locomotion. Counterbalance between two MSN subtypes, enkephalin-positive and substance P-positive MSNs, is crucial for maintaining normal movement. Preferential degeneration of enkephalinergic MSNs in early stage Huntington's disease (HD) contributes to abnormal involuntary movement called chorea. The reasons for this selective vulnerability are unknown. *In vitro* differentiation of pluripotent stem cells (PSCs) to neuronal cells is considered a potential approach for modelling neurodegenerative disorders including HD. Generation of PSC-derived enkephalinergic MSNs would be an ideal tool for dissecting their preferential degeneration. However, an enkephalinergic phenotype has never been reported in PSC-derived MSNs. We, therefore, have generated a mouse embryonic stem cell (mESC) reporter line that expresses enhanced yellow fluorescent protein (EYFP) when the cells are committed to an enkephalinergic fate. Characterisation of this mESC line via chimaera generation showed that all EYFP-positive cells were also enkephalin-positive. We have then optimised an enkephalinergic neuronal differentiation protocol using this ESC line. Interestingly, we found that a combination of Wnt inhibitor Dickkopf-related protein 1 (DKK1), sonic hedgehog (Shh) and brain-derived neurotrophic factor (BDNF), commonly used in addition to basal medium for deriving MSNs from PSCs, had a detrimental effect on enkephalin expression. Absence of these three factors, surprisingly, did not reduce the potential of ESCs to become MSNs nor did it affect the electrophysiological properties of ESC-derived MSNs. Further investigation revealed that *Pre-pro-enkephalin* is down-regulated in the presence of exogenous DKK1 and/or Shh but not in the presence of BDNF. We, therefore, propose that addition of exogenous DKK1 and Shh is unfavourable to derive enkephalinergic MSNs from mouse ESCs. These findings could be used to derive enkephalinergic MSNs *in vitro* allowing the disease in a dish approach for HD modelling.

Acknowledgements

First of all, I would like to express my gratitude to my supervisors, Dr. Liliana Minichiello and Prof. Claus Nerlov. The advice, support and encouragement I have received from them are indispensable.

I would like to thank all members of the Nerlov and the Minichiello laboratories for teaching me the laboratory techniques I need for the project and for being excellent colleagues. I would especially like to thank Dr. Amit Grover, Dr. Mario Buono and Dr. Roy Drissen for helping me on the FACS and tissue culture techniques, Dr. Jacqui Horn for her great work in managing the mouse colonies and for her generous help on proofreading this thesis, Dr. Dario Besusso, Dr. Mirjam Geibel and Dr. Barbara Zonta for their help on histology and immunostaining, and Dr. Supat Thongjuea for introducing me to an interesting field of bioinformatics.

This project could not have been accomplished without the help from technical staff in the FACS facility at both the Centre for Regenerative Medicine, Edinburgh (Dr. Simon Monard and Dr. Olivia Rodrigues) and the Weatherall Institute of Molecular Medicine, Oxford (Paul Sopp, Dr. Sally-Ann Clark, Kevin Clark and Craig Waugh). I would like to thank Jan Ure and Dr. Joe Mee for deriving the enkephalinergic mESC reporter line and chimaera generation. The electrophysiological analyses were done in collaboration with Dr. Andrei-Sorin Illie and Dr. Colin Akerman. I would like to express my thanks to them for their advice and contribution.

I am thankful for all the support from the academic staff at the Centre for Regenerative Medicine, Edinburgh, particularly Dr. Tilo Kunath and Prof. Ian Wilmut. I am also very appreciative for the extraordinary support from Kelly Douglas, who did very her best to ensure that I could get any administrative matters done despite being away from Edinburgh.

I am indeed grateful for the generous financial support of my PhD from the Prince Mahidol Scholarship, Faculty of Medicine Siriraj Hospital, Mahidol University. I also would like to thank the faculties at the Department of Biochemistry, Faculty of Medicine Siriraj Hospital especially Prof. Neelobol Neungton, Dr. Ruchaneekorn Kalpravidh, Dr. Chatchawan Srisawat and Dr. Vorapan Sirivatanauksorn for their invaluable support and advice. I am also appreciated the generous guidance from Dr. Tuempong Wongtawan.

My thanks go to a group of the very best friends, Dr. Pimolrut Lertphokanon, Dr. Duantida Songdej, Pairoa Praihirunkit, Pitchayak Hunnangkul and Dr. Pittaya Dankulchai, who I have shared memorable experiences with during my PhD.

Finally, I would like to express my gratitude to my family for their unconditional support and encouragement.

Table of contents

List of figures

Page

List of tables

Chapter 3

Chapter 4

Abbreviations

ANB	Anterior neural boundary
AVE	Anterior visceral endoderm
BAC	Bacterial artificial chromosome
BDNF	Brain-derived neurotrophic factor
Bmp	Bone morphogenetic protein
cAMP	Cyclic adenosine monophosphate
Cbp	CREB-binding protein
CGE	Caudal ganglionic eminence
ChAT	Choline acetyltransferase
CMN	Cortical motor neuron
CPu	Caudate-putamen
Crbp I	Cellular retinol binding protein I
D1R	Dopamine D1 receptor
D2R	Dopamine D2 receptor
DAB	3,3'-diaminobenzidine
DARPP32	Dopamine- and cAMP-regulated phosphoprotein of 32,000 kDa
dbcAMP	Dibutyryl-cyclic adenosine monophosphate

DKK1	Dickkopf-1
E	Embryonic day
EB	Embryoid body
Enk	Enkephalin or enkephalinergic
ESC	Embryonic stem cell
EYFP	Enhanced yellow fluorescent protein
FACS	Fluorescence-activated cell sorting
FBS	Foetal bovine serum
Fgf	fibroblast growth factor
FMO	Fluorescence minus one
FS	Fast-spiking
FSC	Forward scatter
GABA	Gamma-aminobutyric acid
Gad	Glutamic acid decarboxylase
Gapdh	Glyceraldehyde-3-phosphate dehydrogenase
Gdnf	Glial cell line-derived neurotrophic factor
GP	Globus pallidus
GPe	External segment of globus pallidus
GPi	Internal segment of globus pallidus
Hap1	Huntingtin-associated protein 1

hESC	Human embryonic stem cell
Hip1	Huntingtin-interacting protein 1
Hip2	Huntingtin-interacting protein 2
hiPSC	Human induced pluripotent stem cell
hPSC	Human pluripotent stem cell
Hsp	Heat-shock protein
I_A	Low-voltage-activated potassium current
IGF	Insulin-like growth factor
iPSC	Induced pluripotent stem cell
Kirs	Inwardly rectifying potassium channels
KSR	KnockOut™ serum replacement
Kv1.2	Slow-inactivating potassium channel
Kv4.2	Fast-inactivating A-type potassium channel
Kv7	Kv7 potassium channel
LGE	Lateral ganglionic eminence
Lif	Leukaemia inhibitory factor
mESC	Mouse embryonic stem cell
MGE	Medial ganglionic eminence
MSN	Medium spiny neuron
MZ	Mantle zone

NRSE	Neuron-restrictive silencer element
NT-3	Neurotrophin-3
NT-4/5	Neurotrophin-4/5
PB	Phosphate buffer
PBS	Phosphate buffer saline
PENK	Pro-enkephalin
Penk	Pre-pro-enkephalin
PFA	Paraformaldehyde
PI	Propidium iodide
PKC	Protein kinase C
PLTS	persistent and low-threshold spike
PPP1R1B	Protein phosphatase 1 regulatory subunit 1B
PSC	Pluripotent stem cell
Psd95	Postsynaptic density 95
qRT-PCR	Quantitative reverse transcription polymerase chain reaction
RA	Retinoic acid
Raldh3	Retinaldehyde dehydrogenase 3
RAR	Retinoic acid receptor
Rest-Nrsf	Repressor element 1-silencing transcription factor and neuron-restrictive silencer factor

ROCK	Rho-associated kinase
RT-PCR	Reverse transcription polymerase chain reaction
RXR	Retinoid X receptor
SCID	severe combined immunodeficiency
s.d.	Standard deviation
s.e.m.	Standard error of the mean
SFEBq	Quick-aggregation serum-free culture of embryoid body-like aggregates
SHH	Sonic hedgehog
SN	Substantia nigra
SNc	Substantia nigra pars compacta
SNr	Substantia nigra pars reticulata
SP	Substance P
Sp1	Specificity protein 1
STN	Subthalamic nucleus
SVZ	Subventricular zone
TAN	Tonically active neuron
TBP	TATA-binding protein
TrkB	Tropomyosin-related receptor kinase B
TrkC	Tropomyosin-related receptor kinase C

VA/VL	Ventral-anterior/ventral-lateral nuclei of thalamus
VTA	Ventral tegmental area
VZ	Ventricular zone

Chapter 1: Introduction

1.1 The basal ganglia

1.1.1 Anatomy and physiology

The basal ganglia consist of a number of nuclei within the brain. Their main function is to control voluntary movement. Developmentally most of the basal ganglia structures, including the striatum, the globus pallidus (GP) and the subthalamic nucleus (STN), originate from the forebrain whereas the substantia nigra (SN) derives from the midbrain. The basal ganglia receive signals from the cerebral cortex and relay them to the thalamus, which in turn is the input for the cortex. The basal ganglia are involved not only in the motor function, but also in non-motor functions such as mood and reward-related behaviour (O'Callaghan et al., 2014). Regarding motor function, the basal ganglia are believed to contribute to the selection and execution of, but not the initiation of, voluntary movement (Bear et al., 2001, Wichmann and DeLong, 2013).

The striatum is widely considered the main input of the basal ganglia (Albin et al., 1989, DeLong, 1990, Bolam et al., 2000, Schroll and Hamker, 2013, Wichmann and DeLong, 2013). This structure is also known as the neostriatum or the dorsal striatum. In some mammals including the primates, the striatum is divided into two structures, the caudate nucleus and the putamen. The striatum receives glutamatergic inputs from efferent fibres of cortical and thalamic neurons (Albin et al., 1989, Wichmann and DeLong, 2013). It is also innervated by dopaminergic fibres from the substantia nigra pars compacta (SNc) and the ventral tegmental area (VTA) (Albin et al., 1989, Kreitzer, 2009, Wichmann and DeLong, 2013). Striatal projection neurons (also known as medium spiny neurons or MSNs, for more details see chapter 1.1.2), which are normally quiescent in the resting stage (Bolam et al.,

2000), then relay the signal via GABAergic efferent fibres to their targets after being activated by cortical efferent fibres.

Microscopically, the striatum could be divided into two compartments, the striosome (also known as the patch) and the matrix (Graybiel, 1990, Gerfen, 1992, Mitchell et al., 1999, Kreitzer, 2009). The striosome, which represents approximately 10-20% of striatal volume (Graybiel, 1990, Kreitzer, 2009), is identified by an enrichment of μ-opioid receptor (Herkenham and Pert, 1981) and a lack of acetylcholinesterase (Graybiel and Ragsdale, 1978). Inputs to patch neurons are mainly from the prelimbic and frontal cortices (Kreitzer, 2009, Shepherd, 2013). On the other hand, the matrix compartment is defined by area of dense calbindin (Gerfen et al., 1985), choline acetyltransferase (ChAT) (Graybiel et al., 1986) and acetylcholinesterase (Graybiel and Ragsdale, 1978) staining. Matrix neurons receive input projections from both the cortex and the thalamus (Kreitzer, 2009).

The main outputs of the basal ganglia are neurons in the internal segment of globus pallidus (GPi, also known as medial globus pallidus or entopeduncular nucleus in rodents) and the substantia nigra pars reticulata (SNr) (Albin et al., 1989, DeLong, 1990, Bolam et al., 2000, Schroll and Hamker, 2013). Unlike MSNs, the GABAergic neurons of the GPi/SNr are constantly active unless they receive inhibitory signals. GABAergic inhibitory efferent fibres from both structures then project to the ventral-anterior/ventral-lateral (VA/VL) nuclei of the thalamus. These nuclei in turn send their glutamatergic excitatory axons back to the cortex. In the resting state, thalamic activity is usually suppressed by inhibition from the GPi/SNr and therefore, less signal is transmitted to the cortex.

Connections between the input (striatum) and the output (GPi/SNr) of the basal ganglia are composed of two different pathways, the direct and the indirect (Figure 1.1). The striatal projection neurons in the direct pathway project their inhibitory fibres directly to the basal ganglia output, the GPi and the SNr (Albin et al., 1989, DeLong, 1990, Bolam et al., 2000, Schroll and Hamker, 2013). Upon activation of MSNs in the direct pathway, inhibition discharge from the MSNs

suppresses the activity of the output neurons in the GPi/SNr, which in turn leads to a disinhibition of the projection neurons within the thalamus, a GPi/SNr target. Consequently, thalamic neurons produce the excitation discharge to their targets, the cerebral cortex.

Conversely, another group of MSNs send inhibitory fibres to the external segment of the globus pallidus (GPe, also known as lateral globus pallidus). GABAergic projection neurons within the GPe in turn negatively regulate the activity of subthalamic nucleus (STN) excitatory neurons, which project their axons to the GPi and the SNr (Albin et al., 1989, DeLong, 1990, Bolam et al., 2000, Schroll and Hamker, 2013). It has been found that, in addition to GPe-STN-GPi/SNr circuit, GABAergic neurons of the GPe have a direct connection to output neurons in the GPi/SNr (Bolam et al., 2000, Schroll and Hamker, 2013). Thus, the MSNs in this pathway are indirectly connected to the GPi/SNr via neurons of the GPe and STN. Activation of the striatal projection neurons in the so-called "indirect pathway" leads to a reduction in GABAergic inhibitory activity of the GPe neurons, which in turn causes disinhibition of excitatory discharge from neurons of the STN. Further excitatory input from the STN then stimulates GABAergic discharge from the GPi/SNr, which eventually results in the inhibition of the basal ganglia target, the VA/VL nuclei of the thalamus. Therefore, stimulation of the direct and indirect pathways produces opposite outcomes. Counterbalance of the two pathways provides feedback to the cerebral cortex and is necessary for appropriate voluntary movement initiated from the cortex.

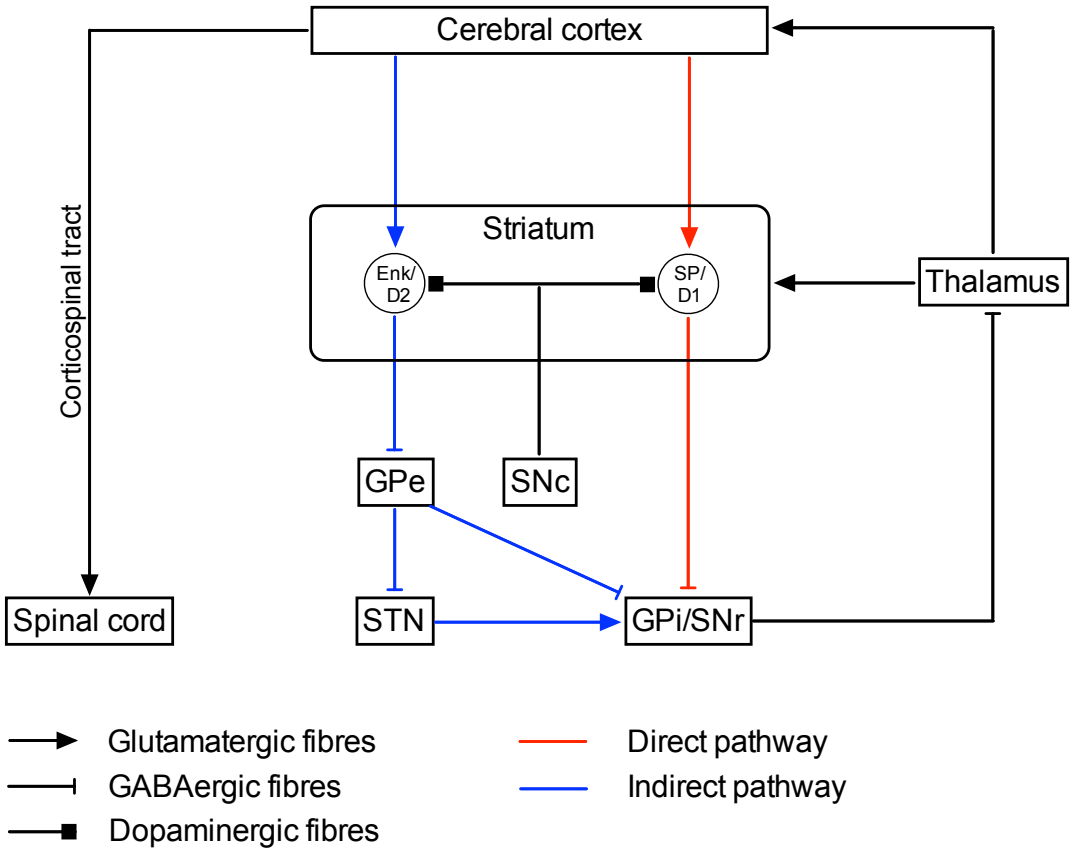

Figure 1.1 The motor circuits of basal ganglia. The cortico-basal ganglia-thalamocortical tracts consist of two parallel pathways within the basal ganglia. Excitatory signals from cerebral cortex and thalamus stimulate two MSN subtypes in the striatum. Activation of the direct pathway MSNs, which are substance P (SP)-positive, express the dopamine D1 receptor and send their inhibitory axons to the GPi/SNr, leads to suppression of GABAergic neurons of the GPi/SNr. Consequently, disinhibition of glutamatergic neurons in the thalamus results in more signal being sent back to the cerebral cortex. In contrast, activation of another group of the MSNs, which are enkephalinergic (Enk, note that enkephalinergic neurons are also found in the granular layer of cerebellum and olfactory bulb and, to a lesser extent, in the cerebral cortex) and express the dopamine D2 receptor, causes an opposite outcome. The MSNs of the indirect pathway inhibits the activity of GABAergic neurons of the GPe by receiving excitatory signals from the cerebral cortex. This subsequently stimulates GPi/SNr inhibitory function. Thus, the cerebral cortex receives less feedback signal from the thalamus. The cerebral cortex then integrates the signals received from the basal ganglia and thalamus before sending the signals through the corticospinal tract to execute motor function. GPe, external segment of globus pallidus; GPi, internal segment of globus pallidus; SNc, substantia nigra pars compacta; STN, subthalamic nucleus.

1.1.2 Neuronal cell types within the striatum

1.1.2.1 Medium spiny neurons

Neuronal cells in the striatum are categorised into two distinct groups according to their function, GABAergic projection neurons called "medium spiny neurons (MSNs)" and aspiny interneurons (Kreitzer, 2009). The majority of neurons (approximately of 95%) in the striatum are MSNs (Mitchell et al., 1999, Gil and Rego, 2008, Kreitzer, 2009). As mentioned in chapter 1.1.1, their main function is to relay a signal from the cerebral cortex to the thalamus via two different pathways, the direct and indirect pathways so regulating movement. Thus, the MSNs can be classified into two subtypes according to the contribution to the specific movement pathway. The MSNs of the direct pathway project their axon to the GPi and SNr. They are, thus, named the striatonigral MSNs, which indicates their location and targets (Kreitzer, 2009). On the other hand, the MSNs of the indirect pathway, which send their axonal terminals to the GPe, are known as the striatopallidal MSNs (Kreitzer, 2009).

Electrophysiologically the two MSN subtypes exhibit unique properties. They possess a hyperpolarised resting membrane potential and low input resistance due to the function of inwardly rectifying potassium channels (Kirs). During depolarisation, the inhibition of Kirs is elicited whilst the fast-inactivating A-type potassium channel (Kv4.2), the slow-inactivating potassium channel (Kv1.2) and the Kv7 potassium channel are active (Kreitzer, 2009). The activation of Kv4.2, Kv1.2 and Kv7 channels results in the hallmark of MSN electrical property, a depolarisation with a delayed onset in generating the initial spike (Kreitzer, 2009) indicated by the presence of a low-voltage-activated potassium current (I_A) (Ericsson et al., 2011). The difference between striatonigral and striatopallidal MSNs in terms of electrical property is subtle. Striatopallidal MSNs were shown to be more excitable than the striatonigral MSNs due to the difference in properties of Kir inactivation (Kreitzer, 2009). Additionally, the striatopallidal MSNs are more responsive to the inhibition of muscarinic M1 receptors compared to the striatonigral counterpart (Shen et al., 2007, Kreitzer, 2009).

Until recently, both MSN subtypes were initially thought to be morphologically identical. Gertler and colleagues have demonstrated that the striatonigral MSNs have higher number of primary dendrites than the striatopallidal subtype (Gertler et al., 2008). Indeed, this morphological distinction contributes, in part, to the electrophysiological differences between two MSN subtypes (Gertler et al., 2008).

In addition to the electrophysiological and morphological dichotomy, both striatonigral and striatopallidal MSNs are distinct in terms of the molecular phenotype (Table 1.1). Although all MSNs are GABA-producing neurons and express a common marker, dopamine- and cAMP-regulated phosphoprotein of 32,000 kDa or Darpp32 (also known as protein phosphatase 1 regulatory subunit 1B or Ppp1r1b), neuropeptides present in each subtype are different. Substance P and dynorphin are selectively produced by the striatonigral MSNs whilst the striatopallidal MSNs preferentially secrete enkephalin (Gerfen and Young, 1988, Gerfen et al., 1990). Differential expression of various receptors in MSN subtypes has also been well described in rodents. The striatonigral MSNs possess dopamine D1 receptor (D1R, encoded from *Drd1a* gene) (Gerfen et al., 1990) and muscarinic M4 receptor (Harrison et al., 1996). In contrast, dopamine D2 receptor (D2R, encoded from *Drd2* gene) (Gerfen et al., 1990) and adenosine A2a receptor (Ferré et al., 1993) is specifically expressed in the striatopallidal MSNs.

Table 1.1: Basic characteristics of the striatonigral and striatopallidal MSNs.

	Striatonigral MSN	**Striatopallidal MSN**
Neuropeptide produced	Subtance P Dynorphin	Enkephalin
Type of dopamine receptor expressed	D1 receptor	D2 receptor
Other receptors expressed	Muscarinic M4 receptor	Adenosine A2a receptor
Axonal projection	Substantia nigra pars reticulata and internal portion of globus pallidus	External portion of globus pallidus
Function	Initiation of voluntary movement (direct pathway)	Suppression of unwanted movement (indirect pathway)
Striatal compartment	Patch and matrix	Patch and matrix
Degeneration in Huntington's disease	Degeneration occurs in the late stage of the disease	Degeneration starts in the early stage of the disease (most vulnerable neuronal population)

MSN, medium spiny neuron.

1.1.2.2 Striatal interneurons

Striatal interneurons represent only a small fraction (approximately 2.3% in rodents) of striatal neuronal cells (Rymar et al., 2004). They receive input from the cerebral cortex and the thalamus. Their major function is to modulate the activity of the MSNs. The striatal interneurons consist of two main groups, the medium-sized GABA-producing interneurons and the large-size cholinergic interneurons (Tepper and Bolam, 2004, Kreitzer, 2009). GABAergic interneurons comprise approximately 2% of total striatal neurons (Rymar et al., 2004) and can be further classified into three subtypes: parvalbumin-positive, somatostatin-positive and calretinin-positive neurons (Rymar et al., 2004, Tepper and Bolam, 2004, Kreitzer, 2009). Parvalbumin-positive interneurons account for about 0.7% of total neurons within the rodent striatum (Rymar et al., 2004) and are the best characterised striatal interneurons. In terms of electrophysiology, they are called fast-spiking (FS) interneurons because they exhibit rapid and sustained firing rates (Tepper and Bolam, 2004, Kreitzer, 2009). They inhibit activity of both striatonigral and striatopallidal MSNs via numerous synaptic connections (Gittis and Kreitzer, 2012, Do et al., 2012) although they preferentially target the former rather than the latter (Gittis et al., 2010). Interestingly, it has been shown that depletion of dopamine leads to a shift of connections between parvalbumin-positive interneurons and MSNs by doubling the parvalbumin-positive interneuron-striatopallidal MSN innervation (Gittis et al., 2011). This increase could result in the induction of aberrant activity of striatopallidal MSNs resulting in the observed motor symptoms in Parkinson's disease (Gittis et al., 2011).

Another GABAergic striatal interneuron subtype, the somatostatin-positive neurons, also expresses high level of neuropeptide Y, NADPH diaphorase and nitric oxide synthase. They make up about 0.8% of total rat striatal cells (Rymar et al., 2004). Due to their typical electrical properties, low threshold spike and prolonged plateau potential mediated by calcium channels, they are called the persistent and low-threshold spike (PLTS) neurons (Tepper and Bolam, 2004). In terms of their function this group of GABAergic interneurons is less well characterised than

parvalbumin-positive interneurons. Potentiation of GABA-mediated inhibition of MSN activity by somatostatin-positive neurons has been described in dopamine depleted condition (Dehorter et al., 2009). Moreover, it has been proposed that somatostatin-positive interneurons might regulate corticospinal synaptic plasticity via their ability to produce nitric oxide (Tepper and Bolam, 2004).

The third group of GABA-producting striatal interneurons is calretinin-positive neurons. They comprise about 0.5% of striatal neurons in rodents (Rymar et al., 2004). Unlike the other striatal interneurons, no electrophysiological properties of calretinin-positive interneurons have been described (Tepper and Bolam, 2004, Kreitzer, 2009, Gittis and Kreitzer, 2012). However, an interesting study on adult neurogenesis of the human brain has recently demonstrated that the striatal calretinin-positive interneurons are being generated throughout life (Ernst et al., 2014). Thus, this group of interneuron might have an important role in co-ordinating and regulating the striatal function.

Unlike GABAergic interneurons, the cholinergic striatal interneurons are large-size, aspiny and can be identified by the presence of ChAT (Tepper and Bolam, 2004, Kreitzer, 2009). They also express dopamine receptors (D2 and D5), and muscarinic receptors (M2 and M4) (Levey et al., 1993, Hersch et al., 1994, Bergson et al., 1995, Guzman et al., 2011). About 0.3% of neostriatal neurons are believed to belong to this group of interneurons (Rymar et al., 2004). They receive GABAergic inputs from the MSNs in addition to glutamatergic inputs from the cerebral cortex and thalamus (Tepper and Bolam, 2004, Kreitzer, 2009). Their axons innervate matrix neurons within the striatum, mainly MSNs, and, to a lesser extent, other GABAergic interneurons (Tepper and Bolam, 2004). Electrical characteristics of the cholinergic interneurons are slow and regular firing with a long duration action potential and slow spike after-hyperpolarisation, which give rise to the name of tonically active neurons (TANs) (Tepper and Bolam, 2004, Kreitzer, 2009). Regarding the function of cholinergic interneurons, they, together with dopaminergic nigrostriatal neurons, are believed to modulate the MSN activity that regulates

reward-based learning and motivated behaviour (Morris et al., 2004, Tepper and Bolam, 2004).

1.2 Huntington's disease

1.2.1 General information

Huntington's disease, originally described as Huntington's chorea, is an autosomal dominant neurodegenerative disorder caused by abnormal expansion of CAG repeats within the first exon of the human huntingtin gene, located on the short arm of chromosome 4. The number of CAG repeats in the general population is normally less than 27 repeats whilst the presence of more than 35 repeats results in Huntington's disease (Roos, 2010). This mutation results in the production of abnormal huntingtin protein that contains excess glutamine residues at its N-terminus. The mutant huntingtin contributes to the loss of neurons in the central nervous system particularly the striatal projection medium spiny neurons. The onset of the disease is mid-adult life, ranging between 35 and 50 years in most patients although the production of mutant huntingtin has been found throughout life. The disease has a prevalence of 4-10 per 100,000 in Western countries (Ross and Tabrizi, 2011).

Given that the disease is caused by an expansion of CAG repeat, it is expected that higher repeats would lead to more severe clinical manifestation. Indeed, it has been shown that the number of CAG repeats correlates directly with neuronal loss. Individuals who have longer CAG repeats have higher degree of cell death in the striatum (Vonsattel and DiFiglia, 1998). However, the number of CAG repeats accounts for only 30-60% of overall variance in age of onset. Other factors affecting the disease onset are other genetic and environmental factors (Wexler et al., 2004, Arning et al., 2005).

1.2.2 Clinical manifestation

The major clinical triad of Huntington's disease consists of cognitive function deterioration, abnormal involuntary movement, known as chorea, and psychiatric disturbances (Roos, 2010). Psychiatric problems are normally the earliest symptoms presented in the patients. Prevalence of these symptoms varies greatly due to different methodologies as well as stages of the disease. In the REGISTRY study, a prospective observation study of Huntington's disease in European countries, apathy was the most prevalent psychiatric symptoms in every stage of the disease (van Duijn et al., 2014). Approximately 28% of patients were diagnosed moderate to severe apathy whilst moderate to severe depression was found in only 12.7% of participants. Other neuropsychiatric problems reported include irritability, aggression, obsessive compulsive behaviour and psychosis (Gil and Rego, 2008, Roos, 2010, van Duijn et al., 2014). Similar to the psychiatric disturbances, cognitive decline can generally be observed long before the emergence of motor symptoms resulting in patients losing their organising ability as well as their memory. In the end stage of the disease, most patients show profound dementia (Gil and Rego, 2008).

The most striking of the triad, and usually the last to appear is motor disturbance. This generally begins with a slightly clumsy gait, the patients later develop slowly progressive involuntary choreatic movement spreading from distal to proximal muscles. The progression of involuntary movement results in an inability to move at their own will, as well as dysarthria (difficulty in articulating words) and dysphagia (difficulty in swallowing). In the late stage of the disease, bradykinesia (slowness of movement) and akinesia (difficulty in starting movement) are present in the majority of patients (Gil and Rego, 2008, Roos, 2010).

In addition to the classical symptoms mentioned above, other symptoms have been described in the patients. One of the most common extraneuronal symptoms is non-choreatic-related weight loss. Pathogenesis of a reduction in body weight in Huntington's disease is unknown but it is believed that the loss of hypothalamic neurons would play a role (Kremer and Roos, 1992, Djoussé et al., 2002). Abnormalities in the endocrine system are also observed. These include an increase

in the level of corticosteroids caused by hypothalamic-pituitary-adrenal axis dysfunction (Heuser et al., 1991, Leblhuber et al., 1995) and a decrease of plasma testosterone (Markianos et al., 2005).

The leading causes of death in Huntington's disease patients are pneumonia and heart disease (Lanska et al., 1988, Sørensen and Fenger, 1992). Pneumonia, which is generally aspiration-related, is responsible for approximately 40% of deaths in Huntington's patients. Although psychiatric problems are commonly present in Huntington's patients, suicide accounts for only 5% or less of total death in these patients (Lanska et al., 1988, Sørensen and Fenger, 1992).

1.2.3 Pathology

Pathologically the hallmark of Huntington's disease is striatal atrophy. Interestingly, it has been found that only the GABAergic striatal projection MSNs mainly degenerate whilst striatal interneurons are relatively preserved (Ferrante 1985, Ferrante 1987, Gil 2008). A neuropathological grading system commonly used for the disease was introduced by Vonsattel and colleagues (Vonsattel et al., 1985). The Vonsattel grading system classifies Huntington's disease into five grades ranging from grade 0 to 4 according to post-mortem examination, both macroscopic and microscopic. Grade 0 is the least severe and macroscopically indistinguishable from control normal brains. In contrast, grade 5 brains showed severe neuronal loss and diffuse astrogliosis in both the caudate nucleus and putamen.

What is interesting regarding the MSN vulnerability in the disease is that degeneration is not equally observed amongst the MSN population (Table 1.2). Preferential loss of enkephalinergic striatopallidal MSNs is found in presymptomatic as well as initial and middle stages of the disease whilst the substance P-positive MSNs are less affected (Reiner et al., 1988, Albin et al., 1990, Albin et al., 1992, Richfield et al., 1995, Deng et al., 2004). Reiner and colleagues have demonstrated using immunohistochemistry that the number of enkephalin-containing fibres, found mainly in the GPe, was drastically reduced in the brains from all stages of Huntington's disease when compared to controls (Reiner et al., 1988). Conversely, the number of substance P-containing axons projecting to the GPi of Vonsattel stage 2 and 3 Huntington brains was similar to that of controls. Both enkephalin- and substance P-positive fibres were, however, markedly depleted in the advanced stage of the disease (Vonsattel grade 4). Interestingly, the activity of glutamic acid decarboxylase (GAD), an enzyme involved in the GABA synthesis, was markedly decreased in the lateral pallidum, but not in the medial pallidum (Spokes, 1980). These findings indicate the preferential loss of enkephalinergic striatal neurons projecting to the GPe in Huntington's disesase (Reiner et al., 1988, Mitchell et al., 1999). Several publications have confirmed these observations. An *in situ* hybridisation study revealed a greater decline of enkephalin-producing neurons

compared to substance P-producing neurons in the caudate nucleus of Huntington's disease patients (Richfield et al., 1995). Albin and colleagues have reported a reduction in the number of enkephalin-positive fibre terminals in the GPe, but not in the number of substance P-containing fibres in the GPi, in the brain of two pre-symptomatic Huntington's disease individuals (Albin et al., 1990, Albin et al., 1992). In addition, studies in Huntington's disease rodent models have also shown similar findings. Two Huntington's disease mouse models, the transgenic R6/2 mice (Mangiarini et al., 1996) and the knock-in (CAG91 and CAG74) mice (Levine et al., 1999), have demonstrated a severe reduction of enkephalin mRNA levels in striatal neurons of mutants (Menalled et al., 2000). However, the expression of substance P, Gad65 and Gad67 in mutant animals was identical to that of controls. Similarly, a reduction in the level of enkephalin mRNA, the number of enkephalinergic neurons in the striatum, as well as a lower intensity of enkephalin-immunoreactive fibres in the GP of R6/2 mice was found (Sun et al., 2002). These findings are in contrast with the number of substance P-positive neurons in the striatum as well as substance P immunoreactive fibre intensities in the GP, which were relatively normal in R6/2 animals.

Preferential degeneration of enkephalinergic striatopallidal MSNs has also been supported by the fact that the levels of other striatopallidal markers were also diminished in all stages of Huntington's disease (Glass et al., 2000). In grade 1 striata, the density of dopamine D2 receptor was markedly decreased to 6-7% of controls whereas moderate reduction (54-56% of controls) was described for dopamine D1 receptor density. The decline of D2 receptor density was even more prominent in the caudate nucleus and putamen of grade 2 and 3 brains (6-10% of normal brain) whilst D1 receptor density was diminished to a lesser degree (26-34%) (Glass et al., 2000). Likewise, the level of adenosine A2a receptor was drastically reduced in the striata of grade 1 Huntington's disease patients, 11-13% compared to controls. At later stages, no detectable level of A2a receptor was found within the caudate nucleus and putamen (Glass et al., 2000). Since the D2 receptor and A2a receptor are specifically expressed in the striatopallidal MSNs, the findings from

Glass and co-workers have further confirmed that the enkephalinergic striatopallidal MSNs are the most vulnerable striatal population in Huntington's disease.

Given that the enkephalinergic striatopallidal MSNs are part of the indirect pathway of the basal ganglia, the loss of this MSN subtype in the early stage of the disease would lead to an imbalance between the direct and indirect pathways. It has been shown that an inactivation of the indirect pathway by an injection of GABA receptor antagonist bicuculline into either the putamen or the GPe resulted in a choreatic movement (Crossman et al., 1988). Indeed, this is consistent with the motor symptoms of early stage Huntington's disease, when the choreatic movement is predominant (Gil and Rego, 2008, Roos, 2010).

Also, Hedreen and Folstein have described the differential degeneration of striatal neurons within patch-matrix compartments of Huntington's disease patients (Hedreen and Folstein, 1995). The cause of the preferential degeneration of patch neurons in the early stage Huntington's disease is unknown. This may be explained by the fact that neurons in this compartment are devoid of the calcium binding protein calbindin. Calcium homeostasis has been implicated in neurodegeneration, and therefore, the absence of calbindin in striosomal neurons might contribute to the selective degeneration (Mitchell et al., 1999).

Atrophy of other regions of the brain also occurs although to a lesser degree. Affected areas include the cerebral cortex, cerebellum, thalamus, hypothalamus, amygdala and substantia nigra (Kassubek et al., 2005, Douaud et al., 2006). The degree of atrophy in non-striatal structures, interestingly, is well correlated with Vonsattel grading system. A good example is the cerebral cortex, which shows only a subtle loss in grade 1 and 2. However, a marked degeneration of the cerebral cortex especially layers III, V and VI is evident in grade 3 and 4 brains (Gil and Rego, 2008). Atrophy of brain structures contributes to a reduction of brain weight, which could be up to 40% in patients with advanced stage of the disease (Gusella, 2001).

Table 1.2: Differential vulnerability of striatal neurons in Huntington's disease (Adapted from Mitchell et al., 1999).

	Least vulnerable	Most vulnerable
Neuronal cell type	Striatal interneuron	MSN
MSN subtypes	Substance P-positive striatonigral MSN	Enkephalinergic striatopallidal MSN
Striatal compartment	Matrix	Patch

MSN, medium spiny neuron.

1.2.4 Pathogenesis and pathophysiology

It is believed that the pathogenesis of Huntington's disease is caused by two mechanisms, loss of function of normal huntingtin protein and toxic gain of function of the mutant protein (Gil and Rego, 2008). Huntingtin is a protein that has at least 3,100 amino acid residues. The precise amount of amino acids within the protein depends on the number of glutamine residues. This protein is found intracellularly in various types of cells throughout the body. Huntingtin is normally located in the cytoplasm although it is also found, to a lesser extent, in the nucleus (Kegel et al., 2002, Gil and Rego, 2008). Huntingtin is associated with the mitochondria, the Golgi body, the endoplasmic reticulum and the microtubules (Young, 2003, Landles and Bates, 2004, Gil and Rego, 2008). Normal huntingtin interacts with many proteins such as the huntingtin-associated protein 1 (Hap1), the huntingtin-interacting protein 1 (Hip1), the huntingtin-interacting protein 2 (Hip2), glyceraldehyde-3-phosphate dehydrogenase (Gapdh) and β-tubulin (Gil and Rego, 2008). Within the central nervous system, huntingtin has been demonstrated to associate with several processes including regulation of brain-derived neurotrophic factor (Bdnf) expression, vesicular transportation of Bdnf and interaction with postsynaptic density 95 (Psd95) (Gil and Rego, 2008). Thereby, it involves several processes, for instance, embryonic development, intracellular transport, transcriptional regulation and anti-apoptotic function. In Huntington's disease, the production of mutant huntingtin causes a disruption of the processes above.

The mutant huntingtin produced in Huntington's disease is found in two forms, soluble and insoluble. The formation of insoluble aggregates of the mutant protein is one of the histological features of the disease. It was previously believed that an accumulation of mutant huntingtin aggregates was a cause of neurodegeneration in the disease (Landles and Bates, 2004, Gil and Rego, 2008). However, recent findings have indicated that, instead of being harmful to the cell, aggregates of mutant huntingtin may be a result of protective process by the cell to sequester the mutant protein and thus may not be pathogenic in the disease (Young, 2003, Gil and Rego, 2008).

The loss of normal huntingtin together with the accumulation of mutant huntingtin contributes to deregulation of several pathways and consequently cell loss in the disease. Mutant huntingtin causes transcriptional deregulation by sequestration of transcription factors. Abnormal interaction between mutant huntingtin and several transcription factors, for example, CREB-binding protein (Cbp), specificity protein 1 (Sp1), TATA-binding protein (Tbp) and p53 has been reported (Landles and Bates, 2004, Gil and Rego, 2008). Depletion of Cbp results in an inhibition of CBP-mediated transcription. Interestingly, genes implicated in Huntington's disease such as pro-enkephalin (*PENK*) are CBP-regulated genes (Huggenvik et al., 1991). Cbp ablation causes an Huntington's disease-like phenotype in mice and down-regulation of CBP-regulated genes has been found in Huntington's disease patients (Landles and Bates, 2004). Abnormal transcriptional processes in Huntington's disease are also related to a loss of normal huntingtin function, for example the transcriptional regulation of the *Bdnf* gene. The inability of mutant huntingtin to bind to the transcription factor complex of repressor element 1-silencing transcription factor and neuron-restrictive silencer factor (Rest-Nrsf) results in nuclear translocation of Rest-Nrsf. The intranuclear Rest-Nrsf then binds to the neuron-restrictive silencer element (NRSE) within the *Bdnf* promoter and consequently suppresses its transcription (Zuccato et al., 2003, Landles and Bates, 2004, Gil and Rego, 2008).

Abnormal protein folding and degradation processes are another key pathologies in Huntington's disease. Sequestration of heat-shock proteins (Hsps), such as Hsp40 and Hsp70, into mutant huntingtin aggregates leads to an accumulation of intracellular misfolded proteins (Landles and Bates, 2004, Gil and Rego, 2008). Abnormally folded proteins inside the cells are normally ubiquitinated and degraded by the proteasome. However, ubiquitin and proteasome subunits are also sequestered in the mutant huntingtin aggregates (Wyttenbach et al., 2000, Landles and Bates, 2004, Gil and Rego, 2008). Thus, the ubiquitin-proteasome system is also impaired in Huntington's disease. Accumulation of mutant huntingtin and misfolded proteins over the course of the disease, consequently, contributes to cell death via apoptosis or autophagy (Landles and Bates, 2004, Gil and Rego, 2008).

Other mutant huntingtin-mediated neuropathology includes axonal transport dysfunction and synaptic dysfunction. Wild-type huntingtin, via an association with Hap1, is involved in both anterograde and retrograde axonal transports. Mutant huntingtin, conversely, could inhibit this activity. This may account for the disruption of microtubule-mediated axonal transport, such as the anterograde transport of Bdnf (Gauthier et al., 2004, Gil and Rego, 2008). Axonal transport malfunction is one of the causes of impaired synaptic transmission via depletion of synaptic vesicles and related proteins at nerve terminals (Gil and Rego, 2008). Moreover, synaptic dysfunction is also a result of other molecular abnormalities observed in Huntington's disease. For instance, a reduction in wild-type huntingtin, which normally interacts with numerous vesicle proteins, brings about the synaptic dysfunction (Li et al., 2003, Gil and Rego, 2008). The presence of mutant huntingtin has also been identified as a main contributor for an alteration in available synaptic proteins as well as causing a functional abnormality in synaptic transmission. Indeed, increased glutamate release from presynaptic terminals, as well as a reduced glutamate clearance capacity, have been proposed as a cause of striatal excitotoxicity (Li et al., 2003, Gil and Rego, 2008). Lastly, transcriptional deregulation mediated by mutant huntingtin would lead to abnormal transcription of genes related to synaptic transmission. All of the abnormalities described above eventually lead to neuronal death. However, the question of why certain types of neurons are more vulnerable than others is still unknown and remains to be elucidated.

1.3 *In vivo* striatal neurogenesis

1.3.1 Development of the central nervous system

In adult mammals, the central nervous system is composed of two main structures, the brain and the spinal cord. They are developmentally derived from the neural tube. Neurulation, the process of forming the neural tube, creates neural folds that eventually fuse together forming a tube. Formation of the neural tube does not happen simultaneously but rather first begins at the anterior portion and then spreads to the posterior part (Gilbert, 2010). It is widely accepted that the neural tissue has an anterior identity by default (Levine and Brivanlou, 2007, Wilson and Houart, 2004). The caudal part of neural tube then acquires the posterior character by exposure to caudalizing factors, for instance, Wnts, Fgfs (fibroblast growth factors), retinoic acid (RA), Bmps (bone morphogenetic proteins) and Nodal, generated from posterior part of embryo. This means posterior identity could be induced in pre-specified anterior neural tissue. Maintenance of anterior neural identity in the anterior portion of neural tube, therefore, requires anticaudalizing agents, which are Wnt and Bmp inhibitor Cerberus, Wnt inhibitor Dickkopf-1 (Dkk1) and Nodal inhibitor Lefty produced from anterior visceral endoderm (AVE) (Kimura et al., 2000).

In parallel to what is happened at cellular and molecular levels, anterior neural tissue undergoes morphological change by bulging into three vesicles, which are prosencephalon (forebrain), mesencephalon (midbrain) and rhombencephalon (hindbrain). All structures in the brain are derived from either one of these vesicles. Table 1.3 shows the adult derivatives of these three structures.

Table 1.3: Structures in embryonic brain and their adult derivatives. Adapted from Gilbert, 2010.

Embryonic structures		Adult derivatives	Functions
Prosencephalon	Telencephalon	Neocortex	Association
		Hippocampus	Memory storage
		Amygdala	Emotional memory storage
		Basal ganglia	Voluntary motor control
		Olfactory bulb	Smelling
	Diencephalon	Epithalamus	Motor and emotional control
		Thalamus	Relay centre for optic and auditory neurons
		Hypothalamus	Temperature, sleep, satiety and breathing regulation
		Optic vesicle	Vision
Mesencephalon		Midbrain	Motor control, eye movement and consciousness
Rhombencephalon	Metencephalon	Cerebellum	Coordination of complex muscular movements
	Myelencephalon	Pons	Fibre tracts between cerebrum and cerebellum
		Medulla	Reflex centre of involuntary activities

1.3.2 Regional patterning of the telencephalon

The prosencephalon is divided into the telencephalon and more caudally the diencephalon. Specification of the telencephalon occurs around embryonic day (E) 8.5 in mice, when the expression of *Foxg1* (*Bf1*) is found in this region (Hébert and Fishell, 2008). This specification is mediated by a number of mechanisms related to the structure called anterior neural boundary (ANB) since the absence of ANB causes loss of expression of telencephalic markers *Foxg1* in mouse (Shimamura and Rubenstein, 1997) and *emx1* in fish models (Houart et al., 1998). Houart and colleagues subsequently identified Tlc, a Wnt signalling antagonist, as the responsible protein for telencephalon-inducing property of ANB in Zebrafish. Transplantation of Tlc-expressing cells into ANB region of ANB-ablated embryos led to a restoration of telencephalic marker *emx1* and *bf1* (Houart et al., 2002). Requirement of WNT antagonists is likely a result of a presence of WNT molecules produced by posterior neural tissue (Wilson and Houart, 2004). In addition to the inhibitory Wnt signalling, activation of the Fgf signalling pathway is necessary for telencephalic specification. Shimamura and Rubenstein have demonstrated that *Fgf8* from the ANB induces expression of *Foxg1* in rodents. Exogenous Fgf8 administration is able to restore *Foxg1* expression in ANB-depleted explants (Shimamura and Rubenstein, 1997). Also, *Fgf8* mutant animals exhibit reduced *Foxg1* expression (Storm et al., 2006). Interestingly, Martynoga and colleagues have reported that *Fgf8* expression is diminished in the telencephalon of *Foxg1*$^{-/-}$ mice (Martynoga et al., 2005) suggesting that *Fgf8* and *Foxg1* may positively regulate each other (Hébert and Fishell, 2008).

Once the anterior neural tissue acquires telencephalic fate, it further expands and subdivided into dorsal (pallial) and ventral (subpallial) telencephalon. A number of transcription factors as well as cell signalling pathways are known to contribute to regional patterning within the telencephalon (Figure 1.2). Dorsal and ventral telencephalon can be defined by the expression of their specific markers. In rodents, dorsal identity is determined by the expression of transcription factors Pax6 and Gli3 whereas ventral identity is specified by the presence of Shh and Fgf8 as well as

transcription factors Nkx2.1 and Gsx2 (Hébert and Fishell, 2008). Pax6 is initially expressed throughout the prospective telencephalon at the late 4-somite stage of mouse embryo (Inoue et al., 2000). Its expression is then lost from the ventral telencephalon around E9.5 (Sousa and Fishell, 2010). Loss of *Pax6* expression in ventral telencephalon is mediated by *Shh* produced from the axial mesendoderm (Macdonald et al., 1995, Shimamura and Rubenstein, 1997). *Pax6* is essential for dorsal telencephalic identity especially in the pallium-subpallium border since the expression of pallial markers in this area is lost in $Pax6^{-/-}$ embryos (Manuel and Price, 2005). Like Pax6, the transcription factor Gli3, is widely expressed in the telencephalon, but later the expression is limited to the dorsal portion only (Hébert and Fishell, 2008). Null mutation of *Gli3* contributes to the loss of expression of the dorsal telencephalic marker *Emx2*, reducing the size of the neocortex as well as the absence of both the hippocampus and choroid plexus (all are dorsal telencephalic structures) in *Gli3* deleted Xt^J/Xt^J mice (Theil et al., 1999). This indicates the requirement of *Gli3* in dorsal telencephalic development.

In contrast to Gli3, Sonic hedgehog (Shh) signalling is the major factor in the ventral telencephalon and suppresses any dorsalisation. In rodents, *Shh* transcript is found initially in the midline mesoderm of the head process around E7.5 (Echelard et al., 1993) and later found in the hypothalamus and ventral telencephalon (Rallu et al., 2002a). In *Shh* mutant mice the ventral telencephalon structures are absent and the expression of dorsal forebrain specific gene *Emx1* is detected throughout the telencephalon (Chiang et al., 1996). Interestingly, structural abnormalities and altered gene expression, observed in either *Gli3* or *Shh* mutant mice, are restored in *Shh/Gli3* double mutants (Rallu et al., 2002b) indicating that Shh suppresses the dorsalisation process by counteracting Gli3 rather than promoting ventral identity. Thus, Gli3 and Shh have an antagonising effect on each other and the interaction between Gli3 and Shh regulates the division of telencephalon into dorsal and ventral regions.

Another important regulator for the acquisition of ventral telencephalic fate in rodents is Fgf signalling. Expression of the ventral telencephalic marker *Nkx2.1* is greatly reduced in *Fgf8* mutant mice (Storm et al., 2006). Furthermore, double

mutation of Fgf receptors *Fgfr1* and *Fgfr2*, leads to the loss of *Nkx2.1*, *Mash1* and *Dlx2* expression. However, the expression of *Pax6* and *Emx2* is unaffected, indicating the loss of ventral telencephalic precursor cells (Gutin et al., 2006). Since the phenotype observed in *Fgfr1/Fgfr2* double mutants resembles that of *Shh* mutants, it is thought that Fgfs may act either downstream, or independently, of Shh. Indeed, it has been shown *Shh* expression is unaffected in *Fgfr1/Fgfr2* double mutants and the loss of *Gli3* does not rescue ventral telencephalic phenotypes in these mutants (Gutin et al., 2006), indicating that Fgf signalling acts downstream of Shh to determine ventral telencephalic identity.

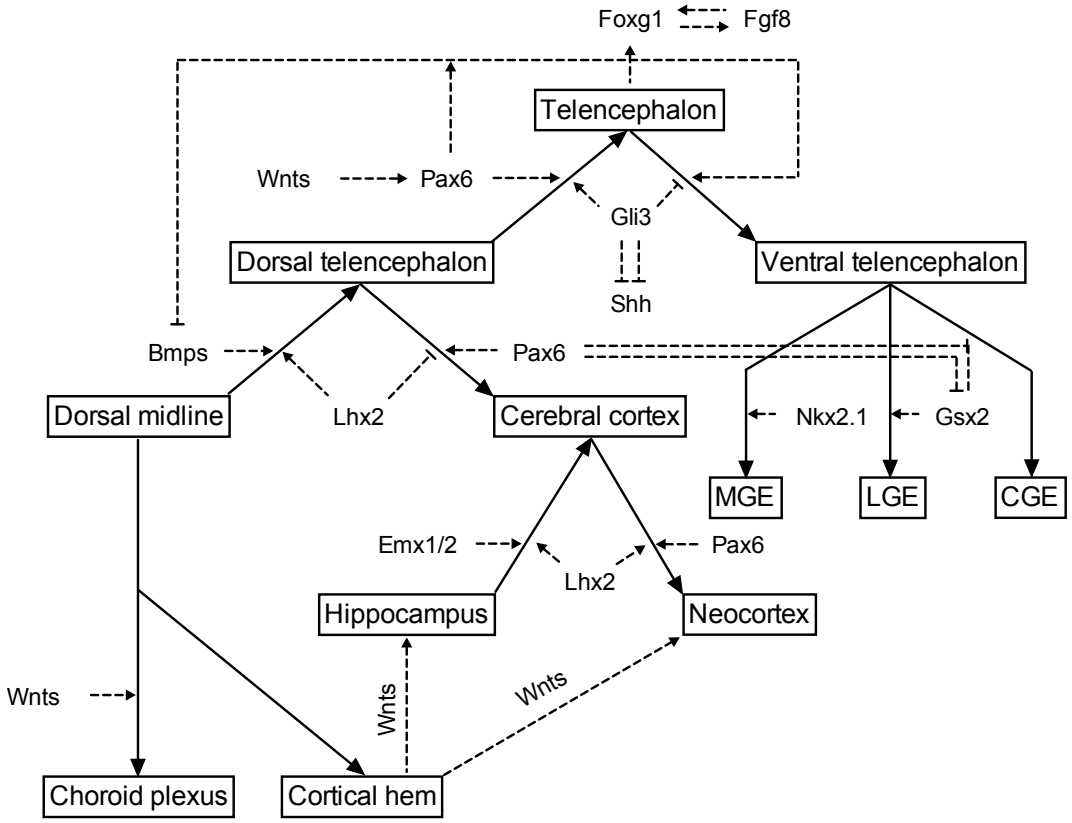

Figure 1.2: Regulation of regional patterning of the telencephalon. Transcription factors involved in the patterning and specification of the murine telencephalon. Foxg1 and Fgf signalling are essential for telencephalic identity. Dorsal telencephalic identity is driven by the activity of Gli3 and Foxg1. Structures derived from dorsal telencephalon then acquire their fate by an expression of Emx1/2, Lhx2 and Pax6. In parallel, Foxg1 and Fgf signalling collaborate with Shh to induce ventral telencephalic fate. The ventral telencephalon is then committed to MGE and LGE fates by the transcription factors Nkx2.1 and Gsx2, respectively. CGE, caudal ganglionic eminence; LGE, lateral ganglionic eminence; MGE, medial ganglionic eminence.

1.3.3 Development of the ventral telencephalon

The murine ventral telencephalon can be divided into three structures, the medial, lateral and caudal ganglionic eminences (MGE, LGE and CGE, respectively), and are born chronologically. The emergence of a transcription factor Nkx2.1 around E9.5 marks the appearance of the prospective MGE. This occurs just after Shh-mediated repression of Pax6 in the ventral area of the forebrain (Sousa and Fishell, 2010). Both Pax6 and Nkx2.1 play an important role in a formation of dorsal-ventral telencephalic boundary at this stage. In addition, expression of Nkx2.1 is implicated in the development of MGE derivatives. *Nkx2.1* mutants lack MGE derivatives such as the GP and cortical interneurons (Butt et al., 2008, Sussel et al., 1999).

At E10, the appearance of transcription factor Gsx2, marks the second eminence, the LGE, and the dorsal-ventral boundary is evident. The sharp boundary of pallial-subpallial telencephalon is now determined by expression of Pax6 and Gsx2 (Hebert and Fishell, 2008, Toresson et al., 2000). Similar to the role of Nkx2.1 in MGE specification, Gsx2 is essential for the expression of genes that are involved in the development of LGE derivatives including striatal neurons. *Gsx2*$^{-/-}$ mice show loss of expression of striatal progenitor genes such as *Dlx1* and *Dlx2* as well as a reduction of *Pre-pro-enkephalin* (*Penk*) and *Drd2* expression (Corbin et al., 2000). Ectopic expression of cortical-enriched genes in the LGE was also noted in *Gsx2* depleted mice (Corbin et al., 2000, Toresson et al., 2000).

The most caudal structure, the CGE, emerges from the ventral telencephalon around E11. Unlike MGE and LGE, the CGE does not have any known region-specific markers and its identity is defined anatomically, an area posterior to the fusion of the MGE and LGE (Nery et al., 2002). The ganglionic eminences generate progenitors contributing to various types of neurons, mainly projection neurons and interneurons, which will distribute throughout the forebrain. Table 1.4 shows the corresponding adult neuronal populations that derive from the ventral telencephalon.

It is widely accepted that Shh is the master regulator of the ventral telencephalon development. Shh was shown to induce Nkx2.1 expression in telencephalic explants of chick embryos (Ericson et al., 1995) and no Nkx2.1 expression was found in *Shh*$^{-/-}$ mice (Rallu et al., 2002b). Likewise, Gsx2 was absent from the forebrain of *Shh*$^{-/-}$ mice (Corbin et al., 2000). This indicates that Nkx2.1 and Gsx2 are both downstream of Shh. Despite its role as a morphogen in governing neuronal cell identity in the ventral telencephalon, Shh also acts as a mitogen. Study from the Fishell lab indicates that conditional knockout of *Shh* after ventral telencephalic patterning was established led to a reduction of progenitors in postnatal subventricular zone (Machold et al., 2003). All of the evidence here indicates that Shh regulates both the specification of the MGE and LGE as well as the proliferation of progenitors in these regions.

Table 1.4: Ganglionic eminences and their adult derivatives (Nery et al., 2002, Takahashi and Liu, 2006).

Embryonic ganglionic eminences	Adult derivatives
Medial ganglionic eminence	Pallidal projection neurons
	Cortical interneurons
	Hippocampal interneurons
Lateral ganglionic eminence	Striatal projection neurons
	Projection neurons in the nucleus accumbens
	Olfactory bulb interneurons
Caudal ganglionic eminence	Interneurons in layer V of neocortex
	Hippocampal neurons
	Neurons in the nucleus accumbens
	Bed nucleus of the stria terminalis
	Neurons in the amygdala
	Striatal neurons
	Pallidal neurons

1.3.4 Development of medium spiny neurons

MSNs derive from progenitor cells in the LGE. In rodents, neurogenesis in this area consists of two distinct temporal waves; early neurogenesis, occurring between E12-13, and late neurogenesis at E14-15 (Martynoga et al., 2005). Neural progenitors in early neurogenesis reside in the ventricular zone (VZ) of the LGE. Another area in the LGE, the subventricular zone (SVZ) is formed later by migrating progenitors from the VZ. The SVZ contains a group of progenitors for late neurogenesis. Early neurogenesis generates striatal neurons in the striosomes (van der Kooy and Fishell, 1987). In contrast, late neurogenesis contributes to matrix neurons (van der Kooy and Fishell, 1987). *In situ* hybridisation and immunohistochemistry studies have demonstrated that enkephalin-positive and substance P-positive MSNs were found in both striosomes and matrix (Graybiel and Chesselet, 1984, Gerfen and Young, 1988, Besson et al., 1990, Song and Harlan, 1994). In rodents, the percentage of pre-pro-enkephalin mRNA-expressing MSNs defined by *in situ* hybridisation in patch and matrix compartments was 65% and 58%, respectively (Gerfen and Young, 1988). These findings indicate that enkephalinergic MSNs are generated by both early and late neurogenesis in the LGE.

1.3.4.1 Roles of transcription factors in development of medium spiny neurons

It has been shown that the two waves of LGE neurogenesis are controlled by different transcriptional regulation (Figure 1.3). Early neurogenesis in the LGE is regulated by the transcription factor Mash1, a downstream target of Gsx2, via Notch signalling (Casarosa et al., 1999, Yun et al., 2002, Mason et al., 2005). Mash1 prevents premature differentiation of VZ cells into SVZ cells in the LGE. VZ cells within the LGE of *Mash1*$^{-/-}$ mice exhibited SVZ markers including *Gad1* (also known as *Gad67*) (Casarosa et al., 1999, Yun et al., 2002), *Dlx5* (Casarosa et al., 1999, Yun et al., 2002), *Dlx6* (Yun et al., 2002), *Brn4* (Yun et al., 2002) and *Six3* (Yun et al., 2002). In addition, expression of Notch ligands *Dll1* and *Dll3*, as well as Notch output gene *Hes5*, was completely lost in the LGE of *Mash1* mutants (Casarosa et al., 1999, Yun et al., 2002). A reduction in the number of early-born patch neurons is also observed in mice with a forebrain-specific *Notch1* deletion

(Mason et al., 2005). Interestingly, later-born matrix neurons were not affected in this mouse model, possibly due to compensation by *Notch3* expression (Mason et al., 2005). *Notch1* however, is not required for the differentiation of neurons once they exit the VZ since both striosomal and matrix neurons develop properly in mice that lack *Notch1* in *Dlx5/6*-postive post-mitotic neurons (Mason et al., 2005). Therefore, Mash1 controls the generation, but not the maturation, of patch neurons by regulating early neurogenesis within the LGE via Notch signalling.

The transcription factors Dlx1 and Dlx2 are the main regulators of late neurogenesis in the murine LGE. *Dlx1* and *Dlx2* are indistinguishably expressed in the VZ and SVZ of the LGE (Bulfone et al., 1993, Anderson et al., 1997). Anderson and colleagues have demonstrated that later-born neurons did not differentiate into mature MSNs in *Dlx1/2* double mutant mice (Anderson et al., 1997). These undifferentiated cells accumulated within the mutant LGE. In contrast, early-born striosomal neurons develop normally. This finding is consistent with the results from several studies which have identified Dlx1 and Dlx2 as the upstream factors that control the expression of late neurogenesis-related transcription factors such as Dlx5 (Anderson et al., 1997, Long et al., 2009), Dlx6 (Anderson et al., 1997, Long et al., 2009), Ikaros-1 (Martin-Ibanez et al., 2010, Long et al., 2009), Foxp1 (Long et al., 2009), Ebf1 (Long et al., 2009) and Arx (Long et al., 2009, Cobos et al., 2005). It should be noted, however, that LGE progenitors from *Dlx1/2* mutants are able to differentiate into Darpp32-positive neurons *in vitro*. This finding suggests that the block of differentiation observed *in vivo* might be a result of an inability of the progenitors to migrate from the SVZ to the developing striatum (Anderson et al., 1997). Interestingly, the transcription factor Arx, a downstream target of Dlx1/2, also plays an important role in the migration of late-born progenitor in the LGE. The phenotype of $Arx^{-/-}$ mice resembles that of *Dlx1/2* mutants; accumulation of progenitors within the SVZ of the LGE and MGE (Colombo et al., 2007). *In vitro* cultivation of these LGE progenitors, however, resulted in the proper differentiation towards mature neurons in which they express Darpp32 (Colombo et al., 2007).

Therefore, it is possible that Dlx1/2 mediates the migration of late-born progenitors to their final destination in the MZ via Arx.

Interaction between Mash1 and Dlx1/2 via Notch signalling has been shown in a study from the Rubenstein lab (Yun et al., 2002). Mash1 acts via Notch signalling to maintain the VZ identity and prevent transformation from VZ cells to SVZ cells (Casarosa et al., 1999, Yun et al., 2002). In contrast, *Dlx1/2* mutants showed ectopic expression of *Mash1*, *Dll1*, *Hes5* and *Notch1* in the SVZ of the LGE. This indicates that Dlx1 and Dlx2 suppress Notch signalling, perhaps through Mash1 repression, driving the differentiation of VZ cells into SVZ progenitors and promoting late neurogenesis within the LGE (Yun et al., 2002). Therefore, Mash1 and Dlx1/2 antagonistically control early and late neurogenesis in the LGE, respectively (Yun et al., 2002).

The function of the Dlx1 and Dlx2-dependent transcription factors in late neurogenesis in the LGE has been well described. *Dlx5* and *Dlx6* are expressed throughout the MGE and LGE. Their expression was found in SVZ and post-mitotic neurons of the mantle zone (MZ), suggesting their role in neuronal differentiation (Wang et al., 2011). Within the MGE, both Dlx5 and Dlx6 regulate the development of parvalbumin-positive cortical interneurons (Wang et al., 2010). In addition, another study demonstrated that ectopic expression of *Dlx5* induces the expression of *Gad65* (also known as *Gad2*), the key gene in GABAergic neuronal differentiation (Stuhmer et al., 2002). Recently, it has been shown that in the striatum of *Dlx6* mutants, the expression of *Dlx5*, Darpp32 and substance P is decreased while *Ikaros* expression is increased (Wang et al., 2011). Expression of D1R and D2R in the striatum of *Dlx6* mutants was, interestingly, identical to controls (Wang et al., 2011).

Foxp1 and Foxp2 are members of the forkhead/winged helix transcription factors. They are expressed in the striatum during development and, unlike most of striatal-specific transcription factors, their expression remains in the adult rodents (Tamura et al., 2004, Kelly et al., 2009). However, their expression pattern within the striatum is not identical. *Foxp1* was first detected in the MZ of the LGE around E14-

14.5 whilst expression of *Foxp2* was found earlier around E12.5-13 (Takahashi et al., 2003). *In situ* hybridisation revealed that *Foxp2* was co-expressed with the μ-opioid receptor, a marker for striatal patch neurons, but did not overlap with the expression of calbindin, a striatal matrix marker (Takahashi et al., 2003). The expression pattern of *Foxp1*, on the other hand, is controversial. Takahashi and colleagues were the first to show that *Foxp1* was expressed in both patch and matrix compartments (Takahashi et al., 2003). A contradictory finding was reported by Tamura and colleagues indicating that *Foxp1* expression was restricted to matrix neurons only (Tamura et al., 2004). Given that *Foxp1* expression was detected at E14, corresponding to the time of late neurogenesis in the LGE, *Foxp1* might be expressed in the later-born matrix neurons (Tamura et al., 2004). Consistent with this, *Foxp1* expression was greatly diminished in *Dlx1/2* mutants, which showed a defect in later-born matrix neurons (Long et al., 2009). *Foxp2*, in contrast, showed a subtle reduction of expression in *Dlx1/2*$^{-/-}$ mice (Long et al., 2009). Thus, Foxp1 may have a role in late neurogenesis within the developing striatum whereas Foxp2 is probably involved in early neurogenesis.

Amongst Dlx-dependent factors, Ikaros plays a critical role in the development of enkephalinergic striatopallidal MSNs. *Ikaros* expression is dependent on *Dlx1/2*, since *Dlx1/2*$^{-/-}$ mice exhibited a severe reduction of *Ikaros* expression (Long et al., 2009). *Ikaros* isoforms 1 and 2 have been shown to be regulators of enkephalinergic striatopallidal neurons differentiation (Agoston et al., 2007). Ikaros expression is found both proliferating and post-mitotic cells in the developing striatum and controls enkephalinergic fate by binding to the Ik-like cis-regulatory element on the *Penk* gene. Mutation in DNA-binding domain of *Ikaros* causes severe reduction in the amount of enkephalin-positive cells whereas the number of substance P-positive and dynorphin-positive neurons is unaffected (Agoston et al., 2007). The role of Ikaros in striatopallidal neurons development is also underscored by the study from Martin-Ibanez and colleagues. In addition to its role in enkephalinergic fate decision, they demonstrated that Ikaros isoform 1 (Ikaros-1) can induce cell cycle arrest via cyclin-dependent kinase inhibitors. This

then leads to transformation of proliferating progenitors into post-mitotic neurons (Martin-Ibanez et al., 2010). *Ikaros*$^{-/-}$ mice exhibit reduced striatal volume as a result of a decrease in the number of enkephalinergic MSNs within the matrix compartment. Furthermore, overexpression of *Ikaros-1* can increase the number of enkephalin-positive neurons in primary LGE cultures. These findings highlight the importance of Ikaros in enkephalinergic differentiation.

In contrast to Ikaros, the transcription factor Ebf1 is known for its role in controlling substance P-positive striatonigral neurons differentiation. Like other Dlx1/2-dependent transcription factors, *Ebf1* expression was reduced in *Dlx1/2* mutants (Long et al., 2009). Within the striatum, *Ebf1* is specifically expressed in the striatonigral MSNs (Lobo et al., 2006). Analysis of postnatal *Ebf1* mutant mice showed that the number of substance P-positive striatonigral MSNs is decreased when compared to wild type whereas no change is observed in the number of striatopallidal MSNs (Lobo et al., 2006).

Despite two different waves of neurogenesis, differentiation of both early- and late-born post-mitotic neurons into mature MSNs in rodents is commonly governed by the transcription factor Ctip2 (also known as Bcl11b). *Ctip2* is first detected at E12.5 in the post-mitotic neurons of the murine LGE and is continuously expressed in the developing striatum until animals reach their adulthood (Arlotta et al., 2005, Arlotta et al., 2008). Within the adult striatum, Ctip2 is exclusively expressed in MSNs but not in striatal interneurons (Arlotta et al., 2008). *Ctip2* knockout mice do not show any abnormality in the neurogenesis within the LGE, but rather exhibit abnormalities in MSN differentiation in both patch and matrix compartments of the striatum. Development of the patch compartment was predominantly affected whilst the matrix compartment displayed less abnormal differentiation (Arlotta et al., 2008). The expression of the mature MSN markers, Darpp32 and FOXP1, as well as the striatonigral specific gene *Chrm4*, was diminished (Arlotta et al., 2008). However, the expression pattern of striatopallidal-enriched genes such as *Penk*, *Adora2a* (encoding for the adenosine A2a receptor) and *Drd2* was not described. Interestingly, a study from Desplats and colleagues has

revealed that many striatal-enriched genes including *Ctip2* itself, *Ppp1r1b*, *Foxp2*, *Adora2a* and *Drd2* have a Ctip2 binding element within their promoter region (Desplats et al., 2008). Therefore, Ctip2 may direct MSN maturation by regulating the expression of striatal specific genes.

1.3.4.2 Roles of signalling molecules in development of medium spiny neurons

In addition to the striatal specific transcription factors, ligands of several cell-signalling pathways are also involved in the maturation of striatal neurons. Amongst these, retinoic acid (RA) and Bdnf are well described. Within the murine telencephalon, high levels of retinoids, produced from radial glia in the LGE as determined by high expression of cellular retinol binding protein I (Crbp I) are found in this area (Toresson et al., 1999). Generation of RA in the LGE is mediated by retinaldehyde dehydrogenase 3 (Raldh3), first detected around E12-12.5 (Li et al., 2000, Molotkova et al., 2007). In fact, the expression of Raldh3 is regulated by Gsx2 since *Gsx2*$^{-/-}$ mice have decreased expression of Raldh3 (Waclaw et al., 2004). This underscores the role of Gsx2 not only in the specification of LGE, but also in the regulation of retinoic acid signalling. Interestingly, a number of reports show that retinoic acid receptors (RARs) and retinoid X receptors (RXRs) are present in the striatum (Ruberte et al., 1993, Toresson et al., 1999). This implies that retinoic acid signalling might have a role in striatal neuronal development. Indeed, it has been shown that retinoic acid signalling regulates MSN maturation by enhancing Darpp32 expression, since LGE cultures treated with RA contain more Darpp32 neurons compared to controls (Toresson et al., 1999). RA activates Darpp32 expression, possibly via Rarβ1, since ectopic expression of Rarβ1 was able to up-regulate Darpp32 in cortical explant cultures (Liao and Liu, 2005). Moreover, it has been shown that retinoic acid signalling is essential for *Nolz1*-mediated neurogenesis. Nolz1, a Gsx2 downstream target, promotes cell cycle exit and neuronal differentiation of progenitor cells in the LGE (Urban et al., 2010). Additionally, the presence of RA is needed for the expression of *Meis2* (Oulad-Abdelghani et al., 1997), a downstream transcription factor of *Dlx1/2* (Long et al., 2009). *Meis2* is initially expressed at E12.5 in the LGE, but not the MGE, and its expression remains

through adulthood in the striatum, albeit at lower levels (Toresson et al., 1999). Although no functional analysis of this gene has been reported, it is known that, in adult striatum, *Meis2* has an expression pattern similar to that of the Darpp32 (Toresson et al., 1999). Therefore, Meis2 may also have a role in the development of striatal projection neurons in the striatum.

Activation of tropomyosin-related receptor kinase B (TrkB) through its ligand Bdnf is believed to modulate the differentiation of striatal MSNs. Analysis of *Bdnf* null mice revealed that both mRNA and protein levels of Darpp32 in the striatum were decreased when compared to wild type animals (Ivkovic et al., 1997). Likewise, administration of Bdnf to *in vitro* LGE cultures resulted in an increased number of Darpp32-positive neurons compared to untreated controls (Ivkovic et al., 1997, Ivkovic and Ehrlich, 1999). Interestingly, addition of neurotrophin-3 (NT-3) and/or neurotrophin-4/5 (NT-4/5) in LGE cultures also induced Darpp32 expression at a level comparable to Bdnf (Ivkovic and Ehrlich, 1999). This finding is not surprising because NT-4/5 binds specifically to TrkB (Chao, 2003) and NT-3 specifically to tropomyosin-related receptor kinase C (TrkC) that are expressed in the striatum (Escandón et al., 1994). However, NT-3 does not compensate for the loss of Bdnf *in vivo* due to temporal and spatial expression differences (Ivkovic and Ehrlich, 1999).

In addition to its roles in striatal maturation, Bdnf is also essential in trophic support to MSNs. It was previously believed that Bdnf was necessary for MSNs survival *in vivo*. The striatum does not produce Bdnf by itself but rather receives Bdnf produced from cortical neurons via anterograde transport through the corticospinal tract (Altar et al., 1997). Also, reduction in numbers of calbindin-positive MSN is found in *Bdnf* null mice (Altar et al., 1997). Interestingly, Baquet and colleagues reported similar finding. By using a mouse model in which Bdnf is deleted from cortical neurons, they showed that the number of striatal neurons was significantly reduced in aged mutant mice. They also observed, in the absence of Bdnf, a reduction in the size of MSNs and a decrease in dendritic spine density (Baquet et al., 2004). However, recent evidence suggests that this might not be the case. A publication from the Minichiello lab has suggested that Bdnf, through

activation of the TrkB receptor, is essential for the correct functioning of enkephalinergic striatopallidal MSNs, but is dispensable for long term survival of this neuronal population (Besusso et al., 2013). Indeed, conditional deletion of Bdnf from cortical neurons would lead to an alteration of cortical neuron morphology (Gorski et al., 2003), impairment of cortical input to the MSNs and, consequently, an increase in striatal vulnerability (Besusso et al., 2013). Recently, analysis of a Huntington's mouse model, the BACHD (Gray et al., 2008), in early symptomatic stage revealed that Bdnf mRNA and protein levels are unaltered. However, the downstream signalling of Bdnf-TrkB is impaired (Plotkin et al., 2014). Thus, abnormal transmission of Bdnf-TrkB signalling, rather than impaired Bdnf transport, might be a major pathophysiology in early stage Huntington's disease.

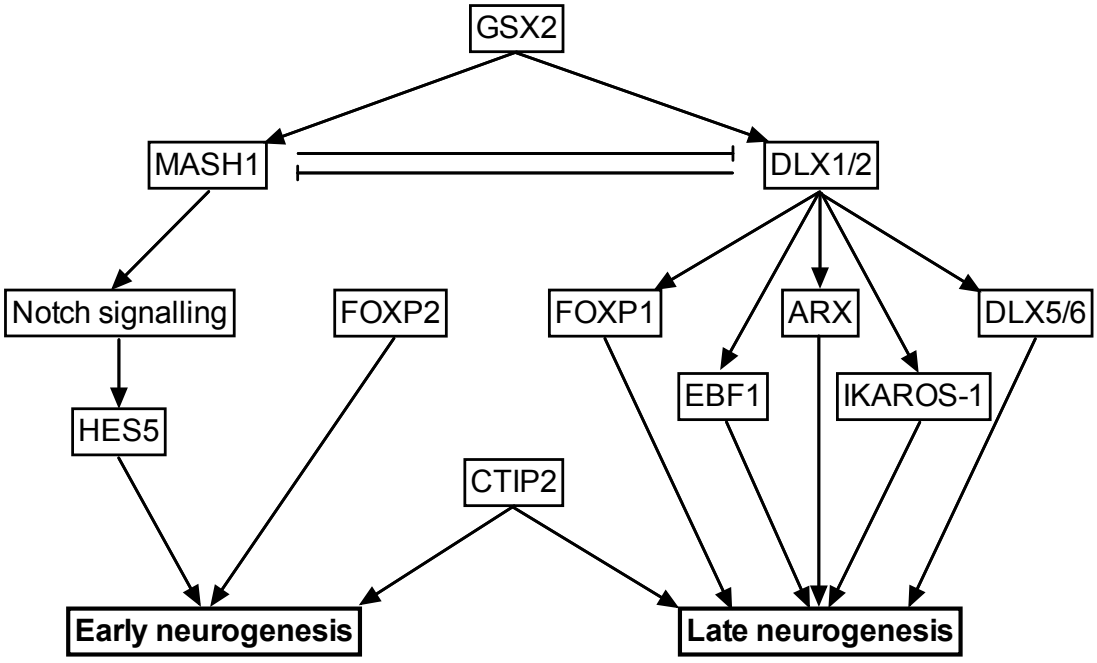

Figure 1.3 Transcriptional regulation of neurogenesis within the LGE. Two peaks of neurogenesis take place in the LGE. Early neurogenesis occurs between E12 and E13 and is mainly regulated by MASH1. In contrast, late neurogenesis starts around E14-15 and involves several transcription factors including DLX1/2 and their targets. E, embryonic day; LGE, lateral ganglionic eminence.

1.4 *In vitro* derivation of medium spiny neurons

There have already been several attempts to derive MSNs from various types of stem/progenitor cells. The generation of stem cell-derived MSNs would allow the modelling of basal ganglia disorders such as Huntington's disease *in vitro* (Carter and Chan, 2012, Perrier and Peschanski, 2012), but also to provide a novel source of striatal cells for transplantation (Kelly et al., 2009, Benraiss and Goldman, 2011, Perrier and Peschanski, 2012, Maucksch et al., 2013). The source of stem/progenitor cells commonly used for deriving striatal neurons in both rodents and human is pluripotent stem cells (PSCs), which may either be embryonic stem cells (ESCs) or induced pluripotent stem cells (iPSCs). The use of striatal neural stem cell lines (El-Akabawy et al., 2011) or primary striatal progenitors established from the LGE (Ivkovic and Ehrlich, 1999) have also been reported, although are less frequently used.

Several differentiation protocols for deriving MSNs from PSCs have been reported. These protocols basically mimic the normal development of ventral telencephalon by adding various ligands and/or inhibitors exogenously. Aubry and colleagues have shown that human embryonic stem cells (hESCs) could be converted to DARPP32-positive neurons (Figure 1.5 A) (Aubry et al., 2008). Initially, hESCs were co-cultured with a mitotically inactivated stromal cell line, MS5, for three weeks to generate neural rosettes. These were then transferred to polyornithine/laminin-coated culture dishes containing N2 medium supplemented with DKK1, SHH and BDNF (cells were re-plated 3-4 times). In the last re-plating step, cells were plated onto coated culture dishes containing N2 medium supplemented with BDNF, dbcAMP and valproic acid. The percentage of DARPP32-positive neurons and GABAergic neurons derived from this protocol after culturing for at least 62 days was approximately 53% and 36% of total neurons, respectively (Aubry et al., 2008). When the striatal progenitors derived from this protocol were transplanted into quinolinic acid-lesioned rat striata, however, the grafts expanded beyond the limit of the striatum. Further analysis of the grafts revealed the major cell types in the overgrowth were NESTIN-positive neural

progenitors and DARPP32-positive neurons. This protocol is, therefore, unlikely to be suitable for deriving clinical grade MSNs. This differentiation scheme may, however, be used for disease modelling providing that more detailed characterisation, such as electrophysiological studies, are performed.

Likewise, Zhang and colleagues used a similar approach to genearate DARPP32-positive neurons (Figure 1.5 B) (Zhang et al., 2010). They first converted human induced pluripotent stem cells (hiPSCs) derived from fibroblasts from a Huntington's disease patient (Park et al., 2008) into NESTIN-positive/SOX1-positive/PAX6-positive neural stem cells by embryoid body formation. Neural rosettes were picked and plated onto polyornithine/laminin-coated dishes containing neural proliferation medium supplemented with bFGF. These neural stem cells were then re-plated and cultured in the medium supplemented with DKK1, SHH, BDNF and Rho-associated kinase (ROCK) inhibitor (Y-26732) for 8-10 days. After that, cells were cultured in medium contained BDNF, cAMP, valproic acid and Y27632 for a further three days. DARPP32-positive/calbindin-positive MSNs comprised 10% of cells obtained with this protocol (Zhang et al., 2010), which is less than that described by Aubry and co-worker. Moreover, neither the molecular phenotype, nor the electrophysiological properties of the DARPP32-positive neurons obtained with this protocol, were fully characterised.

The Sasai group has developed a culture system known as quick-aggregation serum-free culture of embryoid body-like aggregates (SFEBq) to differentiate both mouse embryonic stem cells (mESCs) and hESCs into different types of telencephalic neurons (Watanabe et al., 2005, Eiraku et al., 2008, Danjo et al., 2011). Under these culture conditions a substantial number of neuronal cells generated had forebrain identity as determined by the induction of *Foxg1* expression. The telencephalic fate in SFEBq culture is mediated by a blockage of endogenous Wnt signalling by addition of the Wnt inhibitor Dkk1 into the culture medium (Watanabe et al., 2005). Addition of recombinant Shh at the concentration of 10 nM from day 3 to day 9 of differentiation into SFEBq resulted in an increase of Gsx2-positive cells within the Foxg1-positive forebrain progenitor population (Danjo et al., 2011).

Dosage of Shh, both endogenous and exogenous plays an important role in forebrain patterning, since treatment with the Shh inhibitor cyclopamine led to an increase of Pax6-positive dorsal forebrain progenitor whereas the number of Gsx2-positive LGE progenitors was diminished. Excess Shh signalling stimulation, either by higher Shh concentration or a more potent Shh agonist (Smoothened agonist or SAG), however, drives cells into the MGE lineage as determined by the higher proportion of Nkx2.1-positive cells but a reduced number of Gsx2-positive cells in the culture. Use of SFEBq culture with addition of 10 nM SHH between day 3 and day 9, combined with FACS-sorting of telencephalic cells at day 9, demonstrated that at day 35 of differentiation approximately 50% of the FACS-sorted Foxg1::venus-positive neurons were DARPP32-positive (Figure 1.5 C) (Danjo et al., 2011). These Darpp32-positive neuronal cells also expressed Ctip2 and Gad67, consistent with their *in vivo* counterpart.

Shin and colleagues have described the use of a feeder-free, serum-free adherent culture technique to derive Darpp32-positive MSNs (Figure 1.4 A) (Shin et al., 2011). They initially compared whether three different neural differentiation methods, the embryoid body formation (Bain et al., 1995), the five stage method (Okabe et al., 1996, Lee et al., 2000) and the monolayer culturing (Ying et al., 2003) were equally efficient in terms of GABAergic neuron generation. Analyses showed that all methods yielded similar amount of GABAergic cells ranging between 27-33% of the total cells (Shin et al., 2011). This was the first study to show that the number of GABAergic cells in the serum-free monolayer culture is comparable to that of the other two methods. Due to the fact that the monolayer culture is relatively simpler than others and contains no serum, it has been considered as a potential method for MSN derivation. Indeed, after twenty-one days of differentiation, one third of GABAergic neurons derived from this method were Darpp32-positive (Shin et al., 2011). Interestingly, the electrical properties of the mESC-derived neurons generated with this method showed the presence of active sodium and potassium channels, an ability to fire repetitive action potentials, and membrane properties, some of which were similar to those of rat E15 LGE neurons in primary cultures.

Hence, for the first time and by using the monolayer culture, this study showed that mESC-derived neurons were functionally active. However, it is not clear whether the patched neurons were actually MSNs since post-patching staining for MSN marker was not performed.

A study from Ma and colleagues has demonstrated that DARPP32-positive MSNs could be generated from hESC by using adherent cultures supplemented with SHH (Figure 1.4 B) (Ma et al., 2012). Consistent to what has been reported in Danjo et al., different concentrations of exogenous SHH regulates dorsal-ventral patterning of the telencephalic cells (Danjo et al., 2011, Ma et al., 2012). Addition of 200 ng/mL recombinant SHH to the cultures between day 12 and 18 of differentiation led to a robust induction of DARPP32 expression in hESC-derived GABAergic neurons (89% of GABAergic neurons expressed DARPP32). In contrast, high doses of SHH (e.g. 500 ng/mL) reduced the expression of the LGE-specific marker *GSX2* whilst the expression of MGE progenitor marker *NKX2.1* was dramatically increased. GABAergic neurons derived from this protocol shown to be capable of producing action potentials. Transplantation of LGE-like progenitors derived from this protocol into quinolinic acid-lesioned striata of severe combined immunodeficiency (SCID) mice resulted in the repopulation of DARPP32-positive GABAergic neurons from the graft within the lesioned striatum. Interestingly, motor deficits resulting from destruction of the striatum by quinolinic acid were restored four months after the transplantation of LGE-like progenitors (Ma et al., 2012). Although the quinolinic acid-lesioned model does not completely recapitulate the pathology of Huntington's disease, this study is the first to show a recovery of motor function upon transplantation of ESC-derived striatal-committed progenitors into the striatum.

Another study about MSN derivation from human pluripotent stem cells (hPSCs) has recently been reported by Delli Carri and colleagues (Figure 1.5 D) (Delli Carri et al., 2013a, Delli Carri et al., 2013b). Neural induction in this study was performed by the dual inhibition of SMAD signalling by Noggin and SB431542 (Chambers et al., 2009). Then at day 5 of differentiation, the ventral telencephalic fate was modulated by addition of recombinant DKK1 and SHH for 3 weeks.

Neuronal cells were maintained for at least 80 days in the N2 medium supplemented with B27 and BDNF. The presence of DKK1 and SHH induced the ventral telencephalic fate as determined by a reduction of *EMX2/NKX2.1* expression ratio. Under these conditions they found that approximately 20% of MAP2ab-positive neurons were also DARPP32-positive at day 80 of differentiation. Although the number of DARPP32-positive neurons is considerably lower than that has been reported in previous studies (e.g. Aubry et al. and Ma et al.), this study is the first to show a detailed characterisation of striatal markers such as CTIP2, FOXP1, FOXP2, *DRD1*, D2R and A2a receptor in PSC-derived MSNs (Delli Carri et al., 2013b). Electrophysiological studies demonstrated that the DARPP32-positive MSNs derived with this protocol could fire repetitive action potentials and exhibit the onset delay in the generation of the first spike, a characteristic electrical property of mature MSNs (Delli Carri et al., 2013b). Transplantation of cells cultured for 38 days into the striatum of quinolinic acid-lesioned rats showed integration of nerve fibres from the graft into the host striatum. DARPP32 as well as FOXP1 and FOXP2 expression patterns were also detected within the graft. More importantly, transplanted animals exhibited an enhanced performance in apomorphine-induced rotation tests compared to controls (Delli Carri et al., 2013b). Therefore, this study demonstrated not only the generation of PSC-derived MSNs, but also showed the most comprehensive characterisation of PSC-derived MSNs, replicating molecular, electrophysiological and functional properties observed *in vivo*.

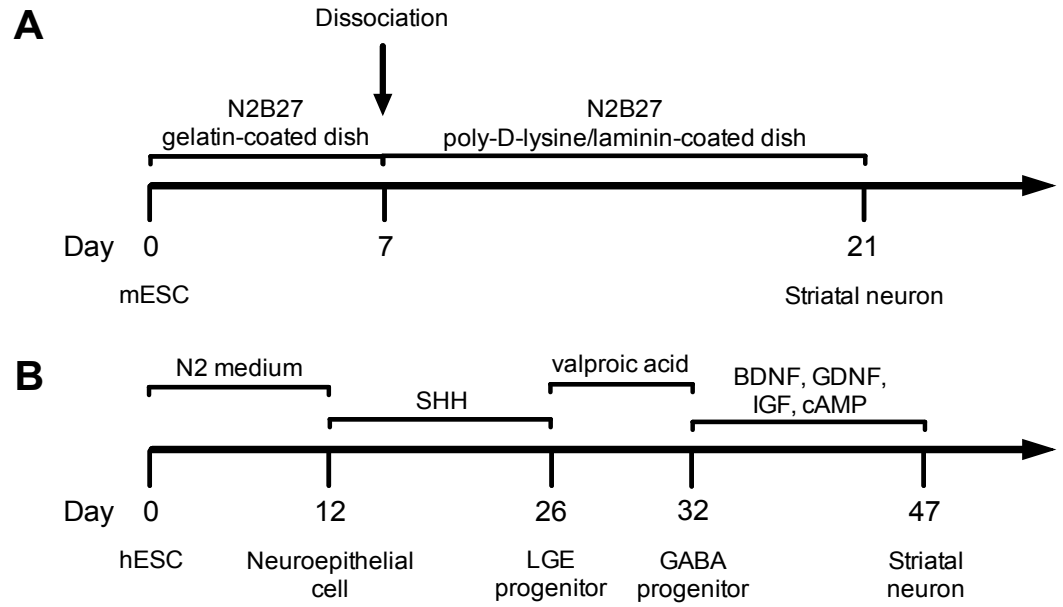

Figure 1.4 Schematic diagram of the published differentiation protocol used for deriving the MSNs. (A) From Shin et al., 2011. **(B)** From Ma et al., 2012. mESC, mouse embryonic stem cell; hESC, human embryonic stem cell; BDNF, brain-derived neurotrophic factor; cAMP, cyclic adenosine monophosphate; GABA, gamma-aminobutyric acid; GDNF, glial cell line-derived neurotrophic factor; IGF, insulin-like growth factor; LGE, lateral ganglionic eminence.

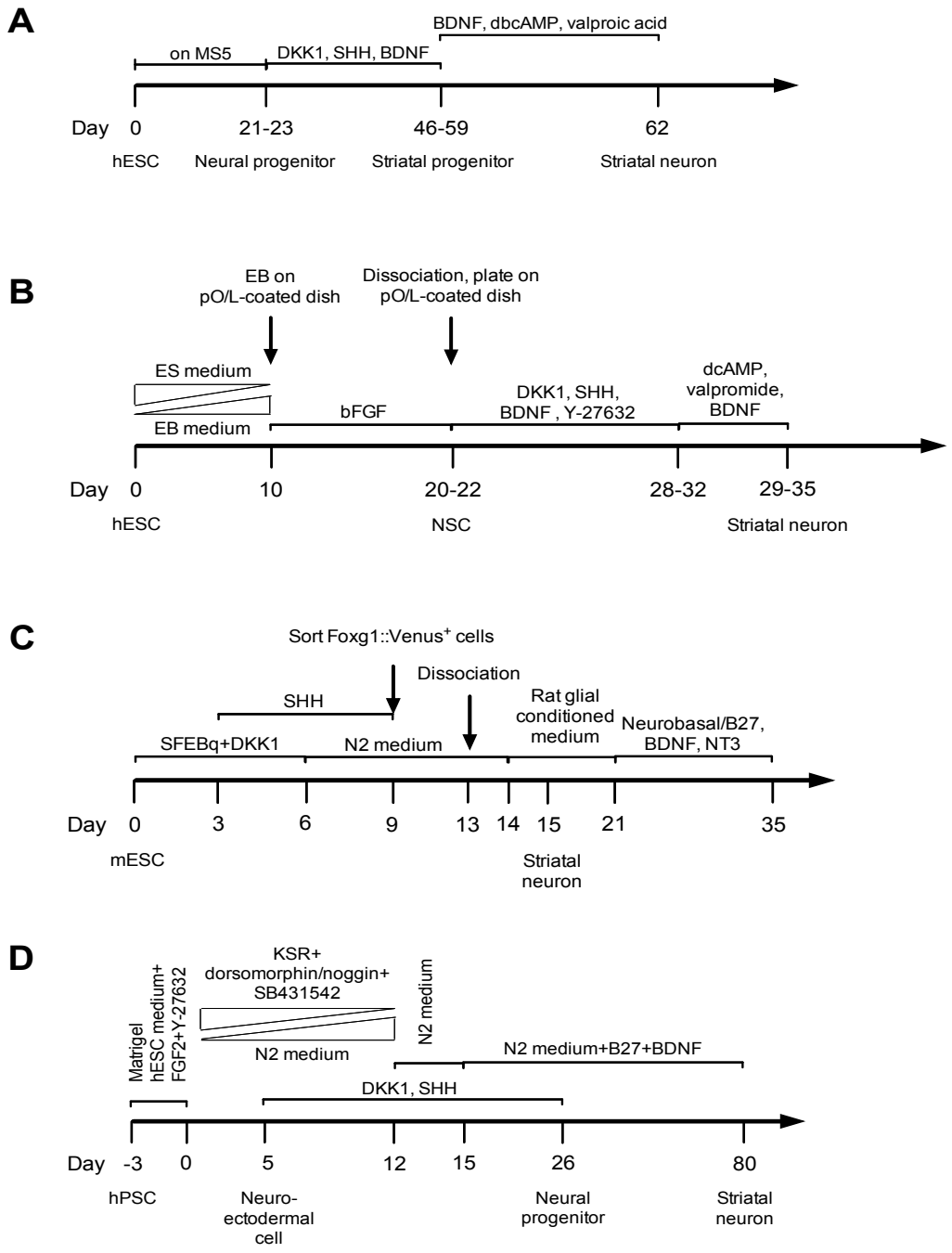

Figure 1.5 Schematic diagram of the published differentiation protocols used DKK1, SHH and BDNF to derive the MSNs. (A) From Aubry et al., 2008. **(B)** From Zhang et al., 2010. **(C)** From Danjo et al., 2011. **(D)** From Delli Carri et al., 2013a and 2013 b. BDNF, brain-derived neurotrophic factor; dbcAMP, dibutyryl-cyclic adenosine monophosphate; EB, embryoid body; hESC, human embryonic stem cell; hPSC, human pluripotent stem cell; KSR, KnockOut™ serum replacement; mESC, mouse embryonic stem cell; NT3, neurotrophin-3; SFEBq, quick-aggregation serum-free culture of embryoid body-like aggregates.

1.5 Aim of the project

Despite the presence of MSN markers including DARPP32 in neuronal cells derived from published *in vitro* differentiation protocols (Aubry et al., 2008, Zhang et al., 2010, Danjo et al., 2011, Shin et al., 2011, Ma et al., 2012, Delli Carri et al., 2013b), the phenotype of MSN subtypes has not been fully characterised. No study so far has demonstrated whether the DARPP32-positive neurons expressed enkephalin or substance P, the two major markers for striatopallidal and striatonigral MSNs, respectively. Although the MSN derived from Delli Carri's protocol exhibited expression of dopamine receptor D1 and D2 as well as adenosine receptor A2a, it was not clear whether they expressed either substance P or enkephalin. The presence of substance P and/or enkephalin in these neurons is essential for the classification of MSN subtypes since the most vulnerable neuronal population in Huntington's disease is identified by enkephalin expression (Reiner et al., 1988), not dopamine receptor D2 or adenosine receptor A2a.

The aim of this thesis, therefore, was to generate one of the MSN subtypes, the enkephalinergic striatopallidal MSNs, from mESCs. We first have generated an enkephalinergic reporter ESC line that allows the expression of enhanced yellow fluorescent protein (EYFP) when the Cre-recombinase is specifically expressed in enkephalin-producing neurons. This reporter line would be useful not only for monitoring enkephalinergic expression during the differentiation, but also to provide a precise marker, which could be used for further analyses/characterisations of the enkephalinergic population within the culture. Using this reporter ESC line, we have optimised a differentiation protocol to derive enkephalinergic MSNs. Further characterisation has revealed the unexpected role of WNT and SHH signalling in the regulation of enkephalin expression. The enkephalinergic MSNs derived from our protocol are electrophysiologically active and exhibit the electrical hallmark of MSNs. Our findings could be used for deriving enkephalinergic MSNs for *in vitro* modelling of Huntington's disease.

Chapter 2: Materials and methods

2.1 Materials

2.1.1 Chemicals

Table 2.1: Chemicals used in this study.

Chemical	Formula	Catalogue number	Manufacturer
Agarose		A9539-500G	Sigma-Aldrich
Ammonium chloride	NH_4Cl	A0171	Sigma-Aldrich
Buffer solution pH4.0 (20°C)		33665-500ML	Fluka
Buffer solution pH7.0 (20°C)		33666-500ML	Fluka
Buffer solution pH10.0 (20°C)		33668-500ML	Fluka
Citric acid monohydrate	$C_6H_8O_7.H_2O$	C1909-25G	Sigma-Aldrich
4′,6-diamidino-2-phenylindole (DAPI)	$C_{22}H_{27}N_5O_6$	D3571	Molecular Probes
Dimethyl sulfoxide (DMSO)	C_2H_6OS	34869-100ML	Sigma-Aldrich
Ethanol (EtOH)	C_2H_6O	20821.330	vWR
Ethidium bromide	$C_{21}H_{20}BrN_3$	E1510-10ML	Sigma-Aldrich
Ethylenedinitrilotetraacetic acid (EDTA) disodium salt dihydrate	$C_{10}H_{14}N_2Na_2O_8.2H_2O$	1084211000	Merck Millipore

Gelatin, from cold water fish skin		G7765-250ML	Sigma-Aldrich
Glycerol	$C_3H_8O_3$	G/0650/08	Fisher Scientific
Glycine	$C_2H_5NO_2$	G/0800/60	Fisher Scientific
Hydrogen peroxide solution (≥30%)	H_2O_2	95321	Fluka
Isopentane (2-methylbutane)	C_5H_{12}	M32631-500ML	Sigma-Aldrich
Isopropanol	C_3H_8O	20842.330	vWR
2-mercaptoethanol (2-ME)	C_2H_6OS	M6250-100ML	Sigma-Aldrich
Paraformaldehyde (PFA)	$OH(CH_2O)_nH$ (n=8-100)	P6148-1KG	Sigma-Aldrich
Phosphate buffered saline (PBS) tablet		P4417-50TAB	Sigma-Aldrich
Sodium azide	NaN_3	S8032-25G	Sigma-Aldrich
Sodium citrate tribasic dihydrate	$C_6H_5Na_3O_7.2H_2O$	C8532-1KG	Sigma-Aldrich
Sodium hydroxide	NaOH	S5881-500G	Sigma-Aldrich
Sodium pentobarbital	$C_{11}H_{17}N_2NaO_3$	P3761-5G	Sigma-Aldrich
Sodium phosphate dibasic dihydrate	$Na_2HPO_4.2H_2O$	71643-1KG	Sigma-Aldrich
Sodium phosphate monobasic monohydrate	$NaH_2PO_4.H2O$	A429146347	Merck

Tris base	$(CH_2OH)_3CNH_2$	BP152-1	Fisher Scientific
Triton X-100	$C_{14}H_{22}O(C_2H_4O)_n$ (n=9-10)	T8787-250ML	Sigma-Aldrich
Tween 20	$C_{58}H_{114}O_{26}$	P1379-500ML	Sigma-Aldrich

2.1.2 Solutions

Cell blocking buffer 10% normal goat serum, 0.3% TritonX-100, 0.2% sodium azide in PBS

Phosphate buffer (PB) 100 mM PB, pH 7.4 (7.74% of 1 M Na_2HPO_4, 2.26% of 1 M NaH_2PO_4)

4% paraformaldehyde 40 g paraformaldehyde in PB, pH 7.4

Quenching solution 0.1 M glycine, 0.1 M NH_4Cl in PBS

TB 50 mM Tris, pH 8.3

10x TBE 890 mM Tris, 890 mM boric acid, 20 mM EDTA, pH 8.3

TBS 50 mM Tris, 150 mM NaCl, pH 7.5

Tissue blocking buffer 1 10% normal goat serum, 0.3% carrageen, 0.5% TritonX-100, 0.2% sodium azide in TBS

Tissue blocking buffer 2 10% normal goat serum, 0.3% TritonX-100, 0.2% sodium azide in TBS

2.1.3 Reagents

Table 2.2: Reagents used in this study.

Reagent	Catalogue number	Manufacturer
DirectPCR lysis reagent (mouse tail)	102-T	Viagen Biotech
KAPA™ universal ladder	KK6303	Kapa Biosystems
LightCycler® 480 Probes Master	04887301001	Roche
$MgCl_2$ solution (25 mM) for PCR	M8787	Sigma-Aldrich
Normal goat serum	S-1000	Vector labs
OCT mounting media	361603E	VWR
Orange G	O3756-100G	Sigma-Aldrich
Proteinase K, recombinant, PCR grade	03115844001	Roche
SIGMA*FAST*™ 3,3'-diaminobenzidine tablets	D4168-5SET	Sigma-Aldrich
Taq DNA polymerase (from *Thermus aquaticus*) with 10x PCR reaction buffer containing $MgCl_2$	D1806-20X250UN	Sigma-Aldrich
Trizol® reagent	15596-018	Ambion
Universal ProbeLibrary Probe 1	04684974001	Roche
Universal ProbeLibrary Probe 5	04685024001	Roche
Universal ProbeLibrary Probe 11	04685105001	Roche

Universal ProbeLibrary Probe 13	04685121001	Roche
Universal ProbeLibrary Probe 17	04686900001	Roche
Universal ProbeLibrary Probe 26	04687574001	Roche
Universal ProbeLibrary Probe 27	04687582001	Roche
Universal ProbeLibrary Probe 32	04687655001	Roche
Universal ProbeLibrary Probe 34	04687671001	Roche
Universal ProbeLibrary Probe 38	04687965001	Roche
Universal ProbeLibrary Probe 40	04687990001	Roche
Universal ProbeLibrary Probe 41	04688007001	Roche
Universal ProbeLibrary Probe 47	04688074001	Roche
Universal ProbeLibrary Probe 56	04688538001	Roche
Universal ProbeLibrary Probe 60	04688589001	Roche
Universal ProbeLibrary Probe 67	04688660001	Roche
Universal ProbeLibrary Probe 75	04688988001	Roche
Universal ProbeLibrary Probe 78	04689011001	Roche
Universal ProbeLibrary Probe 89	04689143001	Roche
Universal ProbeLibrary Probe 95	04692128001	Roche
Universal ProbeLibrary Probe 97	04692144001	Roche
Universal ProbeLibrary Probe 98	04692152001	Roche
Universal ProbeLibrary Probe 100	04692187001	Roche

Universal ProbeLibrary Probe 102	04692209001	Roche
Universal ProbeLibrary Probe 104	04692225001	Roche
Universal ProbeLibrary Probe 110	04692306001	Roche
Vectamount™ mounting medium	H-5000	Vector Laboratories
Vectashield® mounting medium	H-1000	Vector Laboratories

2.1.4 Kits

Table 2.3: Kits used in this study.

Kit	Catalogue number	Manufacturer
MycoAlert™ mycoplasma detection kit	LT07-118	Lonza
MycoAlert™ assay control set	LT07-518	Lonza
Ready-To-Go T-primed first-strand kit	27-9263-01	Amersham
RNeasy® mini kit	74106	Qiagen
RNase-free DNase set	79254	Qiagen
SuperScript® VILO™ cDNA synthesis kit	11754-250	Invitrogen
Vectastain® ABC kit (standard)	PK-4000	Vector Laboratories

2.1.5 Primers

Table 2.4: qRT-PCR primers used in this study.

Gene*	Forward primer	Reverse primer	UPL probe	Amplicon size (bp)
Actb (β-actin)	AAG GCC AAC CGT GAA AAG AT	GTG GTA CGA CCA GAG GCA TAC	56	110
Adora2a (adenosine A2a receptor)	GGT CCT CAC GCA GAG TTC C	TCA CCA AGC CAT TGT ACC G	41	95
Cd24a (CD24)	CTT CTG GCA CTG CTC CTA CC	TGG TGG TAG CGT TAC TTG GA	60	112
Ctip2	TGG ATG CCA GTG TGA GTT GT	GCT GCT GCA TGT TGT GC	97	68
Dkk1	TGG TTG GTG CTT TTG CCT A	GAC CTG AGT TCA TGG GCA TC	75	71
Dlx1	CCG GAG GTT CCA ACA AAC T	TCT GGA ACC ATA TCT TGA CCT G	13	101
Dlx2	GCC TCA CCC AAA CTC AGG T	AGG CAC AAG GAG GAG AAG C	1	126
Drd1a (dopamine D1 receptor)	TGT TTG AAA TGT TTA CAA GGT GTT C	CAG TCA GCC CTT CCT TCA GT	38	74
Drd2 (dopamine D2 receptor)	TGA ACA GGC GGA GAA TGG	CTG GTG CTT GAC AGC ATC TC	17	70
EYFP	GAA GCG CGA TCA	CCA TGC CGA GAG	67	62

	CAT GGT	TGA TCC		
Foxg1	GAA GGC CTC CAC AGA ACG	CAA GGC ATG TAG CAA AAG AGC	26	114
Foxp1	CTG CAC ACC TCT CAA TGC AG	GGA AGC GGT AGT GTA CAG AGG T	102	73
Foxp2	ACA TCG ACA GCA ATG GGA AC	CTT CCT TGA CAT GGA TTG AATG	5	75
Gad1	ATA CAA CCT TTG GCT GCA TGT	TTC CGG GAC ATG AGC AGT	27	60
Gata6	GGT CTC TAC AGC AAG ATG AAT GG	TGG CAC AGG ACA GTC CAA G	40	94
Gfap	TCG AGA TCG CCA CCT ACA G	GTC TGT ACA GGA ATG GTG ATG C	67	67
Gsx2	GTC GGA CCC ACG GAG ATT	TTT TGC CAT TGG GTA CCT G	34	71
Nanog	TTC TTG CTT ACA AGG GTC TGC	AGA GGA AGG GCG AGG AGA	110	67
Ncam1	AGT TCA AGA CAC AGC CAG TCC	GAT GGA GTT CCC GTC CTC T	11	77
Nes	TCC CTT AGT CTG GAA GTG GCT A	GGT GTC TGC AAG CGA GAG TT	67	68
Nkx2.1	AAA ACT GCG GGG ATC TGA G	TGC TTT GGA CTC ATC GAC AT	95	144
Ntrk2 (TrkB)	AAA GCA ATC GGG AGC ATC T	CCA ACT TGA GCA GGA GCA AC	40	96

Pax6	GTT CCC TGT CCT GTG GAC TC	ACC GCC CTT GGT TAA AGT CT	78	61
Penk	CCC AGG CGA CAT CAA TTT	TCT CCC AGA TTT TGA AAG AAG G	47	74
Rbfox3 (NeuN)	AAG AAG CCT GGG AAC CCA TA	GGC CCA TAG ACT GTT CCT ACC	11	68
Plp1	TCA GAG TGC CAA AGA CAT GG	CAG AAC AGT GCC ACT CCA AA	49	114
Oct4	ATT GGA GAA GGT GGA ACC AA	CTC CTT CTG CAG GGC TTT C	95	61
Pax6	GTT CCC TGT CCT GTG GAC TC	ACC GCC CTT GGT TAA AGT CT	78	61
Ppp1r1b (DARPP32)	CCA CCC AAA GTC GAA GAG AC	GCT AAT GGT CTG CAG GTG CT	98	82
Shh	CCA ATT ACA ACC CCG ACA TC	GCA TTT AAC TTG TCT TTG CAC CT	32	91
Sox1	GTG ACA TCT GCC CCC ATC	GAG GCC AGT CTG GTG TCA G	60	60
T Brachyury	CAG CCC ACC TAC TGG CTC TA	GAG CCT GGG GTG ATG GTA	100	72
Tac1	AAG CCT CAG CAG TTC TTT GG	TCT GGC CAT GTC CAT AAA GA	89	100
Tbp	GGC GGT TTG GCT AGG TTT	GGG TTA TCT TCA CAC ACC ATG A	107	83
Tubb3	GCG CAT CAG CGT	TTC CAA GTC CAC	104	73

(βIII-tubulin)	ATA CTA CAA	CAG AAT GG

*Where the gene and protein names differ, the protein name has also been added.

2.1.6 Primary antibodies

Table 2.5: Primary antibodies used in this study.

Antibody	Isotype	Dilution	Catalogue number	Manufacturer
βIII-tubulin (clone TuJ-1)	Mouse IgG_{2a}	1:1,000	MAB1195	R&D Systems
CD133 (clone13A4, biotin conjugated)	Rat IgG1, κ	1:300	13-1331-82	eBioscience
CD24 (clone M1/69, PE-Cy7 conjugated)	Rat IgG2b, κ	1:600	101822	BioLegend
Ctip2	Rat IgG	1:500	ab18465	Abcam
DARPP32	Rabbit IgG	1:500	AB10518	Millipore
GABA	Rabbit IgG	1:1,000	A2052	Sigma-Aldrich
GFAP	Rabbit IgG	1:500	Z0334	Dako
GFP	Chicken IgY	1:1,000	ab13970	Abcam
Nestin	Mouse IgG_1	1:50	Rat-401	DSHB
Oct-3/4	Mouse IgG_{2b}	1:200	sc-5279	Santa-Cruz
Pax6	Mouse $IgG_{1κ}$	1:500	PAX6	DSHB
Pre-pro enkephalin	Rabbit IgG	1:200	RA14124	Neuromics
Pre-pro enkephalin	Rabbit IgG	1:5,000	LS-C23084	Lifespan Biosciences

2.1.7 Secondary antibodies

Table 2.6: Secondary antibodies used in this study.

Antibody	Dilution	Catalogue number	Manufacturer
Alexa Fluor® 350 goat anti-mouse IgG (H+L)	1:500	A-11045	Molecular Probes
Alexa Fluor® 488 goat anti-chicken IgG (H+L)	1:1,000	A-11039	Molecular Probes
Alexa Fluor® 488 goat anti-mouse IgG (H+L)	1:1,000	A-11001	Molecular Probes
Alexa Fluor® 488 goat anti-mouse IgG_1	1:1,000	A-21121	Molecular Probes
Alexa Fluor® 488 goat anti-mouse IgG_{2b}	1:1,000	A-21141	Molecular Probes
Alexa Fluor® 488 goat anti-rabbit IgG (H+L)	1:1,000	A-11008	Molecular Probes
Alexa Fluor® 555 goat anti-mouse IgG (H+L)	1:1,000	A-21422	Molecular Probes
Alexa Fluor® 555 goat anti-rabbit IgG (H+L)	1:1,000	A-21428	Molecular Probes
Alexa Fluor® 555 goat anti-rat IgG (H+L)	1:1,000	A-21434	Molecular Probes
Alexa Fluor® 568 goat anti-mouse IgG_{2a}	1:1,000	A-21134	Molecular Probes

2.1.8 Culture media, supplements and dissociation reagents

Table 2.7: Culture media, supplements and dissociation reagents used.

Medium/supplement/dissociation reagent	Size	Catalogue number	Manufacturer
B27® supplement	10 mL	17504-044	Gibco
B27® supplement minus vitamin A	10 mL	12587-010	Gibco
Bovine serum albumin fraction V	100 g	K41-001P	PAA
Chicken serum	100 mL	C5405-100ML	Sigma-Aldrich
DMEM/F12 without L-glutamine	500 mL	21331-020	Gibco
DPBS without Calcium and Magnesium	100 mL	D8537-100ML	Sigma-Aldrich
Foetal bovine serum (batch number: 41G8502K)	500 mL	10270-106	Gibco
Gelatin (from porcine skin)	100 g	G1890-100G	Sigma-Aldrich
Glasgow Minimum Essential Medium (GMEM) with sodium bicarbonate, without L-glutamine	500 mL	G5154-500ML	Sigma-Aldrich
Laminin (from Engelbreth-Holm-Swarm murine sarcoma), 1 mg/mL	1 mg	L2020-1MG	Sigma-Aldrich
L-glutamine, 200 mM	100 mL	25030-024	Gibco
Lif	550 µL	NA	ISCR tissue culture facility
MEM non-essential amino acids	100 mL	11140-035	Gibco

2-mercaptoethanol	100 mL	M6250-100ML	Sigma-Aldrich
NDiff® N2 neuronal supplement	5 mL	SF-NS-01-005	StemCells Inc
Neurobasal® medium	500 mL	21103-049	Gibco
PBS, pH 7.4	500 mL	10010-015	Gibco
Penicillin/Streptomycin (10,000 U/mL)	100 mL	15140-122	Gibco
0.01% poly-L-ornithine solution	50 mL	P4957-50ML	Sigma-Aldrich
Purmorphamine	5 mg	540220-5MG	Calbiochem
Recombinant human BDNF	100 µg	450-02	Peprotech
Recombinant human BDNF	5 µg	248-BD-005	R&D systems
	25 µg	248-BD-025	
Recombinant human DKK1	10 µg	5439-DK	R&D systems
Recombinant mouse Shh N-terminus, C25II substitution	25 µg	464-SH-025	R&D systems
Sodium pyruvate, 100 mM	100 mL	11260-039	Gibco
StemPro® Accutase® cell dissociation reagent	100 mL	A11105-01	Gibco
TrypLE™ express with phenol red	100 mL	12605-010	Gibco
2.5% trypsin	100 mL	15090-046	Gibco
Y-27632 dihydrochloride	10 mg	ab120129	Abcam
Y-27632 dihydrochloride	1 mg	688000-1MG	Calbiochem

Medium/reagent preparation

mESC medium Glasgow minimum essential medium supplemented with

- Foetal bovine serum (10% v/v final concentration)
- 1 mM sodium pyruvate
- 2 mM L-glutamine
- 1x MEM non-essential amino acid
- 0.1 mM 2-mercaptoethanol
- 1,000 U Lif

Differentiation medium* Glasgow minimum essential medium supplemented with

- 10% foetal bovine serum
- 1 mM sodium pyruvate
- 2 mM L-glutamine
- 1x MEM non-essential amino acid
- 0.1 mM 2-mercaptoethanol
- 10 μM Y-27632 dihydrochloride

N2B27 medium	98 mL Neurobasal® medium and 100 mL DMEM/F12 medium supplemented with - 2 mL B27® supplement - 1 mL NDiff® N2 neuronal supplement - 1 mM L-glutamine - 0.1 mM 2-mercaptoethanol
NB medium**	N2B27 medium supplemented with 10 μM Y-27632 dihydrochloride
0.025% trypsin-EDTA	0.025% trypsin, 1 mM EDTA, 1% chick serum in PBS
1% gelatin	1% porcine gelatin in sterile filtered H_2O

* Differentiation medium is used in the first day of NB and NB+3F differentiation protocols.

** NB medium is used from the second day onwards of NB and NB+3F differentiation protocols.

2.1.9 Consumables

Table 2.8: Consumables used in this study.

Consumable	Catalogue number	Manufacturer
Falcon® 40 µm cell strainers	352340	Becton Dickinson
Combitips advanced®, 0.1 mL, Eppendorf Biopur®	0030089618	Eppendorf
Combitips advanced®, 0.2 mL, Eppendorf Biopur®	0030089626	Eppendorf
13 mm cover glass	631-0149	vWR
Cryogenic vials, internal thread, conical bottom, 1 mL	377224	Nunc
Falcon® 35 mm polystyrene tissue culture dish	353001	Becton Dickinson
Falcon® 60 mm polystyrene tissue culture dish	353004	Becton Dickinson
EasYFlasks™ polystyrene tissue culture flasks, 25 cm^2 growth area	156340	Nunc
EasYFlasks™ polystyrene tissue culture flasks, 75 cm^2 growth area	156472	Nunc
Falcon® polystyrene tissue culture flask, 175 cm^2 growth area	353028	Becton Dickinson
Falcon® polystyrene tissue culture multiple well plates, 6-well, flat bottom	353046	Becton Dickinson
Falcon® polystyrene tissue culture multiple well	353043	Becton

plates, 12-well, flat bottom		Dickinson
Falcon® polystyrene tissue culture multiple well plates, 24-well, flat bottom	353047	Becton Dickinson
Axygen® 1,000 µL Maxymum Recovery® filter tips	TF-1000-L-R-S	Axygen
Axygen® 200 µL Maxymum Recovery® filter tips	TF-200-L-R-S	Axygen
Axygen® 20 µL Maxymum Recovery® filter tips	TF-20-L-R-S	Axygen
Axygen® 10 µL Maxymum Recovery® Gilson-style filter tips	TF-300-L-R-S	Axygen
Hard-Shell® thin-wall 384-well skirted PCR plates	HSP-3805	Bio-Rad
LightCycler® 480 white 384-well plates with sealing foils	04729749001	Roche
MicroAmp® adhesive film applicators	4333183	Applied Biosystems
MicroAmp® fast optical 96-well reaction plates	4346906	Applied Biosystems
MicroAmp® optical adhesive film	4311971	Applied Biosystems
Microseal® 'B' adhesive seals	MSB-1001	Bio-Rad
1.5 mL microcentrifuge tubes	S1615-5599	Starlab
0.2 mL 8-strip PCR tubes	I1402-2908	Starlab
Costar® 5 mL Stripette® serological pipettes	4487	Corning
Costar® 10 mL Stripette® serological pipettes	4488	Corning
Costar® 25 mL Stripette® serological pipettes	4251	Corning

50 mL pipettes	FB55486	Fisher Scientific
Corning® 15 mL polypropylene centrifuge tubes, conical bottom	430790	Corning
Corning® 50 mL polypropylene centrifuge tubes, conical bottom	430829	Corning
Falcon® 5 mL polystyrene FACS tubes with 35 µm cell strainer cap	352235	Becton Dickinson
Falcon® 5 mL polystyrene FACS tubes with snap cap	352054	Becton Dickinson
Purple nitrile gloves, medium size	90627	Kimberly-Clark Professional
RNase AWAY®	83931	Sigma-Aldrich
RNaseZap® solution	AM9780	Ambion
RNaseZap® wipes	AM9786	Ambion
SigmaClean® water bath treatment	S5525-4OZ	Sigma-Aldrich
1,000 µL tips	F167104	Gilson
200 µL tips	F167103	Gilson
10 µL tips	F167101	Gilson
30 mL universal tube	128A/P	Sterilin
150 mm unplugged glass Pasteur pipettes	FB50251	Fisher Scientific

2.1.10 Cell lines

Table 2.9: Cell lines used in this study.

Cell line	Description	Reference
E14tg2a	A wild-type, hypoxanthine phosphoribosyltransferase (HPRT) deficient mESC line, 129/Ola background	Hooper et al., 1987
PNK6	A mESC line generated from the crossing between BAC-Penk-Cre$^{tg/+}$ line and Rosa26-EYFP$^{tg/+}$ line with no Cre-recombinase transgene inherited from parents, C57BL/6J:129 background	This study
PNK18	A reporter mESC line generated from the crossing between BAC-Penk-Cre$^{tg/+}$ line and Rosa26-EYFP$^{tg/+}$ line and expresses EYFP upon Cre-mediated recombination occurred in enkephalinergic neurons, C57BL/6J:129 background	This study

2.1.11 Animals

Table 2.10: Animals used in this study.

Mouse line	Description	Reference
BAC-*Penk-Cre*	A BAC (bacterial artificial chromosome) transgenic line expressing Cre-recombinase under the control of pre-pro-enkephalin promoter	Besusso et al., 2013
Rosa26-EYFP	A reporter line expressing EYFP from the *Rosa26* locus upon Cre-mediated removal of LoxP-flanked stop cassette	Srinivas et al., 2001
Trkb floxed	A Trkb conditional knockout line, which has loxP sites flanking the second exon corresponding to the tyrosine kinase domain of the *Ntrk2* gene	Minichiello et al., 1999

2.1.12 Analytical software

Table 2.11: Analytical software used in this study.

Software	Application	Developer
FlowJo (version 8.8.7)	Flow cytometry analysis	Tree Star
ImageJ (version 1.49b)	Image analysis	National Institutes of Health
Prism 6 for Mac OS X (version 6.0d)	Statistical analysis	GraphPad
Universal ProbeLibrary assay design center (version 2.45-2.50)	Primer design for qRT-PCR with UPL assay	Roche

2.2 Methods

2.2.1 Embryonic stem cell culture

All prepared media and solutions were kept at 4°C. No media that had been prepared for more than one month were used. Culture media, trypsin-EDTA and PBS were heated to 37°C in a water bath before applying to cells. Unless otherwise stated, all tissue culture plasticware was coated with 0.1% porcine gelatin in PBS for at least 30 minutes prior to use.

2.2.1.1 Routine culture

Cells were cultured in a humidified tissue culture incubator with 5% CO_2 at 37°C. Cells were passaged when they reached 80-90% confluence; media were removed, cells were washed once with 5 mL pre-warmed PBS. After aspirating the PBS, 2 mL of 0.025% trypsin-EDTA was added to T25 flask (the amount of trypsin-EDTA added was adjusted according to the size of flasks/plates). The flask was incubated at 37°C for 5 minutes and then tapped several times to dissociate the cells. 8 mL of mESC medium was added to the flask to inactivate the trypsin. The cell suspension was then transferred to a 15 mL tube and centrifuged in a bench top centrifuge at 300 g for 3 minutes. The medium was removed and the cell pellet resuspended in 1 mL pre-warmed mESC medium. Approximately 1/10 to 1/5 of cell suspension, depending on the cell line, was added to a new gelatinised T25 flask with 9 mL pre-warmed mESC medium. The flask was then put in the incubator. Media were replaced every day and cells passaged when confluence (usually every 2-3 days).

2.2.1.2 Freezing cells

Embryonic stem cells were frozen as follows: cells grown in a T25 flask were passaged as usual but resuspended in 2 mL freezing medium (mESC medium, 10% (v/v final concentration) DMSO). The amounts were altered accordingly to the size of flasks used. 1 mL of cell suspension was

transferred to a cryovial labelled with cell line's name, passage number and a date of freezing. The cryovial was put into Mr Frosty™ freezing container before storing in -80°C freezer overnight. The vial was transferred to a liquid nitrogen cell bank the following day.

2.2.1.3 Thawing cells

Cryovials containing frozen cells were removed from liquid nitrogen cell storage and immediately thawed by placing them into a tissue culture water bath set at 37°C. To dilute DMSO, cell suspension was transferred to a 15 mL tube containing 9 mL pre-warmed mESC medium. After centrifugation at 300 g for 3 minutes, medium was aspirated and the cell pellet was gently resuspended in 1 mL mESC medium. The cell suspension was transferred to a gelatin-coated T25 flask containing 9 mL pre-warmed mESC medium. The flask was placed in an incubator with 5% CO2 at 37°C. The mESC medium was changed once after cells had attached to a floor of the flask (3-5 hours after thawing cells).

2.2.1.4 Karyotyping

Chromosome counting was performed by using exponentially growing cells. Cells were washed with PBS and fed with pre-warmed mESC medium supplemented with 0.1 μg/mL (final concentration) demecolcine and incubated at 37°C for 40 minutes prior to trypsinisation. After centrifugation at 300 g for 3 minutes, the media was aspirated and the cell pellet resuspended in 2.5 mL pre-warmed 0.56% KCl. After 6 minutes incubation at room temperature, the cells suspension was centrifuged, resuspended in 200 μL fixative (methanol-acetic acid, 3:1 by volume) and left at 4°C for 30 minutes. The cell suspension was then dropped onto a cleaned glass slide and air-dried. Cells were then stained with 10% Giemsa, pH 7.2 for 20 minutes. Chromosome counting was done using bright field microscopy.

2.2.1.5 *Mycoplasma screening*

Newly derived cell lines were screened for mycoplasma contamination using the MycoAlert™ mycoplasma detection kit (Lonza) as per manufacturer's instructions. Briefly, 100 µL of medium from attached cells was used as a blank control for luminometer. 100 µL MycoAlert™ reagent was added to medium and incubated for 5 miuntes, generating the reading A from the luminometer. 100 µL of the MycoAlert™ substrate was then added and incubated for 10 minutes providing reading B. The ratio between reading A and reading B was calculated and mycoplasma contamination was considered present if the ratio was greater than 1.2. The sensitivity of the luminometer was confirmed by the use of positive and negative control samples from the MycoAlert™ assay control set (Lonza).

2.2.2 N2B27 monolayer neural differentiation

2.2.2.1 Plate/cover slip preparation for neural differentiation

Cover slips (13 mm diameter) were sterilised by treatment in 70% ethanol for 5 minutes. They were dried by placing on the edge of 24-well plate in a vertical position. The completely dry cover slip was placed into each well of a new sterile 24-well plate. Sterile cover slips were rinsed with PBS once before coating with poly-L-ornithine/laminin.

For poly-L-ornithine/laminin coating, one well of 24-well plate or a single cover slip was coated with 400 µL poly-L-ornithine solution (0.01%) for either 2 hours at room temperature or overnight at 4°C. They were then washed once with PBS before coating with 400 µL laminin (10 µg/mL) and incubated at room temperature for 2 hours or overnight at 4°C. The laminin was removed and the well/cover slip washed with PBS. The volume of poly-L-ornithine and laminin used was adjusted accordingly for other sized plastics.

2.2.2.2 Neural differentiation

Neural differentiation of mESCs was performed by N2B27 monolayer culture as described in Ying et al. 2003, with some modifications. Cells used in neural differentiation were in passage 8-20 (PNK18) or 29-40 (E14). One day prior to beginning the differentiation process, confluent mESCs were plated at high density (1/2 of total cell suspension or approximately 3,000,000-3,500,000 cells per T25 flask) in mESC medium. On the first day of differentiation or day 0, the confluent mESCs were trypsinised and plated onto gelatin-coated plasticware containing differentiation medium (Glasgow minimum essential medium supplemented with foetal bovine serum (FBS), sodium pyruvate, L-glutamine, MEM non-essential amino acid, 2-mercaptoethanol and Y-27632 dihydrochloride) at a density of 20,000 cells/mL. Medium was changed to NB medium (N2B27 supplemented with Y-27632 dihydrochloride) on day 1. Cells were fed every

day until they reached analytical time point at either day 15 or day 21. At day 7 of differentiation, cells were washed with PBS and dissociated with accutase at 37°C for 10 minutes. After centrifugation, cell pellet was resuspended in 1 mL NB medium. Cells were replated onto poly-L-ornithine/laminin-coated plastics/cover slip containing NB medium at a density of 5 x 10^4 cells/cm^2. For NB+3F culture, 100 ng/mL recombinant human DKK1, 200 ng/mL recombinant mouse Shh and 20 ng/mL recombinant human BDNF were added from day 1 to day 6 of differentiation, day 3 to day 9 of differentiation and day 12 of differentiation onwards, respectively.

2.2.3 Animals

2.2.3.1 Mouse line

All animals were kept on a mixed genetic background (C57BL/6J:129). Colonies were maintained by Dr. Jacqui Horn. Three mouse lines were used in this project. The BAC-*Penk-Cre* transgenic line was generated by pronuclear injection of circular BAC carrying Cre-recombinase under the control of pre-pro-enkephalin promoter (Besusso et al., 2013). The *Gt(ROSA)26Sor*$^{tm1(EYFP)Cos}$/J (also known as *Rosa26-EYFP*) is a reporter line, which contains a LoxP-flanked stop cassette in front of a cDNA for the enhanced yellow fluorescent protein (EYFP) inserted into the *Gt(ROSA)26Sor* (also known as *Rosa26* or *R26*) locus (Srinivas et al., 2001). This line expresses EYFP only when the stop cassette is removed in the presence of Cre-recombinase. The *Trkb* floxed line (*Trkb*$^{lx/lx}$) has LoxP sites flanking the second exon of the *Ntrk2* gene; corresponding to the tyrosine kinase domain (Minichiello et al., 1999). Excision of the second exon by Cre recombination leads to a disruption of gp145^{TrkB} receptor expression whilst expression of truncated Trkb isoforms is intact.

2.2.3.2 Animal husbandry, maintenance and procedures

Animals were housed in designated facility at the Institute for Stem Cell Research, University of Edinburgh and the Department of Pharmacology, University of Oxford. Animal husbandry was performed by staff from Biological Services (Edinburgh), and Biomedical Services (Oxford). Mice were housed separately according to their sex. The maximum number of animals per cage was six. In a case of males, only littermates were housed together whereas female animals from different litters could be pooled. For breeding purposes, one male was housed with two females. The minimal age of breeding was 6 weeks for females, or 7 weeks for males. Litters were weaned after P19. An ear biopsy was collected from each mouse at P14-21 for identification purposes and for genotyping. The project had ethical approval. All animal welfares and procedures, including Schedule 1 of

the Animal (Scientific Procedures) Act 1986, were conducted under University of Edinburgh and University of Oxford ethical committee guidelines and in adherence with Home Office legislation, Animals (Scientific procedures) Act 1986, and EU legislation for the protection of animals used for scientific purposes, Directive 2010/63/EU. The project licence number and personal licence number are PPL60/4193 and PIL60/13118, respectively.

2.2.3.3 *Genotyping*

All genotyping was performed by Dr. Jacqui Horn.

DNA isolation

DNA used for genotyping was isolated from ear and tail biopsies, which had been kept at -20°C until processed. Ear punches were collected between P14-21 and used for genotyping. Tail biopsies were taken from experimental animals to confirm animals' genotype at time of death. Samples were digested in 100 µL directPCR lysis reagent for mouse tail (Bioquote) with 1.5 µL PCR grade, recombinant proteinase K (16.4 mg/mL, Roche) at 56°C for a minimum of 4 hours. Heat inactivation at 85°C was then performed for 45 minutes. For each PCR reaction, 1 µL of DNA preparation was used.

Polymerase chain reaction (PCR)

Lyophilised primers were ordered from Sigma-Aldrich, dissolved in nuclease-free H_2O (Ambion) to 100 µM and stored at -20°C. PCR reaction for each target was set accordingly. All PCR reactions were set up in 0.2 mL 8-strip PCR tubes (Starlab) and run on DNAEngine Peltier Thermal Cycler (Bio-Rad).

BAC-*Penk-Cre* PCR

Primers:	LM40	5’ - AGG CAC CCG GGG AGG TTG TT - 3’
	LM41	5’ - CCA CGA CCG GCA AAC GGA CA - 3’
	LM42	5’ - CTC CTG CCA CGC ACC TTC CG - 3’

Reaction contained:

1 µL gDNA

5 µL 5x buffer

2.5 µL $MgCl_2$ (25 mM stock)

0.625 µL dNTPs

(10 mM stock, 2.5 mM for each dNTP)

0.5 µL LM40 primer (10 µM stock)

0.5 µL LM41 primer (10 µM stock)

0.5 µL LM42 primer (10 µM stock)

0.05 µL Taq polymerase (Sigma-Aldrich)

14.325 µL neuclease-free H_2O

Total reaction volume: 25 µL

Cycling conditions: Denaturation for 2 minutes at 94°C

35 cycles of 15 seconds at 94°C

15 seconds at 64°C

1 minute at 72°C

Final extension for 5 minutes at 72°C

Product size: Wild type 371 bp

Mutant 527 bp

Rosa26-EYFP PCR

Primers: LM17 5' - AAA GTC GCT CTG AGT TGT TAT - 3'

LM18 5' - GCG AAG AGT TTG TCC TCA ACC - 3'

LM19 5' - GGA GCG GGA GAA ATG GAT ATG - 3'

Reaction contained: 1 µL gDNA

5 µL 5x buffer

2.5 µL $MgCl_2$ (25 mM stock)

0.625 µL dNTPs

(10 mM stock, 2.5 mM for each dNTP)

0.5 µL LM17 primer (10 µM stock)

0.5 µL LM18 primer (10 µM stock)

0.5 µL LM19 primer (10 µM stock)

0.1 µL Taq polymerase (Sigma-Aldrich)

14.275 µL neuclease-free H_2O

Total reaction volume: 25 µL

Cycling conditions: Denaturation for 2 minutes at 94°C

35 cycles of 15 seconds at 94°C

15 seconds at 58°C

1 minute at 72°C

Final extension for 5 minutes at 72°C

Product size: Wild type 602 bp

Mutant 298 bp

TrkB floxed PCR

Primers: LM11 5' - TGA AGG ACG CCA GCG ACA ATG CAC G - 3'

LM12 5' - CCA AGG TGA TCA ACA GCC CAA GTC - 3'

Reaction contained: 1 µL gDNA

2.5 µL 10x buffer

2.5 µL $MgCl_2$ (25 mM stock)

0.625 µL dNTPs

(10 mM stock, 2.5 mM for each dNTP)

0.5 µL LM11 primer (10 µM stock)

0.5 µL LM12 primer (10 µM stock)

0.1 µL Taq polymerase (Sigma-Aldrich)

17.275 µL nuclease-free H_2O

Total reaction volume: 25 µL

Cycling conditions: Denaturation for 2 minutes at 94°C

40 cycles of 15 seconds at 94°C

15 seconds at 68°C

1 minute 30 seconds at 72°C

Final extension for 5 minutes at 72°C

Product size: Wild type 857 bp

Mutant 913 bp

Agarose gel electrophoresis

Gel electrophoresis of PCR reactions was done on 2% agarose gel in 0.5x TBE buffer. The gel was prepared by melting Agarose (Sigma-Aldrich) in a microwave oven until completely dissolved. After the agarose had been allowed to cool to 55°C, ethidium bromide (10 mg/mL; Sigma-Aldrich) was added to make a final concentration of 50 ng/mL. Agarose was poured onto a gel tray where both of its ends were sealed with tape and the appropriate comb inserted. Once solidified, the gel was placed into an electrophoretic chamber containing 0.5x TBE. 5 µL KAPA universal ladder (KAPA Biosystems) and 15 µL PCR reactions (with 3 µL of loading buffer added) were loaded into each well of the agarose. Gel was applied with 170 V electricity until the bands were clearly separated. Images of the bands were taken with either Gel DocTM XR+ system (Bio-Rad) or PhotoDoc-It^{TM} imaging system (UVP).

2.2.4 Immunostaining for brain tissues

2.2.4.1 Perfusion and fixation

For eliminating blood from a brain as much as possible, mice were perfused with 0.1 M phosphate buffer (PB) pH 7.4. Initially, animals were intraperitoneally injected with 50 μL sodium pentobarbital (50 mg/mL, Sigma-Aldrich). To test whether mice were unconscious, their hind paws and tail were pinched and no further procedure would be carried unless the mice were totally unresponsive. After that, a tip of tail was collected for genotyping and the mouse pinned to a cork board. The abdominal wall of mouse was opened and the right atrium was cut to allow the blood to drain out. 20 mL PB was flushed through the animal via perfusion tubing attached to 30G needle and a perfusion pump at a rate of 3-4 mL/min (Masterflex L/S easyload II, Cole Parmer) to slowly perfuse the PB through the left ventricle of the animals. Perfusion with PB was performed until the liver cleared and only clear liquid was observed from the opening of right atrium. After that perfusion with 20 mL of 4% PFA in PB was performed. After decapitation, the skull was opened and the brain removed and placed in 4% PFA on ice for three hours or overnight (Brains were initially left in 4%PFA overnight but it has been found that some primary antibodies did not worked well on over fixed tissues). Tissues were then washed twice in PBS and transferred to 30% sucrose in Tris-Azide buffer. Brains were left in sucrose at 4°C until they sank to the bottom of a tube (usually 2-3 days). Brains were embedded in a plastic mold containing OCT and quickly frozen in dry ice-cold isopentane for 1 minute before long-term storage at -80°C.

2.2.4.2 Immunohistochemistry

OCT-embedded brains were transferred from -80°C freezer to the Cryostat chamber (-20°C) and left to equilibrate for at least 30 minutes. Sagittal sections of the brain were cut at 30 μm thickness using a Cryostat CM3030 S (Leica Biosystems). Sections were treated with 3% hydrogen peroxide (in TBS) at room temperature for 20 minutes. Three washes (10

minutes each) with TBS were done. Tissues were incubated in tissue blocking buffer 1 (10% normal goat serum, 0.3% carrageen, 0.5% TritonX-100, 0.2% sodium azide in TBS) at room temperature for 1 hour. Tissues were then incubated with the primary antibody (chicken anti-GFP, abcam, 1:1,000) diluted in 1% normal goat serum, 0.3% carrageen, 0.5% TritonX-100 in TBS at room temperature overnight. After three washes with TBS, sections were incubated with the secondary antibody, biotinylated goat anti-chicken (1:200, Novex) diluted in 1% normal goat serum, 0.3% carrageen, 0.5% TritonX-100 in TBS at room temperature for 2 hours. After three washes, sections were incubated in Vectastain® ABC solution (Vector laboratories) at room temperature for 30 minutes. Tissues were washed three times (15 minutes each) with TBS followed by two washes (15 minutes each) with TB. Tissues were then incubated in DAB solution for 1-2 minutes. When colour developed, the reaction was stopped by adding cold TB. Sections were mounted on gelatin-coated slides and air-dried in a fume hood for 2 hours. Mounted sections were dehydrated in 90% and 100% ethanol, each for 1 minute before incubating in xylene for 10 minutes. Vectamount permanent mounting medium (Vector laboratories) was then applied on the slide before cover slip was placed.

2.2.4.3 Immunofluorescence

OCT-embedded brains were transferred from -80°C freezer to the Cryostat chamber (-20°C) and left equilibrated for at least 30 minutes. Sagittal section of the brain was cut at 30 μm thickness using Cryostat CM3030 S (Leica Biosystems). Sections were washed with TBS for three times (15 minute each). Heat-induced antigen retrieval was performed to reveal the masked epitope from protein cross-linking mediated by paraformaldehyde. Sections were immersed in 10 mM sodium citrate buffer pH 6.0 and incubated at 80°C for 1 hour. After antigen retrieval was done, sections were washed three times (15 minute each) with TBS. Sections were then incubated in tissue blocking buffer 2 (10% normal goat serum, 0.3%

TritonX-100, 0.2% sodium azide in TBS) at room temperature for 2 hours. Sections were incubated with primary antibodies diluted in tissue blocking buffer 2 (rabbit anti-pre-pro enkephalin, Lifespan Biosciences, 1:5,000 and chicken anti-GFP, abcam, 1:1,000) at room temperature overnight. After three washes with TBS, sections were incubated with secondary antibodies diluted in tissue blocking buffer 2 (goat anti-chicken Alexa Fluor 488 and goat anti-rabbit Alexa Fluor 555, Molecular Probes, 1:1,000) in the dark at room temperature for 3 hours. Sections were washed three times (15 minutes each) with TBS. Sections were then counterstained with 100 ng/mL DAPI at room temperature for 10 minutes, washed three times with TBS (15 minutes each), transferred to gelatin-coated slides, mounted using Vectashield Mounting Medium (Vector laboratories) and covered with a cover slip. Images were taken with a Leica AF6000 Modular System microscope (Leica Microsystems). LAS AF software (Leica Microsystems) was used for image processing.

2.2.5 Immunofluorescence of cultured cells

Cells grown on 13 mm cover slips were washed once with PBS. Fixation was done at room temperature in 4% PFA for either 5 minutes (for enkephalin immunostaining) or 20 minutes (for other stainings). Cells were washed three times with PBS. Fixed cells could be kept at 4°C for several days if desired. A quenching step was done by incubating fixed cells in quenching solution (0.1 M ammonium chloride, 0.1 M glycine in PBS) at room temperature for 10 minutes. After quenching, cover slips were washed with PBS for three times. Cells were incubated in cell blocking buffer (10% normal goat serum, 0.3% TritonX-100, 0.2% sodium azide in PBS) at room temperature for 30 minutes and incubated with primary antibodies diluted in cell blocking buffer at room temperature overnight. After three washes with PBS, cells were incubated with secondary antibodies diluted in cell blocking buffer in the dark at room temperature for 1 hour. After three washes with PBS, cells were stained with 100 ng/mL DAPI in the dark at room temperature for 10 minutes. Cover slips were then washed with PBS for three times and transferred to a glass slide. Mounting was done using Vectashield Mounting Medium (Vector laboratories). Images were taken with a Leica AF6000 Modular System microscope (Leica Microsystems). LAS AF software (Leica Microsystems) was used for image processing.

2.2.6 Flow cytometry and fluorescence-activated cell sorting (FACS)

2.2.6.1 Cell dissociation

Cells grown in a well of 12-well plate were washed once with 1 mL PBS. Enzymatic dissociation was done by adding 400 µL Accutase and incubating at 37°C, 5% CO2 for 15 minutes. The plates were tapped five times to dissociate cells. 1.6 mL of N2B27 medium was then added. The cell suspension was pipetted up and down 15 times using 1 mL filter tip to create a single cell suspension. Samples were kept on ice until the staining step was performed.

2.2.6.2 Antibody staining

The cell suspension was centrifuged in a bench-top centrifuge at 300 g, room temperature, for 4 minutes. Cells were then incubated with primary antibodies (PE-Cy7-conjugated rat anti-CD24, 1:600 per 1,000,000 cells, Biolegend; biotinylated rat anti-CD133, 1:300 per 1,000,000 cells, eBioscience) at 4°C in the dark for 15 minutes. Cells were washed by adding 1 mL PBS before centrifugation at 300 g, 4°C for 3 minutes. For CD133 staining, cells were incubated in streptavidin conjugated APC at 4°C in the dark for 15 minutes. Cells were washed with 1 mL PBS then resuspended in 200 µL FACS buffer. 0.2 µg/mL DAPI was added into samples to exclude dead cells. All samples were kept on ice until analysis/sorting was performed.

2.2.6.3 Analysis

Cells were analysed with a BD LSRFortessa cell analyser (Becton Dickinson). E14 (Hooper et al., 1987) -derived neural cells were used for setting forward and side scatter gate and calibrating DAPI, EYFP, PE-Cy7 and APC signals. Single-labelled samples (DAPI-positive, EYFP-positive, PE-Cy7-positive and APC-positive controls) and fluorescence minus one (FMO) controls (FMO-DAPI, FMO-EYFP, FMO-PE-Cy7 and FMO-APC) were used to compensate fluorescent overlap in different channels and to set gates. Data was acquired and saved in FCS formats with BD

FACSDiva™ software (Becton Dickinson). Analysis was performed with FlowJo software version 8.8.7 (Tree Star).

2.2.6.4 Cell sorting

Cells were sorted with either a BD FACSAriaII or BD FACSAriaIII cell sorters (BD Biosciences). Gates were set with unstained E14 (Hooper et al., 1987) neural cells, single-labelled controls and FMO controls as described in chapter 2.2.6.3. An 100 μm nozzle was used for cell sorting. Pre-sort purity analysis was performed prior to the actual sort to determine the purity of the sorted cells. Most sorted samples were at least 90% purity. Two thousand cells were sorted directly into a 1.5 mL tube contained 800 μL Trizol. After sorting, cells were mixed by inverting the collection tubes for several times. The tubes were briefly centrifuged and quickly frozen in dry ice. Frozen Trizol samples were kept at -80°C until RNA isolation was performed.

2.2.7 RNA isolation

2.2.7.1 RNA isolation from cultured cells

Total RNA was extracted from cultured cells using the RNeasy Mini kit (Qiagen). Briefly, cells were lysed in 350 µL buffer RLT, 10 µL/mL 2-mercaptoethanol. Homogenisation was done by passing lysate five times through a 21-gauge needle connected to an 1 mL RNase-free syringe. The lysate was transferred to RNeasy spin column. After washing, on column genomic DNA digestion was done by adding 2.73 Kunitz units of DNase I. The final RNA was eluted with 40 µL RNase-free water (Qiagen).

2.2.7.2 RNA isolation from sorted cells and brain tissues

Total RNA was isolated from both sorted cells and brain tissues with Trizol (Ambion). For sorted cell samples, 2,000 cells were FACS-sorted into 1.5 mL tube contained 800 µL Trizol. For brain tissues, up to 100 mg of tissue was placed in 1 mL Trizol. Chloroform was added (200 µL per 1 mL Trizol) to all sample types. After centrifugation, the aqueous phase, which contains RNA, was transferred to a new tube. RNA was precipitated, first with isopropanol and then with 75% ethanol. The RNA pellet was air dried and resuspended in either 15 µL (sorted cells) or 40 µL (brain tissues) nuclease-free water (Ambion).

2.2.7.3 RNA concentration measurement

RNA quantification was done using an UV spectrophotometer Nanodrop ND-1000 (Thermo Scientific), NanoVue Plus (GE Healthcare Life Sciences) or NanoPhotometer P 300 (Implen). The UV absorbance was converted to an RNA concentration using the Beer-Lambert law with an extinction coefficient of 40.

2.2.8 cDNA synthesis

2.2.8.1 T-primed kit (Amersham)

One microgramme of total RNA was diluted with RNase-free water to a volume of 33 μL in 1.5 mL tube. RNA was heated at 65°C for 5 minutes, then at 37°C for 5 minutes. While RNA was incubating at 37°C, the first-strand reaction mix tube was also warm to 37°C for 5 minutes. RNA was then transferred to the first-strand reaction mix tube and incubated at 37°C for 5 minutes. The contents in the tube were mixed by gentle vortexing, then spun down briefly before incubating at 37°C for another 60 minutes. The resulting cDNA was either used immediately for quantitative RT PCR or kept at -20°C.

2.2.8.2 Superscript VILO kit (Invitrogen)

One to two microgrammes of total RNA was added to 200 μL tube containing 4 μL of 5x VILO reaction mix and RNase-free H2O (to 18 μL) and 2 μL of 10x SuperScript enzyme mix was then added. The amount of 5x VILO reaction mix, 10x SuperScript enzyme mix and total volume could sometimes be scaled up to 50 μL depending on the RNA concentration used. After gentle mixing, the tube was incubated at 25°C for 10 minutes, then at 42°C for another 2 hours. The reaction was terminated by heating the tube at 85°C for 5 minutes. The cDNA was either used instantly or kept at -20°C for further applications.

2.2.9 Quantitative RT PCR (qRT-PCR)

2.2.9.1 Primer design

Primers were designed using the Roche Universal ProbeLibrary Assay Design Centre software. Chosen primers have a melting temperature between 59°C and 60°C. Primers with intron spanning assay were chosen to avoid genomic DNA amplification with an exception of EYFP primers, which does not contain any introns.

2.2.9.2 qRT-PCR

qRT PCR was done using an UPL assay on a LightCycler 480 Instrument (Roche), ABI 7500 Fast Real-Time PCR System (Applied Biosystems) or CFX384 Touch Real-Time PCR Detection System (Bio-Rad). PCR settings are shown in Table 2.12.

Table 2.12: PCR setting for UPL assay

Step	Temperature (°C)	Duration (hh:mm:ss)	Accquisition mode
Pre-incubation	95	00:10:00	None
Amplification	95	00:00:10	None
	60	00:00:30	None
	72	00:00:01	Single
Cooling	40	00:00:30	None

The Ct threshold value was either set automatically (in the LightCycler 480 Instrument and CFX384 Touch Real-time PCR Detection System) or manually (in the 7500 Fast Real Time PCR System) for each experiment. Data was analysed using the corresponding software. Ct values of each gene were normalised to that of a housekeeping gene, such as *Actb,* (ΔCt) of a same sample. Data was represented as either expression level relative to *Actb* or as fold difference to a reference sample (log2 scale) by ΔΔCt method.

2.2.10 Electrophysiological studies

All of the electrophysiological analyses were performed by Dr. Andrei-Sorin Illie, a postdoctoral research scientist in Dr. Colin Akerman's group at the Department of Pharmacology, University of Oxford.

All recordings were performed using the whole-cell patch-clamp technique in voltage- or current-clamp configurations. Patch pipettes were pulled from filamental borosilicate glass capillaries (1.2 mm outer diameter and 0.69 mm inner diameter; Harvard Apparatus) using a horizontal puller (Sutter P-97). The pipettes (5-8 MΩ tip resistance) were filled with an intracellular solution containing 130 mM potassium gluconate, 4 mM NaCl, 2 mM $MgCl_2$, 2 mM Na_2ATP, 0.3 mM Na_3GTP, 5 mM phosphocreatine, 1 mM EGTA and 10 mM HEPES (Delli Carri et al., 2013a). Osmolarity was adjusted to 290 mOsm and the pH was adjusted to 7.25 with KOH.

The PNK18 mESC line was cultured with either NB or NB+3F media to allow for neural differentiation. Cells were dissociated and re-plated at 50,000 cells/cm^2 density on poly-L-ornithine/laminin-coated 13 mm diameter cover slips. At day 22-24 of differentiation, cells were transferred from the incubator to the recording chamber. The cells were bathed in extracellular solution containing 140 mM NaCl, 3 mM KCl, 10 mM glucose, 10 mM HEPES, 2 mM $CaCl_2$, 1 mM $MgCl_2$, pH 7.36 (adjusted with NaOH) (Delli Carri et al., 2013a). All recordings were performed at room temperature (22-24°C). Neurons were visualised under a 60x, water-immersion objective (Olympus BX51WI). Epifluorescence was used to visualise and identify EYFP-expressing neurons, which were then selected for patch-clamp recordings. Following formation of a tight seal between the pipette and the underlying plasma membrane (>1 GΩ), whole-cell configuration was achieved by gently applying negative pressure via suction. Access resistance was calculated from -10 mV steps applied in voltage clamp from a holding voltage of -70 mV. Only recordings where access resistance was <50 MΩ were included. Recordings were made using an Axopatch 1D amplifier (Axon Instruments) and data was acquired using WinWCP Strathclyde whole cell analysis software (V.3.9.7; University of

Strathclyde) and stored on a PC for offline analysis. All voltages were corrected offline for a calculated junction potential of -15.8 mV.

Voltage-clamp recordings were used to measure membrane resistance, membrane capacitance and voltage-activated currents. Membrane resistance and membrane capacitance were calculated from -10 mV voltage steps from a holding voltage of -70 mV. Voltage-activated fast inward sodium currents and delayed outward potassium currents were recorded by holding the cell at -90 mV and applying a series of depolarising voltage steps, progressively increasing by 10 mV and sequentially moving the membrane potential from -80 to +30 mV. Leak currents were removed by performing offline leak current subtraction. The current density of voltage-activated currents for each recording was calculated by dividing the peak amplitude of the current by membrane capacitance of the neuron.

To check for the presence of a voltage-gated, fast inactivating, transient potassium current (I_A) we used an IA-isolaing protocol in voltage-clamp mode in the presence of tetrodotxin (TTX, 1 μM) to block voltage-gated sodium currents (Delli Carri et al., 2013a). The membrane potential was held at -110 mV and the I_A was activated with a series of depolarising test potentials in which the membrane potential was moved to a range between -40 and +70 mV in 10 mV increments. The I_A current is completely abolished when the test potential is preceded by a 50 ms prepulse at -40 mV (Delli Carri et al., 2013a). Under these conditions, only delayed potassium currents are active. The I_A was then isolated offline by subtracting traces containing the prepulse from those without the prepulse.

Current-clamp recordings were used to measure resting membrane potential and action potential. The resting membrane potential was calculated from current-clamp recordings with holding current (I_{hold}) at 0 A. To test for spiking activity, a series of depolarising current steps were injected from a membrane potential of -80 mV in 5 pA increments. The rheobase was determined as the value of the injected current required for triggering the first action potential. Maximal firing rate was determined as the highest firing rate in response to suprathreshod current injection.

2.2.11 Statistical analysis

Unless stated otherwise, results are reported as mean ± standard error of mean. Statistical analyses were performed using Prism 6 for Mac OS X (version 6.0d, GraphPad). Statistical significance was assessed by student's t-test, one- or two-way ANOVA with either Tukey's multiple comparison test or uncorrected Fisher's LSD test. Differences were considered statistically significant when p value is less than 0.05.

Chapter 3: Results

3.1 Generation/characterisation of an enkephalinergic reporter embryonic stem cell line

3.1.1 Generation of reporter cell lines

Two mouse lines were utilised for generating enkephalinergic reporter embryonic stem cell lines, the *Rosa26-EYFP* and the BAC-*Penk-Cre* lines. The *Rosa26-EYFP* reporter line harbours LoxP flanked stop cassette followed by EYFP in the *Rosa26* locus (Srinivas et al., 2001). Removal of the stop cassette by Cre-recombinase allows expression of EYFP in these cells. The BAC-*Penk-Cre* line, where Cre-recombinase expression is under the control of the *Pre-pro-enkephalin* (*Penk*) promoter, was generated in the Minichiello laboratory and characterised by Drs. Dana Kramer and Dario Besusso. Some of those characterisations (Besusso et al., 2013) relevant to this work is reported in figure 3.1 A-E and described below. The recombination pattern of the BAC-*Penk-Cre* line was analysed by crossing the line with the *Z/EG* reporter line (Novak et al., 2000) as well as the *Rosa26-EYFP* reporter line (Srinivas et al., 2001). Cre-recombinase-mediated expression of GFP in adult animals was detected in the caudoputamen (Figure 3.1 A), nucleus accumbens, granular layer of olfactory bulb and cerebellum, layers II, V and VI of the cerebral cortex and in the hippocampal formation, similar to the *in situ* hybridisation data of *Penk* expression described in the Allen Brain Atlas Data Portal (http://mouse.brain-map.org/). To evaluate recombination specificity within the striatum, double immunofluorescence using anti-GFP (which also binds to EYFP) and anti-pre-pro-enkephalin antibodies was done on the brain of adult *BAC-Penk-Cre*$^{tg/+}$*,Rosa26-EYFP*$^{yfp/+}$ mice. Cre-mediated EYFP expression was found in the majority (98%) of enkephalinergic MSNs, and only 4% of EYFP-expressing cells had no enkephalinergic phenotype (Figure 3.1 B). Double immunostaining for EYFP and the generic MSN marker Ctip2 (Figure 3.1 C) showed 43.28%±3.77 Ctip2-positive

neuronal cells expressing EYFP (Figure 3.1 E, value is mean ± standard deviation). Markers for striatal interneurons including Calretinin, Choline acetyltransferase, Parvalbumin and Somatostatin were not detected in EYFP-positive neurons within the striatum (Figure 3.1 D).

Enkephalinergic reporter embryonic stem cell lines were generated by collecting morula stage embryos from a *Rosa26-EYFP* female mouse that was crossed with a BAC-*Penk-Cre* male (Figure 3.1 F). The morulae were extracted by Jan Ure and Dr. Joe Mee, Transgenic Unit, Institute for Stem Cell Research, University of Edinburgh. The ESC lines were designated "PNK". Four clones were successfully obtained, clone 6, 8, 13 and 18. Genotyping revealed that only clone 8 and 18 carried the Cre-recombinase transgene. Clone 18 (PNK 18) was selected and used for this study. As mentioned above, EYFP would be detected upon expression of Cre-recombinase under the *Penk* promoter. Therefore, EYFP is only detectable once the cells have differentiated into enkephalinergic neurons but not in pluripotent stage (Figure 3.1 G).

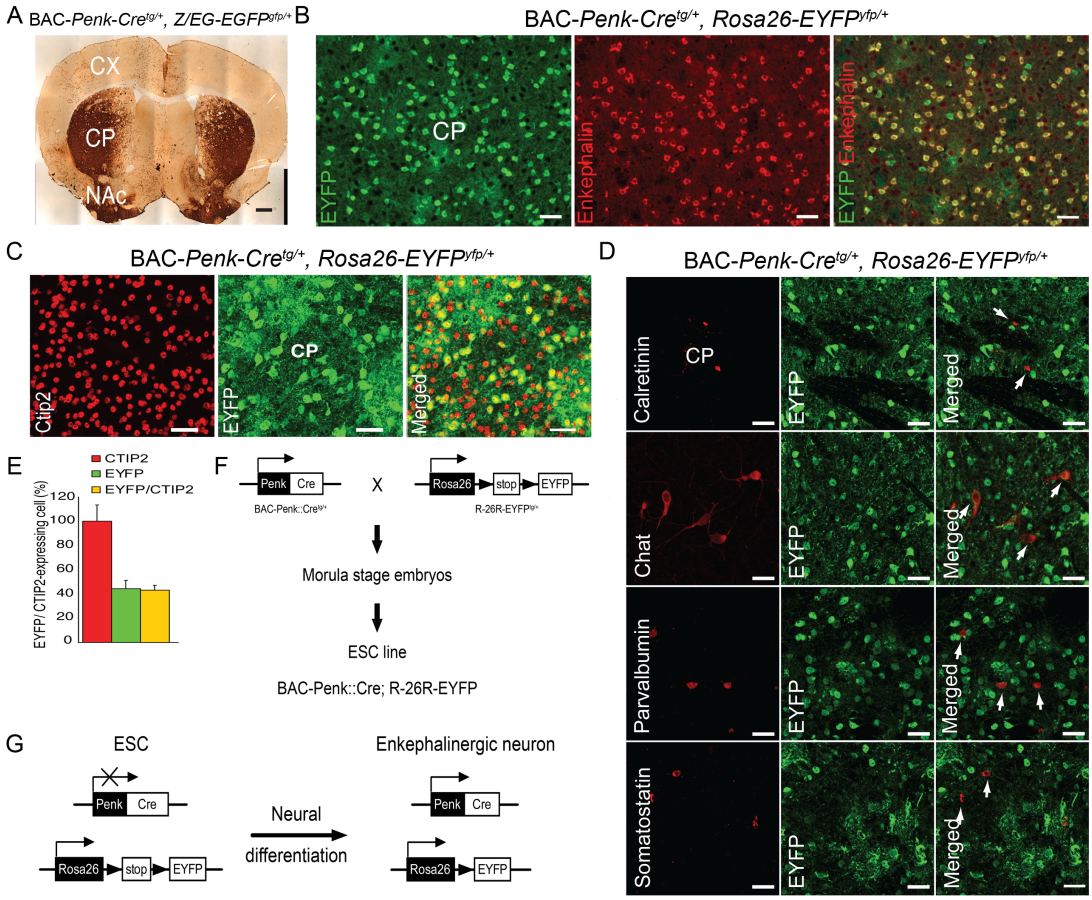

Figure 3.1: Generation of enkephalinergic reporter ESC line. (A) DAB staining against EYFP showed Cre-mediated EYFP expression in the caudoputamen (CP) and nucleus accumbens (NAc). **(B)** Immunofluorescence staining of adult *BAC-Penk-Cre*$^{tg/+}$*,Rosa26-EYFP*$^{yfp/+}$ brain revealed co-localisation between enkephalin and EYFP in the striatum. **(C and E)** Double immunostaining **(C)** of Ctip2 and enkephalin showed that approximately two fifths of Ctip2-positive MSNs are enkephalinergic (quantification shown in **E**). **(D)** Striatal interneuron markers did not co-localise with enkephalin-expressing cells. **(F)** Diagram depicting the generation of reporter ESC line. **(G)** Schematic representation of Cre-mediated EYFP expression in PNK18 ESC line undergoing enkephalinergic differentiation. Figure A-E are from Besusso et al., 2013. Scale bars are 500 µm (A) or 50 µm (B, C and D). Values are mean ± standard deviation (s.d). CX, cerebral cortex; ESC, embryonic stem cell; DAB, 3,3'-diaminobenzidine; EYFP, enhanced yellow fluorescent protein.

3.1.2 Characterisation of the PNK18 reporter cell line

Characterisation of the PNK18 line was performed to confirm that during the ESC stage, the line did not express EYFP. Immunofluorescence for Oct4, the protein expressed in undifferentiated ESCs, demonstrated a presence of Oct4 in all cells. As expected, and in contrast to Oct4, EYFP immmunoreactivity was not detected at this stage (Figure 3.2 A). These findings confirmed that recombination specificity of the line was intact since no Cre-recombination was observed in undifferentiated ESCs.

We next tested the ability of this ESC line to contribute to all germ layers by generating chimaeras. Chromosomes analysis determined that 75% of metaphase spreads (18/24) were euploid (Figure 3.2 B), indicating that chimaeras generated from the PNK18 line should have good contribution from the stem cells to all tissues including germ line. Chimaeras were generated by injecting PNK18 ESC clones into blastocysts. Seventeen pups were obtained from clone 18 injections. The percentage of chimaerism was assessed and five mice that showed high ESC contribution were chosen for further characterisation (Syto9 melt curve performed by Dr. Amit Grover). To examine the recombination pattern in these chimaeras, perfusion with 4% paraformaldehyde was done. Immunohistochemistry using 3,3'-diaminobenzidine (DAB) detected EYFP expression in the caudoputamen, hippocampal dentate gyrus and cerebellum of three out of five mice (Figure 3.2 C).

Cell type specificity of recombination was checked in one brain of the three EYFP-positive adult chimaeras by double immunofluorescence staining of EYFP and pre-pro-enkephalin. EYFP-positive cells were found in the expected areas including the striatum, however, at the first attempt, enkephalin immunoreactiviy was not detected (data not shown). We hypothesised that prolonged fixation in paraformaldehyde could mask the epitope of pre-pro-enkephalin peptide. We, therefore, performed heat-induced epitope retrieval prior to immunostaining. Both EYFP and pre-proenkephalin were detected successfully in the sections. Co-localisation between EYFP and pre-pro-ennkephalin was observed in all EYFP-positive cells in the striatum (Figure 3.2 D). However, only half of the striatal

enkephalinergic neurons showed EYFP staining. This can be explained by the fact that these animals were chimaeras so not all cells may derive from the injected ESCs.

In conclusion, the PNK18 ESC line was shown to possess pluripotency properties and to be a precise reporter for enkephalinergic neurons.

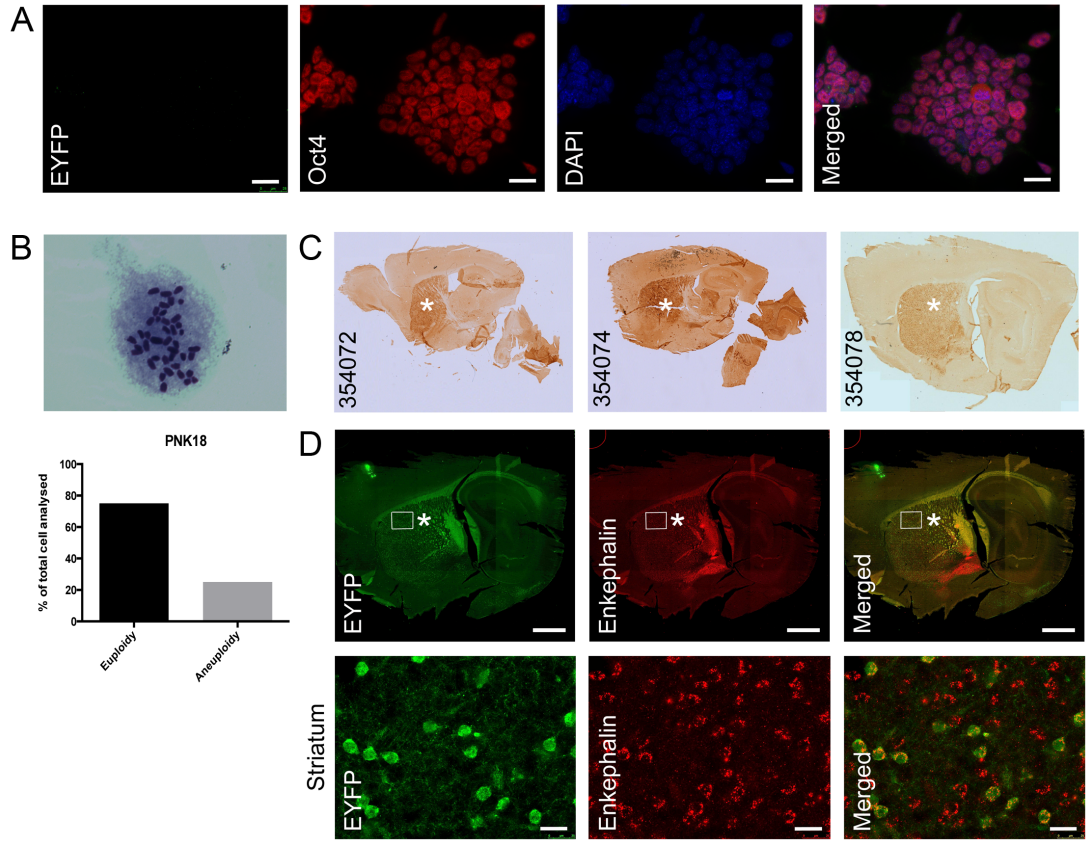

Figure 3.2: Characterisation of the PNK18 enkephalinergic reporter line. (A) Immunofluorescence staining showed Oct4 expression but not EYFP in PNK18 ESCs. **(B)** Chromosome counting from metaphase spreads with Giemsa stain demonstrated that the majority of spreads analysed (75%) were euploid (n=24). **(C)** DAB staining depicted EYFP immunoreactivity within the striata (asterisks) of three chimaeras. **(D, upper panel)** Double immunohistofluorescence staining for EYFP and enkephalin of the brain one of the chimaeras (ID 354072) showed most of the EYFP-positive cells were found mainly in the striatum (asterisks). **(D, lower panel)** Higher magnification of the inlet in the upper panel revealed co-localisation of EYFP and enkephalin in the striatum. All scale bars are 25 µm with an exception for the top panel of **(D)**, which are 1 mm. EYFP, enhanced yellow fluorescent protein; ESCs, embryonic stem cells.

3.2 Enkephalinergic differentiation from mouse embryonic stem cells

3.2.1 Neural differentiation using N2B27 monolayer culture

Monolayer neural differentiation (Ying and Smith, 2003) was selected as a platform for the differentiation. Initially, confluent ESCs were trypisinised and plated onto gelatin-coated tissue culture dish containing N2B27 medium at three densities, 7,500, 15,000 and 30,000 cells/cm^2. It was found that higher initial cell densities gave greater yield of cells that survived the differentiation process. However, a significant number of undifferentiated cells were evident in the highest suggested density, in particular at 30,000 cells/cm^2. For this reason, we selected 15,000 cells/cm^2 as an optimal plating density. We noticed that neural differentiation was slightly different between the control PNK6 line (a line without Cre-recombinase transgene) and the PNK18 line. By qualitative analysis at the same time point, PNK6 culture had more cells with mature morphology (Figure 3.3 A). This is not unexpected since variability amongst cell lines in neural differentiation efficiency has previously been reported (Ying and Smith, 2003). At day 12 of differentiation, immunocytofluorescence was performed to check whether the cultures contained any neural cell lineages. Nestin-positive progenitors and post-mitotic neurons, shown by βIII-tubulin (also known as TuJ1) staining, were found in the PNK6 cultures (Figure 3.3 B). Interestingly, Pax6, a marker commonly used to define forebrain identity, was also expressed in the PNK6 cultures. Expression of Ctip2, a transcription factor shown to be specific to corticospinal motor neurons (Arlotta et al., 2005) and all MSNs (Arlotta et al., 2008), was also detected in some cells (Figure 3.3 C). To investigate whether this differentiation protocol could generate any enkephalinergic neural cells, PNK18 cells at day 10 of differentiation (ND day 10) were harvested and processed for flow cytometric analysis (Figure 3.4). A percentage of EYFP-positive cells, reflecting enkephalinergic neurons, were increased nearly thirty fold when compared ESCs (Figure 3.4 B and C). Control PNK6 and E14 lines did not show any significant amount of EYFP-positive cells in both ESC stage and ND day

10 (Figure 3.4 D and E). This finding demonstrated that N2B27 cultures could be used as a basal medium for deriving enkephalinergic neurons from mESCs.

Due to the fact that this protocol is not specific to enkephalinergic differentiation, we speculated that addition and/or withdrawal of factors (both stimulators and inhibitors), which have a major role in striatal neuronal development to the culture medium would, in theory, lead to higher number of striatal neurons including enkphalinergic MSNs. In addition, we also observed a huge amount of cell death during differentiation, which, in some experiments, resulted in loss of the entire culture. For these reasons we optimised N2B27 culture medium by adding or removing certain factors to improve both the differentiation efficiency and cell survival. We also tested whether re-plating cells on optimal substrata would improve neural differentiation and cell viability.

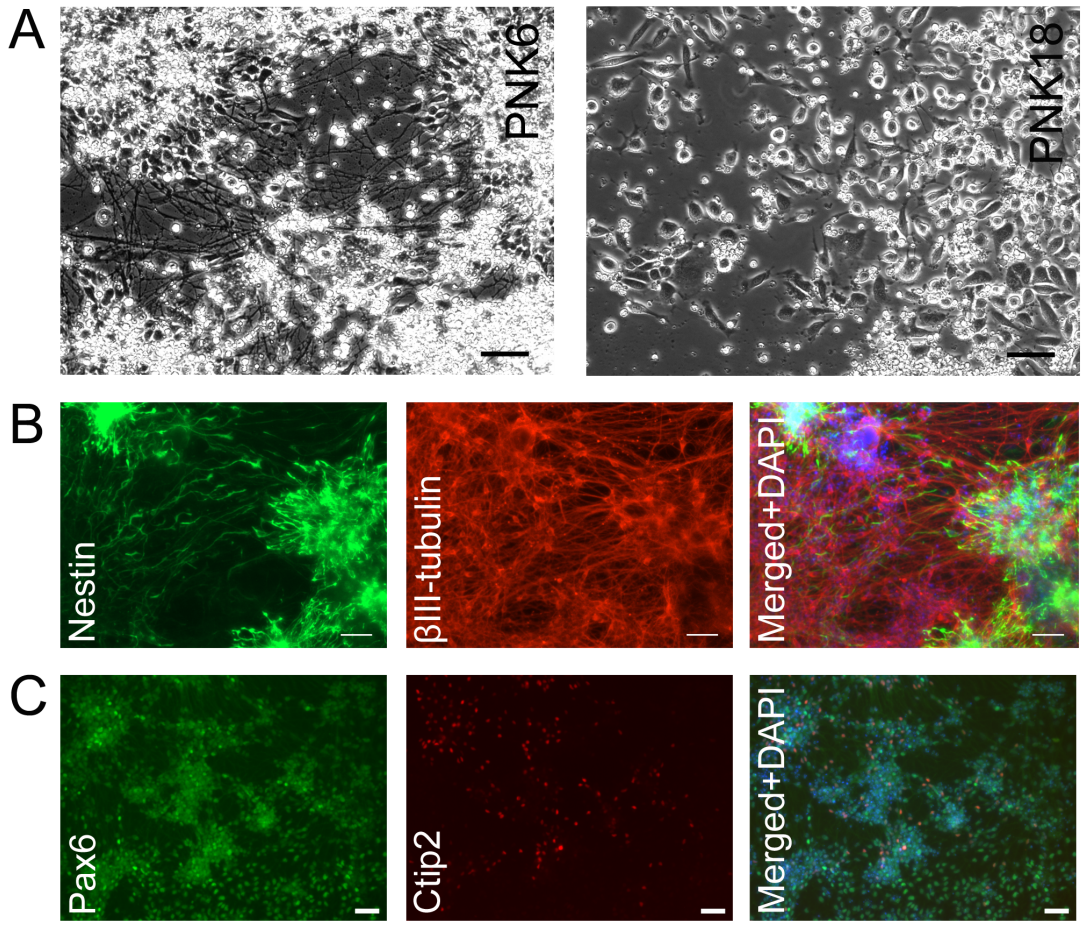

Figure 3.3: N2B27 monolayer neural differentiation in PNK18 and PNK6 ESC lines. **(A)** Images taken at day 8 of differentiation showed N2B27 neural differentiation of PNK6 (left) and PNK18 (right) lines. **(B)** Immunofluorescence staining showing Nestin-positive neural progenitors and βIII-tubulin-positive neuronal cells in PNK6 line cultured in N2B27 at day 12 of differentiation. **(C)** Expression of the forebrain progenitor marker Pax6 and MSN-specific marker Ctip shown by immunofluorescence of day 12 cultures of PNK6 line. All scale bars are 50 μm. ESC, embryonic stem cell; MSN, medium spiny neuron.

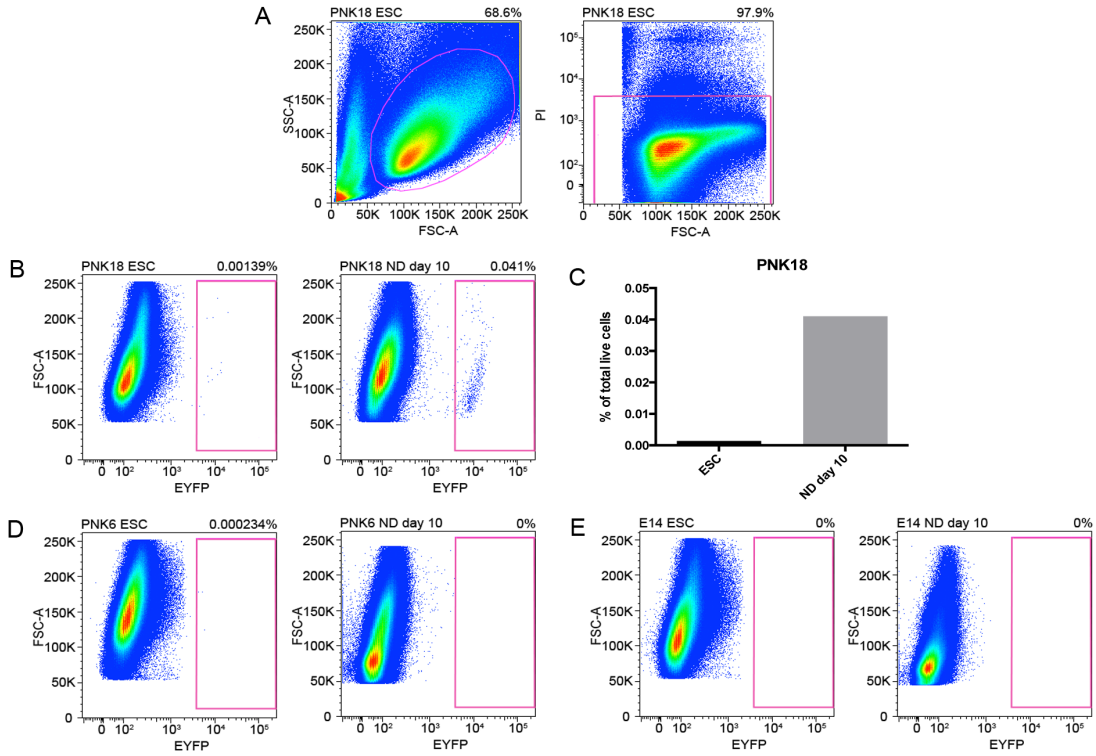

Figure 3.4: Presence of enkephalinergic neural cells in N2B27 monolayer culture. Flow cytometric analysis of PNK18, PNK6 and E14 lines was performed at ESC stage and day 10 of N2B27 neural differentiation. **(A)** Gate setting on forward and side scatter plot (left), and the viability gate (right), was set to exclude dead cells (as determined by a high propridium iodide (PI) signal). **(B and C)** Increased EYFP-positive cells in the PNK18 line at day 10 of differentiation compared to ESCs. **(B)** Flow cytometric plots of EYFP intensity in X axis vs forward scatter (FSC) in Y axis and **(C)** graph showing the percentage of EYFP-positive cells from total live cells. **(D and E)** In contrast, PNK6 **(D)** and E14 **(E)** lines, which were negative controls (no Cre-recombinase transgene), did not show any EYFP-positive cells in either stage. ESC, embryonic stem cell; EYFP, enhanced yellow fluorescent protein.

3.2.2 Role of retinoic acid signalling in monolayer neural differentiation

Retinoic acid (RA) is one of the crucial factors involved in most steps of ESC differentiation towards MSN. It has been shown that RA promotes differentiation via FGF signalling pathway (Stavridis et al., 2010). After neural fate is acquired, RA plays an important role in neural patterning together with other caudalising factors by inhibiting anterior neural identity (Gaspard and Vanderhaeghen, 2010). For this reason, absence of these factors, including RA, is mandatory for forebrain structures to retain their identity. Interestingly, during maturation of striatal MSNs, RA treatment increases the number of Darpp32-positive cells in E13.5 LGE cultures (Toresson et al., 1999). Since the B27 supplement added to N2B27 medium contains retinyl acetate, which can be converted to RA, we, therefore, investigated whether a removal of retinyl acetate would affect neural differentiation by using B27 supplement that did not contain retinyl acetate (B27-vitA supplement). The retinyl acetate deficient medium was called N2B27-vitA.

The E14 ESC line was cultured in either N2B27 or N2B27-vitA media for 20 days before cells were collected for analysis. In addition to N2B27 and N2B27-vitA cultures, we tested a third culture condition, which consisted of E14 ESC cultivated in N2B27 medium for two days before changing the medium to N2B27-vitA from day 2 of differentiation onwards (N2B27-vitA d2 onwards). The reason for adding the third culture condition was to lower the proportion of undifferentiated cells in the cultures since RA signalling is needed for neural differentiation (Stavridis et al., 2010). Quantitative reverse transcription polymerase chain reaction (qRT-PCR) analysis at day 20 of differentiation (Figure 3.5) showed a surprising finding, the expression of *Oct4* was highest in the N2B27-vitA d2 onwards condition, but not N2B27-vitA culture condition. The N2B27 culture, however, showed lower expression of *Oct4* compared to the other two culture conditions. We observed a trend of lower expression of the MGE marker *Nkx2.1*, and higher expression of the LGE marker *Gsx2*, in the N2B27 culture medium compared to the other conditions. However, statistical analysis could not be obtained since only one biological replicate was performed. Neural differentiation appeared to be more efficient in the

N2B27 culture as determined by the highest level of expression of the pan-neuronal marker *Tubb3* (gene encodes for βIII-tubulin). MSN-specific markers *Ctip2* and *Ppp1r1b* (gene encodes for Darpp32) showed a tendency to be slightly up-regulated in the N2B27-vitA d2 onwards culture condition.

No obvious difference in terms of the expression of striatal neuronal genes was observed in the two culture conditions (with and without the presence of vitamin A) at the time point analysed (day 20). Due to the potential problems of omitting vitamin A, such as an accumulation of undifferentiated cells in cultures, reduced striatal cell fate commitment but higher MGE-lineage priming, and lower neuronal differentiation efficiency, we continued to use the regular B27 supplement (with retinyl acetate) in our culture system.

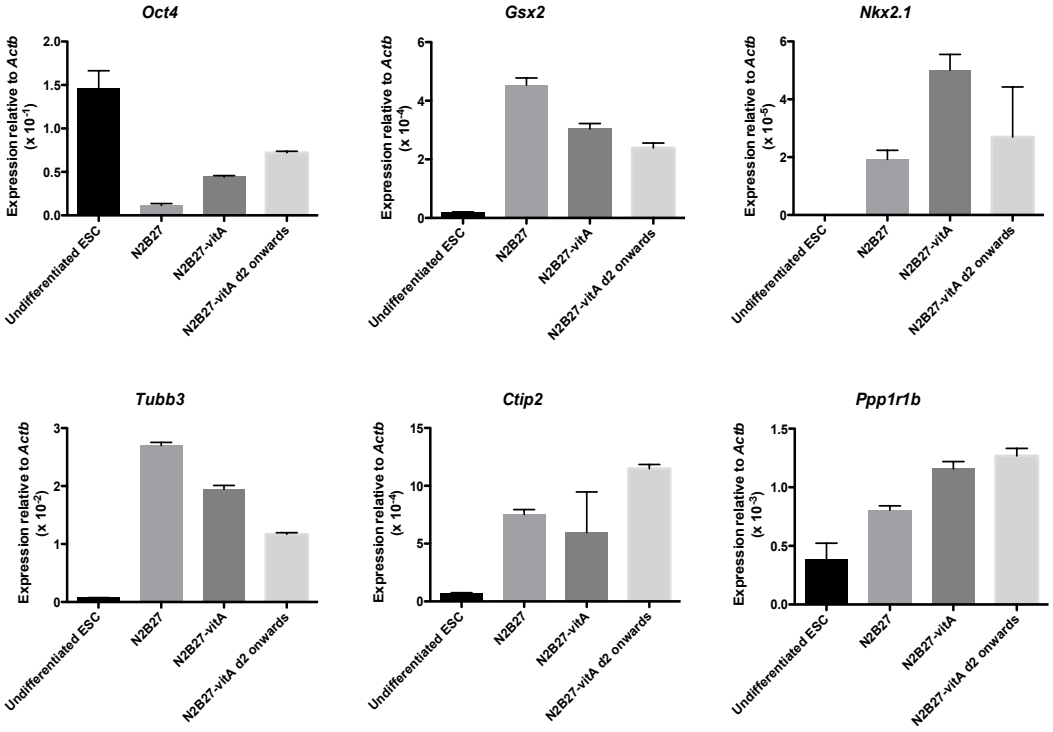

Figure 3.5: Pluripotency and neural gene expression in cultures with and without vitamin A. The E14 ESC line was cultured in either N2B27, N2B27-vitA or in N2B27 on the first two days then in N2B27-vitA (N2B27-vitA d2 onwards). Cells were processed for qRT-PCR analysis at day 20 of differentiation. Expression of the pluripotency gene *Oct4* and the MGE marker *Nkx2.1* in both vitamin A-deficient cultures showed an increased trend when compared to that of the standard N2B27 cultures. The striatal progenitor marker *Gsx2* and pan-neuronal gene *Tubb3* also showed a minimal trend of enrichment in N2B27 sample. MSN-specific genes *Ctip2* and *Ppp1r1b* were expressed at higher levels in N2B27-vitA d2 onwards culture compared to N2B27. No statistical analysis performed; n=1 for each group; Values are mean ± s.d from technical replicates. ESC, embryonic stem cell; MGE, medial ganglionic eminence; MSN, medium spiny neuron.

3.2.3 Effects of DKK1, Shh and BDNF in enkephalinergic differentiation

Several published differentiation protocols used extrinsic factors to derive DARPP32-positive neurons from both mouse and human PSCs. Amongst these, a combination of WNT inhibitor DKK1, SHH and BDNF is the most common cocktail used (Aubry et al., 2008, Zhang et al., 2010, Danjo et al., 2011, Delli Carri et al., 2013b). To test whether enkephalinergic neurons could be obtained when those factors were present in the culture medium, we added the three factors (recombinant murine Shh, recombinant human DKK1 and BDNF) into N2B27 neural culture at the specified time points (Figure 3.6 A). Flow cytometric analysis performed at day 30 of differentiation showed that the percentage of EYFP-positive cells from N2B27 culture supplemented with the three factors (N2B27+3F) was higher than that of N2B27 culture without any factor added (Figure 3.5 B and C). Thus, the addition of these factors resulted in a higher percentage of enkephalinergic neurons. Additionally, qRT-PCR analysis of key markers of E14 ESC undergoing neural differentiation in either of the two culture conditions (N2B27 or N2B27+3F) revealed higher expression of *Oct4* and *Gsx2* in N2B27 cultures compared to that of N2B27+3F (Figure 3.5 D). In contrast, expression of the pan-neuronal gene *Tubb3*, MSN markers *Ctip2* and *Ppp1r1b* was more robust in cultures with the three factors.

In conclusion, the N2B27+3F culture medium produced more mature neuronal cells and decreased the proportion of undifferentiated cells in the culture, as determined by lower expression of *Oct4* compared to the factor-free N2B27 culture condition. Further analysis showed higher expression of MSN-specific markers such as *Ctip2* and *Ppp1r1b* in N2B27+3F cultures. Moreover, N2B27+3F cultures exhibited more EYFP-positive cells, indicated the presence of enkephalinergic neurons.

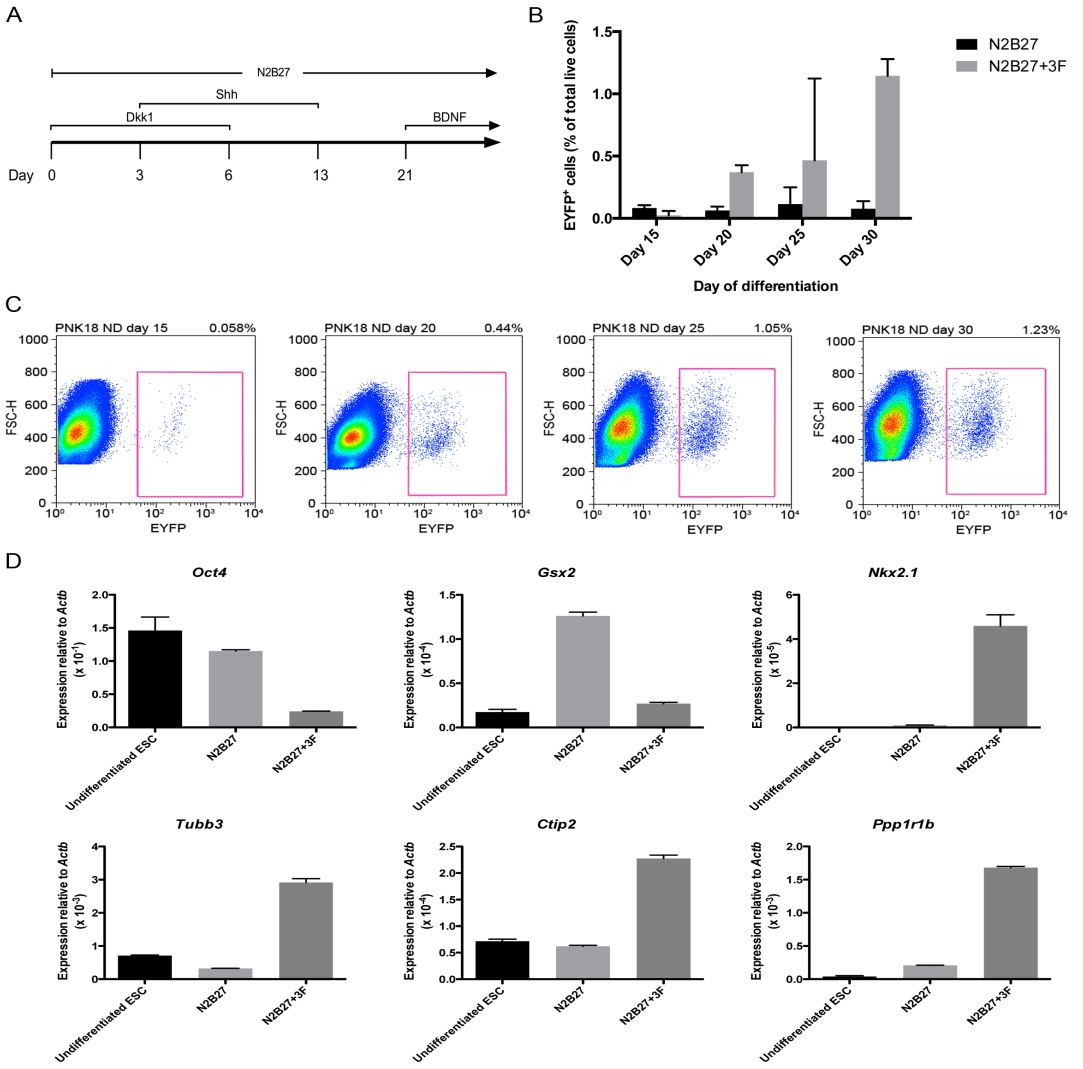

Figure 3.6: Enrichment of EYFP-positive cells and MSN-specific genes in the N2B27+3F culture. (A) Schematic representation of the differentiation protocol used. **(B and C)** Flow cytometric analysis of EYFP-positive cells obtained from PNK18 cell line cultured in either N2B27 or N2B27+3F. **(B)** Graph shows percentage of EYFP-positive cells from total live cells analysed. **(C)** Plots show an increase in the proportion of EYFP population during neural differentiation in the presence of the three factors. **(D)** qRT-PCR analysis of pluripotency marker (*Oct4*), LGE marker (*Gsx2*), MGE marker (*Nkx2.1*), pan-neuronal marker *Tubb3* and MSN markers (*Ctip2* and *Ppp1r1b*) of the E14 cell line in undifferentiated ESC, day 35 of N2B27 culture (N2B27) and day 32 of N2B27 with the three factors (N2B27+3F). No statistical analysis performed; n=1 for each group; Values are mean ± s.d from technical replicates. EYFP, enhanced yellow fluorescent protein; MSN, medium spiny neuron; LGE, lateral ganglionic eminence; MGE, medial ganglionic eminence; ESC, embryonic stem cell.

3.2.4 Improvement of cell survival during neural differentiation by using a modified culture medium

It is known that up to 50% of cells may die when cells cultured in serum-containing medium are transferred to serum-free medium (Ying and Smith, 2003). Cell viability can be increased by several strategies. We have taken three approaches to address this issue. Firstly, by either the addition of leukaemia inhibitory factor (Lif) into N2B27 medium or replacement of N2B27 with ESC medium on the first day of differentiation. Secondly, by adding a proliferation factor such as Fgf2, a potent mitogen for neural progenitors. Lastly, the use of an anti-apoptotic reagent, Rho-associated kinase (ROCK) inhibitor Y-27632. The four culture conditions tested are detailed in Table 3.1, and the number of live cells remaining at day 4 and day 11 of differentiation were calculated.

Table 3.1: Details of media used in four culture conditions

Culture condition	Medium used on		
	Day 0	**Day 1**	**Day 2 onwards**
1	GMEM+FBS+Fgf2+ ROCK inhibitor	N2B27+Fgf2+ ROCK inhibitor	N2B27+ ROCK inhibitor
2	GMEM+FBS+ ROCK inhibitor	N2B27+ ROCK inhibitor	N2B27+ ROCK inhibitor
3	N2B27+Lif+Fgf2+ ROCK inhibitor	N2B27+Fgf2+ ROCK inhibitor	N2B27+ ROCK inhibitor
4	N2B27+Lif+ ROCK inhibitor	N2B27+ ROCK inhibitor	N2B27+ ROCK inhibitor

FBS, foetal bovine serum.

Cell survival was comparable in all culture conditions at day 4 of differentiation, however, massive cell death was observed in culture conditions 3 and 4 at differentiation day 11. It is clear that the use of ESC medium without Lif on the first day of neural differentiation (culture conditions 1 and 2) has an enhanced effect on cell survival when compared to the use of N2B27 with Lif (culture conditions 3 and 4) at day 11 of differentiation (Figure 3.7 A). Culture condition 2 showed significantly higher numbers of live cells than that of culture conditions 1, 3 and 4 (Figure 3.7 A; two-way ANOVA, interaction between culture condition and time point: $F_{(3,6)}$=13.63, p=0.0044; effect of culture condition: $F_{(3,6)}$=15.09, p=0.0033; effect of time point: $F_{(1,6)}$=0.04629, p=0.8368; Tukey's multiple comparison test: p=0.0050 condition 1 vs condition 2 day 11; p=0.0016 condition 2 vs condition 3 day 11; p=0.0017 condition 2 vs condition 4 day 11; n=2 per group except day 11 of culture condition 3 and 4, n=1). Likewise, the proportion of DAPI-negative (viable) cells from flow cytometric analysis at day 11 of differentiation showed higher cell viability in culture conditions 1 and 2 compared to culture condition 3 and 4 (Figure 3.7 B; two-way ANOVA, interaction between culture condition and time point: $F_{(3,6)}$=200.2, p<0.0001; effect of culture condition: $F_{(3,6)}$=221.1, p<0.0001; effect of time point: $F_{(1,6)}$=1173, p<0.0001; Tukey's multiple comparison test: p=0.0237 condition 1 vs condition 2 day 11; p<0.0001 condition 1 vs condition 3 day 11; p<0.0001 condition 1 vs condition 4 day 11; p<0.0001 condition 2 vs condition 3 day 11; p<0.0001 condition 2 vs condition 4 day 11; n=2 per group except day 11 of culture conditions 3 and 4, n=1). Surprisingly, addition of Fgf2 in culture conditions 1 and 3 did not show a beneficial effect on cell viability. Based on these findings we decided to use culture condition 2 as a basal medium for neural differentiation. We designated this culture "modified N2B27 (NB)" culture.

We next tested whether Y-27632 effect on cell survival would be preserved if the treatment time was restricted to only the first day of differentiation. We compared the number and percentage of live cells between two cultures, NB and a new culture condition (NB+R), which is similar to NB culture except Y-27632 was added on day 0 only. Although there was a considerable amount of live cells in both

cultures at day 15 of differentiation, we found that both total number and percentage of live cells in NB+R cultures were significantly lower than that of NB culture (Figure 3.8; p=0.0004 for total cell number and p=0.0203 for percentage of viable cells, unpaired Student's t-test, n=3 per group). This underscored the anti-apoptotic effect of Y-27632 and supported its addition in the medium throughout the entire differentiation period.

To ensure that addition of Y-27632 would not interfere with the neural differentiation process or direct cells to other lineages, we performed gene expression analysis of different markers on cells from NB and NB+R cultures. The presence of Y-27632 in cultures, regardless of duration, led to an enrichment of the neural progenitor marker *Sox1* compared to ordinary N2B27 culture (Figure 3.9). This correlated with a reduction of the pluripotency marker *Nanog* expression in NB and NB+R cultures. Consistent with what has been reported in literature that ROCK is involved in the maintenance of undifferentiated state of ESCs and its inhibition induces neural differentiation (Chang et al., 2010, Frisca et al., 2013). Interestingly, longer duration of Y-27632 treatment resulted in an increase in the expression of both forebrain progenitor genes *Foxg1* and *Pax6*, and LGE marker *Gsx2*, which is more specific for the neuronal population of interest here. Expression of striatal markers *Dlx1* and *Dlx2*, downstream targets of *Gsx2*, however, was identical between NB and NB+R cultures. To ensure that the persistent administration of Y-27632 did not bias differentiation towards other lineages, we checked and found that both mesodermal marker *Brachyury* (*T*) and endodermal marker *Gata6* were expressed in a comparable level in both NB and NB+R cultures. These results indicate that the prolonged exposure to ROCK inhibitor had a beneficial effect on cell survival and on neural differentiation.

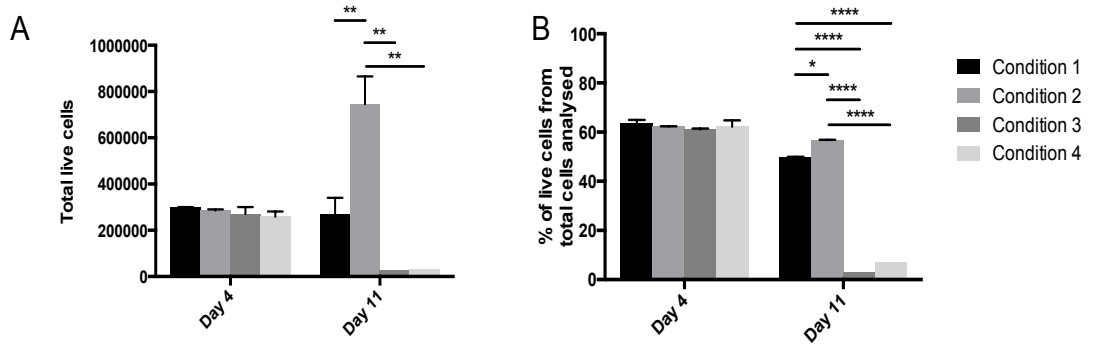

Figure 3.7: Cell survival is enhanced using ESC medium without Lif the first day of differentiation together with Y-27632 treatment. Culture conditions 1-4 are detailed in table 3.1. **(A)** Total number of live cells per one well of a 12-well plate assessed by trypan blue staining at days 4 and 11 of differentiation. Culture condition 2 had the highest number of live cells at day 11 of differentiation. **(B)** Flow cytometric analysis of individual cultures showing the percentage of live cells to the total number of cells analysed. Approximately 49% and 56% of total cells analysed in culture conditions 1 and 2, respectively, were alive at day 11 of differentiation. The proportion of live cells in culture was significantly less in culture conditions 3 and 4. Two-way ANOVA with Tukey's post-hoc analysis; * $p<0.05$; ** $p<0.01$; **** $p<0.0001$; p are adjusted p-value from Tukey's test; n=2 for each group except day 11 of culture condition 3 and 4, n=1; Values are mean ± standard error of the mean (s.e.m.). ESC, embryonic stem cell

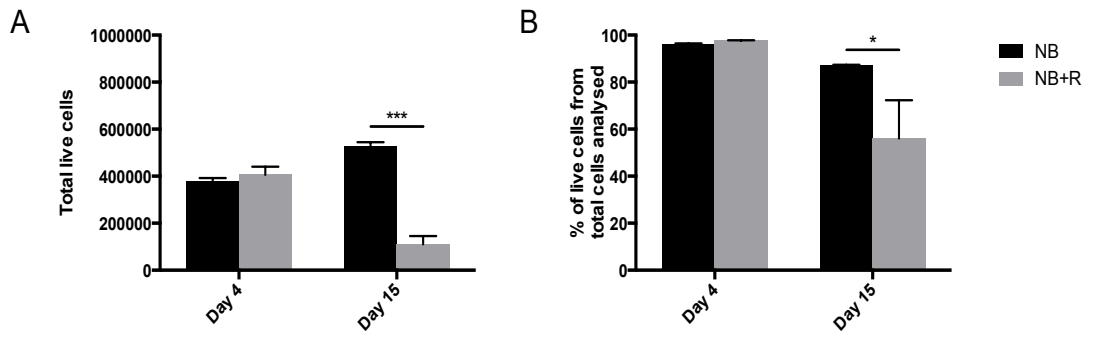

Figure 3.8: ROCK inhibitor enhances cell survival. The PNK18 line was cultured in either NB or NB+R media before analysis was performed on day 4 and day 15 of differentiation **(A)** Total number of live cells per one well of a 12-well plate assessed by trypan blue staining. Total number of live cells in NB culture was significantly higher than that of NB+R culture at day 15 of differentiation. **(B)** Percentage of live cells to the total number of cells analysed by flow cytometric analysis. At day 15 of differentiation, proportion of live cells in NB culture was significantly higher than NB+R culture. Unpaired Student's t-test; * $p<0.05$; *** $p<0.001$; n=3 for each group; Values are mean ± s.e.m.

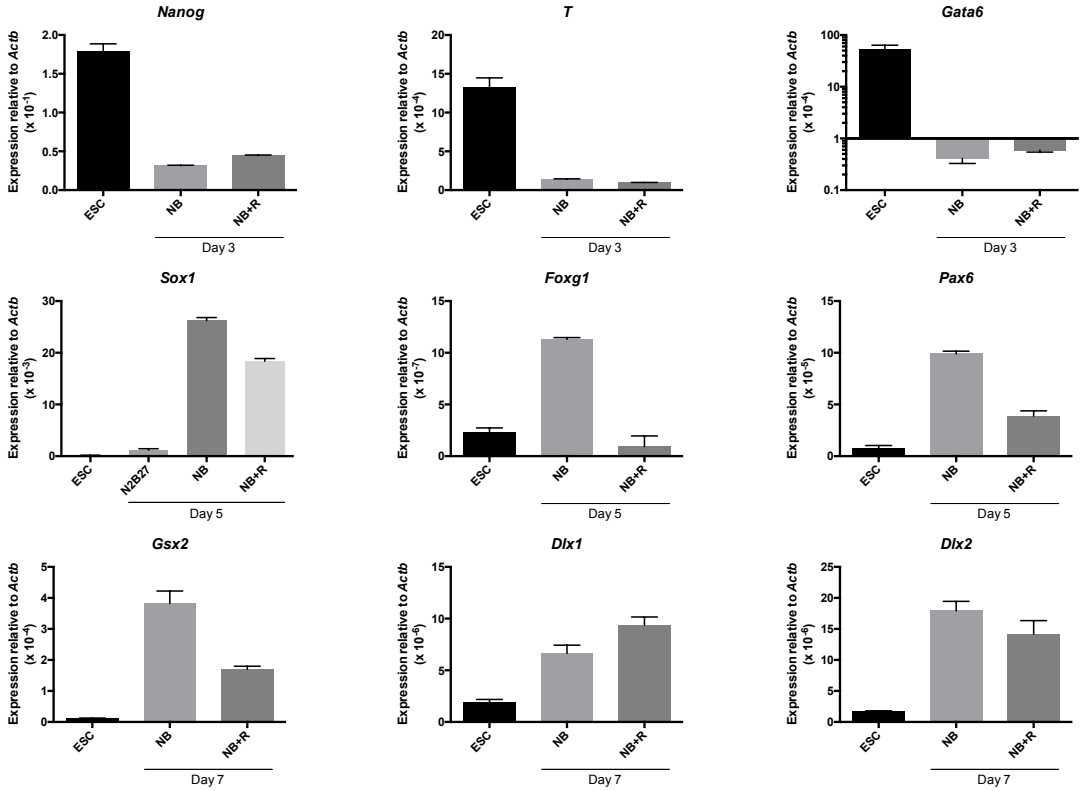

Figure 3.9: Gene expression analysis of cells from NB and NB+R cultures. The PNK18 line was cultured in either NB or NB+R media. Cells were harvested at time points indicated in each graph for qRT-PCR analysis. Down-regulation of *Nanog*, *Brachyury* (*T*) and *Gata6* was observed in both NB and NB+R cultures at day 3 of differentiation. *Sox1* was highly expressed in cultures treated with Y-27632. NB cultures showed higher expression of *Foxg1*, *Pax6* and *Gsx2* whilst *Dlx1* and *Dlx2* were expressed in a similar manner in both cultures. No statistical analysis performed; n=1 for each group; Values are mean ± s.d from technical replicates.

3.2.5 Re-plating increases neural differentiation efficiency

Another factor known to promote neural differentiation efficiency is the use of positively charged substrates, such as poly-L-ornithine, poly-lysine and laminin (Ying and Smith, 2003, Lorincz, 2006). It is also possible that re-plating cells onto a new culture dish may reduce the number of undifferentiated cells in culture and remove the paracrine effect of high cell densities that might impede neural differentiation. Moreover, PNK18 neural cells detached from the plates when maintained in gelatin-coated Petri dishes for long term, indicating that gelatin is not an ideal substrate for culturing neuronal cells. We, therefore, tested whether re-plating differentiating cells on gelatin-coated plates to those coated with poly-L-ornithine/laminin improved neural differentiation efficiency as well as cell survival. PNK18 neural cells at day 4 of N2B27 differentiation were dissociated and plated at a density of 50,000 cells/cm^2 onto new culture plates coated with either 0.1% gelatin or 0.01% poly-L-ornithine/10 μg/mL laminin. Images of live cells taken at day 5 of differentiation showed that cells re-plated onto poly-L-ornithine/laminin-coated dishes were properly attached (Figure 3.10 A) whereas almost all the cells re-plated onto gelatin-coated dishes had detached and were floating and clustered in clumps (Figure 3.10 B). This finding demonstrates that poly-L-ornithine and laminin are better substrates for neuronal attachment after re-plating.

To further investigate the status of the re-plated cells on the different substrata (gelatin and poly-L-ornithine/laminin), they were processed in parallel for immunofluorescence staining and qRT-PCR analysis. PNK18 and E14 neural cells were cultured on gelatin-coated dish for four days before re-plating onto new plates coated with either gelatin or poly-L-ornithine/laminin. For each condition, we did re-plate cells with four different densities (25,000 cells/cm^2, 50,000 cells/cm^2, 75,000 cells/cm^2 and 100,000 cells/cm^2) to determine an optimal re-plating density. At day 12 of differentiation, cells were processed for immunofluorescence staining for the pluripotency marker Oct4 and post-mitotic neuronal marker βIII-tubulin. Regardless of the re-plating density, very few βIII-tubulin-positive cells were seen when cells were re-plated onto gelatin-coated dishes and no Oct4 staining was detected (Figure

3.11 A and B; cultures re-plated at 25,000 cells/cm^2 and 75,000 cells/cm^2 showed similar recovery to that of the 50,000 cells/cm^2 and 100,000 cells/cm^2, respectively, data not shown). This confirms gelatin is not a good substratum for neural differentiation cultures. Conversely, βIII-tubulin-positive neuronal cells were abundantly found when poly-L-ornithine/laminin was used as substrate (Figure 3.11 C and D). Although a few Oct4 expressing cells were present, most of them were clustered in clumps, clearly distinguishable from differentiated βIII-tubulin-positive cells.

Quantitative RT-PCR was performed using cDNA prepared from RNA of PNK18 line cultured in low and high re-plating densities (50,000 and 75,000 cells/cm^2, respectively). Expression of the neural progenitor marker *Nestin* (*Nes*), post-mitotic neuronal marker *Tubb3*, MSN-specific marker *Ppp1r1b* and enkephalineric MSN-specific marker *Penk* was enriched in cultures maintained on poly-L-ornithine/laminin compared to those on gelatin (Figure 3.12). In contrast, *Oct4* expression level was higher in cultures on gelatin substratum. There was a subtle difference between low and high re-plating densities on both substrata used for the expression analysis of all the genes mentioned.

From these results, it is clear that the use of poly-L-ornithine/laminin substratum for neural differentiation is better than gelatin. The advantages include higher number of neuronal cells present, higher expression of neuronal/striatal markers and lower expression of *Oct4*. There was not any obvious difference between the different plating densities tested in terms of the proportion of differentiated and undifferentiated cells based on immunoflourescence staining or the expression of genes by qRT-PCR. However, for long-term cultures, higher cell densities would complicate the analysis due to the difficulty in distinguishing single cells and the increase of multilayer cultures. Therefore, the low re-plating density, 50,000 cells/ cm^2, was chosen as the optimal one.

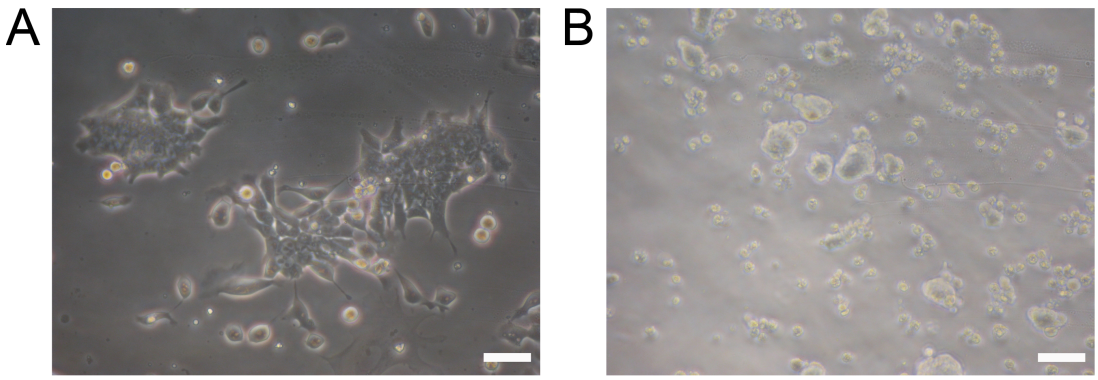

Figure 3.10: Re-plating on poly-L-ornithine/laminin-coated dish reduced cell detachment during neural differentiation. The PNK18 line was cultured on gelatin-coated plates at the start of the differentiation process. At day 4, cells were dissociated and re-plated on poly-L-ornithine/laminin- or gelatin-coated dishes. Live images taken at day 5 of differentiation showing that most of cells plated on poly-ornithine/laminin substrates were properly attached **(A)** whilst the majority of cells re-plated on gelatin-coated wells were detached **(B)**. All scale bars are 50 µm.

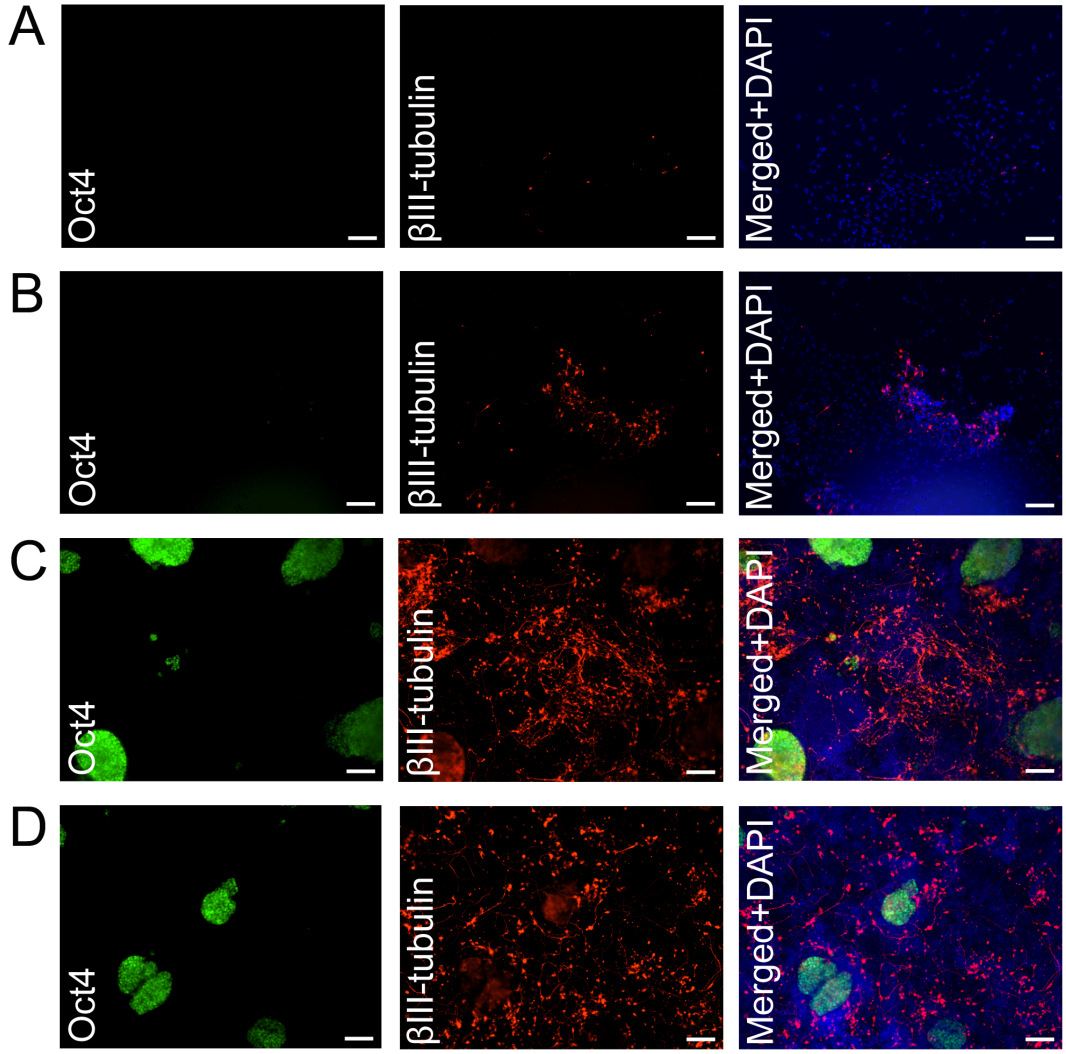

Figure 3.11: Oct4 and βIII-tubulin were highly expressed in cultures re-plated on poly-L-ornithine/laminin. The PNK18 line cultured on gelatin-coated dishes in N2B27 medium was dissociated and re-plated on gelatin- **(A and B)** or poly-L-ornithine/laminin- **(C and D)** coated dishes at day 4 of differentiation at different re-plating densities (**A and C**, 50,000 cells/cm^2, and **B and D**, 100,000 cells/cm^2). **(A and B)** Immunofluorescence staining for Oct4 and βIII-tubulin at day 12 of differentiation demonstrated no Oct4-positive cells and few βIII-tubulin-positive cells on gelatin-coated dishes at either density. **(C and D)** Higher numbers of βIII-tubulin-positive cells were found in poly-L-ornithine/laminin-coated dishes regardless of re-plating densities. All scale bars are 75 μm.

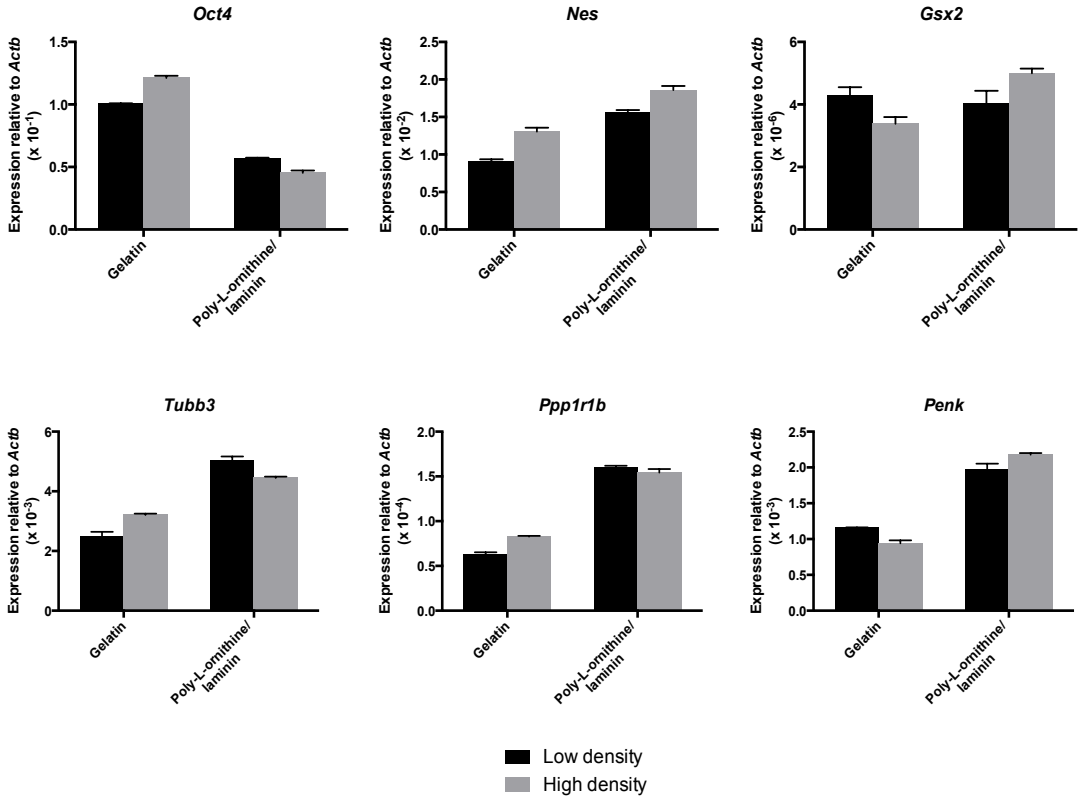

Figure 3.12: Expression of key genes from neural cells cultured on either gelatin- or poly-L-ornithine/laminin-coated dishes. PNK18 line was cultivated on gelatin-coated dishes prior to re-plating at day 4 of differentiation at either low (50,000 cells/cm^2) or high (75,000 cells/cm^2) density on either gelatin- or poly-L-ornithine/laminin-coated dishes. qRT-PCR analysis was performed at day 12 of differentiation. Enrichment of *Oct4* expression was detected in cells cultured on gelatin substratum whereas *Tubb3*, *Ppp1r1b* and *Penk* expression was more prominent in cells grown on poly-L-ornithine/laminin-coated plates. No obvious dissimilarities in gene expression were detected between low and high re-plating densities. No statistical analysis performed; n=1 for each group; Values are mean ± s.d from technical replicates.

3.2.6 Addition of DKK1, Shh and BDNF in modified N2B27 culture

We have demonstrated that both NB culture and re-plating cells on poly-L-ornithine/laminin-coated dishes contributed to increasing cell survival. We next investigated whether these two strategies, when combined with the exogenous addition of the three factors (DKK1, Shh and BDNF) would result in a higher enkephalinergic neuronal yield in cultures. PNK18 line was then cultivated in a newly generated protocol we called NB+3F (Figure 3.13 A). Cells were dissociated and re-plated onto poly-L-ornithine/laminin-coated dishes at day 7 of differentiation and flow cytometric analysis was performed at the indicated time points (Figure 3.13 B and F). As expected, we found a significant increase in the percentage of EYFP-positive cells in culture when compared to control NB cultures at day 15 and day 21 of differentiation (EYFP percentage at day15: NB 0.217±0.109, NB+3F 1.632±0.394; EYFP percentage at day 21: NB 0.158±0.048, NB+3F 1.661±0.477; values are mean ± s.e.m.; two-way ANOVA, interaction between culture condition and time point: $F_{(3,14)}$=4.432, p=0.0217; effect of culture condition: $F_{(1,14)}$=17.03, p=0.0010; effect of time point: $F_{(3,14)}$=5.096, p=0.0136; Tukey's multiple comparison test: p=0.0221 NB day 15 vs NB+3F day 15; p=0.0315 NB day 21 vs NB+3F day 21; n=3 per group). In addition, qRT-PCR analysis at day 21 showed that *Ctip2* was slightly higher expressed in NB+3F culture (Figure 3.13 E), although this did not reach a level of significant difference (p=0.3134, unpaired Student's t-test; n=4 per group). These findings suggested that the NB+3F cultures might have more EYFP-positive (and consequently more enkephalinergic) MSNs compared to NB cultures. Expression level of post-mitotic neuronal marker *Tubb3* was higher, but not significant, in NB+3F cultures (Figure 3.13 E; p=0.1788, unpaired Student's t-test; n=4 per group). This indicates that neural cells cultured with NB+3F are slightly more mature than those cultured in NB medium. The finding was consistent with the morphology observed in live images (Figure 3.13 C and D), which clearly show that the NB+3F culture contained more morphologically mature neurons. All data have supported the superiority of NB+3F over NB cultures in terms of EYFP-positive

(enkephalinergic) MSN generation. We, therefore, have used the NB+3F culture as a standard protocol for deriving enkephalinergic MSN from mESC.

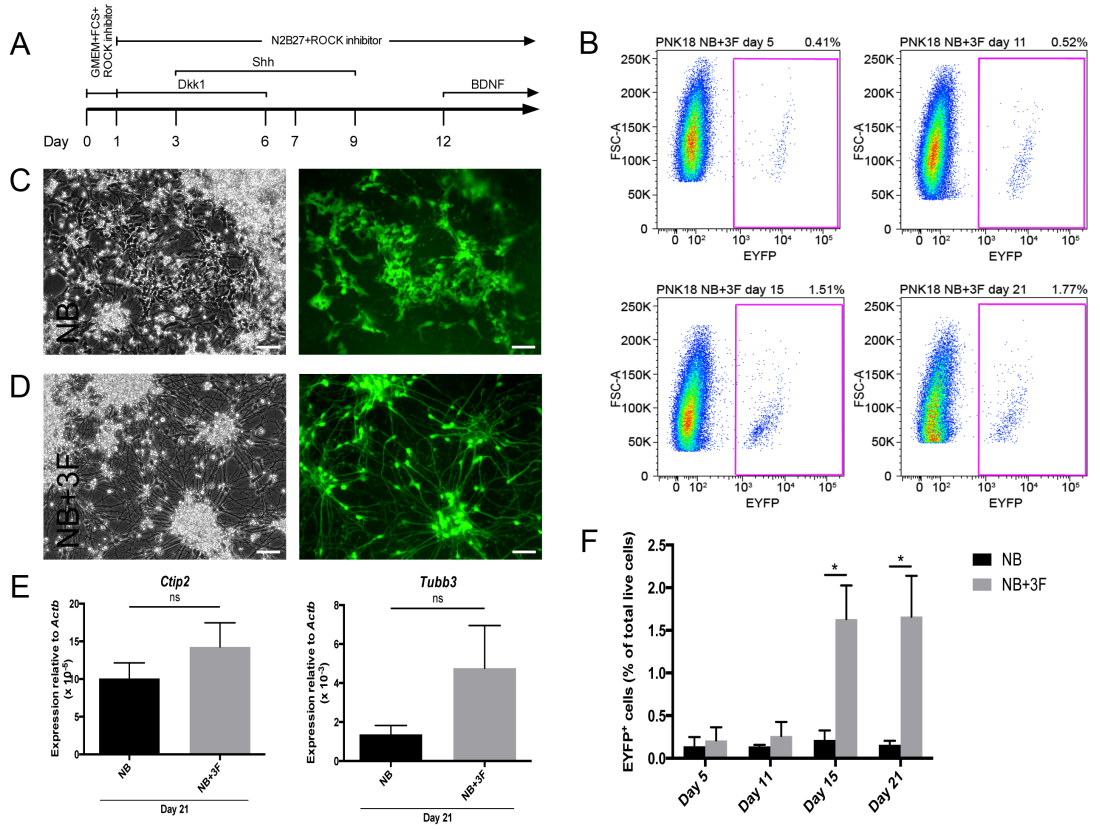

Figure 3.13: Enkephalinergic neuronal differentiation in NB+3F cultures. (A) Schematic representation of the differentiation protocol used. **(B and F)** Flow cytometric analysis at four time points during differentiation showed a gradual increase of EYFP percentage in NB+3F cultures with significant differences between NB and N3F were observed in day 15 and 21 of differentiation. **(B)** Flow cytometric plots of EYFP intensity in X axis vs FSC in Y axis and **(F)** graph showed percentage of EYFP-positive cells from total live cells analysed in the NB and NB+3F cultures (Two-way ANOVA with Tukey's post-hoc analysis; * $p<0.05$; p is adjusted p-value from Tukey's test; n=3 for each group). **(C and D)** Brightfield and fluorescent live images of NB **(C)** and NB+3F **(D)** cultures at day 23 of differentiation. EYFP-positive neural cells in NB+3F culture exhibited a more mature neuronal morphology compared to those in NB cultures. **(E)** At day 21 of differentiation, expression MSN-specific gene *Ctip2* in neural cells from NB+3F culture was slightly higher than that of NB culture. Expression of post-mitotic neuronal marker *Tubb3* expression was higher in NB+3F cultures, albeit not statistically significant (Unpaired Student's t-test; n.s., no significance; n=4 per group). This confirmed the findings from live imaging **(C and D)** that neuronal cells in NB+3F were more mature. Scale bars in **(C)** and **(D)** are 50 µm. Values are mean ± s.e.m. EYFP, enhanced yellow fluorescent protein; FSC, forward scatter; MSN, medium spiny neuron.

3.3 Surface marker identification of neural cells in culture

3.3.1 CD24 is highly expressed in differentiating neural cells but not in undifferentiated embryonic stem cells

Monolayer neural differentiation cultures are not homogeneous but composed of undifferentiated cells, neural progenitors and post-mitotic neuronal cells (Ying et al., 2003, Lorincz, 2006). In the N2B27 culture medium without re-plating step, a moderate level of *Oct4* expression is found even in day 35 of differentiation (Figure 3.6 D), indicating that there are still pluripotent cells present in the culture. To distinguish between undifferentiated and differentiated cells by flow cytometry, we sought surface markers described in the literature, which could be used to distinguish between these two populations. Amongst many markers the heat stable antigen CD24 has been described to define a neuronal population derived from hPSCs, when used together with CD15 and CD29 (Pruszak et al., 2009) or CD15, CD44 and CD184 (Yuan et al., 2011). Interestingly, CD24 is expressed at a low level in mESCs and its expression level increases gradually along neural differentiation with strongest expression observed in post-mitotic neurons (Pruszak et al., 2009). These findings encouraged us to address whether CD24 alone was sufficient to isolate neuronal populations from undifferentiated ESCs in culture. ESCs and cells from three time points (day 5, 15 and 21) throughout NB differentiation were stained with CD24 antibody prior to flow cytometric analysis. The majority of cells from all of the differentiation time points analysed were found to express higher levels of CD24 compared to ESCs (Figure 3.14 A and B). When cells were classified into two groups, CD24-low and CD24-high, there was a significant difference in terms of percentage of the two populations in all time point analysed (Figure 3.14 A and C; two-way ANOVA, interaction between CD24 expression level and time point: $F_{(3,16)}=88.83$, $p<0.0001$; effect of CD24 expression level: $F_{(1,16)}=70.25$, $p<0.0001$; effect of time point: $F_{(3,16)}=0.2518$, $p=0.8589$; Tukey's multiple comparison test: $p<0.0001$ ESC, day 15 and day 21 $CD24^{lo}$ vs $CD24^{hi}$; and $p=0.0003$ day 5 $CD24^{lo}$ vs $CD24^{hi}$; n=3 per group). Approximately 78% of the live ESCs analysed could be

classified as CD24-low (Figure 3.14 A and C; $CD24^{lo}$: 78.20±4.09, $CD24^{hi}$: 9.65±0.39; values are mean of percentage of live cells analysed ± s.e.m.) whilst the majority of differentiating neural cells at any stage were CD24-high with less than a quarter of live cells remaining as CD24-low (Figure 3.14 A and C; $CD24^{lo}$: 24.40±7.25 (day 5), 9.50±5.70 (day 15) and 11.61±1.24 (day 21), $CD24^{hi}$: 68.23±2.41 (day 5), 86.63±5.73 (day 15) and 78.40±3.34 (day 21); values are mean of percentage of live cells analysed ± s.e.m.). The data indicates that ESCs and differentiating neural cells express distinct levels of CD24. It also confirms the finding from Pruszak and colleagues that CD24 expression is increased during mESC differentiation towards neural lineages (Pruszak et al., 2009).

Confirmation of the gating settings used for the CD24-low and CD24-high populations was achieved by measuring the level of *Cd24a* (the gene encoding CD24) expression by qRT-PCR of cells sorted from the two populations (Figure 3.14 D). *Cd24a* expression in the CD24-low fraction was significantly lower than in the CD24 high population in all the differentiating samples but not in ESCs (two-way ANOVA, interaction between CD24 expression level and time point: $F_{(3,10)}=3.004$, $p=0.0815$; effect of CD24 expression level: $F_{(1,10)}=73.71$, $p<0.0001$; effect of time point: $F_{(3,10)}=6.239$, $p=0.0117$; Uncorrected Fisher's LSD test: $p=0.1510$ ESC $CD24^{lo}$ vs $CD24^{hi}$; $p=0.0004$ day 5 $CD24^{lo}$ vs $CD24^{hi}$; $p=0.0006$ day 15 $CD24^{lo}$ vs $CD24^{hi}$; and $p=0.0002$ day 21 $CD24^{lo}$ vs $CD24^{hi}$; n=2 per group for ESCs, day 5 and day 15, and n=3 for day 21). This confirms the gating we used reflects the exact expression of *Cd24a*.

Since EYFP will be expressed when cells are committed to an enkephalinergic neural fate, we hypothesised that most of the EYFP-positive cells should be CD24-high. Flow cytometric analysis revealed that EYFP-positive cells were equally resided in both CD24 low and CD24 high fractions when cells were pluripotent (Figure 3.14 E and F). In contrast, there was an enrichment of EYFP-positive cells in the CD24-high fraction in differentiating neural cells. The proportion of CD24-high/EYFP-positive cells was significantly higher than that of CD24-low/EYFP-positive cells suggesting higher CD24 expression in more mature cells.

(two-way ANOVA, interaction between CD24 expression level and time point: $F_{(3,16)}$=11.41, p=0.0003; effect of CD24 expression level: $F_{(1,16)}$=93.47, p<0.0001; effect of time point: $F_{(3,16)}$=8.004 x 10^{-14}, p>0.999; Tukey's multiple comparison test: p<0.001 for day 5 % $EYFP^+$ cells in $CD24^{lo}$ vs % $EYFP^+$ cells in $CD24^{hi}$; p<0.001 for day 15 % $EYFP^+$ cells in $CD24^{lo}$ vs % $EYFP^+$ cells in $CD24^{hi}$; and p=0.007 for day 21 % $EYFP^+$ cells in $CD24^{lo}$ vs % $EYFP^+$ cells in $CD24^{hi}$; n=3 per group).

To investigate this further cells were sorted from both CD24-low and CD24-high populations from ESCs and differentiating cells at day 5, 15 and 21, and qRT-PCR performed (Figure 3.15). In addition to pluripotency gene (*Oct4*) and pan-neuronal genes (*Tubb3*, *Rbfox3* and *Ncam1*), neural progenitor genes (*Sox1*, *Nes* and *Pax6*), the oligodendrocyte marker (*Plp1*) and glial marker (*Gfap*) were included in the analysis. As expected, significant difference in *Oct4* expression were observed in two populations (based on CD24 gating) and the four time points (Figure 3.15 and Table 3.2 for post-hoc analysis; two-way ANOVA, interaction between CD24 expression level and time point: $F_{(3,10)}$=6.394, p=0.0108; effect of CD24 expression level: $F_{(1,10)}$=78.50, p<0.0001; effect of time point: $F_{(3,10)}$=15.41, p=0.0004; n=2 per group for ESCs, day 5, day 15 and n=3 for day 21). Expression of *Oct4*, was very high in the ESC sample regardless of CD24 expression level (no statistical difference between two populations). *Oct4* was also highly expressed in CD24-low population throughout neural differentiation. In contrast, *Oct4* expression in the CD24-high fraction declined during the differentiation process.

The expression of three neural progenitor markers *Sox1*, *Nes* and *Pax6* was statistically different between CD24 low and CD24 high fractions (Figure 3.15 and Table 3.2 for post-hoc analysis; two-way ANOVA, interaction between CD24 expression level and time point: $F_{(3,10)}$=2.543, p=0.1151 for *Sox1*; $F_{(3,10)}$=0.6658, p=0.5919 for *Nes*; and $F_{(3,10)}$=13.27, p=0.0008 for *Pax6*; effect of CD24 expression level: $F_{(1,10)}$=15.83, p=0.0026 for *Sox1*; $F_{(1,10)}$=11.49, p=0.0069 for *Nes*; and $F_{(1,10)}$=48.61, p<0.0001 for *Pax6*; effect of time point: $F_{(3,10)}$=3.172, p=0.0723 for *Sox1*; $F_{(3,10)}$=0.7846, p=0.5293 for *Nes*; and $F_{(3,10)}$=21.63, p=0.0001 for *Pax6*; n=2 per group for ESCs, day 5, day 15 and n=3 for day 21). These markers were

expressed in a constant and relatively low level in CD24-low fraction during differentiation. This suggests that the majority of cells in CD24-low population do not acquire a neural fate.

Likewise, expression of neuronal genes such as *Tubb3*, *Rbfox3* and *Ncam1* was also found to be significantly different between CD24-low and CD24-high populations (Figure 3.15 and Table 3.3 for post-hoc analysis; two-way ANOVA, interaction between CD24 expression level and time point: $F_{(3,10)}$=2.688, p=0.1031 for *Tubb3*; $F_{(3,10)}$=6.180, p=0.0120 for *Rbfox3*; and $F_{(3,10)}$=2.093, p=0.1649 for *Ncam1*; effect of CD24 expression level: $F_{(1,10)}$=8.556, p=0.0152 for *Tubb3*; $F_{(1,10)}$=25.88, p=0.0005 for *Rbfox3*; and $F_{(1,10)}$=9.707, p=0.0110 for *Ncam1*; effect of time point: $F_{(3,10)}$=3.101, p=0.0760 for *Tubb3*; $F_{(3,10)}$=6.856, p=0.0086 for *Rbfox3*; and $F_{(3,10)}$=2.378, p=0.1310 for *Ncam1*; n=2 per group for ESCs, day 5, day 15 and n=3 for day 21). Significant enrichment of *Tubb3* (day 21), *Rbfox3* (days 15 and day 21) and *Ncam1* (day 15 and day 21) expression in the CD24-high population was observed. These pan-neuronal genes were steadily expressed at a minimal level in CD24-low cells at all stages analysed but showed an upward trend of expression in the CD24-high subset as differentiation progressed.

Unlike neural progenitor and neuronal genes, the oligodendrocyte-specific gene *Plp1,* and the astrocytic-specific gene *Gfap,* showed no difference in terms of their expression at any stage analysed (Figure 3.15; two-way ANOVA, interaction between CD24 expression level and time point: $F_{(3,10)}$=1.306, p=0.3260 for *Plp1*; and $F_{(3,10)}$=0.5638, p=0.6511 for *Gfap*; effect of CD24 expression level: $F_{(1,10)}$=3.797, p=0.0800 for *Plp1*; $F_{(1,10)}$=0.4654, p=0.5106 for *Gfap*; effect of time point: $F_{(3,10)}$=1.570, p=0.2573 for *Plp1*; $F_{(3,10)}$=0.8338, p=0.5054 for *Gfap*; n=2 per group for ESCs, day 5, day 15 and n =3 for day 21). This could be explained by the fact that oligodendroglial lineages are born later than neuronal cells *in vivo* (Qian et al., 2000). Expression of these two markers, therefore, is expected to start at the later stages of differentiation. In agreement with this, expression of these genes in the CD24-high subset exhibited a sharp increase from day 15 onwards, whereas the increased expression of pan-neuronal genes began from day 5 onwards.

Overall, these findings support the idea that CD24 is beneficial in distinguishing differentiated cells from any pluripotent cells that might remain in the culture.

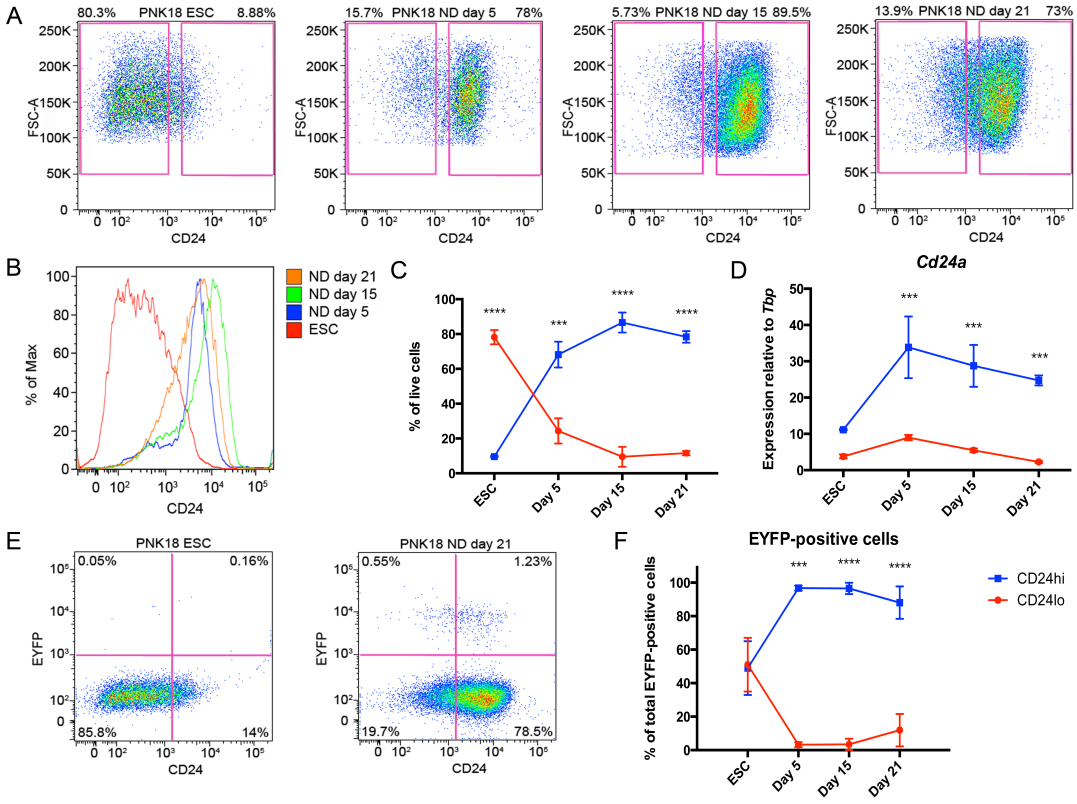

Figure 3.14: Distinct level of CD24 expression profiles differs between ESCs and differentiating neural cells. Flow cytometric analysis of CD24-positive cells from PNK18 ESCs and cells underwent neural differentiation from three time points of neural differentiation (day 5, 15 and 21). **(A)** Plots show the gates for CD24-low and CD24-high populations on the left and right halves, respectively. **(B)** Summary of CD24 expression profiles from all samples is shown in a histogram. **(C)** CD24-low is the main population in ESCs whilst differentiating cells are mostly CD24-high. **(D)** qRT-PCR analysis of *Cd24a* expression in CD24 low and CD24 high populations. **(E)** Plots between CD24 (X axis) and EYFP (Y axis) and **(F)** a graph showing percentage of EYFP-positive cells in each population in differentiating neural cells and ESCs. An enrichment of EYFP-positive cells in CD24-high fraction is observed in differentiating neural cells but not in ESCs. **(C, D and F)** $CD24^{lo}$ (in red), CD24-low fraction; $CD24^{hi}$ (in blue), CD24-high fraction. **(C and F)** Two-way ANOVA with Tukey's post-hoc analysis; *** $p<0.001$; **** $p<0.0001$; p are adjusted p-value from Tukey's test; n=3 for each group. **(D)** Two-way ANOVA with uncorrected Fisher's LSD test; *** $p<0.001$; n=2 except day 21, n=2; Values are mean ± s.e.m. ESCs, embryonic stem cells; EYFP, enhanced yellow fluorescent protein.

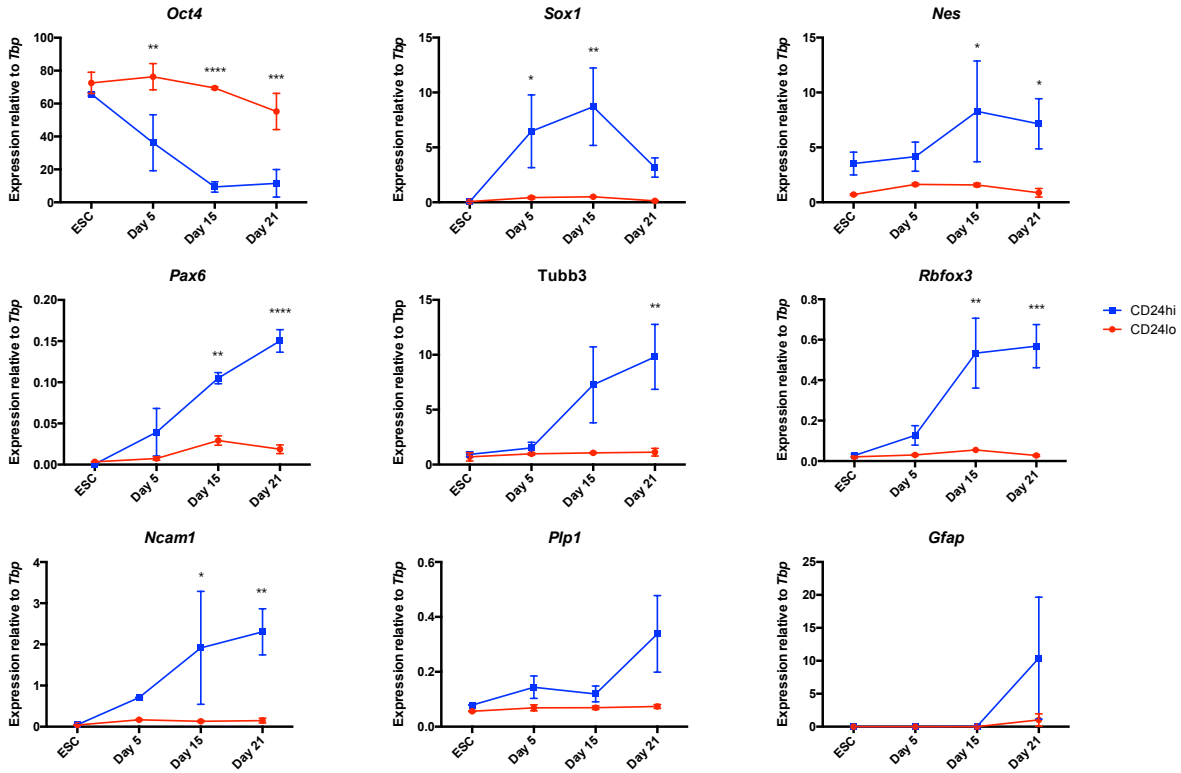

Figure 3.15: Expression of pluripotency gene and neural genes in CD24-low and CD24-high populations during neural differentiation. CD24-low and CD24-high fractions from ESCs and cells from three differentiation time points (day 5, 15 and 21) were sorted by FACS. qRT-PCR showed consistently high level of *Oct4* in CD24-low population regardless of time points analysed. Additionally, expression of neural progenitors genes (*Sox1*, *Nes* and *Pax6*), pan-neuronal genes (*Tubb3*, *Rbfox3* and *Ncam1*), and oligodendrocyte gene (*Plp1*) in CD24-low fraction of differentiating culture remained relatively low and comparable to their expression in ESCs. In CD24-high population, an opposite trend between *Oct4* and neural gene expression was observed, *Oct4* expression was declining along differentiation whereas the expression of most neural genes was increasing as differentiation progressed. $CD24^{lo}$ (in red), CD24-low population; $CD24^{hi}$ (in blue), CD24-high population. Two-way ANOVA with uncorrected Fisher's LSD test; * p<0.05; ** p<0.01; *** p<0.001; **** p<0.0001; n=2 for each group except day 21, n=3; Values are mean ± s.e.m. ESCs, embryonic stem cells; FACS, fluorescence-activated cell sorting.

Table 3.2: Statistical analysis of expression of pluripotency and neural progenitor genes during neural differentiation (related to Figure 3.15)

Gene	Time point	Population compared	P-value
Oct4	ESC	$CD24^{lo}$ vs $CD24^{hi}$	0.4608
	Day 5	$CD24^{lo}$ vs $CD24^{hi}$	0.0011
	Day 15	$CD24^{lo}$ vs $CD24^{hi}$	<0.0001
	Day 21	$CD24^{lo}$ vs $CD24^{hi}$	0.0001
Sox1	ESC	$CD24^{lo}$ vs $CD24^{hi}$	0.9952
	Day 5	$CD24^{lo}$ vs $CD24^{hi}$	0.0237
	Day 15	$CD24^{lo}$ vs $CD24^{hi}$	0.0047
	Day 21	$CD24^{lo}$ vs $CD24^{hi}$	0.1319
Nes	ESC	$CD24^{lo}$ vs $CD24^{hi}$	0.3398
	Day 5	$CD24^{lo}$ vs $CD24^{hi}$	0.3926
	Day 15	$CD24^{lo}$ vs $CD24^{hi}$	0.0393
	Day 21	$CD24^{lo}$ vs $CD24^{hi}$	0.0214
Pax6	ESC	$CD24^{lo}$ vs $CD24^{hi}$	0.8701
	Day 5	$CD24^{lo}$ vs $CD24^{hi}$	0.1017
	Day 15	$CD24^{lo}$ vs $CD24^{hi}$	0.0016
	Day 21	$CD24^{lo}$ vs $CD24^{hi}$	<0.0001

P-value from uncorrected Fisher's LSD test; n=2 for each group except day 21, n=3. ESC, embryonic stem cell; $CD24^{lo}$, CD24-low population; $CD24^{hi}$, CD24-high population

Table 3.3: Statistical analysis of neuronal gene expression during neural differentiation (related to Figure 3.15)

Gene	Time point	Population compared	P-value
Tubb3	ESC	$CD24^{lo}$ vs $CD24^{hi}$	0.9364
	Day 5	$CD24^{lo}$ vs $CD24^{hi}$	0.8493
	Day 15	$CD24^{lo}$ vs $CD24^{hi}$	0.0509
	Day 21	$CD24^{lo}$ vs $CD24^{hi}$	0.0035
Rbfox3	ESC	$CD24^{lo}$ vs $CD24^{hi}$	0.9587
	Day 5	$CD24^{lo}$ vs $CD24^{hi}$	0.4200
	Day 15	$CD24^{lo}$ vs $CD24^{hi}$	0.0020
	Day 21	$CD24^{lo}$ vs $CD24^{hi}$	0.0002
Ncam1	ESC	$CD24^{lo}$ vs $CD24^{hi}$	0.9902
	Day 5	$CD24^{lo}$ vs $CD24^{hi}$	0.4884
	Day 15	$CD24^{lo}$ vs $CD24^{hi}$	0.0394
	Day 21	$CD24^{lo}$ vs $CD24^{hi}$	0.0056

P-value from uncorrected Fisher's LSD test; n=2 for each group except day 21, n=3. ESC, embryonic stem cell; $CD24^{lo}$, CD24-low population; $CD24^{hi}$, CD24-high population

3.3.2 CD133 does not distinguish between neural progenitors and post-mitotic neurons

Although the use of CD24 excludes pluripotent cells in differentiating neural cultures, we further sought other surface antigens that could be used for labelling neural progenitors. This allows further characterisation of the enkephalinergic neurons and may be useful for future applications such as transplantation of purified neural progenitors. A literature search suggested CD133 (also known as Prominin-1), as a candidate marker. It is highly expressed in neural progenitor cells and has been used to purify mouse neural progenitor from postnatal forebrain (Corti et al., 2007) and cerebellum (Lee et al., 2005). Therefore, we tested the feasibility of using this marker to define a neural progenitor population in culture. The majority of ESCs did not express CD133 (Figure 3.16; $CD133^-$: 71.53±21.81, $CD133^+$: 12.81±10.66; n=3 per group, values are mean of percentage of live cells analysed ± s.e.m.) and consistent with previous studies, a proportion of cells in CD133-negative fraction became less prominent and was comparable to that of CD133-positive fraction as differentiation progresses. (Figure 3.16; $CD133^-$: 32.90±7.18, $CD133^+$: 45.67±8.67 for day 5; $CD133^-$: 37.53±11.93, $CD133^+$: 47.20±14.86 for day 15; $CD133^-$: 42.00±15.73, $CD133^+$: 45.50±16.20 for day 21; two-way ANOVA, interaction between CD133 expression level and time point: $F_{(3,16)}$=2.883, p=0.0683; effect of CD133 expression level: $F_{(1,16)}$=0.6891, p=0.4187; effect of time point: $F_{(3,16)}$=0.03812, p=0.9897; n=3 per group, values are mean of percentage of live cells analysed ± s.e.m.).

Since the CD133-negative population in differentiating cultures will consist of both undifferentiated ESCs and post-mitotic neuronal cells, we decided to use a combination of CD133 and CD24 to define three populations in culture. We hypothesised that CD24-high/CD133-positive and CD24-high/CD133-negative populations would define neural progenitors and post-mitotic neural cells, respectively, whilst CD24-low subset would label undifferentiated cells.

As we have previously shown (Chapter 3.3.1) the CD24-low fraction defines undifferentiated cells in culture, we, therefore, excluded this population from further

analysis. (Figure 3.17 A). The percentage of CD24-high/CD133-negative and CD24-high/CD133-positive populations is not significantly different at any time point analysed (Figure 3.17 B; two-way ANOVA, interaction between CD24/CD133 expression level and time point: $F_{(3,16)}$=0.3785, p=0.7698; effect of CD24/CD133 expression level: $F_{(1,16)}$=1.375, p=0.2581; effect of time point: $F_{(3,16)}$=3.342, p=0.0458; n=3 per group). This was unexpected, however, it is possible that during differentiation, neural progenitors proliferate at the same rate as cells exiting the progenitor stage thus the percentage of cells in both fractions remains unchanged.

To confirm that the two populations, CD24-high/CD133-negative and CD24-high/CD133-positive are post-mitotic cells and neural progenitors, respectively, cells were sorted from both fractions at different stages and qRT-PCR analysis performed for key genes involved in ESC neural differentiation. Unexpectedly, no significant difference in expression levels was found in most of the genes examined in the two populations (Figure 3.18). The level of *Oct4* expression exhibited a significant reduction coincident with differentiation progress but no statistical difference was observed between the CD24-high/CD133-negative and CD24-high/CD133-positive fractions. (Figure 3.18; two-way ANOVA, interaction between CD24/CD133 expression level and time point: $F_{(3,8)}$=0.3436, p=0.7948; effect of CD24/CD133 expression level: $F_{(1,8)}$=1.304, p=0.2865; effect of time point: $F_{(3,8)}$=15.05, p=0.0012; n=2 per group). Expression of neural progenitor genes *Sox1*, *Nes* and *Pax6* were also identical in both populations (Figure 3.18; two-way ANOVA, interaction between CD24/CD133 expression level and time point: $F_{(3,8)}$=0.02115, p=0.9955 for *Sox1*; $F_{(3,8)}$=0.1361, p=0.9357 for *Nes*; and $F_{(3,8)}$=0.3716, p=0.7759 for *Pax6*; effect of CD24/CD133 expression level: $F_{(1,8)}$=0.09059, p=0.7711 for *Sox1*; $F_{(1,8)}$=0.2868, p=0.6069 for *Nes*; and $F_{(1,8)}$=1.527, p=0.2517 for *Pax6*; effect of time point: $F_{(3,8)}$=4.106, p=0.0489 for *Sox1*; $F_{(3,8)}$=1.651, p=0.2535 for *Nes*; and $F^{(3,8)}$=2.295, p=0.1546 for *Pax6*; n=2 per group) and reached peak expression at day15. Expression of the pan-neuronal marker *Tubb3* showed a significant difference between populations at day 15 and 21 of differentiation (Figure 3.18; two-way ANOVA, interaction between CD24/CD133 expression level and time point:

$F_{(3,8)}$=2.150, p=0.1721; effect of CD24/CD133 expression level: $F_{(1,8)}$=7.148, p=0.0282; effect of time point: $F_{(3,8)}$=4.523, p=0.0390; Uncorrected Fisher's LSD test: p=0.9700 ESC $CD24^{hi}/CD133^{-}$ vs $CD24^{hi}/CD133^{+}$; p=0.9244 day 5 $CD24^{hi}/CD133^{-}$ vs $CD24^{hi}/CD133^{+}$; p=0.0278 day 15 $CD24^{hi}/CD133^{-}$ vs $CD24^{hi}/CD133^{+}$; and p=0.0354 day 21 $CD24^{hi}/CD133^{-}$ vs $CD24^{hi}/CD133^{+}$; n=2 per group). The neuronal genes *Rbfox3* and *Ncam1* and oligodendroglial genes (*Plp1* and *Gfap*) revealed no difference in their expression pattern (Figure 3.18; two-way ANOVA, interaction between CD24/CD133 expression level and time point: $F_{(3,8)}$=0.9586, p=0.4577 for *Rbfox3*; $F_{(3,8)}$=0.1456, p=0.9296 for *Ncam1*; $F_{(3,8)}$=1.152, p=0.3858 for *Plp1*; and $F_{(3,8)}$=0.8773, p=0.4923 for *Gfap*; effect of CD24/CD133 expression level: $F_{(1,8)}$=2.673, p=0.1407 for *Rbfox3*; $F_{(1,8)}$=0.04795, p=0.8321 for *Ncam1*; $F_{(1,8)}$=0.6277, p=0.4511 for *Plp1*; and $F_{(1,8)}$=0.8714, p=0.3779 for *Gfap*; effect of time point: $F_{(3,8)}$=3.823, p=0.0574 for *Rbfox3*; $F_{(3,8)}$=2.905, p=0.1012 for *Ncam1*; $F_{(3,8)}$=0.6890, p=0.5838 for *Plp1*; and $F_{(3,8)}$=1.134, p=0.3919 for *Gfap*; n=2 per group). These findings indicated that both the CD24-high/CD133-negative and CD24-high/CD133-positive populations have similar expression profiles of the genes examined. Therefore use of both CD24 and CD133 was not beneficial to further discriminate neural progenitors from post-mitotic neural cells in NB cultures. For this reason we decided to use only CD24 for further flow cytometric analyses.

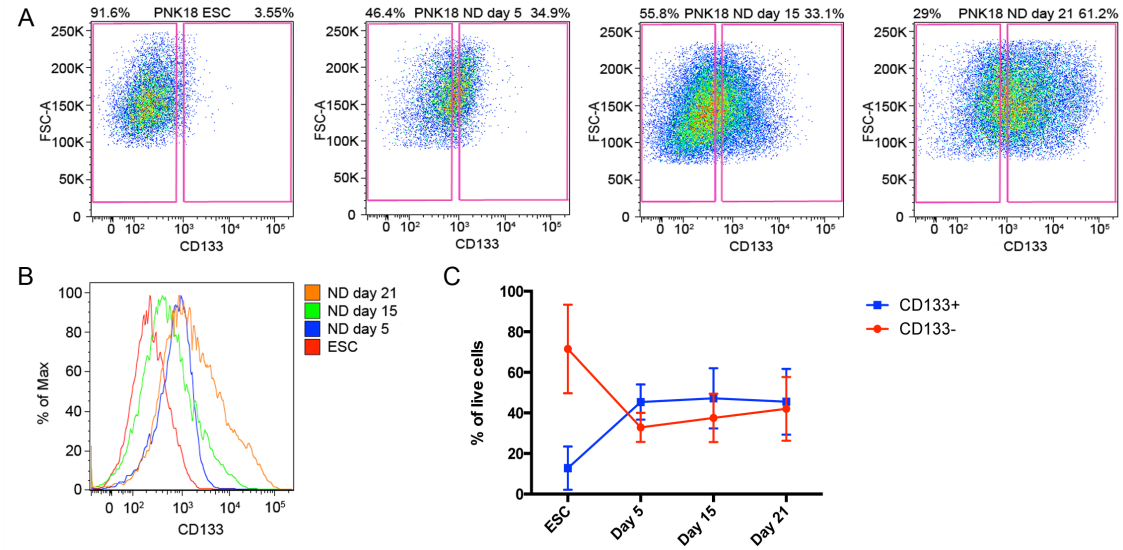

Figure 3.16: Expression of CD133 in ESCs and differentiating cells in NB cultures. Flow cytometric analysis of ESCs and cells at three differentiation time points (day 5, 15 and 21) stained with a CD133 antibody. **(A)** Plots show gating for CD133-negative (left) and CD133-positive (right) subsets. **(B)** Summary of CD133 expression showing a nearly identical pattern of expression in all stages analysed. **(C)** CD133 expression profile throughout differentiation. ESC sample had high percentage of CD133-negative population in contrast to differentiating cells, which show a similar proportion of CD133-negative and CD133-positive populations. Two-way ANOVA; No significant difference was found; n=3 for each group; Values are mean ± s.e.m. ESCs, embryonic stem cells.

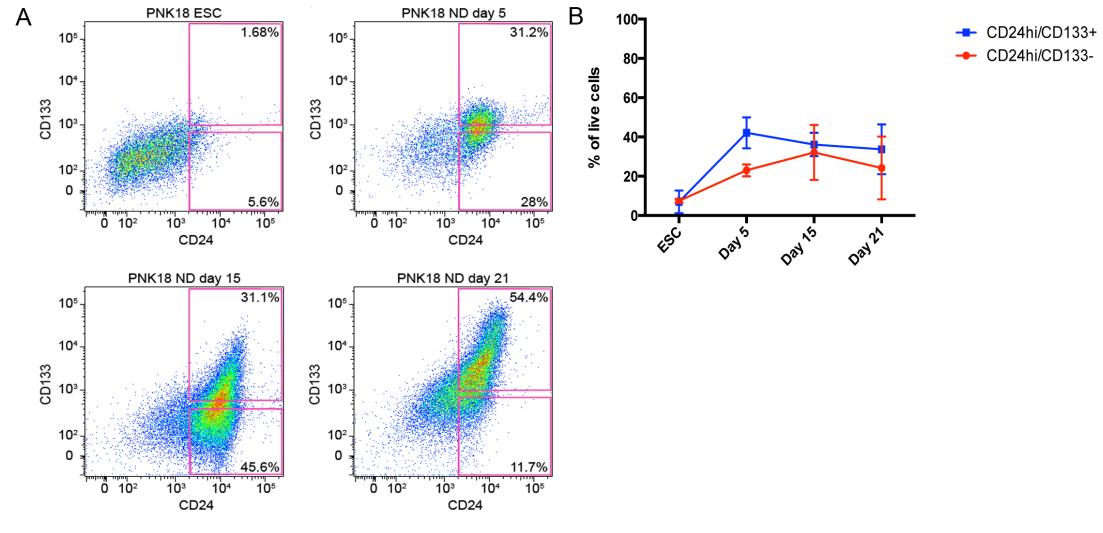

Figure 3.17: The use of CD24 and CD133 to define subpopulations of cells during neural differentiation. Flow cytometric analysis of CD24 and CD133 in ESCs and differentiating cells. **(A)** Plots gated for CD24-high/CD133-negative and CD24-high/CD133-positive populations. **(B)** Quantification of the percentage of cells in both fractions at all time point analysed. $CD24^{hi}/CD133^{-}$ (in red), CD24 high/CD133-negative fraction; $CD24^{hi}/CD133^{+}$ (in blue), CD24 high/CD133-positive fraction. Two-way ANOVA; No significant difference was found; n=3 for each group; Values are mean ± s.e.m. ESCs, embryonic stem cells.

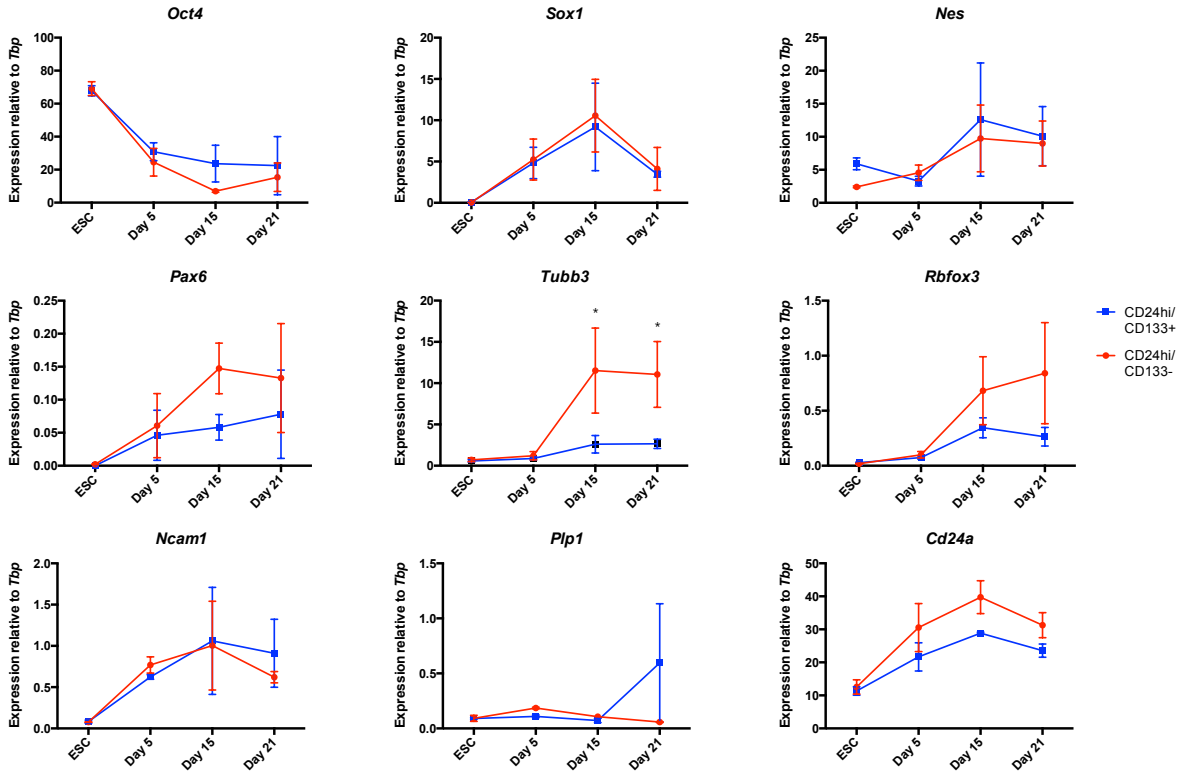

Figure 3.18: Gene expression profiles of CD24-high/CD133-negative and CD24-high/CD133-positive populations during neural differentiation. CD24-high/ CD133-negative and CD24-high/CD133-positive fractions from ESCs and cells at three differentiation time points (day 5, 15 and 21) were sorted by FACS. qRT-PCR analysis shows the expression pattern of most genes (except *Tubb3* at day 15 and day 21 of differentiation) in the two populations were similar. $CD24^{hi}/CD133^{-}$ (in red), CD24 high/CD133-negative fraction; $CD24^{hi}/CD133^{+}$ (in blue), CD24 high/CD133-positive fraction. Two-way ANOVA with uncorrected Fisher's LSD test; * $p<0.05$; n=2 for each group; Values are mean ± s.e.m. ESCs, embryonic stem cells; FACS, fluorescence-activated cell sorting.

3.4 *In vitro* characterisation of embryonic stem cell-derived enkephalinergic neurons

3.4.1 Characterisation of embryonic stem cell-derived EYFP-positive neural cells in NB and NB+3F cultures

We have shown that the NB+3F culture medium resulted in a higher percentage of EYFP-positive cells compared to NB medium (Chapter 3.2.6). To confirm the identity of EYFP-positive cells, which were expected to be enkephalinergic MSNs, we next characterised the phenotype of the EYFP-positive neurons in both culture conditions by immunocytofluorescence staining. Consistent with the FACS analysis (Figure 3.13), we found that the number of EYFP-positive cells (by qualitative analysis) in NB culture was lower than that in the NB+3F culture. However, only a few EYFP neurons were enkephalin-positive (Figure 3.19 A and 3.20 A). This finding was more obvious in the NB+3F culture. Staining of E14 (wild-type) mESCs cultured similarly demonstrated that those grown in the NB medium had a higher proportion of βIII-tubulin-positive/enkephalin-positive neurons than NB+3F (Figure 3.21 A and B; qualitative analysis), confirming what was found in the PNK18 line. This discrepancy could be explained by the fact that enkephalin is a neurotransmitter, which is released by neurons in the central nervous system, therefore, hindering co-localisation. Another possibility is that the EYFP-positive/ enkephalin-negative neurons had previously been enkephalinergic. EYFP expression results from the expression of, and recombination by, Cre-recombinase, which is controlled by the *Penk* promoter. Activation of *Penk* promoter leads to Cre-mediated removal of the stop cassette in front of the EYFP reporter gene. Transient activation of the *Penk* promoter could potentially produce recombination and EYFP expression. However, the endogenous *Penk* promoter could have been inactive at the time of analysis and no enkephalin would be made from such cells. To understand which one of the two hypotheses was the cause of the absence of enkephalin in EYFP-positive neurons, we performed qRT-PCR analysis of *Penk* mRNA levels from bulk cultures at day 21 of differentiation (Figure 3.22) in the two culture conditions. If the first hypothesis was true; enkephalin was still produced from the EYFP neurons but is

undetectable because it was released from the cells, the *Penk* mRNA levels in NB+3F culture should be higher than that of the NB culture. However, if the EYFP neurons in the NB+3F culture were not expressing enkephalin at the time of analysis, the *Penk* mRNA levels in the NB+3F culture should be lower than that of the NB culture. We found that the expression of *Penk* was, indeed, significantly down-regulated in the NB+3F culture (p=0.0018, unpaired Student's t-test, n=4 per group), confirming the finding from the immunostaining data. Thus, the EYFP-positive cells in the NB+3F culture may have committed to an enkephalinergic fate during differentiation but they subsequently lost that identity. To investigate this possibility, we performed qRT-PCR analysis of PNK18 line cultured in NB or NB+3F conditions on earlier stages of differentiation, at the ESC stage, day 3, day 5, day 7 and day 15 of differentiation. The first three time points are prior to the addition of BDNF in the NB+3F differentiation protocol, therefore, are called NB+D+S (Figure 3.23 A). Expression of *Penk* in NB+D+S (NB+3F) culture was significantly up-regulated at day 5 of differentiation compared to controls (Figure 3.23 B and C; one-way ANOVA: $F_{(2,3)}$=404.1, p=0.0002; Tukey's multiple comparison test: p=0.0020 ESC vs NB day 5; p=0.0001 ESC vs NB+D+S day 5; p=0.0013 NB day 5 vs NB+D+S day 5; n=2 for each group) *Penk* mRNA levels in NB+D+S (NB+3F) culture dropped sharply at day 7 of differentiation, reaching the lowest levels at day 15 and 21 (Figure 3.23 B). In contrast, the expression of *Penk* in the NB culture showed only modest changes with no obvious fluctuation. This, therefore, provides an explanation of the higher proportion of EYFP-positive cells despite the lower expression of *Penk* in NB+3F cultures at the later time point of differentiation.

The expression of other striatopallidal markers, such as *Adora2a* and *Drd2* at day 21 of differentiation were slightly up-regulated in NB+3F culture compared to NB culture, although not at a significantly different level (Figure 3.22; p=0.4648 for *Adora2a* and p=0.2903 for *Drd2*, unpaired Student's t-test, n=4 per group). All of the data provided here indicated that the addition of the three factors in the NB medium had a detrimental effect on enkephalin expression, but not on *Adora2a* and *Drd2*.

We then investigated whether EYFP-positive neurons demonstrated other features of a medium spiny neuron phenotype. Immunostaining analysis showed that some EYFP neurons in both culture conditions were Darpp32-positive (Figure 3.19 B and 3.20 B) and GABAergic (Figure 3.19 C and 3.20 C), resembling the *in vivo* MSNs. A GABAergic phenotype was also found in the E14 line cultured in both media for 21 days (Figure 3.21 C and D). The expression profiles of both *Ppp1r1b* and *Gad1* (Figure 3.22), the genes that encode for Darpp23 and the enzyme used for GABA synthesis, respectively, showed no difference between the NB and NB+3F cultures (p=0.4631 for *Ppp1r1b* and p=0.2003 for *Gad1*, unpaired Student's t-test, n=4 per group), although there was a higher trend in the NB+3F sample. Likewise, other MSN markers such as *Foxp1* and *Foxp2* were similarly expressed in both culture conditions (Figure 3.22; NB vs NB+3F cultures; p=0.8694 for *Foxp1* and p=0.6905 for *Foxp2*, unpaired Student's t-test, n=4 per group). Lastly, we also checked the expression of substance P (also known as tachykinin or *Tac1*) and *Drd1a*, markers for striatonigral MSNs. Although no significant difference in expression levels was detected between the two cultures (Figure 3.22; p=0.1318 for *Tac1* and p=0.1831 for *Drd1a*, unpaired Student's t-test, n=4 per group), the NB+3F culture showed higher trend of expression compared to the NB culture.

We next corroborated the gene expression finding from bulk cultures by analysing defined populations of cells within the cultures. We FACS sorted CD24-high/EYFP-positive cells and CD24-high/EYFP-negative cells from day 21 of both NB and NB+3F cultures (Figure 3.24). Quantitative RT-PCR analysis demonstrated a significant difference in *Penk* expression between different culture conditions and populations (Figure 3.24; two-way ANOVA, interaction between population and culture condition: $F_{(1,9)}$=5.141, p=0.0496; effect of population: $F_{(1,9)}$=6.176, p=0.0347; effect of culture condition: $F_{(1,9)}$=14.78, p=0.0039; n=3 per group except CD24-high/EYFP-negative in NB culture, n=4). Similar to data from bulk culture, *Penk* was significantly down-regulated in CD24-high/EYFP-positive cells from NB+3F culture compared to NB culture (Tukey's multiple comparison test: p=0.0104). In the absence of the three factors, *Penk* is statistically enriched in EYFP-

positive population compared to the negative population (Tukey's multiple comparison test: p=0.0293). This supported the specificity of EYFP reporter expression. To confirm the purity of our FACS sorted populations, we checked EYFP expression and found a significant difference between population (CD24-high/EYFP-positive cells vs CD24-high/EYFP-negative cells) but not culture condition (Figure 3.24; two-way ANOVA, interaction between population and culture condition: $F_{(1,5)}$=2.349, p=0.1859; effect of population: $F_{(1,5)}$=.115.2, p=0.0001; effect of culture condition: $F_{(1,5)}$=1.171, p=0.3287; n=2 per group except CD24-high/EYFP-negative in NB culture, n=3). Indeed, EYFP expression was enriched in CD24-high/EYFP-positive cells when compared to CD24-high/EYFP-negative cells in both NB and NB+3F cultures (Tukey's multiple comparison test: p=0.0010 in NB culture and p=0.0059 in NB+3F culture).

No significant difference between population nor culture condition in terms of expression profiles was found in any of the other striatal genes. *Adora2a* and *Ppp1r1b* were similarly expressed amongst both populations in both culture conditions (Figure 3.24; two-way ANOVA, interaction between population and culture condition: $F_{(1,5)}$=0.1253, p=0.7378 for *Adora2a*; and $F_{(1,7)}$=0.7254, p=0.4226 for *Ppp1r1b*; effect of population: $F_{(1,5)}$=1.278, p=0.3095 for *Adora2a*; $F_{(1,7)}$=0.4770, p=0.5120 for *Ppp1r1b*; effect of culture condition: $F_{(1,5)}$=0.5356, p=0.4971 for *Adora2a*; $F_{(1,7)}$=0.1229, p=0.7362 for *Ppp1r1b*; n=2 per group for *Adora2a* except CD24-high/EYFP-negative in NB culture, n=3 and n=2 for *Ppp1r1b* except CD24-high/EYFP-negative in NB culture, n=4 and CD24-high/EYFP-negative in NB+3F culture, n=3). Interestingly, expression of *Drd2* in the EYFP-negative fraction from both cultures showed a higher trend when compared to the EYFP-positive population, although it did not reach any significant level (Figure 3.24; two-way ANOVA, interaction between population and culture condition: $F_{(1,7)}$=0.01412, p=0.9087; effect of population: $F_{(1,7)}$=3.635, p=0.0982; effect of culture condition: $F_{(1,7)}$=1.054, p=0.3388; n=2 per group except CD24-high/EYFP-negative in NB culture, n=4 and CD24-high/EYFP-negative in NB+3F culture, n=3). This gene, however, is less specific to striatopallidal MSNs than *Penk* and *Adora2a* since it is

also highly expressed in striatal cholinergic interneurons (Guzman et al., 2011). Lastly, we found that *Tubb3* expression showed a non-significant enrichment in the EYFP-negative population (Figure 3.24; two-way ANOVA, interaction between population and culture condition: $F_{(1,9)}$=0.1831, p=0.6788; effect of population: $F_{(1,9)}$=1.602, p=0.2374; effect of culture condition: $F_{(1,9)}$=0.8593, p=0.3781; n=3 per group except CD24-high/EYFP-negative in NB culture, n=4). This may be due to the fact that the EYFP-negative population was composed of various types of neuronal cells including those that were more mature.

From these findings, we concluded that both cultures were able to generate GABAergic striatal neurons with comparable efficiency. A striatonigral phenotype of ESC-derived MSNs could be obtained by both culture conditions. However, the striatopallidal phenotype, in particular enkephalin expression, is enriched in the NB culture.

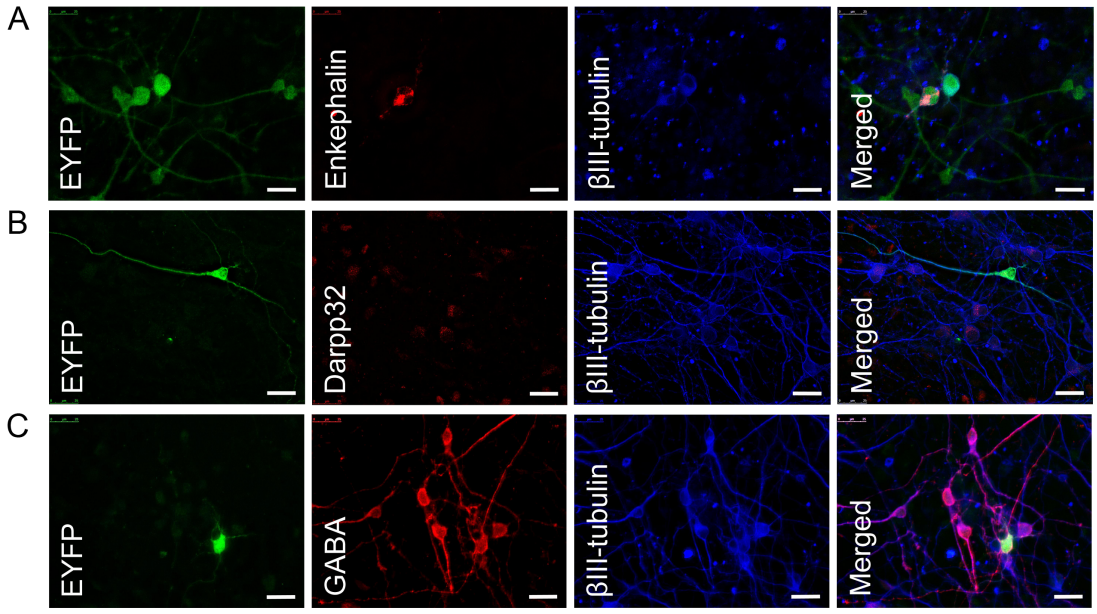

Figure 3.19: Enkephalinergic MSN phenotype of EYFP-positive neurons cultured in NB medium. Immunofluorescence staining for EYFP, βIII-tubulin and other key markers **(A)** enkephalin, **(B)** Darpp32 and **(C)** GABA at day 21 of differentiation. Co-localisation between **(A)** EYFP and enkephalin, **(B)** EYFP and Darpp32 and **(C)** EYFP and GABA was found in some but not all EYFP-positive cells. All scale bars are 25 μm. MSN, medium spiny neuron; EYFP, enhanced yellow fluorescent protein.

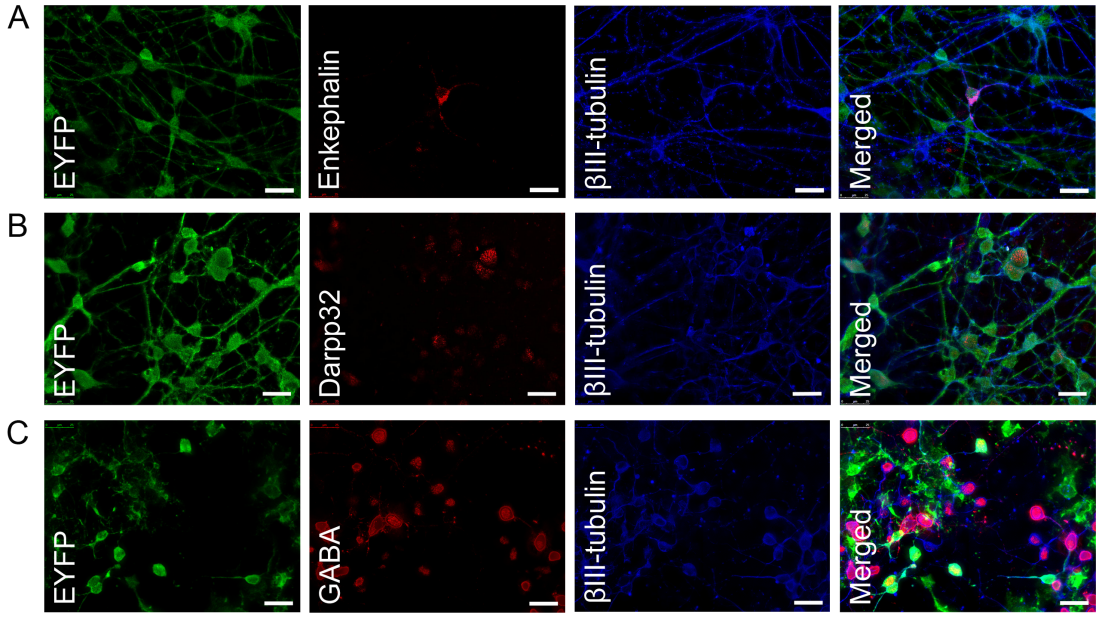

Figure 3.20: Enkephalinergic MSN phenotype of EYFP-positive neurons cultured in NB+3F medium. Immunofluorescence staining for EYFP, enkephalin, Darpp32, GABA and βIII-tubulin at day 21 of differentiation. **(A)** Only a fraction of EYFP-positive cells expressed enkephalin whilst the majority of them did not. Darpp32 **(B)** and GABA **(C)** were expressed in some EYFP-positive cells. All scale bars are 25 µm. MSN, medium spiny neuron; EYFP, enhanced yellow fluorescent protein.

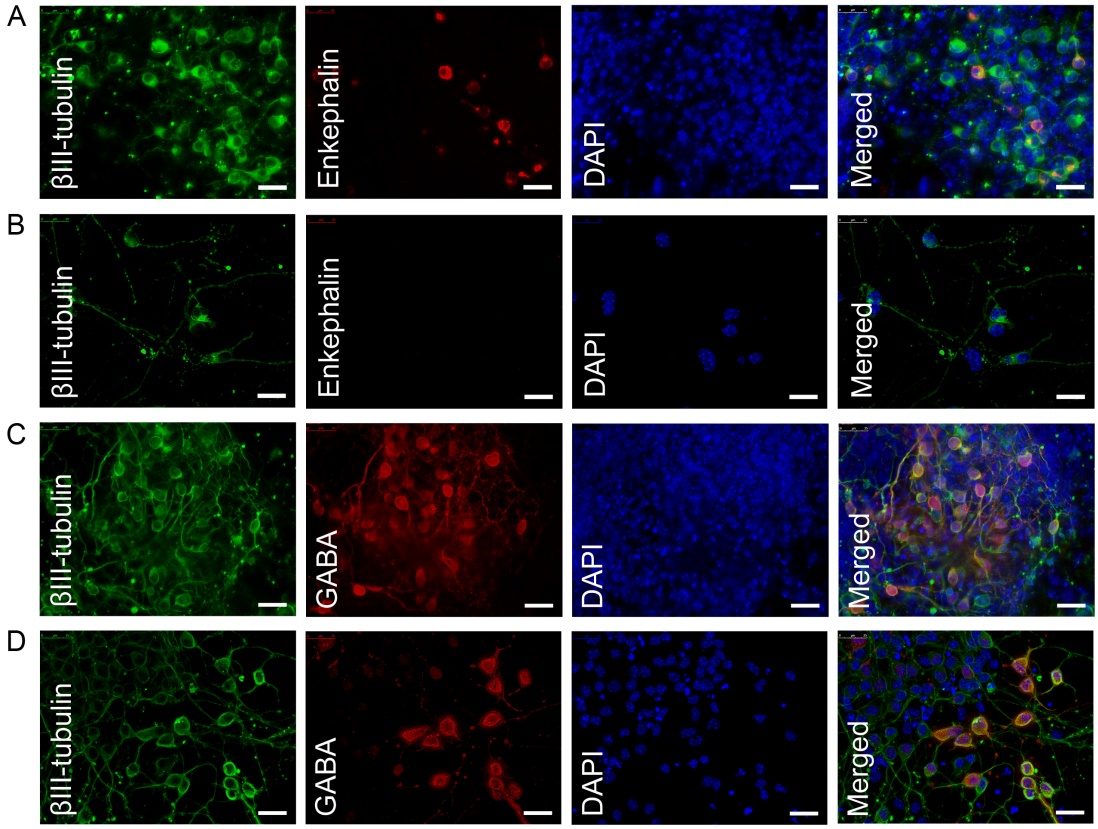

Figure 3.21: Enkephalinergic and GABAergic phenotypes of E14 neuronal cells. Immunofluorescence staining of the E14 line grown in NB **(A and C)** and NB+3F **(B and D)** media. **(A and B)** Cells were fixed and stained for βIII-tubulin and enkephalin at day 21 of differentiation. The NB culture showed more enkephalin-positive cells than NB+3F. **(C and D)** βIII-tubulin and GABA staining at day 21 of differentiation showed both NB and NB+3F cultures exhibited GABAergic neurons. All scale bars are 25 μm.

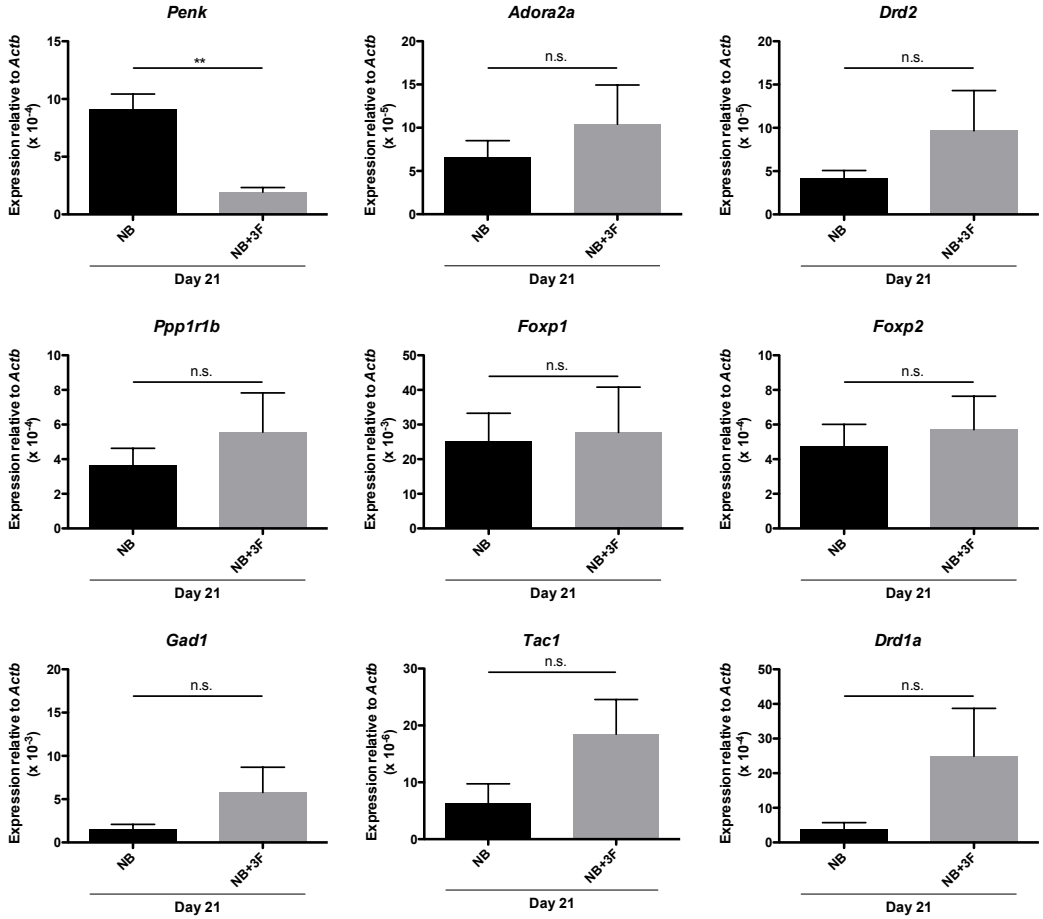

Figure 3.22: Gene expression analysis of cells from NB and NB+3F cultures: qRT-PCR analysis of the PNK18 line cultured in NB or NB+3F media was performed at day 21 of differentiation. Only *Penk* showed a significant difference between the culture conditions. Other striatopallidal markers, *Adora2a* and *Drd2*, were similarly expressed. Expression of MSN markers such as *Ppp1r1b*, *Foxp1* and *Foxp2* and GABAergic neuronal marker *Gad1* was identical in both culture conditions. Increased expression of the striatonigral genes, *Tac1* and *Drd1a*, was observed in NB+3F although it did not reach a significant level. Unpaired Student's t-test; ** $p<0.01$; n.s., no significance; n=4 for both culture conditions; Values are mean ± s.e.m. MSN, medium spiny neuron.

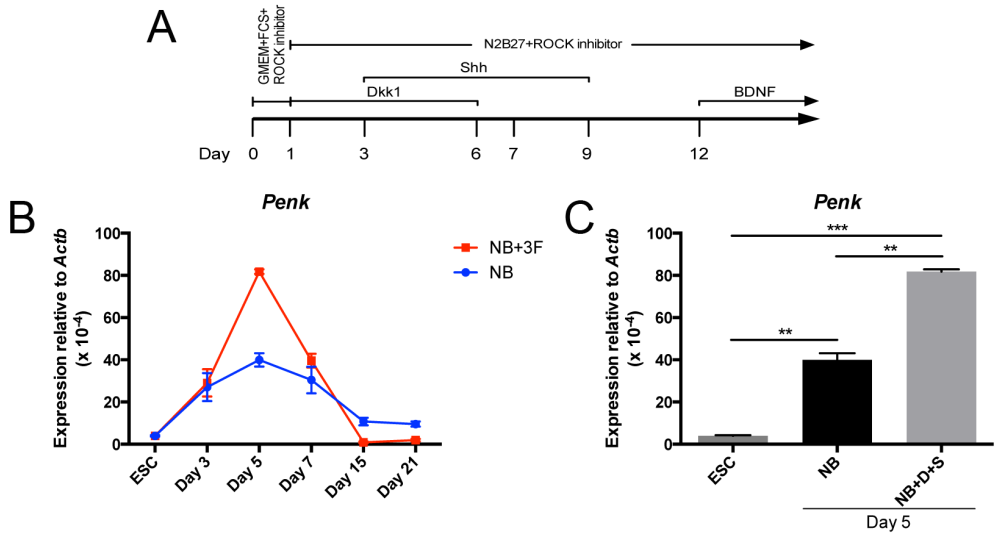

Figure 3.23: *Penk* expression in NB and NB+3F cultures throughout differentiation. (A) Schematic representation of the NB+3F (or NB+D+S if samples were analysed at early time points prior to the addition of BDNF) differentiation protocol. **(B)** qRT-PCR analysis of the PNK18 ESC and differentiated PNK18 line in NB and NB+3F cultures at day 3, day 5, day 7, day 15 and day 21 of differentiation. **(C)** Differentiated cells from the two culture conditions at day 5 showed a significant enrichment of *Penk* compared to ESC. One-way ANOVA with Tukey's post-hoc analysis; ** $p<0.01$; *** $p<0.001$; p are adjusted p-value from Tukey's test; n=2 for each group; Values are mean ± s.e.m. ESC, embryonic stem cell.

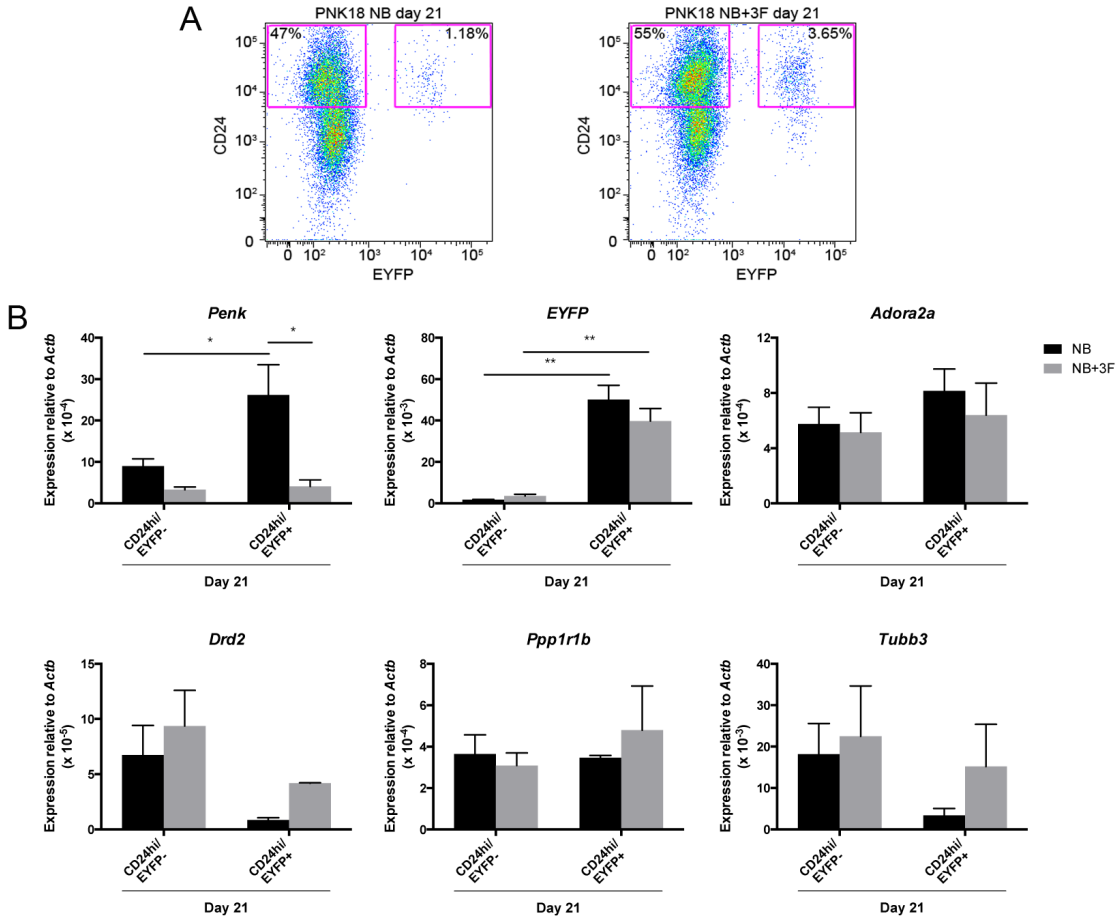

Figure 3.24: Gene expression analysis of CD24^{hi}/EYFP^{-} and CD24^{hi}/EYFP^{+} populations in NB and NB+3F cultures. The PNK18 line was cultured in NB or NB+3F medium. Sorting was performed at day 21 of differentiation to collect CD24^{hi}/EYFP^{-} and CD24^{hi}/EYFP^{+} fractions. **(A)** Plots showed the gating used for sorting two populations. **(B)** qRT-PCR analysis of sorted samples revealed a significant enrichment of *Penk* expression in the CD24^{hi}/EYFP^{+} fraction compared to the CD24^{hi}/EYFP^{-} fraction in NB cultures. Expression of *Penk* in the NB+3F culture, in contrast, did not show a difference between the two populations. When compared CD24^{hi}/EYFP^{+} subset between two culture conditions, *Penk* expression was significantly higher in NB cultures. EYFP was highly expressed in the CD24^{hi}/EYFP^{+} population of both cultures. Other genes including striatopallidal markers *Adora2a* and *Drd2*, MSN marker *Ppp1r1b* and post-mitotic neuronal marker *Tubb3* were similar in terms of their expression, regardless of the culture conditions and populations. Two-way ANOVA with Tukey's post-hoc analysis; * p<0.05; ** p<0.01; p are adjusted p-value from Tukey's test; n=3 for each group except CD24^{hi}/EYFP^{-} in NB culture, n=4; Values are mean ± s.e.m. EYFP, enhanced yellow fluorescent; MSN, medium spiny neuron.

3.4.2 Penk expression is suppressed by addition of either DKK1 or Shh

We have shown that the NB+3F culture condition resulted in the down-regulation of *Penk*. It is likely that this is due to the addition of one or more of the factors in the NB+3F culture. We, however, believed that Bdnf via an activation of its high affinity receptor TrkB is essential, at least *in vivo*, for the *Penk* expression. This has been demonstrated in the work of Dr. Dario Besusso in the Minichiello lab (Besusso et al., 2013). *In situ* hybridisation analysis of the BAC-*Penk-Cre*$^{tg/+}$, *Trkb*$^{lx/lx}$ line, in which the TrkB receptor was deleted specifically in enkephalinergic neurons, showed that the *Penk* transcript was significantly reduced in the striata of these animals compared to their control littermates (Figure 3.25 A; p=0.036, unpaired Student's t-test, n= 3 per group). We have also confirmed this finding by qRT-PCR analysis of striata from the *BAC-Penk-Cre*$^{tg/+}$, *Trkb*$^{lx/lx}$ mice (Figure 3.25 B). Indeed, expression of *Penk* was significantly diminished in the absence of Bdnf-TrkB signalling in enkephalinergic striatal neurons (p=0.0016, unpaired Student's t-test, n= 3 per group). From the data above, we hypothesised that the presence of exogenous human DKK1 and/or murine Shh in NB+3F culture led to *Penk* down-regulation.

To address which factor(s) in NB+3F contributed to the reduction of *Penk* transcript, we cultured the PNK18 line in three novel culture conditions, which contained only one or two factors used in NB+3F culture in addition to NB and NB+3F cultures (no Shh, NB+D+B; no DKK1, NB+S+B; and no DKK1 or Shh, NB+B; Table 3.4). Gene expression analysis was then performed at day 15 of differentiation. We found a significant reduction in *Penk* expression in the NB+3F, NB+D+B and NB+S+B cultures when compared to the NB culture (Figure 3.26; one-way ANOVA: $F_{(4,13)}$=12.74, p=0.0002; Tukey's multiple comparison test: p=0.0054 for NB vs NB+3F; p=0.0218 for NB vs NB+D+B; p=0.0300 for NB vs NB+S+B; n=4 for NB and NB+3F and n=3 for NB+D+B and NB+S+B). This indicated that addition of either DKK1 or Shh led to suppression of *Penk* expression. Consistent with *in vivo* findings, we can exclude the detrimental effect of BDNF on *Penk* expression since we did not find a difference in *Penk* mRNA level between NB

and NB+B cultures (Tukey's multiple comparison test: p=0.6985; n=4 for NB+B). In reality, *Penk* expression was slightly higher in NB+B than NB cultures. When compared to other cultures, the expression of *Penk* in NB+B cultures was significantly higher than that of NB+3F, NB+D+B and NB+S+B cultures (Tukey's multiple comparison test: p=0.0006 for NB+B vs NB+3F; p=0.0026 for NB+B vs NB+D+B; p=0.0035 for NB+B vs NB+S+B). We conclude that the presence of exogenous DKK1 and/or Shh but not BDNF down-regulates *Penk* expression at day 15 of differentiation. Addition of exogenous BDNF, interestingly, did not enhance the *Penk* expression in cultures.

To corroborate the findings above, we repeated the same analysis at day 21 of differentiation (Figure 3.26). Consistent with day 15 data, *Penk* was highly expressed in NB culture but not in NB+3F, NB+D+B or NB+S+B cultures (one-way ANOVA: $F_{(4,13)}$=13.82, p=0.0001; Tukey's multiple comparison test: p=0.0007 for NB vs NB+3F; p=0.0011 for NB vs NB+D+B; p=0.0004 for NB vs NB+S+B; n=4 for NB and NB+3F and n=3 for NB+D+B and NB+S+B). We also found a significant difference of *Penk* expression between the NB+B and NB+3F (Tukey's multiple comparison test: p=0.0414; n= 4 for NB+B) and between the NB+B and NB+S+B (Tukey's multiple comparison test: p=0.0169) cultures. Addition of BDNF in NB+B culture, however, did not affect *Penk* expression in comparison to the NB culture (Tukey's multiple comparison test: p=0.1912 for NB vs NB+B). Interestingly, the level of *Penk* expression at day 21 of differentiation was lower than that of day 15, although only NB+B culture showed statistically difference (unpaired t test: p=0.8127 for NB, p=0.1914 for NB+3F, p=0.6841 for NB+D+B, p=0.3082 for NB+S+B and p=0.0326 for NB+B). This indicates that the maintenance of *Penk* expression at later time points in our culture system requires other supporting factor(s) in addition to BDNF.

Analysis of other striatopallidal markers such as *Adora2a* and *Drd2* (Figure 3.26), unlike *Penk*, showed no difference in their expression at both day 15 (one-way ANOVA: $F_{(4,13)}$=1.575, p=0.2394 for *Adora2a*; $F_{(4,13)}$=0.1526, p=0.9585 for *Drd2*; n=4 for NB, NB+3F and NB+B and n=3 for NB+D+B and NB+S+B) and day 21 of

differentiation (one-way ANOVA: $F_{(4,13)}$=1.511, p=0.2562 for *Adora2a*; $F_{(4,13)}$=0.9896, p=0.4472 for *Drd2*; n=4 for NB, NB+3F and NB+B and n=3 for NB+D+B and NB+S+B). Likewise, expression of the MSN markers *Ppp1r1b*, *Foxp1*, *Foxp2* and *Ctip2* (Figure 3.27) was identical amongst all culture conditions at day 21 of differentiation (one-way ANOVA: $F_{(4,13)}$=1.386, p=0.2924 for *Ppp1r1b*; $F_{(4,13)}$=1.963, p=0.1598 for *Foxp1*; $F_{(4,13)}$=0.4396, p=0.7780 for *Foxp2*; $F_{(4,13)}$=2.382, p=0.1051 for *Ctip2*; n=4 for NB, NB+3F and NB+B and n=3 for NB+D+B and NB+S+B). We also checked for the expression of striatonigral markers *Tac1*, *Drd1a*. Although *Drd1a* showed slightly higher expression in NB+3F, no significant difference was detected (one-way ANOVA: $F_{(4,13)}$=1.199, p=0.3574 for *Tac1*; $F_{(4,13)}$=1.820, p=0.1852 for *Drd1a*; n=4 for NB, NB+3F and NB+B and n=3 for NB+D+B and NB+S+B). To ensure that all culture conditions used had no bias in term of neuronal subtypes specification, we confirmed that expression of *Gad1* was unchanged. A slight, but not significant increase was observed only in NB+3F compared to NB cultures (one-way ANOVA: $F_{(4,13)}$=1.480, p=0.2647; n=4 for NB, NB+3F and NB+B and n=3 for NB+D+B and NB+S+B). This confirmed that similar numbers of GABAergic neurons were generated amongst all culture conditions used. A non-significant increase in *Gad1* expression in NB+3F culture might result from higher *Tubb3* expression, despite not significantly difference, in this culture condition compared to NB culture (one-way ANOVA: $F_{(4,13)}$=2.041, p=0.1476, n=4 for NB, NB+3F and NB+B and n=3 for NB+D+B and NB+S+B).

Lastly, to ensure that cells in cultures could respond to BDNF with no bias, we checked whether TrkB receptor (encoded by *Ntrk2* gene) expression was similar in all culture conditions (Figure 3.27). As expected we found that all cultures expressed a comparable amount of *Ntrk2* (one-way ANOVA: $F_{(4,13)}$=1.634, p=0.2248, n=4 for NB, NB+3F and NB+B and n=3 for NB+D+B and NB+S+B).

Neural specification is regulated by several signalling pathway including the Wnt and Shh pathways. We, therefore, checked whether the addition of exogenous DKK1 and/or Shh to the cultures affected the transcriptional level of their endogenous counterparts. Quantitative RT-PCR analysis of *Dkk1* demonstrated its

constant expression of in all culture conditions at both days 15 and 21 of differentiation (Figure 3.28; one-way ANOVA: $F_{(4,13)}$=1.096, p=0.3990 for day 15; $F_{(4,13)}$=0.2248, p=0.9197 for day 21; n=4 for NB, NB+3F and NB+B and n=3 for NB+D+B and NB+S+B). In contrast, exogenous addition of both DKK1 and Shh led to significant changes of the endogenous *Shh* transcript level at both days 15 and 21 of differentiation (one-way ANOVA: $F_{(4,13)}$=5.961, p=0.0060 for day 15; $F_{(4,13)}$=5.498, p=0.0081 for day 21; Tukey's multiple comparison test: p=0.0126 for day 15 NB vs NB+3F; and p=0.0277 for day 21 NB vs NB+3F; n=4 for NB, NB+3F and NB+B and n=3 for NB+D+B and NB+S+B). The addition of either DKK1 or Shh individually in the culture media was not sufficient to produce a similar increase in *Shh* expression. (Tukey's multiple comparison test: NB vs NB+D+B: p=0.9541 for day15 and p=0.8849 for day 21; NB+3F vs NB+D+B: p=0.0061 for day 15 and p=0.0085 for day 21; NB vs NB+S+B: p=0.9798 for day 15 and p>0.9999 for day 21; NB+3F vs NB+S+B: p= 0.0567 for day 15 and p= 0.0412 for day 2).

To further investigate the direct effect of exogenous DKK1 and Shh in NB+3F culture, we performed a similar analysis at earlier time points of differentiation (ESC stage, day 3, day 5 and day 7), corresponding to the period where both recombinant proteins were added to the cultures (Figure 3.29 A and B). In contrast to that observed at the later time points, endogenous *Dkk1* and *Shh* levels in NB cultures were higher than in NB+D+S (NB+3F) cultures with a significant up-regulation observed at day 7 of differentiation (two-way ANOVA, interaction between culture condition and time point: $F_{(3,8)}$=34.98, p<0.0001 for *Dkk1*; and $F_{(3,8)}$=19.14, p=0.0005 for *Shh*; effect of time point: $F_{(3,8)}$=48.48, p<0.0001 for *Dkk1*; $F_{(3,8)}$=31.90, p<0.0001 for *Shh*; effect of culture condition: $F_{(1,8)}$=55.37, p<0.0001 for *Dkk1*; $F_{(1,8)}$=33.84, p=0.0004 for *Shh*; Tukey's multiple comparison test: p<0.0001 for *Dkk1* day 7 NB vs NB+D+S and p=0.0002 for *Shh* day 7 NB vs NB+D+S; n=2 per group). Thus, the presence of DKK1 and Shh in NB+D+S (NB+3F) cultures leads to the suppression of endogenous *Dkk1* and *Shh* production at day 7 of differentiation. However, by day 15 of differentiation the expression of *Shh* has recovered and was higher in NB+3F cultures (Figure 3.28). This may be a result of

the abrupt withdrawal of exogenous Shh at day 9 of the differentiation process, leading to an over-compensatory production of *Shh* in the NB+3F culture.

Specification of LGE progenitors requires both Shh signalling and Wnt inhibition, from this data we hypothesised that the endogenous level of *Shh* and *Dkk1* is enough to drive ESCs towards a LGE fate. Addition of exogenous DKK1 and Shh at the concentration and duration we have used, however, may influence ESCs to acquire other neuronal fates. It is known that higher concentrations of Shh can induce ESCs to acquire a MGE fate rather than a LGE fate (Danjo et al., 2011, Ma et al., 2012). The neurons in the NB+3F cultures may, therefore, be MGE derivatives rather than LGE-derived striatal neurons. To address this we measured the expression of the MGE marker *Nkx2.1* in the two culture conditions at day 7 of differentiation (Figure 3.29 C). Indeed, we found a significant enrichment of *Nkx2.1* expression but not of a forebrain marker *Foxg1* in the NB+D+S (NB+3F) culture (Figure 3.29 C and D; p=0.0358 for *Nkx2.1* and p=0.0612 for *Foxg1*, unpaired Student's t-test, n=2 per group), indicating that cells in the N+D+S (NB+3F) culture are more MGE primed. This may explain the down-regulation of *Penk* expression in NB+3F culture (Figure 3.22). However, other striatal markers are similarly expressed in both NB and NB+3F cultures, therefore, there may be other unknown mechanisms that contribute to this reduction.

In summary, our data shows that the reporter ESC line we have generated is capable of acquiring a GABAergic MSN phenotype in all culture conditions tested. However, only the NB culture condition was able to acquire the enkephalinergic phenotype typical of striatopallidal MSNs. Enkephalin was highly expressed in the absence of exogenous DKK1 and Shh. Therefore, we propose that *Penk* down-regulation is a consequence of excess exogenous DKK1 and Shh in the culture medium. We, however, also believe that other signalling pathways might be involved in this process. Finally, we propose that both NB and NB+B cultures are ideal conditions for deriving enkephalinergic MSNs from mESCs.

Table 3.4: Culture conditions used in this chapter

Culture condition	Day of differentiation	Medium used
NB	Day 0	GMEM+FBS+ROCK inhibitor
	Day 1 onwards	N2B27+ROCK inhibitor
NB+3F	Day 0	GMEM+FBS+ROCK inhibitor
	Day 1-2	N2B27+DKK1+ROCK inhibitor
	Day 3-6	N2B27+DKK1+Shh+ROCK inhibitor
	Day 7-9	N2B27+Shh+ROCK inhibitor
	Day 10-11	N2B27+ROCK inhibitor
	Day 12 onwards	N2B27+BDNF+ROCK inhibitor
NB+D+B	Day 0	GMEM+FBS+ROCK inhibitor
	Day 1-6	N2B27+DKK1+ROCK inhibitor
	Day 7-11	N2B27+ROCK inhibitor
	Day 12 onwards	N2B27+BDNF+ROCK inhibitor
NB+S+B	Day 0	GMEM+FBS+ROCK inhibitor
	Day 1-2	N2B27+ROCK inhibitor
	Day 3-9	N2B27+Shh+ROCK inhibitor
	Day 10-11	N2B27+ROCK inhibitor
	Day 12 onwards	N2B27+BDNF+ROCK inhibitor
NB+B	Day 0	GMEM+FBS+ROCK inhibitor
	Day 1-11	N2B27+ROCK inhibitor
	Day 12 onwards	N2B27+BDNF+ROCK inhibitor

FBS, foetal bovine serum.

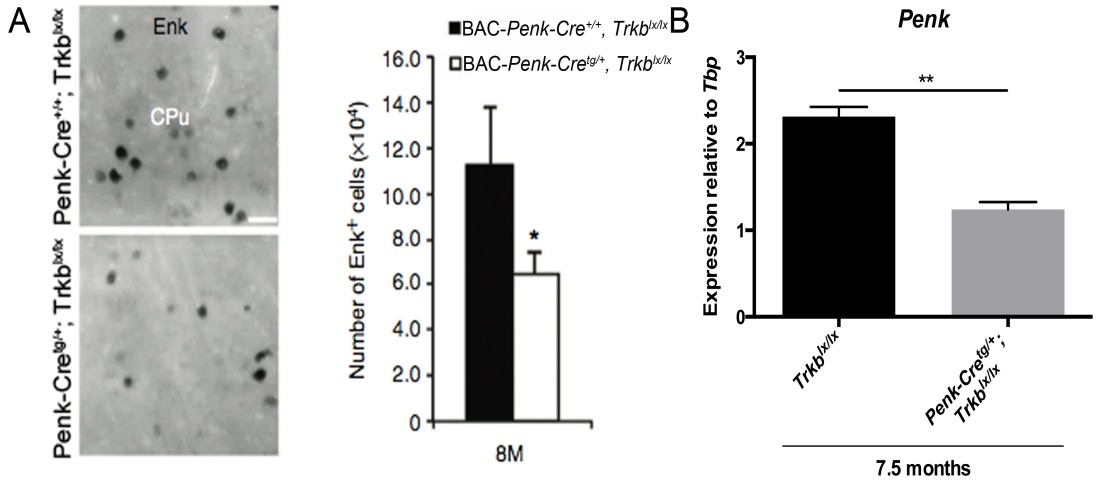

Figure 3.25: *Penk* is down-regulated in the absence of Bdnf-TrkB signalling. (A) *In situ* hybridisation of the *Penk* transcript in the caudate-putamen (CPu) of eight months old *BAC-Penk-Cre$^{tg/+}$, Trkb$^{lx/lx}$* animals showed a significant reduction of enkephalin in comparison to their control littermates (*BAC-Penk-Cre$^{+/+}$; Trkb$^{lx/lx}$*). **(B)** qRT-PCR analysis demonstrated a significant decrease in *Penk* expression level in *BAC-Penk-Cre$^{tg/+}$; Trkb$^{lx/lx}$* striata compared to *Trkb$^{lx/lx}$* controls. Figure A is from Besusso et al., 2013. Scale bar is 50 µm. Unpaired Student's t-test; * p<0.05; ** p<0.01; n=3 for each group; Values are mean ± s.e.m.

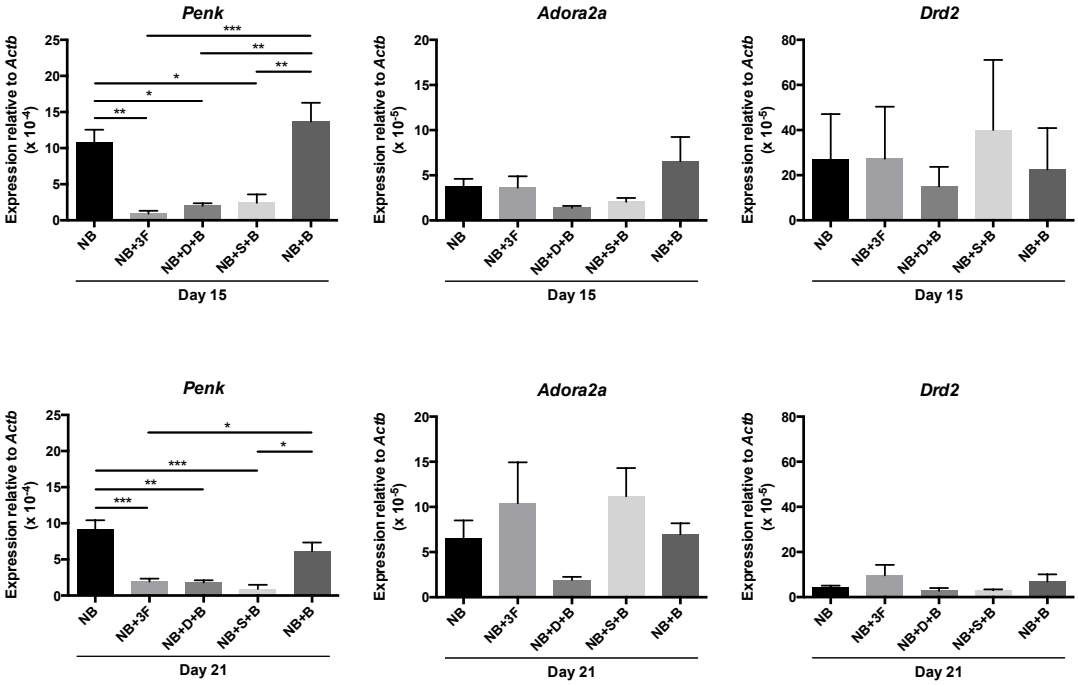

Figure 3.26: Expression of striatopallidal-specific genes in differentiating neural cells. PNK18 cells were cultured in combinations of NB medium and exogenous factors (no factor added, NB; three factors added, NB+3F; no Shh, NB+D+B; no DKK1, NB+S+B; and no DKK1 or Shh, NB+B). Quantitative RT-PCR analysis was performed at day 15 and day 21 of differentiation. At both time points, *Penk* was highly expressed in NB and NB+B cultures but not in NB+3F, NB+D+B nor NB+S+B. Expression of *Adora2a* and *Drd2* showed no significant difference amongst all culture conditions. One-way ANOVA with Tukey's post-hoc analysis; * $p<0.05$; ** $p<0.01$; *** $p<0.001$; p are adjusted p-value from Tukey's test; n=4 for NB, NB+3F and NB+B and n=3 for NB+D+B and NB+S+B; Values are mean ± s.e.m.

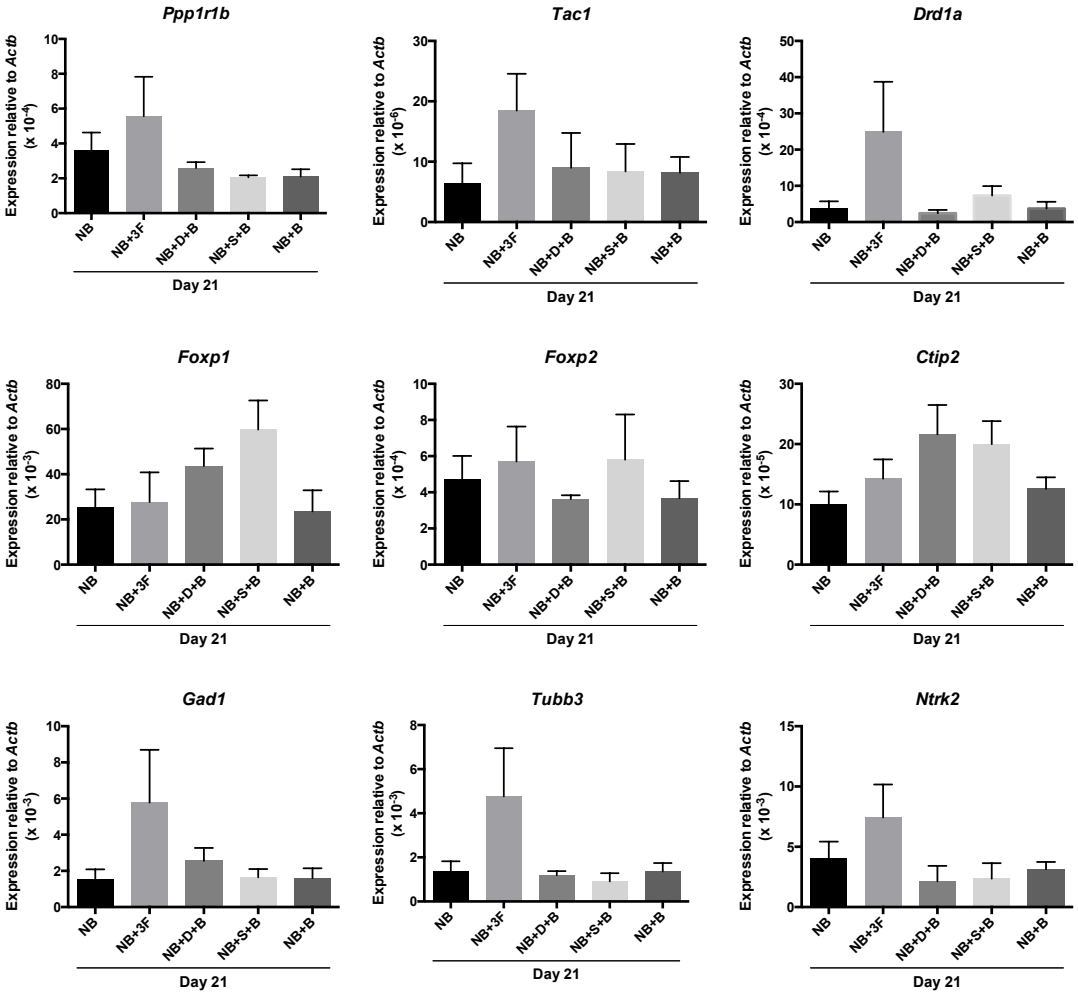

Figure 3.27: Gene expression analysis of MSN-specific and other important markers in differentiating neural cells. PNK18 cells were cultured in combinations of NB medium and exogenous factors (no factor added, NB; three factors added, NB+3F; no Shh, NB+D+B; no DKK1, NB+S+B; and no DKK1 or Shh, NB+B). Quantitative RT-PCR analysis was performed at day 21 of differentiation for the expression of MSN markers (*Ppp1r1b*, *Foxp1*, *Foxp2* and *Ctip2*), striatonigral markers (*Tac1* and *Drd1a*), GABAergic marker (*Gad1*), Post-mitotic neuronal marker (*Tubb3*) and TrkB (*Ntrk2*). One-way ANOVA; No statistical difference was observed in all genes analysed; n=4 for NB, NB+3F and NB+B and n=3 for NB+D+B and NB+S+B; Values are mean ± s.e.m. MSN, medium spiny neuron.

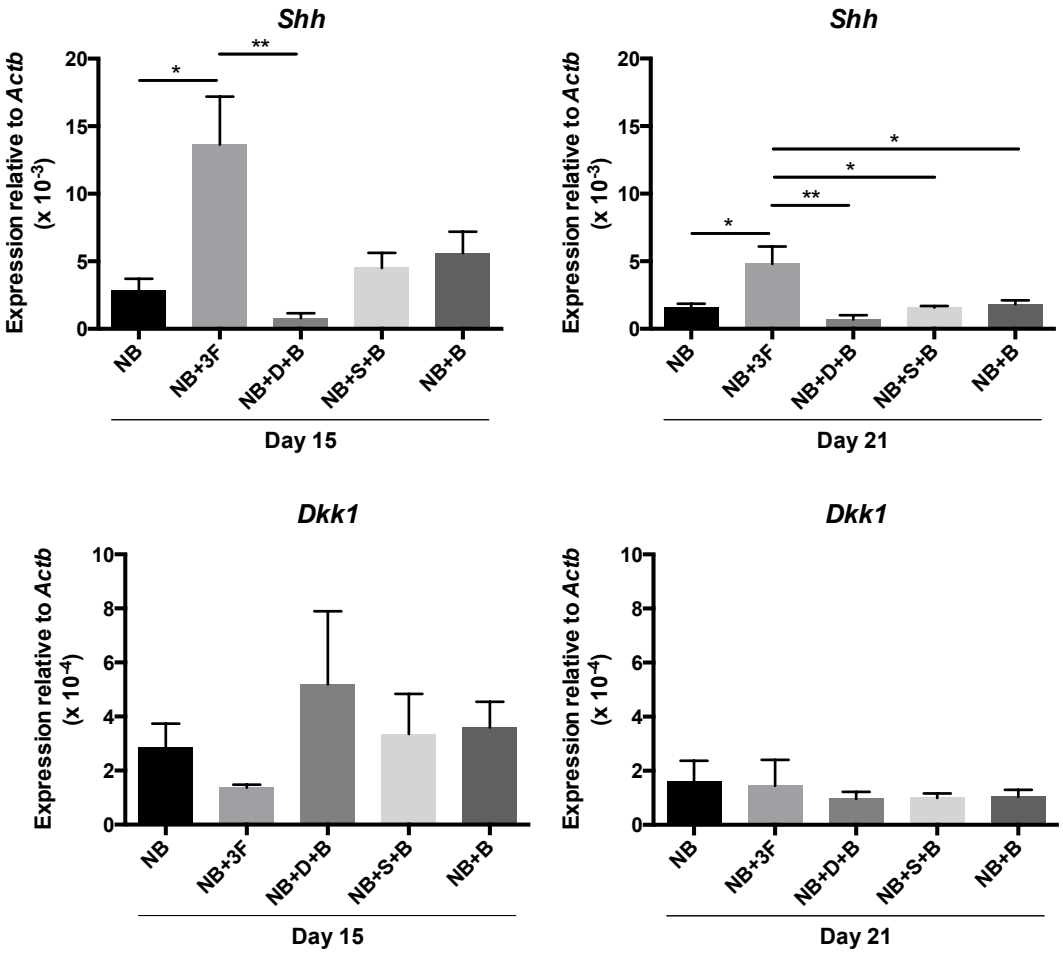

Figure 3.28: Up-regulation of *Shh* in NB+3F culture at day 15 and 21 of differentiation. qRT-PCR analysis showed that presence of recombinant human DKK1 and mouse Shh in NB+3F culture significantly increased *Shh* transcript compared to NB (both at day 15 and day 21) or NB+B (day 21 only) cultures. This effect was abolished when either DKK1 or Shh was added individually into cultures (NB+D+B or NB+S+B, respectively). In contrast, *Dkk1* transcript level at day 15 and 21 of differentiation was not influenced by exogenous treatment of DKK1 and Shh. One-way ANOVA with Tukey's post-hoc analysis; * $p<0.05$; ** $p<0.01$; p are adjusted p-value from Tukey's test; n=4 for NB, NB+3F and NB+B and n=3 for NB+D+B and NB+S+B; Values are mean ± s.e.m.

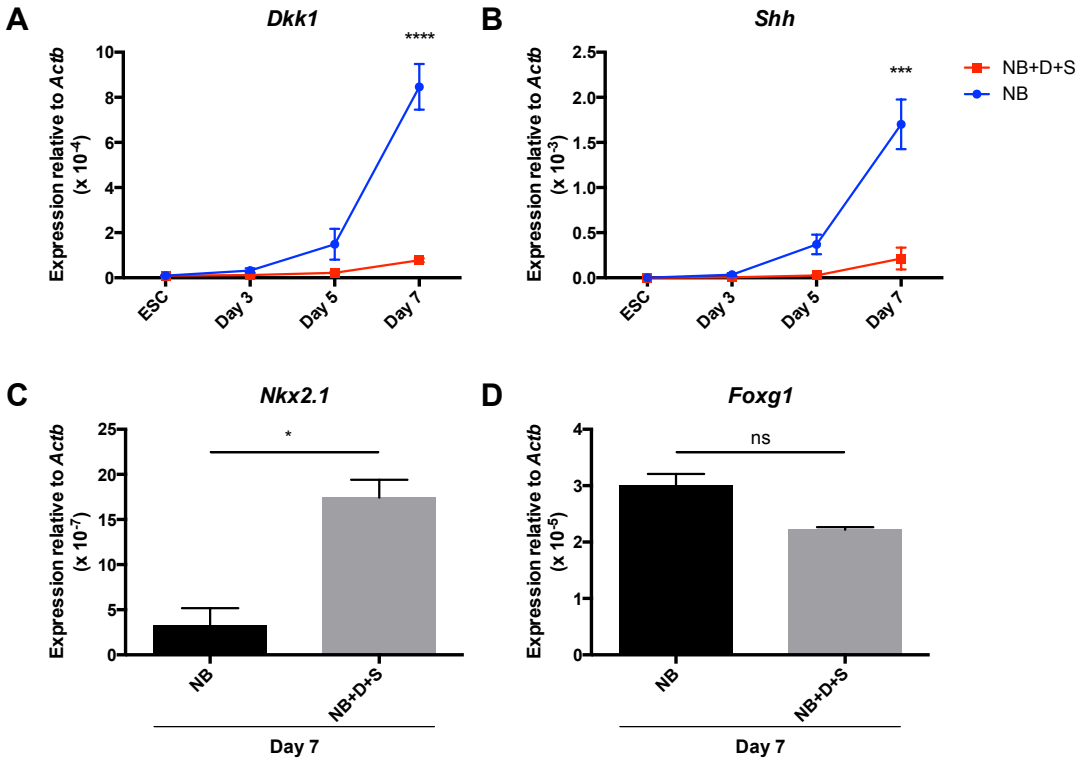

Figure 3.29: Suppression of endogenous levels of *Dkk1* and *Shh* by addition of exogenous DKK1 and Shh leads to up-regulation of *Nkx2.1*. (A and B) qRT-PCR analysis of ESCs and differentiating cells at day 3, day 5 and day 7 of differentiation demonstrated that the presence of recombinant DKK1 and Shh in NB+D+S (NB+3F) culture inhibits endogenous production of **(A)** *Dkk1* and **(B)** *Shh* transcripts. This inhibitory effect was gradually increased as differentiation progressed and the difference in *Dkk1* and *Shh* expression level between NB and NB+D+S (NB+3F) cultures reached a significant level at day 7. As a result, expression of the MGE marker *Nkx2.1* at the same time point (day 7) in NB+D+S (NB+3F) culture was statistically higher than that of the NB culture. This indicated that the NB+D+S (NB+3F) culture exhibited more MGE-primed neurons than the NB culture. Expression of forebrain progenitor marker *Foxg1* in NB+D+S (NB+3F) culture at day 7, in contrast, was similar to that of NB culture, indicating that forebrain specification was not altered with exogenous treatment of DKK1 and Shh. Two-way ANOVA with Tukey's post-hoc analysis; * $p<0.05$; *** $p<0.001$; **** $p<0.0001$; p are adjusted p-value from Tukey's test; n=2 for each group; Values are mean ± s.e.m. ESCs, embryonic stem cells; MGE, medial ganglionic eminence.

3.4.3 Electrophysiological properties of embryonic stem cell-derived EYFP-positive neurons

All of the electrophysiological analyses were conducted by Dr. Andrei-Sorin Illie, a postdoctoral research scientist in Dr. Colin Akerman's group at the Department of Pharmacology, University of Oxford.

We have shown in the previous sections that we were successful in deriving EYFP-positive neurons that were enkephalinergic and exhibited the molecular phenotype of the MSNs. To test whether these neurons possess electrophysiological properties of functional neurons, we performed whole-cell patch-clamp recording in current- and voltage-clamp configurations. EYFP-expressing neurons were targeted for patch-clamp recording between day 22 and 24 of differentiation (Figure 3.30 A). Passive membrane properties of EYFP-expressing neurons of both NB and NB+3F cultures were identical (Figure 3.30 B, C and D). The resting membrane potential of neurons from NB and NB+3F cultures was -58.1±2.5 mV and -58.2±3.3 mV, respectively (Figure 3.30 B; values are mean ± s.e.m., p=0.79, unpaired Student's t-test, n=12 per group). The cell capacitance was 36.3±5.4 pF for EYFP-positive neurons from the NB culture and 35.3±9.5 pF for EYFP-expressing neurons from the NB+3F culture (Figure 3.28 C; values are mean ± s.e.m., p=0.76, unpaired Student's t-test, n=13 for NB and n=12 for NB+3F,). Lastly, the membrane resistance of EYFP-expressing cells from NB culture was 1.13±0.17 GΩ whereas that of NB+3F-derived EYFP-positive cells was 1.50±0.32 GΩ (Figure 3.28 D; values are mean ± s.e.m., p=0.20, unpaired Student's t-test, n=12 per group,). These values are consistent with electrophysiological data from hPSC-derived MSNs (Delli Carri et al., 2013b) and also confirm that mESC-derived YFP-positive neurons from both cultures have similar electrophysiological properties.

It has been demonstrated that PSC-derived MSNs could produce repetitive action potential when stimulated with a current injection (Shin et al., 2011, Ma et al., 2012, Delli Carri et al., 2013b) This is considered an important property of functional neurons. To test whether the EYFP-positive neurons from both NB and NB+3F cultures could fire action potential and exhibit repetitive spiking activity, we injected

a series of depolarising currents in current clamp mode, in steps of 5 pA from a membrane potential of -80 mV (Figure 3.31 A). We found that all recorded EYFP-positive cells in NB and NB+3F culture fired repetitive action potentials. The minimal current needed for inducing action potentials (also known as rheobase) was identical between the two groups of EYFP-expressing cells (Figure 3.31 B; 36.6±9.8 pA for neurons from NB culture, and 56.0±9.4 pA for neurons from NB+3F culture, values are mean ± s.e.m., p=0.41, unpaired Student's t-test, n=6 for neurons from NB culture and n=5 for neurons from NB+3F culture). Interestingly, the maximal firing rate in response to suprathreshold stimulation was significantly higher in neurons derived from NB+3F culture compared to NB-derived neurons (Figure 3.31 C; 17.1±1.7 spikes/sec for neurons from NB+3F and 12.5±1.3 spikes/sec for neuron from NB, values are mean ± s.e.m., $p<0.05$, unpaired student's t-test, n=6 per group,). A possible explanation of this could be that the neurons in the NB+3F culture are more mature, supported by the observation of longer processes (Figure 3.13 C and D). Next, we checked whether voltage-activated currents, which underlie spiking activity was present in EYFP-expressing neurons. Voltage-clamp recordings with a series of 12 voltage steps, gradually increasing by +10 mV from a holding voltage of -90 mV, were performed. All EYFP-positive neurons from both NB and NB+3F cultures exhibited voltage-activated fast inward and delayed outward currents, which represent sodium and potassium currents, respectively (Figure 3.31 D; n=7 for NB culture and n=6 for NB+3F culture). The current densities of the inward sodium currents and outward potassium currents of NB- and NB+3F-derived neurons were not different (Figure 3.31 E and F). These data confirm that EYFP-positive neurons derived from NB and NB+3F cultures are functionally active.

MSNs have been shown to express one type of potassium channel, which causes a voltage-gated, fast inactivating potassium currents resembling the A-type potassium current (I_A) (Surmeier et al., 1988, Nisenbaum et al., 1996, Ericsson et al., 2011). The presence of this current in MSNs contributes to their unique firing property, which is a delay in the initiation of first spike of action potentials (Ericsson et al., 2011). Interestingly, we did observe that the first action potential generated

could be delayed in neurons from both cultures (black traces in Figure 3.31 A). This is in accordance with the presence of an I_A-like current in EYFP-positive neurons. To confirm the existence of an I_A-like current in EYFP-expressing cells, we performed voltage-clamp recordings in the presence of 1 μM tetrodotoxin to block the voltage-gated sodium channels (Delli Carri et al., 2013a). Cells were held at -110 mV and a series of depolarising test potentials were applied. The I_A current can be completely inactivated when the test potential is preceded by a 50 ms prepulse to -40 mV (Delli Carri et al., 2013a). The fast inactivating I_A current was isolated by subtracting traces containing a -40 mV prepulse from traces elicited without a prepulse. We found that I_A currents could be recorded from EYFP-positive neurons in both NB and NB+3F cultures (Figure 3.32 A). The majority of EYFP-positive cells in the NB (71.4%, 5 out of 7) and NB+3F (66.6%, 4 out of 6) cultures analysed possess I_A currents (Figure 3.32 B). The maximal I_A current density was similar between neurons derived from two culture conditions (Figure 3.32 C; 16.1±4.5 pA/pF for NB-derived neurons and 15.2±3.4 pA/pF for NB+3F-derived neurons, values are mean ± s.e.m., p=0.88, unpaired Student's t-test). Thus, both culture conditions give rise to EYFP-positive neurons that exhibit the electrophysiological characteristics of MSNs.

To conclude, electrophysiological data indicates that the EYFP-positive neurons derived from both NB and NB+3F cultures are functionally active. They exhibit voltage-activated fast inward sodium and delayed persistent potassium currents and are able to fire repetitive action potentials, which are basic properties of functional neurons. The majority of EYFP-positive neurons generated also possess the fast inactivating I_A current, the hallmark electrical property of MSNs.

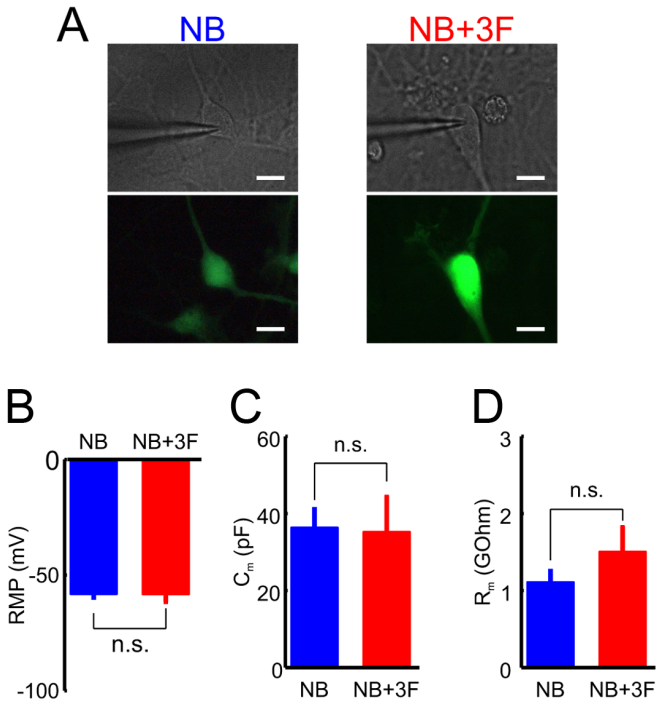

Figure 3.30: Electrophysiological properties of EYFP-positive neurons derived in NB and NB+3F cultures. The PNK18 line was cultured in NB and NB+3F conditions for at least 22 days. Patch clamp analysis of EYFP-positive cells was performed between day 22 and 24 of differentiation. **(A)** Representative images in bright field and green fluorescent channel showed the patched EYFP-positive neurons in both culture conditions. An average **(B)** resting membrane potential (RMP; n=12 for each group), **(C)** membrane capacitance (C_m; n=13 for NB and n=12 for NB+3F) and **(D)** membrane resistance (R_m; n=12 for each group) of EYFP-positive neurons from NB and NB+3F cultures showed no significant difference of these parameters between EYFP-expressing neurons derived from NB and NB+3F cultures. Scale bars are 10 µm. Unpaired Student's t-test; n.s., no significance; Values are mean ± s.e.m. EYFP, enhanced yellow fluorescent protein.

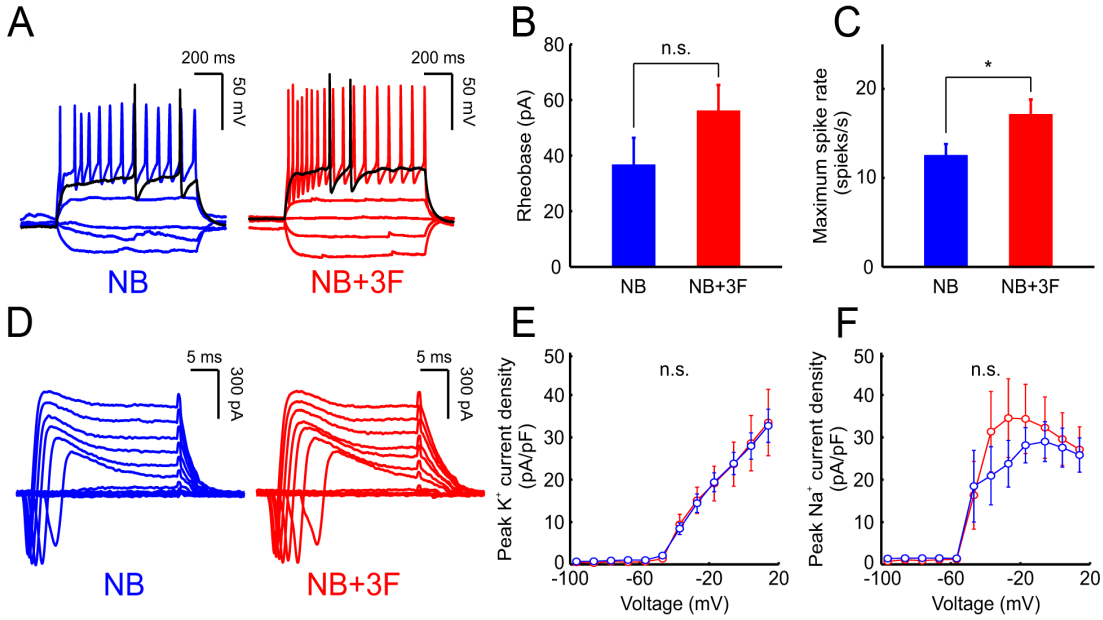

Figure 3.31: EYFP-positive neurons from NB and NB+3F cultures are capable of firing repetitive action potentials and possess functional sodium and potassium channels. The PNK18 line was cultured in NB and NB+3F conditions for at least 22 days. Patch clamp analysis of EYFP-positive cells was performed between day 22 and 24 of differentiation. **(A)** Tracings from current clamp recordings show repetitive action potentials after stimulated with increasing suprathreshold currents in EYFP-positive neurons from NB and NB+3F cultures. Black traces show the minimal current injections to generate action potentials. The delay in generating the first spike is noted. **(B)** Average of the minimal current necessary for initiating depolarisation (n=6 for NB and n=5 for NB+3F) and **(C)** maximum spike rate after suprathreshold current injection (n=6 for each group) in EYFP-positive cells. Neurons from the NB+3F culture had a significantly higher spike rate than neurons from the NB culture. **(D)** Tracings from voltage clamp recordings show groups of inward and outward voltage-activated currents, representing functional sodium and potassium channels, respectively, in EYFP-positive neurons derived in NB and NB+3F cultures. No difference in **(E)** potassium and **(F)** sodium current density of EYFP-positive neurons from NB and NB+3F cultures (n=7 for NB and n=6 for NB+3F). Data from NB-derived neurons and NB+3F-derived neurons are represented in blue and red, respectively. Unpaired Student's t-test; * $p<0.05$; n.s., no significance; Values are mean ± s.e.m. EYFP, enhanced yellow fluorescent protein.

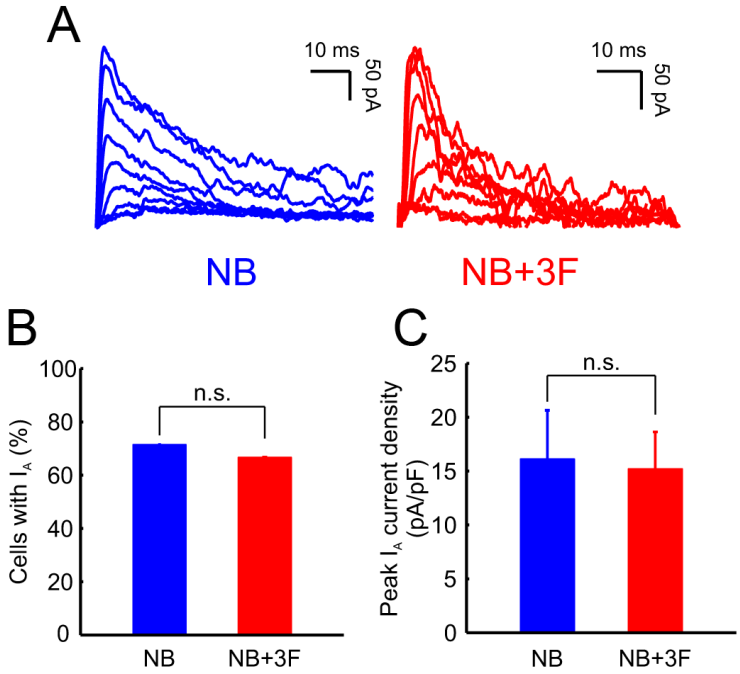

Figure 3.32: EYFP-positive neurons from NB and NB+3F cultures exhibited I_A currents. **(A)** Tracings from voltage clamp recordings showed families of fast-inactivating A-type potassium current (I_A) of EYFP-positive neurons from NB and NB+3F cultures. **(B)** The majority of EYFP-expressing cells (5 out of 7 in NB and 4 out of 6 in NB+3F) exhibited I_A currents. **(C)** The average maximal I_A current density (n=5 for NB and n=4 for NB+3F) was identical between EYFP-positive cells from both cultures. Unpaired Student's t-test; n.s., no significance; Values are mean ± s.e.m. EYFP, enhanced yellow fluorescent protein

Chapter 4: Discussion

4.1 Characterisation of an enkephalinergic reporter embryonic stem cell line

We have reported here the generation of an enkephalinergic reporter mESC line (PNK18), which can be used as a tool for studying enkephalinergic differentiation from mESCs. The PNK18 reporter line was generated by crossing a male BAC-*Penk*-*Cre* mouse (Besusso et al., 2013) to a female *Rosa26*-*EYFP* mouse (Srinivas et al., 2001) (Figure 3.1 F). Initial characterisation by Oct4 immunostaining implied the pluripotent potential of this line. Additionally, EYFP expression was not detected in PNK18 ESCs indicating that Cre-recombination had not occurred during the pluripotency stage and supported the specificity of the reporter. The PNK18 line was further characterised by chimaera generation via blastocyst injection. We found that three out of five animals analysed showed EYFP expression in the expected brain regions and cell types including the striatum, hippocampal dentate gyrus and cerebellum. Double immunofluorescence staining demonstrated that approximately half of the enkephalinergic neurons also expressed EYFP (Figure 3.2 D). However, all EYFP-positive neurons were enkephalin-positive ensuring the specificity of the line. Thus, the PNK18 ESC line is pluripotent and is a precise reporter for enkephalinergic neurons.

Despite of the specificity of the PNK18 line, one of its limitations is when the reporter is activated by Cre-mediated deletion of the stop cassette, the cells will continue to express EYFP throughout its life, even if it subsequently loses its enkephalinergic phenotype. For most applications such as *in vivo* labelling of enkephalinergic neurons in normal condition, this reporter would be ideal. However, for some application including *in vivo* labelling of enkephalinergic neurons in Huntington's disease models and *in vitro* differentiation of enkephalinergic neurons from ESCs, the possibility that enkephalin expression does not last for the lifespan of the neurons should be taken into consideration. Therefore, the PNK18 line may be

superior for some applications that aim to investigate the cause of *Penk* down-regulation in enkephalinergic neurons, an observation also seen in early stage Huntington's disease.

4.2 Enkephalinergic differentiation from mouse embryonic stem cells

4.2.1 N2B27 monolayer culture as a platform for neural differentiation

There are two widely used approaches to derive neuronal cell lineages from embryonic stem cells: the embryoid body (EB) formation (Bain et al., 1995) and monolayer differentiation (Ying et al., 2003). For MSN derivation, both approaches have been demonstrated to generate the DARPP32-positive MSNs with variable efficiency (Aubry et al., 2008, Zhang et al., 2010, Danjo et al., 2011, Shin et al., 2011, Ma et al., 2012, Delli Carri et al., 2013b). However, the monolayer culture is superior to the EB formation method from our perspective for the following reasons. Firstly, differentiated cells found in EB formation are more heterogeneous and consist of higher proportion of mesodermal and endodermal lineages compared to the monolayer protocol. Secondly, due to the nature of adherent cultures, cells undergoing differentiation via monolayer cultures are more easily monitored throughout the process. For these reasons, we have selected the N2B7 monolayer culture as a platform for neural differentiation.

It is known that, in monolayer cultures, the plating density needs to be adjusted empirically for each cell line. We found that an optimal plating density for the PNK18 line in the N2B27 culture is 15,000 cells/cm^2. Lower densities (7,500 cells/cm^2) exhibit massive cell death whereas higher plating densities (30,000 cells/cm^2), although reduce the amount of cell death, result in an increased percentage of undifferentiated cells in the culture.

Initial characterisation of cells cultured in the N2B27 monolayer protocol showed the presence of Ctip2-positive cells indicating that the culture was already committed to striatal fate to some degree since Ctip2 is expressed in post-mitotic MSNs (Arlotta et al., 2008) (Figure 3.3 C). Ctip2 is also found in cortical motor neurons (CMNs). However, it is unlikely that the Ctip2-positive cells in our cultures

were CMNs since it has been shown previously that the specification of dorsal forebrain identity from mESCs using monolayer culture requires inhibition of endogenous *Shh* (Gaspard et al., 2008), which did not happen in our culture system.

Retinoic acid (RA) signalling plays an important role in mESC differentiation from neural induction to neuronal subtype specification. Activation of retinoic acid signalling induces ESC differentiation towards both neural and non-neural lineages (Stavridis et al., 2010). After neural fate is acquired, RA contributes to rostro-caudal patterning of neural tube by inducing caudal identity (Gaspard and Vanderhaeghen, 2010). We, therefore, checked whether the presence of the RA precursor retinyl acetate in B27 supplement affected neural induction and patterning. We found that *Oct4* was expressed at higher levels in both cultures deficient in vitamin A than in N2B27 medium. The opposite was true for *Tubb3* expression (Figure 3.5). This indicates that the RA precursor may be needed for the loss of pluripotency of ESCs during differentiation. The expression of striatal markers such as *Ctip2* and *Ppp1r1b*, showed a higher trend of expression in the N2B27-vitA d2 onwards condition, which could be explained by the fact that this culture condition could have more forebrain neurons since RA was absent during neural patterning. However, expression of these striatal genes in all culture conditions analysed was only marginally different. We, therefore, selected N2B27 as a basal medium in order to minimise the number of undifferentiated cells remaining in the culture

4.2.2 Enhancement of cell survival during neural differentiation by modifying the culture medium

Cell death during monolayer neural differentiation is an issue encountered in this protocol. The severity of this problem may vary amongst different cell lines. The PNK18 reporter line, for example, has a lower survival rate compared to the E14 line, not uncommon in transgenic cell lines. For this reason we have optimised the culture conditions to increase the survival rate during differentiation in several ways. We first added Lif to the N2B27 medium on the first day of differentiation (Ying and Smith, 2003). In parallel to this, we added the anti-apoptotic molecule Y-27632 throughout the differentiation process. Under this condition, however, we still observed a vast amount of cell death at later stages of differentiation. In contrast, when we used ESC medium without Lif supplemented with the ROCK inhibitor (Y-27632) at day 0, then transferred to N2B27 medium supplemented with Y-27632 throughout differentiation, cell survival improved (Figure 3.7). This indicates that the presence of foetal bovine serum (FBS) in the ESC medium but not Lif in the culture at the time of plating is essential for cell survival during differentiation, at least for the PNK18 line.

Next, we checked whether the presence of the ROCK inhibitor for enhancing cell survival was needed throughout the differentiation (NB culture) or only on the first day of differentiation (NB+R culture). Indeed, the NB culture contained more live cells compared to NB+R condition at day 15 of differentiation, confirming the anti-apoptotic property of Y-27632 (Figure 3.8). Moreover, expression of the neural progenitor marker *Sox1*, the forebrain markers *Foxg1* and *Pax6* as well as the LGE marker *Gsx2* was enriched in NB compared to NB+R cultures (Figure 3.9). This is consistent with the literature suggesting that the inhibition of ROCK could induce neural differentiation (Chang et al., 2010, Frisca et al., 2013),

We have also tested whether addition of the neural progenitor mitogen Fgf2 would increase cell proliferation during differentiation. Although we found that this was not the case, an explanation might be the timing we chose to add Fgf2, which was day 0-1 of differentiation, was too early. Finding from Ying and colleagues

demonstrated that Fgf4 but not Fgf2, could enhance neural specification via an increase in the number of *Sox1*-positive progenitor cells (Ying et al., 2003). Fgf2, however, is known to be a potent mitogen for Sox1-positive neural progenitors, so an appropriate time point for adding exogenous Fgf2 would be a later time point (e.g. day 3-5) rather than the first two days of differentiation like we did.

4.2.3 Addition of exogenous DKK1, Shh and BDNF to improve striatal differentiation

Lastly, it has been demonstrated in several publications that addition of extrinsic factors could improve the efficiency of PSC-derived MSN generation. The most commonly use factors are the WNT inhibitor DKK1, SHH and BDNF. DKK1 is normally used during the early days of differentiation to induce neural specification as well as to instruct the rostral patterning once neural induction is occurred (Watanabe et al., 2005, Aubry et al., 2008, Zhang et al., 2010, Danjo et al., 2011, Delli Carri et al., 2013b). SHH instead, is used to specify forebrain neural cell to ventral fate since the MSNs originates from one of the ventral forebrain structure, the LGE (Aubry et al., 2008, Zhang et al., 2010, Danjo et al., 2011, Ma et al., 2012, Delli Carri et al., 2013b). BDNF is then added at a later stage to support neuronal maturation (Aubry et al., 2008, Zhang et al., 2010, Danjo et al., 2011, Ma et al., 2012, Delli Carri et al., 2013b). Since the enkephalinergic phenotype of DARPP32-positive MSNs generated using these three factors has not yet been demonstrated, we checked the whether enkephalinergic neurons could be produced and if so, more efficiently, from cultures using this cocktail. Our preliminary data showed that addition of these three factors to our culture (NB+3F) led to an increase in the percentage of EYFP-positive cells when compared to the control NB culture suggesting that enkephalinergic neurons could be generated from the NB+3F culture (Figure 3.13).

4.3 The use of surface markers to identify neural cells in culture

Cells in monolayer cultures are heterogeneous and, therefore, purification of neural lineage cells is necessary prior to gene expression profiling to avoid misinterpretation. One of the most commonly used techniques to select cells of interest is the fluorescence-activated cell sorting (FACS) technique, which is based on the light scattering and fluorescent properties, as well as the combination of different surface antigens, expressed by each subpopulation. We have shown here that CD24 is highly expressed in differentiating neural cells. A CD24-high population shows higher expression of neural progenitor and post-mitotic neuronal genes whilst the expression of a pluripotency marker was diminished (Figure 3.15). In contrast, the CD24-low fraction, a minority in differentiating cultures, comprised undifferentiated cells as determined by a high level of *Oct4* expression. The findings here are consistent with previous study by Pruszak and colleagues (Pruszak et al., 2009), which demonstrated increased CD24 expression level during ESC differentiation toward a neuronal phenotype.

In addition to CD24, we tested whether another surface marker, CD133, was helpful for separating neural progenitors from neuronal cells. CD133 is highly expressed in mouse CNS progenitor cells (Corti et al., 2007). So this marker could probably be used to label neural progenitors in our *in vitro* culture system. We speculated that the CD24-high/CD133-positive population would be neural progenitors whereas CD24-high/CD133-negative would label neuronal cells. However, qRT-PCR analysis showed that only the post-mitotic neuronal marker *Tubb3* was enriched in the CD24-high/CD133-negative fraction. No enrichment of other post-mitotic neuronal genes (e.g. *Rbfox3* and *Ncam1*) was found in such population (Figure 3.18). Likewise, the expression of the neural progenitor markers *Sox1*, *Nes* and *Pax6* was equally expressed in both populations analysed. This unexpected finding could be explained by the fact that CD133 has been widely used to identify CNS progenitor cells *in vivo* (Uchida et al., 2000, Lee et al., 2005, Panchision et al., 2007, Corti et al., 2007). To our knowledge, no publications have

demonstrated the use of this marker to label mESC-derived neural progenitor cells. It is possible that CD133 expression pattern in ESC-derived neural cells is not identical to their *in vivo* counterpart. To test this hypothesis, one approach would be to sort both CD133-negative and CD133-positive fractions and check whether they could proliferate when putting them back into culture. Alternatively, qRT-PCR analysis for neural progenitor genes of sorted CD133-negative and CD133-positive fractions would also be helpful.

Nevertheless, the use of CD24 is likely sufficient to distinguish neural progenitors from neurons. Although the use of CD24 with the established gating strategy, which eliminates undifferentiated cells from neural cells, was sufficient for the analyses performed. Further optimisation of gating strategies to obtain a more homogeneous population would be required prior to transplantation of neural progenitors into murine striata. Setting gates on three distinct subpopulations, CD24-low, -intermediate and -high followed by qRT-PCR analysis from these three subpopulations may assist homogeneity. The expectation would be that CD24-low fraction contains mainly *Oct4*-positive undifferentiated cells whilst CD24-intermediate and CD24-high would label neural progenitor and post-mitotic neurons, respectively.

4.4 *In vitro* characterisation of embryonic stem cell-derived enkephalinergic neurons

4.4.1 Penk expression in NB and NB+3F cultures

The discovery of only a proportion of EYFP-positive cells that co-expressed enkephalin in the PNK18 line was unexpected. One hypothesis was that the enkephalin peptide is continuously released and not stored in the cell and, thus, is difficult to detect. Alternatively, and, perhaps, the most likely, is that the EYFP-positive cells no longer expressed enkephalin at the time of analysis. The PNK18 line was constructed to express EYFP upon activation of *Pre-pro-enkephalin* promoter that would express Cre recombinase, which in turn would delete the conditional stop cassette. Therefore, EYFP would label any cells that acquired an enkephalinergic fate (including transiently) at any point in their life.

To test the first possibility (a secretory effect), we performed qRT-PCR analysis of the *Penk* transcript in both NB and NB+3F cultures. Data from bulk cultures demonstrated that *Penk* expression was diminished in the NB+3F culture (Figure 3.22). This finding ruled out the first hypothesis and was in favour of the second one. It could be argued that the analysis of bulk culture was not precisely reflecting what was happening in EYFP-positive cells. However, we believe that most of the *Penk* mRNA detected in the culture should be generated by EYFP-positive cells, with little possibility that the EYFP-negative cells would contribute to any *Penk* transcript found in the culture. Additionally, a similar finding was found from analysis of a more defined subpopulation, the CD24-high/EYFP-positive cells fraction sorted from both culture conditions (Figure 3.24). Furthermore, *Penk* expression was found to peak at day 5 of differentiation (Figure 3.23 B). By day 15 and day 21 of differentiation, *Penk* expression levels in the NB+3F culture dropped dramatically. Expression of *Penk* in NB culture was also decreased at later time points of differentiation (day 15 and 21) but to a milder extent compared to NB+3F culture. However, EYFP is highly expressed in NB+3F culture condition as a result

of the activation of the *Penk* promoter at earlier time point during differentiation as well as a proliferative effect of BDNF added to the cultures.

4.4.2 Role of BDNF

In vivo data from the previous work in the Minichiello lab by Dr. Dario Besusso showed that absence of Bdnf-TrkB signalling in striatopallidal MSNs contributed to loss of enkephalin expression (Besusso et al., 2013). This indicated that Bdnf is not responsible for the reduction of enkephalin expression observed in NB+3F culture. Instead, Bdnf itself, through TrkB signalling, maintains the enkephalinergic phenotype in striatopallidal MSNs *in vivo*. Our *in vitro* finding also supports this since an addition of BDNF in NB+B culture did not alter enkephalin expression. We initially expected that expression of enkephalin would be higher in the presence of exogenous BDNF although our data did not show so (Figure 3.26). Perhaps, the endogenous level of Bdnf in the culture may be enough to maintain enkephalin expression and, therefore, addition of exogenous BDNF is not required.

It should be noted that the expression level of *Penk* in both NB and NB+B cultures at day 21 of differentiation was slightly lower than that of day 15 despite no statistical significance (Figure 3.26). One explanation may be the lack of factors that are essential for both neuronal survival and maintenance of an enkephalinergic phenotype in the cultures. For instance, it is known that expression of *Penk* is regulated by cyclic adenosine monophosphate (cAMP) and protein kinase C (PKC) (Comb et al., 1986, Hyman and Borsook, 1996). Addition of cAMP may, therefore, maintain the enkephalin level in cultures. Furthermore, the glial cell line-derived neurotrophic factor (Gdnf) has been showed to be necessary for a survival of midbrain dopaminergic neurons, motor neurons and peripheral neurons (Lin et al., 1993, Airaksinen and Saarma, 2002). Enkephalinergic MSNs may also require such glial cell support for survival and GDNF was present in the cocktail used to derive MSNs from hESCs (Ma et al., 2012).

4.4.3 Role of exogenous DKK1 and Shh

Addition of either human DKK1 (in NB+D+B culture) or murine Shh (in NB+S+B culture), contrary to BDNF, led to a huge reduction in *Penk* transcript levels comparable to that observed in the NB+3F cultures (Figure 3.26). These data demonstrate that addition of exogenous DKK1 and Shh, at least with the same concentration and duration we used, should be avoided if an enkephalinergic phenotype is desired. We are aware that the loss of enkephalinergic phenotype might be due to the differences in duration or concentration of both factors in our system compared to others. However, the DKK1 and Shh concentrations used in our study was similar to that used by the majority of PSC-derived MSN reports (Table 4.1) (Aubry et al., 2008, Zhang et al., 2010, Danjo et al., 2011, Ma et al., 2012, Delli Carri et al., 2013b). Likewise, the duration of treatment was the same reported in the study that used mESC for deriving the MSN (Danjo et al., 2011). Thus, the likelihood that the concentration as well as the duration of treatment for DKK1 and Shh we have used are not suitable for MSN derivation is minimal. The discovery of increased *Nkx2.1* in the presence of exogenous DKK1 and Shh, indicating that these cultured cells had acquired other neuronal fates. This explains why the enkephalinergic phenotype has not been found in PSC-derived MSNs generated from those protocols.

It has been demonstrated that mESC-derived neural progenitors produced by monolayer differentiation devoid of any addition of exogenous ligands related to Shh and Wnt signalling pathway are ventral forebrain primed. This is due to an endogenous production of SHH in the culture (Gaspard et al., 2008). Likewise, a study from Shin and colleagues showed that Darpp32-positive MSNs could be derived from mESCs with simple monolayer culture (no exogenous Dkk1 or Shh added) (Shin et al., 2011). Consistent with this, we found that the NB culture exhibited a significant level of *Shh* transcript at day 7 of differentiation. Thus, endogenous Shh in NB culture may be enough for instructing cells to become LGE-primed progenitors. Addition of recombinant Shh in NB+D+S (NB+3F) culture, may result in excessive concentrations for LGE fate induction, but falls into an optimal

level for MGE commitment. Indeed, the higher expression of *Nkx2.1* at day 7 of the NB+D+S (NB+3F) culture confirms this hypothesis.

Transcription of *Dkk1* and *Shh* is regulated by a negative feedback loop. It is known that activation of the canonical Wnt signalling pathway induces *Dkk1* transcription to negatively regulate β-catenin-mediated transcription of target genes (Chamorro et al., 2005, González-Sancho et al., 2005). Inhibition of canonical Wnt signalling by exogenous DKK1, therefore, results in a decrease of *Dkk1* transcript, as observed in the NB+D+S (NB+3F) culture. Likewise, Shh positively regulates the expression of the Bmp family, which in turn suppresses *Shh* transcription (Bastida et al., 2009). Excess Shh by exogenous administration in the NB+D+S (NB+3F) culture, therefore, could inhibit endogenous production of *Shh*.

The reason why *Shh* was up-regulated in NB+3F culture at day 15 and 21 of differentiation is not clear (Figure 3.28). Perhaps, this was a transient over-compensation due to the removal of exogenous Shh at day 9 of differentiation since *Shh* up-regulation was less prominent at day 21 of differentiation. However, if this is the case, up-regulation of *Shh* should be evident in NB+S+B culture as well. The up-regulation of *Shh* in the presence of both exogenous DKK1 and Shh at day 15 and 21 of differentiation would imply an interaction between the two signalling pathways. Consistent with this, it has been shown that activation of Wnt signalling is required for Shh expression (Yang and Niswander, 1995).

It is very interesting that other striatopallidal markers such as *Adora2a* and *Drd2* are not influenced by exogenous DKK1 and Shh. Likewise, the MSN markers *Ppp1r1b*, *Ctip2*, *Foxp1* and *Foxp2* are similarly expressed in all culture conditions. This finding further confirms that, for MSN derivation from mESC, the addition of exogenous DKK1 and Shh is dispensable and causes down-regulation of *Penk*. Thus, our finding underscores the benefit of using the NB medium to derive enkephalinergic MSNs from mESCs, especially for modelling HD.

Table 4.1: Concentration and duration of treatment for recombinant DKK1 and SHH in published protocols.

	DKK1		SHH	
	Concentraion (ng/mL)	**Duration (day)**	**Concentraion (ng/mL)**	**Duration (day)**
Aubry et al., 2008*	100	25 (day 21-46)	200	25 (day 21-46)
Zhang et al., 2010*	100	8-10 (day 22-30)	250	8-10 (day 22-30)
Danjo et al., 2011**	200	6 (day 0-6)	200	6 (day 3-9)
Shin et al., 2012**	-	-	-	-
Ma et al., 2012*	-	-	200	14 (day 12-26)
Delli Carri et al., 2013*	100	21 (day 5-26)	200	21 (day 5-26)

* Differentiation protocol for hPSCs.

** Differentiation protocol for mESCs.

4.4.4 Electrophysiological analyses of EYFP-positive neurons

In order to confirm that the EYFP-positive cells grown in the NB and NB+3F cultures are physiologically functional, we analysed their electrophysiological properties using whole cell patch clamp technique. Basic properties such as resting membrane potential, membrane capacitance and membrane resistance were similar between EYFP-positive cells in NB and NB+3F cultures. Neurons from both cultures also exhibited functional sodium and potassium channels. Moreover, when stimulated with currents above a depolarising threshold, EYFP-positive neuronal cells from both cultures spiked multiple action potentials. Based on the maximum spike rate of EYFP-positive neurons, we found that NB+3F condition had more mature EYFP-expressing neurons compared to NB culture as they had a higher spike frequency. Furthermore, we also demonstrated that the majority of EYFP-positive neurons analysed from both culture conditions (approximately 70 per cent) possess an A-type potassium current (I_A), which is considered a hallmark for MSNs (Ericsson et al., 2011, Delli Carri et al., 2013b). The I_A current density was identical between EYFP cells derived from NB and NB+3F cultures. These data, therefore, indicated that both the electrophysiologically more mature EYFP-positive neurons grown in NB+3F and those grown in NB media are functional and exhibit electrical properties resembling *in vivo* MSNs.

Chapter 5: Conclusion and future directions

5.1 Conclusion

We have shown that the enkephalinergic MSNs can be generated from mESCs using a modified N2B27 monolayer culture. Striatopallidal enkephalinergic MSNs have been described as the most vulnerable neuronal population in the inherited polyglutamine-induced neurodegenerative disorder Huntington's disease (Reiner et al., 1988, Albin et al., 1990, Albin et al., 1992, Richfield et al., 1995, Deng et al., 2004). Currently there is no curative treatment and the development of an *in vitro* platform for deriving the enkephalinergic MSNs would be useful for both disease modelling and the development of cell-based therapies.

To allow dissection of enkephalinergic differentiation from mESCs, we generated an enkephalinergic reporter mESC line, the BAC-*Penk-Cre*$^{tg+}$, *Rosa26-EYFP*$^{yfp/+}$ (PNK18) line. Activation of the *Penk* promoter in any cells is visualised by EYFP expression resulting from the Cre-recombinase deletion of a stop cassette upstream of EYFP. Characterisation of the PNK18 line revealed that all of the EYFP-positive neurons within the striatum of chimaeras generated by PNK18 injection into blastocyst were enkephalinergic, confirming the specificity of the line. When the PNK18 line was cultured in the N2B27 neural differentiation medium, neural progenitors and post-mitotic neurons were found abundantly in the culture. Furthermore, use of the modified N2B27 culture (NB culture), in which the ROCK inhibitor Y-27632 was added into the culture throughout differentiation, greatly enhanced cell survival during neural differentiation.

By using a cell surface marker, CD24, we have set up a FACS strategy to purify neural cells from any undifferentiated cells remaining in the culture. This would exclude the possibility of having EYFP-positive undifferentiated cells contamination in the analyses.

We have shown that the percentage of EYFP-positive neurons in NB cultures can be increased approximately ten times by the addition of recombinant human DKK1 (100 ng/mL from day 1 to day 6) and recombinant mouse Shh (200 ng/mL from day 3 to day 9) into the culture medium (NB+3F). However, the higher number of EYFP-positive cells did not correlate with the expression level of *Penk* as determined by minimal *Penk* expression in sorted CD24-high/EYFP-positive cells. We subsequently demonstrated a transient peak of *Penk* expression in NB+3F cultures at day 5 of differentiation, which may account for the higher number of EYFP-expressing cells in this culture condition. Further investigation indicated that the addition of exogenous DKK1 and/or Shh causes down-regulation of *Penk* in NB+3F cultures. Interestingly, expression of other striatopallidal markers, *Adora2a* and *Drd2*, and the striatal markers, *Ppp1r1b*, *Ctip2*, *Foxp1* and *Foxp2*, were not affected by the presence of exogenous DKK1 and Shh.

Finally, we have shown that the EYFP-positive neurons from both NB and NB+3F cultures possessed electrical properties resembling functional MSNs. The A-type potassium current (I_A) was present in the majority of EYFP-expressing neurons from both culture conditions. Despite the similarity of the molecular and electrical phenotypes of the MSNs from both cultures, the enkephalinergic phenotype of striatopallidal MSNs was mainly found in the EYFP-positive neurons derived from the NB culture. Therefore, we propose that the presence of exogenous DKK1 and Shh in culture is unfavourable to derive enkephalinergic MSNs from mESCs. The absence of exogenous DKK1 and Shh in the culture, in contrast, results in the generation of enkephalinergic MSNs without affecting the molecular or electrophysiological signature of such neurons. These findings could be used to derive the enkephalinergic MSNs from mESCs for other applications including *in vitro* disease modelling.

5.2 Future directions

Further studies have been planned to confirm the identity of EYFP-positive neurons derived from NB and NB+3F cultures. Although we have shown by qRT-PCR that, other than *Penk*, the expression of other key markers for striatopallidal MSNs, as well as general markers for MSNs, is similar in both cultures, a comparison of the transcriptome of EYFP-positive neurons derived from both cultures would be useful for dissecting the cellular phenotypes of the EYFP neurons. At present we have performed RNA sequencing from FACsorted CD24-high/EYFP-positive neurons derived from both NB and NB+3F cultures and are awaiting differential expression and pathway analysis. In parallel, we are optimising FACS of enkephalinergic neurons from the striatum of transgenic animals (BAC-*Penk*-*Cre*$^{tg/+}$, *Ai9*$^{tm/+}$), in which enkephalinergic neurons are labelled with the tdTomato reporter (Madisen et al., 2010). Once this is achieved, enkephalinergic MSNs will be sorted from the striatum and RNA sequencing will be performed. Transcriptomic analysis will be performed to elucidate the similarities and discrepancies between the *in vitro* and the *in vivo* neurons.

Additionally, it is important to investigate whether the derivation of human enkephalinergic MSNs resembles the findings we have shown in mouse. It is highly likely that, developmentally, different species may behave differently. Indeed, a good example comes from two studies, which used either mESC or hESC to derive forebrain neurons. When monolayer culture was used without addition of Shh, the majority of mESC-derived forebrain neurons express ventral marker including *Gsx2* (Gaspard et al., 2008). In contrast, expression of ventral forebrain markers is minimal in hESC-derived telencephalic neurons cultures in medium devoid of exogenous SHH (Ma et al., 2012). Therefore, it might be possible that the default neural differentiation of mESC is towards ventral telencephalic fate whilst hESC-derived neurons are dorsally telencephalic primed.

Increasing the efficiency of the proportion of enkephalinergic neuron in the culture is essential for further applications. This could be achieved by further optimisation of the culture conditions. Alternatively, a more powerful approach is to

over-express transcription factors involved in enkephalinergic striatal differentiation in the differentiating cultures. This would, in theory, lead to an enrichment of the number of enkephalinergic MSN in the cultures.

Finally, to determine whether the EYFP-positive enkephalinergic cells could be engrafted and differentiated *in vivo*, transplantation of such cells should be performed. Since neural progenitor cells are more capable of surviving and integrating into host tissue, the EYFP-positive cells would be sorted during the differentiation stage found to contain the highest number of LGE-committed progenitor cells. To do this, we could use the CD24 with a new gating strategy to separate progenitors from post-mitotic neurons, or seek a new surface marker that is able to label neural progenitors. The sorted EYFP-positive progenitor would then be transplanted into the brain of Huntington's disease model animals such as the R6/2 mice (Mangiarini et al., 1996) or the YAC128 mice (Slow et al., 2003). Functional assessment for any improvement of motor deficit would then be performed. This would address whether the EYFP-positive neurons are capable of restoring the phenotypes related to striatal degeneration.

References

AGOSTON, D. V., SZEMES, M., DOBI, A., PALKOVITS, M., GEORGOPOULOS, K., GYORGY, A. & RING, M. A. 2007. Ikaros is expressed in developing striatal neurons and involved in enkephalinergic differentiation. *J Neurochem,* 102**,** 1805-16.

AIRAKSINEN, M. S. & SAARMA, M. 2002. The GDNF family: signalling, biological functions and therapeutic value. *Nat Rev Neurosci,* 3**,** 383-94.

ALBIN, R. L., REINER, A., ANDERSON, K. D., DURE, L. S., HANDELIN, B., BALFOUR, R., WHETSELL, W. O., PENNEY, J. B. & YOUNG, A. B. 1992. Preferential loss of striato-external pallidal projection neurons in presymptomatic Huntington's disease. *Ann Neurol,* 31**,** 425-30.

ALBIN, R. L., YOUNG, A. B. & PENNEY, J. B. 1989. The functional anatomy of basal ganglia disorders. *Trends Neurosci,* 12**,** 366-75.

ALBIN, R. L., YOUNG, A. B., PENNEY, J. B., HANDELIN, B., BALFOUR, R., ANDERSON, K. D., MARKEL, D. S., TOURTELLOTTE, W. W. & REINER, A. 1990. Abnormalities of striatal projection neurons and N-methyl-D-aspartate receptors in presymptomatic Huntington's disease. *N Engl J Med,* 322**,** 1293-8.

ALTAR, C. A., CAI, N., BLIVEN, T., JUHASZ, M., CONNER, J. M., ACHESON, A. L., LINDSAY, R. M. & WIEGAND, S. J. 1997. Anterograde transport of brain-derived neurotrophic factor and its role in the brain. *Nature,* 389**,** 856-60.

ANDERSON, S. A., QIU, M., BULFONE, A., EISENSTAT, D. D., MENESES, J., PEDERSEN, R. & RUBENSTEIN, J. L. 1997. Mutations of the homeobox genes Dlx-1 and Dlx-2 disrupt the striatal subventricular zone and differentiation of late born striatal neurons. *Neuron,* 19**,** 27-37.

ARLOTTA, P., MOLYNEAUX, B. J., CHEN, J., INOUE, J., KOMINAMI, R. & MACKLIS, J. D. 2005. Neuronal subtype-specific genes that control corticospinal motor neuron development in vivo. *Neuron,* 45**,** 207-21.

ARLOTTA, P., MOLYNEAUX, B. J., JABAUDON, D., YOSHIDA, Y. & MACKLIS, J. D. 2008. Ctip2 controls the differentiation of medium spiny neurons and the establishment of the cellular architecture of the striatum. *J Neurosci,* 28**,** 622-32.

ARNING, L., KRAUS, P. H., VALENTIN, S., SAFT, C., ANDRICH, J. & EPPLEN, J. T. 2005. NR2A and NR2B receptor gene variations modify age at onset in Huntington disease. *Neurogenetics,* 6**,** 25-8.

AUBRY, L., BUGI, A., LEFORT, N., ROUSSEAU, F., PESCHANSKI, M. & PERRIER, A. L. 2008. Striatal progenitors derived from human ES cells mature into DARPP32 neurons in vitro and in quinolinic acid-lesioned rats. *Proc Natl Acad Sci U S A,* 105**,** 16707-12.

BAIN, G., KITCHENS, D., YAO, M., HUETTNER, J. E. & GOTTLIEB, D. I. 1995. Embryonic stem cells express neuronal properties in vitro. *Dev Biol,* 168**,** 342-57.

BAQUET, Z. C., GORSKI, J. A. & JONES, K. R. 2004. Early striatal dendrite deficits followed by neuron loss with advanced age in the absence of anterograde cortical brain-derived neurotrophic factor. *J Neurosci,* 24**,** 4250-8.

BASTIDA, M. F., SHETH, R. & ROS, M. A. 2009. A BMP-Shh negative-feedback loop restricts Shh expression during limb development. *Development,* 136**,** 3779-89.

BEAR, M. F., CONNORS, B. W. & PARADISO, M. A. 2001. Brain control of movement. *In:* BEAR, M. F., CONNORS, B. W. & PARADISO, M. A. (eds.) *Neuroscience : exploring the brain.* 2nd ed. Baltimore, Md.: Lippincott Williams & Wilkins.

BENRAISS, A. & GOLDMAN, S. A. 2011. Cellular therapy and induced neuronal replacement for Huntington's disease. *Neurotherapeutics,* 8**,** 577-90.

BERGSON, C., MRZLJAK, L., SMILEY, J. F., PAPPY, M., LEVENSON, R. & GOLDMAN-RAKIC, P. S. 1995. Regional, cellular, and subcellular variations in the distribution of D1 and D5 dopamine receptors in primate brain. *J Neurosci,* 15**,** 7821-36.

BESSON, M. J., GRAYBIEL, A. M. & QUINN, B. 1990. Co-expression of neuropeptides in the cat's striatum: an immunohistochemical study of substance P, dynorphin B and enkephalin. *Neuroscience,* 39**,** 33-58.

BESUSSO, D., GEIBEL, M., KRAMER, D., SCHNEIDER, T., PENDOLINO, V., PICCONI, B., CALABRESI, P., BANNERMAN, D. M. & MINICHIELLO, L. 2013. BDNF-TrkB signaling in striatopallidal neurons controls inhibition of locomotor behavior. *Nat Commun,* 4**,** 2031.

BOLAM, J. P., HANLEY, J. J., BOOTH, P. A. & BEVAN, M. D. 2000. Synaptic organisation of the basal ganglia. *J Anat,* 196 (Pt 4)**,** 527-42.

BULFONE, A., PUELLES, L., PORTEUS, M. H., FROHMAN, M. A., MARTIN, G. R. & RUBENSTEIN, J. L. 1993. Spatially restricted expression of Dlx-1, Dlx-2 (Tes-1), Gbx-2, and Wnt-3 in the embryonic day 12.5 mouse forebrain defines potential transverse and longitudinal segmental boundaries. *J Neurosci,* 13**,** 3155-72.

BUTT, S. J., SOUSA, V. H., FUCCILLO, M. V., HJERLING-LEFFLER, J., MIYOSHI, G., KIMURA, S. & FISHELL, G. 2008. The requirement of Nkx2-1 in the temporal specification of cortical interneuron subtypes. *Neuron,* 59**,** 722-32.

CARTER, R. L. & CHAN, A. W. 2012. Pluripotent stem cells models for Huntington's disease: prospects and challenges. *J Genet Genomics,* 39**,** 253-9.

CASAROSA, S., FODE, C. & GUILLEMOT, F. 1999. Mash1 regulates neurogenesis in the ventral telencephalon. *Development,* 126**,** 525-34.

CHAMBERS, S. M., FASANO, C. A., PAPAPETROU, E. P., TOMISHIMA, M., SADELAIN, M. & STUDER, L. 2009. Highly efficient neural conversion of human ES and iPS cells by dual inhibition of SMAD signaling. *Nat Biotechnol,* 27**,** 275-80.

CHAMORRO, M. N., SCHWARTZ, D. R., VONICA, A., BRIVANLOU, A. H., CHO, K. R. & VARMUS, H. E. 2005. FGF-20 and DKK1 are transcriptional targets of beta-catenin and FGF-20 is implicated in cancer and development. *EMBO J,* 24**,** 73-84.

CHANG, T. C., CHEN, Y. C., YANG, M. H., CHEN, C. H., HSING, E. W., KO, B. S., LIOU, J. Y. & WU, K. K. 2010. Rho kinases regulate the renewal and neural differentiation of embryonic stem cells in a cell plating density-dependent manner. *PLoS One,* 5**,** e9187.

CHAO, M. V. 2003. Neurotrophins and their receptors: a convergence point for many signalling pathways. *Nat Rev Neurosci,* 4**,** 299-309.

CHIANG, C., LITINGTUNG, Y., LEE, E., YOUNG, K. E., CORDEN, J. L., WESTPHAL, H. & BEACHY, P. A. 1996. Cyclopia and defective axial patterning in mice lacking Sonic hedgehog gene function. *Nature,* 383**,** 407-13.

COBOS, I., BROCCOLI, V. & RUBENSTEIN, J. L. 2005. The vertebrate ortholog of Aristaless is regulated by Dlx genes in the developing forebrain. *J Comp Neurol,* 483**,** 292-303.

COLOMBO, E., COLLOMBAT, P., COLASANTE, G., BIANCHI, M., LONG, J., MANSOURI, A., RUBENSTEIN, J. L. & BROCCOLI, V. 2007. Inactivation of Arx, the murine ortholog of the X-linked lissencephaly with ambiguous genitalia gene, leads to severe disorganization of the ventral telencephalon with impaired neuronal migration and differentiation. *J Neurosci,* 27**,** 4786-98.

COMB, M., BIRNBERG, N. C., SEASHOLTZ, A., HERBERT, E. & GOODMAN, H. M. 1986. A cyclic AMP- and phorbol ester-inducible DNA element. *Nature,* 323**,** 353-6.

CORBIN, J. G., GAIANO, N., MACHOLD, R. P., LANGSTON, A. & FISHELL, G. 2000. The Gsh2 homeodomain gene controls multiple aspects of telencephalic development. *Development,* 127**,** 5007-20.

CORTI, S., NIZZARDO, M., NARDINI, M., DONADONI, C., LOCATELLI, F., PAPADIMITRIOU, D., SALANI, S., DEL BO, R., GHEZZI, S., STRAZZER, S., BRESOLIN, N. & COMI, G. P. 2007. Isolation and characterization of murine neural stem/progenitor cells based on Prominin-1 expression. *Exp Neurol,* 205**,** 547-62.

CROSSMAN, A. R., MITCHELL, I. J., SAMBROOK, M. A. & JACKSON, A. 1988. Chorea and myoclonus in the monkey induced by gamma-aminobutyric acid antagonism in the lentiform complex. The site of drug action and a hypothesis for the neural mechanisms of chorea. *Brain,* 111 (Pt 5)**,** 1211-33.

DANJO, T., EIRAKU, M., MUGURUMA, K., WATANABE, K., KAWADA, M., YANAGAWA, Y., RUBENSTEIN, J. L. & SASAI, Y. 2011. Subregional specification of embryonic stem cell-derived ventral telencephalic tissues by timed and combinatory treatment with extrinsic signals. *J Neurosci,* 31**,** 1919-33.

DEHORTER, N., GUIGONI, C., LOPEZ, C., HIRSCH, J., EUSEBIO, A., BEN-ARI, Y. & HAMMOND, C. 2009. Dopamine-deprived striatal GABAergic interneurons burst and generate repetitive gigantic IPSCs in medium spiny neurons. *J Neurosci,* 29**,** 7776-87.

DELLI CARRI, A., ONORATI, M., CASTIGLIONI, V., FAEDO, A., CAMNASIO, S., TOSELLI, M., BIELLA, G. & CATTANEO, E. 2013a. Human pluripotent stem cell differentiation into authentic striatal projection neurons. *Stem Cell Rev,* 9**,** 461-74.

DELLI CARRI, A., ONORATI, M., LELOS, M. J., CASTIGLIONI, V., FAEDO, A., MENON, R., CAMNASIO, S., VUONO, R., SPAIARDI, P., TALPO, F., TOSELLI, M., MARTINO, G., BARKER, R. A., DUNNETT, S. B., BIELLA, G. & CATTANEO, E. 2013b. Developmentally coordinated extrinsic signals drive human pluripotent stem cell differentiation toward authentic DARPP-32+ medium-sized spiny neurons. *Development,* 140**,** 301-12.

DELONG, M. R. 1990. Primate models of movement disorders of basal ganglia origin. *Trends Neurosci,* 13**,** 281-5.

DENG, Y. P., ALBIN, R. L., PENNEY, J. B., YOUNG, A. B., ANDERSON, K. D. & REINER, A. 2004. Differential loss of striatal projection systems in Huntington's disease: a quantitative immunohistochemical study. *J Chem Neuroanat,* 27**,** 143-64.

DESPLATS, P. A., LAMBERT, J. R. & THOMAS, E. A. 2008. Functional roles for the striatal-enriched transcription factor, Bcl11b, in the control of striatal gene expression and transcriptional dysregulation in Huntington's disease. *Neurobiol Dis,* 31**,** 298-308.

DJOUSSÉ, L., KNOWLTON, B., CUPPLES, L. A., MARDER, K., SHOULSON, I. & MYERS, R. H. 2002. Weight loss in early stage of Huntington's disease. *Neurology,* 59**,** 1325-30.

DO, J., KIM, J. I., BAKES, J., LEE, K. & KAANG, B. K. 2012. Functional roles of neurotransmitters and neuromodulators in the dorsal striatum. *Learn Mem,* 20**,** 21-8.

DOUAUD, G., GAURA, V., RIBEIRO, M. J., LETHIMONNIER, F., MAROY, R., VERNY, C., KRYSTKOWIAK, P., DAMIER, P., BACHOUD-LEVI, A. C., HANTRAYE, P. & REMY, P. 2006. Distribution of grey matter atrophy in Huntington's disease patients: a combined ROI-based and voxel-based morphometric study. *Neuroimage,* 32**,** 1562-75.

ECHELARD, Y., EPSTEIN, D. J., ST-JACQUES, B., SHEN, L., MOHLER, J., MCMAHON, J. A. & MCMAHON, A. P. 1993. Sonic hedgehog, a member of a family of putative signaling molecules, is implicated in the regulation of CNS polarity. *Cell,* 75**,** 1417-30.

EIRAKU, M., WATANABE, K., MATSUO-TAKASAKI, M., KAWADA, M., YONEMURA, S., MATSUMURA, M., WATAYA, T., NISHIYAMA, A., MUGURUMA, K. & SASAI, Y. 2008. Self-organized formation of polarized cortical tissues from ESCs and its active manipulation by extrinsic signals. *Cell Stem Cell,* 3**,** 519-32.

EL-AKABAWY, G., MEDINA, L. M., JEFFRIES, A., PRICE, J. & MODO, M. 2011. Purmorphamine increases DARPP-32 differentiation in human striatal neural stem cells through the Hedgehog pathway. *Stem Cells Dev,* 20**,** 1873-87.

ERICSON, J., MUHR, J., PLACZEK, M., LINTS, T., JESSELL, T. M. & EDLUND, T. 1995. Sonic hedgehog induces the differentiation of ventral forebrain neurons: a common signal for ventral patterning within the neural tube. *Cell,* 81**,** 747-56.

ERICSSON, J., SILBERBERG, G., ROBERTSON, B., WIKSTRÖM, M. A. & GRILLNER, S. 2011. Striatal cellular properties conserved from lampreys to mammals. *J Physiol,* 589**,** 2979-92.

ERNST, A., ALKASS, K., BERNARD, S., SALEHPOUR, M., PERL, S., TISDALE, J., POSSNERT, G., DRUID, H. & FRISÉN, J. 2014. Neurogenesis in the striatum of the adult human brain. *Cell,* 156**,** 1072-83.

ESCANDÓN, E., SOPPET, D., ROSENTHAL, A., MENDOZA-RAMÍREZ, J. L., SZÖNYI, E., BURTON, L. E., HENDERSON, C. E., PARADA, L. F. & NIKOLICS, K. 1994. Regulation of neurotrophin receptor expression during embryonic and postnatal development. *J Neurosci,* 14**,** 2054-68.

FERRÉ, S., O'CONNOR, W. T., FUXE, K. & UNGERSTEDT, U. 1993. The striopallidal neuron: a main locus for adenosine-dopamine interactions in the brain. *J Neurosci,* 13**,** 5402-6.

FRISCA, F., CROMBIE, D. E., DOTTORI, M., GOLDSHMIT, Y. & PÉBAY, A. 2013. Rho/ROCK pathway is essential to the expansion, differentiation, and morphological rearrangements of human neural stem/progenitor cells induced by lysophosphatidic acid. *J Lipid Res,* 54**,** 1192-206.

GASPARD, N., BOUSCHET, T., HOUREZ, R., DIMIDSCHSTEIN, J., NAEIJE, G., VAN DEN AMEELE, J., ESPUNY-CAMACHO, I., HERPOEL, A., PASSANTE, L., SCHIFFMANN, S. N., GAILLARD, A. & VANDERHAEGHEN, P. 2008. An intrinsic mechanism of corticogenesis from embryonic stem cells. *Nature,* 455**,** 351-7.

GASPARD, N. & VANDERHAEGHEN, P. 2010. Mechanisms of neural specification from embryonic stem cells. *Curr Opin Neurobiol,* 20**,** 37-43.

GAUTHIER, L. R., CHARRIN, B. C., BORRELL-PAGÈS, M., DOMPIERRE, J. P., RANGONE, H., CORDELIÈRES, F. P., DE MEY, J., MACDONALD, M. E., LESSMANN, V., HUMBERT, S. & SAUDOU, F. 2004. Huntingtin controls neurotrophic support and survival of neurons by enhancing BDNF vesicular transport along microtubules. *Cell,* 118**,** 127-38.

GERFEN, C. R. 1992. The neostriatal mosaic: multiple levels of compartmental organization. *Trends Neurosci,* 15**,** 133-9.

GERFEN, C. R., BAIMBRIDGE, K. G. & MILLER, J. J. 1985. The neostriatal mosaic: compartmental distribution of calcium-binding protein and parvalbumin in the basal ganglia of the rat and monkey. *Proc Natl Acad Sci U S A,* 82**,** 8780-4.

GERFEN, C. R., ENGBER, T. M., MAHAN, L. C., SUSEL, Z., CHASE, T. N., MONSMA, F. J. & SIBLEY, D. R. 1990. D1 and D2 dopamine receptor-regulated gene expression of striatonigral and striatopallidal neurons. *Science,* 250**,** 1429-32.

GERFEN, C. R. & YOUNG, W. S. 1988. Distribution of striatonigral and striatopallidal peptidergic neurons in both patch and matrix compartments: an in situ hybridization histochemistry and fluorescent retrograde tracing study. *Brain Res,* 460**,** 161-7.

GERTLER, T. S., CHAN, C. S. & SURMEIER, D. J. 2008. Dichotomous anatomical properties of adult striatal medium spiny neurons. *J Neurosci,* 28**,** 10814-24.

GIL, J. M. & REGO, A. C. 2008. Mechanisms of neurodegeneration in Huntington's disease. *Eur J Neurosci,* 27**,** 2803-20.

GILBERT, S. F. 2010. The emergence of the ectoderm: Central nervous system and epidermis. *In:* GILBERT, S. F. (ed.) *Develpmental Biology.* 9th ed. Sunderland, MA: Sinauer Associates.

GITTIS, A. H., HANG, G. B., LADOW, E. S., SHOENFELD, L. R., ATALLAH, B. V., FINKBEINER, S. & KREITZER, A. C. 2011. Rapid target-specific remodeling of fast-spiking inhibitory circuits after loss of dopamine. *Neuron,* 71**,** 858-68.

GITTIS, A. H. & KREITZER, A. C. 2012. Striatal microcircuitry and movement disorders. *Trends Neurosci,* 35**,** 557-64.

GITTIS, A. H., NELSON, A. B., THWIN, M. T., PALOP, J. J. & KREITZER, A. C. 2010. Distinct roles of GABAergic interneurons in the regulation of striatal output pathways. *J Neurosci,* 30**,** 2223-34.

GLASS, M., DRAGUNOW, M. & FAULL, R. L. 2000. The pattern of neurodegeneration in Huntington's disease: a comparative study of cannabinoid, dopamine, adenosine and GABA(A) receptor alterations in the human basal ganglia in Huntington's disease. *Neuroscience,* 97**,** 505-19.

GONZÁLEZ-SANCHO, J. M., AGUILERA, O., GARCÍA, J. M., PENDÁS-FRANCO, N., PEÑA, C., CAL, S., GARCÍA DE HERREROS, A., BONILLA, F. & MUÑOZ, A. 2005. The Wnt antagonist DICKKOPF-1 gene is a downstream target of beta-catenin/TCF and is downregulated in human colon cancer. *Oncogene,* 24**,** 1098-103.

GORSKI, J. A., ZEILER, S. R., TAMOWSKI, S. & JONES, K. R. 2003. Brain-derived neurotrophic factor is required for the maintenance of cortical dendrites. *J Neurosci,* 23**,** 6856-65.

GRAY, M., SHIRASAKI, D. I., CEPEDA, C., ANDRÉ, V. M., WILBURN, B., LU, X. H., TAO, J., YAMAZAKI, I., LI, S. H., SUN, Y. E., LI, X. J., LEVINE, M. S. & YANG, X. W. 2008. Full-length human mutant huntingtin with a stable polyglutamine repeat can elicit progressive and selective neuropathogenesis in BACHD mice. *J Neurosci,* 28**,** 6182-95.

GRAYBIEL, A. M. 1990. Neurotransmitters and neuromodulators in the basal ganglia. *Trends Neurosci,* 13**,** 244-54.

GRAYBIEL, A. M., BAUGHMAN, R. W. & ECKENSTEIN, F. 1986. Cholinergic neuropil of the striatum observes striosomal boundaries. *Nature,* 323**,** 625-7.

GRAYBIEL, A. M. & CHESSELET, M. F. 1984. Compartmental distribution of striatal cell bodies expressing [Met]enkephalin-like immunoreactivity. *Proc Natl Acad Sci U S A,* 81**,** 7980-4.

GRAYBIEL, A. M. & RAGSDALE, C. W. 1978. Histochemically distinct compartments in the striatum of human, monkeys, and cat demonstrated by acetylthiocholinesterase staining. *Proc Natl Acad Sci U S A,* 75**,** 5723-6.

GUSELLA, J. F. 2001. Huntington Disease. *Encyclopedia of Life Sciences* [Online].

GUTIN, G., FERNANDES, M., PALAZZOLO, L., PAEK, H., YU, K., ORNITZ, D. M., MCCONNELL, S. K. & HÉBERT, J. M. 2006. FGF signalling generates ventral telencephalic cells independently of SHH. *Development,* 133**,** 2937-46.

GUZMAN, M. S., DE JAEGER, X., RAULIC, S., SOUZA, I. A., LI, A. X., SCHMID, S., MENON, R. S., GAINETDINOV, R. R., CARON, M. G., BARTHA, R., PRADO, V. F. & PRADO, M. A. 2011. Elimination of the vesicular acetylcholine transporter in the striatum reveals regulation of behaviour by cholinergic-glutamatergic co-transmission. *PLoS Biol,* 9**,** e1001194.

HARRISON, M. B., TISSOT, M. & WILEY, R. G. 1996. Expression of m1 and m4 muscarinic receptor mRNA in the striatum following a selective lesion of striatonigral neurons. *Brain Res,* 734**,** 323-6.

HEBERT, J. M. & FISHELL, G. 2008. The genetics of early telencephalon patterning: some assembly required. *Nat Rev Neurosci,* 9**,** 678-85.

HEDREEN, J. C. & FOLSTEIN, S. E. 1995. Early loss of neostriatal striosome neurons in Huntington's disease. *J Neuropathol Exp Neurol,* 54**,** 105-20.

HERKENHAM, M. & PERT, C. B. 1981. Mosaic distribution of opiate receptors, parafascicular projections and acetylcholinesterase in rat striatum. *Nature,* 291**,** 415-8.

HERSCH, S. M., GUTEKUNST, C. A., REES, H. D., HEILMAN, C. J. & LEVEY, A. I. 1994. Distribution of m1-m4 muscarinic receptor proteins in the rat striatum: light and electron microscopic immunocytochemistry using subtype-specific antibodies. *J Neurosci,* 14**,** 3351-63.

HEUSER, I. J., CHASE, T. N. & MOURADIAN, M. M. 1991. The limbic-hypothalamic-pituitary-adrenal axis in Huntington's disease. *Biol Psychiatry,* 30**,** 943-52.

HOOPER, M., HARDY, K., HANDYSIDE, A., HUNTER, S. & MONK, M. 1987. HPRT-deficient (Lesch-Nyhan) mouse embryos derived from germline colonization by cultured cells. *Nature,* 326**,** 292-5.

HOUART, C., CANEPARO, L., HEISENBERG, C., BARTH, K., TAKE-UCHI, M. & WILSON, S. 2002. Establishment of the telencephalon during gastrulation by local antagonism of Wnt signaling. *Neuron,* 35**,** 255-65.

HOUART, C., WESTERFIELD, M. & WILSON, S. W. 1998. A small population of anterior cells patterns the forebrain during zebrafish gastrulation. *Nature,* 391**,** 788-92.

HUGGENVIK, J. I., COLLARD, M. W., STOFKO, R. E., SEASHOLTZ, A. F. & UHLER, M. D. 1991. Regulation of the human enkephalin promoter by two isoforms of the catalytic subunit of cyclic adenosine 3',5'-monophosphate-dependent protein kinase. *Mol Endocrinol,* 5**,** 921-30.

HYMAN, S. E. & BORSOOK, D. 1996. Mechanisms regulating proenkephalin gene expression: contributions of transgenic models. *NIDA Res Monogr,* 161**,** 59-71.

HÉBERT, J. M. & FISHELL, G. 2008. The genetics of early telencephalon patterning: some assembly required. *Nat Rev Neurosci,* 9**,** 678-85.

INOUE, T., NAKAMURA, S. & OSUMI, N. 2000. Fate mapping of the mouse prosencephalic neural plate. *Dev Biol,* 219**,** 373-83.

IVKOVIC, S. & EHRLICH, M. E. 1999. Expression of the striatal DARPP-32/ARPP-21 phenotype in GABAergic neurons requires neurotrophins in vivo and in vitro. *J Neurosci,* 19**,** 5409-19.

IVKOVIC, S., POLONSKAIA, O., FARINAS, I. & EHRLICH, M. E. 1997. Brain-derived neurotrophic factor regulates maturation of the DARPP-32 phenotype in striatal medium spiny neurons: studies in vivo and in vitro. *Neuroscience,* 79**,** 509-16.

KASSUBEK, J., JUENGLING, F. D., ECKER, D. & LANDWEHRMEYER, G. B. 2005. Thalamic atrophy in Huntington's disease co-varies with cognitive performance: a morphometric MRI analysis. *Cereb Cortex,* 15**,** 846-53.

KEGEL, K. B., MELONI, A. R., YI, Y., KIM, Y. J., DOYLE, E., CUIFFO, B. G., SAPP, E., WANG, Y., QIN, Z. H., CHEN, J. D., NEVINS, J. R., ARONIN, N. & DIFIGLIA, M. 2002. Huntingtin is present in the nucleus, interacts with the transcriptional corepressor C-terminal binding protein, and represses transcription. *J Biol Chem,* 277**,** 7466-76.

KELLY, C. M., DUNNETT, S. B. & ROSSER, A. E. 2009. Medium spiny neurons for transplantation in Huntington's disease. *Biochem Soc Trans,* 37**,** 323-8.

KIMURA, C., YOSHINAGA, K., TIAN, E., SUZUKI, M., AIZAWA, S. & MATSUO, I. 2000. Visceral endoderm mediates forebrain development by suppressing posteriorizing signals. *Dev Biol,* 225**,** 304-21.

KREITZER, A. C. 2009. Physiology and pharmacology of striatal neurons. *Annu Rev Neurosci,* 32**,** 127-47.

KREMER, H. P. & ROOS, R. A. 1992. Weight loss in Huntington's disease. *Arch Neurol,* 49**,** 349.

LANDLES, C. & BATES, G. P. 2004. Huntingtin and the molecular pathogenesis of Huntington's disease. Fourth in molecular medicine review series. *EMBO Rep,* 5**,** 958-63.

LANSKA, D. J., LAVINE, L., LANSKA, M. J. & SCHOENBERG, B. S. 1988. Huntington's disease mortality in the United States. *Neurology,* 38**,** 769-72.

LEBLHUBER, F., PEICHL, M., NEUBAUER, C., REISECKER, F., STEINPARZ, F. X., WINDHAGER, E. & MASCHEK, W. 1995. Serum dehydroepiandrosterone and cortisol measurements in Huntington's chorea. *J Neurol Sci,* 132**,** 76-9.

LEE, A., KESSLER, J. D., READ, T. A., KAISER, C., CORBEIL, D., HUTTNER, W. B., JOHNSON, J. E. & WECHSLER-REYA, R. J. 2005. Isolation of neural stem cells from the postnatal cerebellum. *Nat Neurosci,* 8**,** 723-9.

LEE, S. H., LUMELSKY, N., STUDER, L., AUERBACH, J. M. & MCKAY, R. D. 2000. Efficient generation of midbrain and hindbrain neurons from mouse embryonic stem cells. *Nat Biotechnol,* 18**,** 675-9.

LEVEY, A. I., HERSCH, S. M., RYE, D. B., SUNAHARA, R. K., NIZNIK, H. B., KITT, C. A., PRICE, D. L., MAGGIO, R., BRANN, M. R. & CILIAX, B. J. 1993. Localization of D1 and D2 dopamine receptors in brain with subtype-specific antibodies. *Proc Natl Acad Sci U S A,* 90**,** 8861-5.

LEVINE, A. J. & BRIVANLOU, A. H. 2007. Proposal of a model of mammalian neural induction. *Dev Biol,* 308**,** 247-56.

LEVINE, M. S., KLAPSTEIN, G. J., KOPPEL, A., GRUEN, E., CEPEDA, C., VARGAS, M. E., JOKEL, E. S., CARPENTER, E. M., ZANJANI, H., HURST, R. S., EFSTRATIADIS, A., ZEITLIN, S. & CHESSELET, M. F. 1999. Enhanced sensitivity to N-methyl-D-aspartate receptor activation in transgenic and knockin mouse models of Huntington's disease. *J Neurosci Res,* 58**,** 515-32.

LI, H., WAGNER, E., MCCAFFERY, P., SMITH, D., ANDREADIS, A. & DRÄGER, U. C. 2000. A retinoic acid synthesizing enzyme in ventral retina and telencephalon of the embryonic mouse. *Mech Dev,* 95**,** 283-9.

LI, J. Y., PLOMANN, M. & BRUNDIN, P. 2003. Huntington's disease: a synaptopathy? *Trends Mol Med,* 9**,** 414-20.

LIAO, W. L. & LIU, F. C. 2005. RARbeta isoform-specific regulation of DARPP-32 gene expression: an ectopic expression study in the developing rat telencephalon. *Eur J Neurosci,* 21**,** 3262-8.

LIN, L. F., DOHERTY, D. H., LILE, J. D., BEKTESH, S. & COLLINS, F. 1993. GDNF: a glial cell line-derived neurotrophic factor for midbrain dopaminergic neurons. *Science,* 260**,** 1130-2.

LOBO, M. K., KARSTEN, S. L., GRAY, M., GESCHWIND, D. H. & YANG, X. W. 2006. FACS-array profiling of striatal projection neuron subtypes in juvenile and adult mouse brains. *Nat Neurosci,* 9**,** 443-52.

LONG, J. E., SWAN, C., LIANG, W. S., COBOS, I., POTTER, G. B. & RUBENSTEIN, J. L. 2009. Dlx1&2 and Mash1 transcription factors control striatal patterning and differentiation through parallel and overlapping pathways. *J Comp Neurol,* 512**,** 556-72.

LORINCZ, M. T. 2006. Optimized neuronal differentiation of murine embryonic stem cells: role of cell density. *Methods Mol Biol,* 330**,** 55-69.

MA, L., HU, B., LIU, Y., VERMILYEA, S. C., LIU, H., GAO, L., SUN, Y., ZHANG, X. & ZHANG, S. C. 2012. Human embryonic stem cell-derived GABA neurons correct locomotion deficits in quinolinic acid-lesioned mice. *Cell Stem Cell,* 10**,** 455-64.

MACDONALD, R., BARTH, K. A., XU, Q., HOLDER, N., MIKKOLA, I. & WILSON, S. W. 1995. Midline signalling is required for Pax gene regulation and patterning of the eyes. *Development,* 121**,** 3267-78.

MACHOLD, R., HAYASHI, S., RUTLIN, M., MUZUMDAR, M. D., NERY, S., CORBIN, J. G., GRITLI-LINDE, A., DELLOVADE, T., PORTER, J. A., RUBIN, L. L., DUDEK, H., MCMAHON, A. P. & FISHELL, G. 2003. Sonic hedgehog is required for progenitor cell maintenance in telencephalic stem cell niches. *Neuron,* 39**,** 937-50.

MADISEN, L., ZWINGMAN, T. A., SUNKIN, S. M., OH, S. W., ZARIWALA, H. A., GU, H., NG, L. L., PALMITER, R. D., HAWRYLYCZ, M. J., JONES, A. R., LEIN, E. S. & ZENG, H. 2010. A robust and high-throughput Cre reporting and characterization system for the whole mouse brain. *Nat Neurosci,* 13**,** 133-40.

MANGIARINI, L., SATHASIVAM, K., SELLER, M., COZENS, B., HARPER, A., HETHERINGTON, C., LAWTON, M., TROTTIER, Y., LEHRACH, H., DAVIES, S. W. & BATES, G. P. 1996. Exon 1 of the HD gene with an expanded CAG repeat is sufficient to cause a progressive neurological phenotype in transgenic mice. *Cell,* 87**,** 493-506.

MANUEL, M. & PRICE, D. J. 2005. Role of Pax6 in forebrain regionalization. *Brain Res Bull,* 66**,** 387-93.

MARKIANOS, M., PANAS, M., KALFAKIS, N. & VASSILOPOULOS, D. 2005. Plasma testosterone in male patients with Huntington's disease: relations to severity of illness and dementia. *Ann Neurol,* 57**,** 520-5.

MARTIN-IBANEZ, R., CRESPO, E., URBAN, N., SERGENT-TANGUY, S., HERRANZ, C., JAUMOT, M., VALIENTE, M., LONG, J. E., PINEDA, J. R., ANDREU, C., RUBENSTEIN, J. L., MARIN, O., GEORGOPOULOS, K., MENGOD, G., FARINAS, I., BACHS, O., ALBERCH, J. & CANALS, J. M. 2010. Ikaros-1 couples cell cycle arrest of late striatal precursors with neurogenesis of enkephalinergic neurons. *J Comp Neurol,* 518**,** 329-51.

MARTYNOGA, B., MORRISON, H., PRICE, D. J. & MASON, J. O. 2005. Foxg1 is required for specification of ventral telencephalon and region-specific regulation of dorsal telencephalic precursor proliferation and apoptosis. *Dev Biol,* 283**,** 113-27.

MASON, H. A., RAKOWIECKI, S. M., RAFTOPOULOU, M., NERY, S., HUANG, Y., GRIDLEY, T. & FISHELL, G. 2005. Notch signaling coordinates the patterning of striatal compartments. *Development,* 132**,** 4247-58.

MAUCKSCH, C., VAZEY, E. M., GORDON, R. J. & CONNOR, B. 2013. Stem cell-based therapy for Huntington's disease. *J Cell Biochem,* 114**,** 754-63.

MENALLED, L., ZANJANI, H., MACKENZIE, L., KOPPEL, A., CARPENTER, E., ZEITLIN, S. & CHESSELET, M. F. 2000. Decrease in striatal enkephalin mRNA in mouse models of Huntington's disease. *Exp Neurol,* 162**,** 328-42.

MINICHIELLO, L., KORTE, M., WOLFER, D., KÜHN, R., UNSICKER, K., CESTARI, V., ROSSI-ARNAUD, C., LIPP, H. P., BONHOEFFER, T. & KLEIN, R. 1999. Essential role for TrkB receptors in hippocampus-mediated learning. *Neuron,* 24**,** 401-14.

MITCHELL, I. J., COOPER, A. J. & GRIFFITHS, M. R. 1999. The selective vulnerability of striatopallidal neurons. *Prog Neurobiol,* 59**,** 691-719.

MOLOTKOVA, N., MOLOTKOV, A. & DUESTER, G. 2007. Role of retinoic acid during forebrain development begins late when Raldh3 generates retinoic acid in the ventral subventricular zone. *Dev Biol,* 303**,** 601-10.

MORRIS, G., ARKADIR, D., NEVET, A., VAADIA, E. & BERGMAN, H. 2004. Coincident but distinct messages of midbrain dopamine and striatal tonically active neurons. *Neuron,* 43**,** 133-43.

NERY, S., FISHELL, G. & CORBIN, J. G. 2002. The caudal ganglionic eminence is a source of distinct cortical and subcortical cell populations. *Nat Neurosci,* 5**,** 1279-87.

NISENBAUM, E. S., WILSON, C. J., FOEHRING, R. C. & SURMEIER, D. J. 1996. Isolation and characterization of a persistent potassium current in neostriatal neurons. *J Neurophysiol,* 76**,** 1180-94.

NOVAK, A., GUO, C., YANG, W., NAGY, A. & LOBE, C. G. 2000. Z/EG, a double reporter mouse line that expresses enhanced green fluorescent protein upon Cre-mediated excision. *Genesis,* 28**,** 147-55.

O'CALLAGHAN, C., BERTOUX, M. & HORNBERGER, M. 2014. Beyond and below the cortex: the contribution of striatal dysfunction to cognition and behaviour in neurodegeneration. *J Neurol Neurosurg Psychiatry,* 85**,** 371-8.

OKABE, S., FORSBERG-NILSSON, K., SPIRO, A. C., SEGAL, M. & MCKAY, R. D. 1996. Development of neuronal precursor cells and functional postmitotic neurons from embryonic stem cells in vitro. *Mech Dev,* 59**,** 89-102.

OULAD-ABDELGHANI, M., CHAZAUD, C., BOUILLET, P., SAPIN, V., CHAMBON, P. & DOLLÉ, P. 1997. Meis2, a novel mouse Pbx-related homeobox gene induced by retinoic acid during differentiation of P19 embryonal carcinoma cells. *Dev Dyn,* 210**,** 173-83.

PANCHISION, D. M., CHEN, H. L., PISTOLLATO, F., PAPINI, D., NI, H. T. & HAWLEY, T. S. 2007. Optimized flow cytometric analysis of central nervous system tissue reveals novel functional relationships among cells expressing CD133, CD15, and CD24. *Stem Cells,* 25**,** 1560-70.

PARK, I. H., ARORA, N., HUO, H., MAHERALI, N., AHFELDT, T., SHIMAMURA, A., LENSCH, M. W., COWAN, C., HOCHEDLINGER, K. & DALEY, G. Q. 2008. Disease-specific induced pluripotent stem cells. *Cell,* 134**,** 877-86.

PERRIER, A. & PESCHANSKI, M. 2012. How can human pluripotent stem cells help decipher and cure Huntington's disease? *Cell Stem Cell,* 11**,** 153-61.

PLOTKIN, J. L., DAY, M., PETERSON, J. D., XIE, Z., KRESS, G. J., RAFALOVICH, I., KONDAPALLI, J., GERTLER, T. S., FLAJOLET, M., GREENGARD, P., STAVARACHE, M., KAPLITT, M. G., ROSINSKI, J., CHAN, C. S. & SURMEIER, D. J. 2014. Impaired TrkB receptor signaling underlies corticostriatal dysfunction in Huntington's disease. *Neuron,* 83**,** 178-88.

PRUSZAK, J., LUDWIG, W., BLAK, A., ALAVIAN, K. & ISACSON, O. 2009. CD15, CD24, and CD29 define a surface biomarker code for neural lineage differentiation of stem cells. *Stem Cells,* 27**,** 2928-40.

QIAN, X., SHEN, Q., GODERIE, S. K., HE, W., CAPELA, A., DAVIS, A. A. & TEMPLE, S. 2000. Timing of CNS cell generation: a programmed sequence of neuron and glial cell production from isolated murine cortical stem cells. *Neuron,* 28**,** 69-80.

RALLU, M., CORBIN, J. G. & FISHELL, G. 2002a. Parsing the prosencephalon. *Nat Rev Neurosci,* 3**,** 943-51.

RALLU, M., MACHOLD, R., GAIANO, N., CORBIN, J. G., MCMAHON, A. P. & FISHELL, G. 2002b. Dorsoventral patterning is established in the telencephalon of mutants lacking both Gli3 and Hedgehog signaling. *Development,* 129**,** 4963-74.

REINER, A., ALBIN, R. L., ANDERSON, K. D., D'AMATO, C. J., PENNEY, J. B. & YOUNG, A. B. 1988. Differential loss of striatal projection neurons in Huntington disease. *Proc Natl Acad Sci U S A,* 85**,** 5733-7.

RICHFIELD, E. K., MAGUIRE-ZEISS, K. A., VONKEMAN, H. E. & VOORN, P. 1995. Preferential loss of preproenkephalin versus preprotachykinin neurons from the striatum of Huntington's disease patients. *Ann Neurol,* 38**,** 852-61.

ROOS, R. A. 2010. Huntington's disease: a clinical review. *Orphanet J Rare Dis,* 5**,** 40.

ROSS, C. A. & TABRIZI, S. J. 2011. Huntington's disease: from molecular pathogenesis to clinical treatment. *Lancet Neurol,* 10**,** 83-98.

RUBERTE, E., FRIEDERICH, V., CHAMBON, P. & MORRISS-KAY, G. 1993. Retinoic acid receptors and cellular retinoid binding proteins. III. Their differential transcript distribution during mouse nervous system development. *Development,* 118**,** 267-82.

RYMAR, V. V., SASSEVILLE, R., LUK, K. C. & SADIKOT, A. F. 2004. Neurogenesis and stereological morphometry of calretinin-immunoreactive GABAergic interneurons of the neostriatum. *J Comp Neurol,* 469**,** 325-39.

SCHROLL, H. & HAMKER, F. H. 2013. Computational models of basal-ganglia pathway functions: focus on functional neuroanatomy. *Front Syst Neurosci,* 7**,** 122.

SHEN, W., TIAN, X., DAY, M., ULRICH, S., TKATCH, T., NATHANSON, N. M. & SURMEIER, D. J. 2007. Cholinergic modulation of Kir2 channels selectively elevates dendritic excitability in striatopallidal neurons. *Nat Neurosci,* 10**,** 1458-66.

SHEPHERD, G. M. 2013. Corticostriatal connectivity and its role in disease. *Nat Rev Neurosci,* 14**,** 278-91.

SHIMAMURA, K. & RUBENSTEIN, J. L. 1997. Inductive interactions direct early regionalization of the mouse forebrain. *Development,* 124**,** 2709-18.

SHIN, E., PALMER, M. J. & LI, M. 2011. GABAergic neurone from mouse embryonic stem cells possess functional properties of striatal nuerons in vitro, and develop into striatal neurons in vivo in a mouse model of Huntington's disease. *Stem Cell Rev and Rep,* 8**,** 19.

SLOW, E. J., VAN RAAMSDONK, J., ROGERS, D., COLEMAN, S. H., GRAHAM, R. K., DENG, Y., OH, R., BISSADA, N., HOSSAIN, S. M., YANG, Y. Z., LI, X. J., SIMPSON, E. M., GUTEKUNST, C. A., LEAVITT, B. R. & HAYDEN, M. R. 2003. Selective striatal neuronal loss in a YAC128 mouse model of Huntington disease. *Hum Mol Genet,* 12**,** 1555-67.

SONG, D. D. & HARLAN, R. E. 1994. The development of enkephalin and substance P neurons in the basal ganglia: insights into neostriatal compartments and the extended amygdala. *Brain Res Dev Brain Res,* 83**,** 247-61.

SOUSA, V. H. & FISHELL, G. 2010. Sonic hedgehog functions through dynamic changes in temporal competence in the developing forebrain. *Curr Opin Genet Dev,* 20**,** 391-9.

SPOKES, E. G. 1980. Neurochemical alterations in Huntington's chorea: a study of post-mortem brain tissue. *Brain,* 103**,** 179-210.

SRINIVAS, S., WATANABE, T., LIN, C. S., WILLIAM, C. M., TANABE, Y., JESSELL, T. M. & COSTANTINI, F. 2001. Cre reporter strains produced by targeted insertion of EYFP and ECFP into the ROSA26 locus. *BMC Developmental Biology,* 1**,** 4-4.

STAVRIDIS, M. P., COLLINS, B. J. & STOREY, K. G. 2010. Retinoic acid orchestrates fibroblast growth factor signalling to drive embryonic stem cell differentiation. *Development,* 137**,** 881-90.

STORM, E. E., GAREL, S., BORELLO, U., HEBERT, J. M., MARTINEZ, S., MCCONNELL, S. K., MARTIN, G. R. & RUBENSTEIN, J. L. 2006. Dose-dependent functions of Fgf8 in regulating telencephalic patterning centers. *Development,* 133**,** 1831-44.

STUHMER, T., ANDERSON, S. A., EKKER, M. & RUBENSTEIN, J. L. 2002. Ectopic expression of the Dlx genes induces glutamic acid decarboxylase and Dlx expression. *Development,* 129**,** 245-52.

SUN, Z., DEL MAR, N., MEADE, C., GOLDOWITZ, D. & REINER, A. 2002. Differential changes in striatal projection neurons in R6/2 transgenic mice for Huntington's disease. *Neurobiol Dis,* 11**,** 369-85.

SURMEIER, D. J., BARGAS, J. & KITAI, S. T. 1988. Voltage-clamp analysis of a transient potassium current in rat neostriatal neurons. *Brain Res,* 473**,** 187-92.

SUSSEL, L., MARIN, O., KIMURA, S. & RUBENSTEIN, J. L. 1999. Loss of Nkx2.1 homeobox gene function results in a ventral to dorsal molecular respecification within the basal telencephalon: evidence for a transformation of the pallidum into the striatum. *Development,* 126**,** 3359-70.

SØRENSEN, S. A. & FENGER, K. 1992. Causes of death in patients with Huntington's disease and in unaffected first degree relatives. *J Med Genet,* 29**,** 911-4.

TAKAHASHI, H. & LIU, F. C. 2006. Genetic patterning of the mammalian telencephalon by morphogenetic molecules and transcription factors. *Birth Defects Res C Embryo Today,* 78**,** 256-66.

TAKAHASHI, K., LIU, F. C., HIROKAWA, K. & TAKAHASHI, H. 2003. Expression of Foxp2, a gene involved in speech and language, in the developing and adult striatum. *J Neurosci Res,* 73**,** 61-72.

TAMURA, S., MORIKAWA, Y., IWANISHI, H., HISAOKA, T. & SENBA, E. 2004. Foxp1 gene expression in projection neurons of the mouse striatum. *Neuroscience,* 124**,** 261-7.

TEPPER, J. M. & BOLAM, J. P. 2004. Functional diversity and specificity of neostriatal interneurons. *Curr Opin Neurobiol,* 14**,** 685-92.

THEIL, T., ALVAREZ-BOLADO, G., WALTER, A. & RUTHER, U. 1999. Gli3 is required for Emx gene expression during dorsal telencephalon development. *Development,* 126**,** 3561-71.

TORESSON, H., MATA DE URQUIZA, A., FAGERSTRÖM, C., PERLMANN, T. & CAMPBELL, K. 1999. Retinoids are produced by glia in the lateral ganglionic eminence and regulate striatal neuron differentiation. *Development,* 126**,** 1317-26.

TORESSON, H., POTTER, S. S. & CAMPBELL, K. 2000. Genetic control of dorsal-ventral identity in the telencephalon: opposing roles for Pax6 and Gsh2. *Development,* 127**,** 4361-71.

UCHIDA, N., BUCK, D. W., HE, D., REITSMA, M. J., MASEK, M., PHAN, T. V., TSUKAMOTO, A. S., GAGE, F. H. & WEISSMAN, I. L. 2000. Direct isolation of human central nervous system stem cells. *Proc Natl Acad Sci U S A,* 97**,** 14720-5.

URBAN, N., MARTIN-IBANEZ, R., HERRANZ, C., ESGLEAS, M., CRESPO, E., PARDO, M., CRESPO-ENRIQUEZ, I., MENDEZ-GOMEZ, H. R., WACLAW, R., CHATZI, C., ALVAREZ, S., ALVAREZ, R., DUESTER, G., CAMPBELL, K., DE LERA, A. R., VICARIO-ABEJON, C., MARTINEZ, S., ALBERCH, J. & CANALS, J. M. 2010. Nolz1 promotes striatal neurogenesis through the regulation of retinoic acid signaling. *Neural Dev,* 5**,** 21.

VAN DER KOOY, D. & FISHELL, G. 1987. Neuronal birthdate underlies the development of striatal compartments. *Brain Res,* 401**,** 155-61.

VAN DUIJN, E., CRAUFURD, D., HUBERS, A. A., GILTAY, E. J., BONELLI, R., RICKARDS, H., ANDERSON, K. E., VAN WALSEM, M. R., VAN DER MAST, R. C., ORTH, M., LANDWEHRMEYER, G. B. & GROUP, T. E. H. S. D. N. B. P. W. 2014. Neuropsychiatric symptoms in a European Huntington's disease cohort (REGISTRY). *J Neurol Neurosurg Psychiatry*.

VONSATTEL, J. P. & DIFIGLIA, M. 1998. Huntington disease. *J Neuropathol Exp Neurol,* 57**,** 369-84.

VONSATTEL, J. P., MYERS, R. H., STEVENS, T. J., FERRANTE, R. J., BIRD, E. D. & RICHARDSON, E. P. 1985. Neuropathological classification of Huntington's disease. *J Neuropathol Exp Neurol,* 44**,** 559-77.

WACLAW, R. R., WANG, B. & CAMPBELL, K. 2004. The homeobox gene Gsh2 is required for retinoid production in the embryonic mouse telencephalon. *Development,* 131**,** 4013-20.

WANG, B., LUFKIN, T. & RUBENSTEIN, J. L. 2011. Dlx6 regulates molecular properties of the striatum and central nucleus of the amygdala. *J Comp Neurol*.

WANG, Y., DYE, C. A., SOHAL, V., LONG, J. E., ESTRADA, R. C., ROZTOCIL, T., LUFKIN, T., DEISSEROTH, K., BARABAN, S. C. & RUBENSTEIN, J. L. 2010. Dlx5 and Dlx6 regulate the development of parvalbumin-expressing cortical interneurons. *J Neurosci,* 30**,** 5334-45.

WATANABE, K., KAMIYA, D., NISHIYAMA, A., KATAYAMA, T., NOZAKI, S., KAWASAKI, H., WATANABE, Y., MIZUSEKI, K. & SASAI, Y. 2005. Directed differentiation of telencephalic precursors from embryonic stem cells. *Nat Neurosci,* 8**,** 288-96.

WEXLER, N. S., LORIMER, J., PORTER, J., GOMEZ, F., MOSKOWITZ, C., SHACKELL, E., MARDER, K., PENCHASZADEH, G., ROBERTS, S. A., GAYÁN, J., BROCKLEBANK, D., CHERNY, S. S., CARDON, L. R., GRAY, J., DLOUHY, S. R., WIKTORSKI, S., HODES, M. E., CONNEALLY, P. M., PENNEY, J. B., GUSELLA, J., CHA, J. H., IRIZARRY, M., ROSAS, D., HERSCH, S., HOLLINGSWORTH, Z., MACDONALD, M., YOUNG, A. B., ANDRESEN, J. M., HOUSMAN, D. E., DE YOUNG, M. M., BONILLA, E., STILLINGS, T., NEGRETTE, A., SNODGRASS, S. R., MARTINEZ-JAURRIETA, M. D., RAMOS-ARROYO, M. A., BICKHAM, J., RAMOS, J. S., MARSHALL, F., SHOULSON, I., REY, G. J., FEIGIN, A., ARNHEIM, N., ACEVEDO-CRUZ, A., ACOSTA, L., ALVIR, J., FISCHBECK, K., THOMPSON, L. M., YOUNG, A., DURE, L., O'BRIEN, C. J., PAULSEN, J., BRICKMAN, A., KRCH, D., PEERY, S., HOGARTH, P., HIGGINS, D. S., LANDWEHRMEYER, B. & PROJECT, U. S.-V. C. R. 2004. Venezuelan kindreds reveal that genetic and environmental factors modulate Huntington's disease age of onset. *Proc Natl Acad Sci U S A,* 101**,** 3498-503.

WICHMANN, T. & DELONG, M. R. 2013. The basal ganglia. *In:* KANDEL, E. R., SCHWARTZ, J. H., JESSEL, T. M., SIEGELBAUM, S. A. & HUDSPETH, A. J. (eds.) *Principles of neural science.* 5th ed. New York: McGraw-Hill.

WILSON, S. W. & HOUART, C. 2004. Early steps in the development of the forebrain. *Dev Cell,* 6**,** 167-81.

WYTTENBACH, A., CARMICHAEL, J., SWARTZ, J., FURLONG, R. A., NARAIN, Y., RANKIN, J. & RUBINSZTEIN, D. C. 2000. Effects of heat shock, heat shock protein 40 (HDJ-2), and proteasome inhibition on protein aggregation in cellular models of Huntington's disease. *Proc Natl Acad Sci U S A,* 97**,** 2898-903.

YANG, Y. & NISWANDER, L. 1995. Interaction between the signaling molecules WNT7a and SHH during vertebrate limb development: dorsal signals regulate anteroposterior patterning. *Cell,* 80**,** 939-47.

YING, Q. L. & SMITH, A. G. 2003. Defined conditions for neural commitment and differentiation. *Methods Enzymol,* 365**,** 327-41.

YING, Q. L., STAVRIDIS, M., GRIFFITHS, D., LI, M. & SMITH, A. 2003. Conversion of embryonic stem cells into neuroectodermal precursors in adherent monoculture. *Nat Biotechnol,* 21**,** 183-6.

YOUNG, A. B. 2003. Huntingtin in health and disease. *J Clin Invest,* 111**,** 299-302.

YUAN, S. H., MARTIN, J., ELIA, J., FLIPPIN, J., PARAMBAN, R. I., HEFFERAN, M. P., VIDAL, J. G., MU, Y., KILLIAN, R. L., ISRAEL, M. A., EMRE, N., MARSALA, S., MARSALA, M., GAGE, F. H., GOLDSTEIN, L. S. & CARSON, C. T. 2011. Cell-surface marker signatures for the isolation of neural stem cells, glia and neurons derived from human pluripotent stem cells. *PLoS One,* 6**,** e17540.

YUN, K., FISCHMAN, S., JOHNSON, J., HRABE DE ANGELIS, M., WEINMASTER, G. & RUBENSTEIN, J. L. 2002. Modulation of the notch signaling by Mash1 and Dlx1/2 regulates sequential specification and differentiation of progenitor cell types in the subcortical telencephalon. *Development,* 129**,** 5029-40.

ZHANG, N., AN, M. C., MONTORO, D. & ELLERBY, L. M. 2010. Characterization of Human Huntington's Disease Cell Model from Induced Pluripotent Stem Cells. *PLoS Curr,* 2**,** RRN1193.

ZUCCATO, C., TARTARI, M., CROTTI, A., GOFFREDO, D., VALENZA, M., CONTI, L., CATAUDELLA, T., LEAVITT, B. R., HAYDEN, M. R., TIMMUSK, T., RIGAMONTI, D. & CATTANEO, E. 2003. Huntingtin interacts with REST/NRSF to modulate the transcription of NRSE-controlled neuronal genes. *Nat Genet,* 35**,** 76-83.